HYDROMETEOROLOGICAL REPORT NO. 43

Probable Maximum Precipitation, Northwest States

REPRINTED WITH REVISION OF APRIL 1981

U.S. DEPARTMENT OF COMMERCE
ENVIRONMENTAL SCIENCE SERVICES ADMINISTRATION
WEATHER BUREAU
Washington
November 1966

HYDROMETEOROLOGICAL REPORTS

*No. 1. Maximum possible precipitation over the Ompompanoosuc Basin above Union Village, Vt. 1943.
*No. 2. Maximum possible precipitation over the Ohio River Basin above Pittsburgh, Pa. 1942.
*No. 3. Maximum possible precipitation over the Sacramento Basin of California. 1943.
*No. 4. Maximum possible precipitation over the Panama Canal Basin. 1943.
*No. 5. Thunderstorm rainfall. 1947.
*No. 6. A preliminary report on the probable occurrence of excessive precipitation over Fort Supply Basin, Okla. 1938.
*No. 7. Worst probable meteorological condition on Mill Creek, Butler and Hamilton Counties, Ohio. 1937. (Unpublished.) Supplement, 1938.
*No. 8. A hydrometeorological analysis of possible maximum precipitation over St. Francis River Basin above Wappapello, Mo. 1938.
*No. 9. A report on the possible occurrence of maximum precipitation over White River Basin above Mud Mountain Dam site, Wash. 1939.
*No. 10. Maximum possible rainfall over the Arkansas River Basin above Caddoa, Colo. 1939. Supplement, 1939.
*No. 11. A preliminary report on the maximum possible precipitation over the Dorena, Cottage Grove, and Fern Ridge Basins in the Willamette Basin, Oreg. 1939.
*No. 12. Maximum possible precipitation over the Red River Basin above Denison, Tex. 1939.
*No. 13. A report on the maximum possible precipitation over Cherry Creek Basin in Colorado. 1940.
*No. 14. The frequency of flood-producing rainfall over the Pajaro River Basin in California. 1940.
*No. 15. A report on depth-frequency relations of thunderstorm rainfall on the Sevier Basin, Utah. 1941.
*No. 16. A preliminary report on the maximum possible precipitation over the Potomac and Rappahannock River Basins. 1943.
*No. 17. Maximum possible precipitation over the Pecos Basin of New Mexico. 1944. (Unpublished.)
*No. 18. Tentative estimates of maximum possible flood-producing meteorological conditions in the Columbia River Basin. 1945.
*No. 19. Preliminary report on depth-duration-frequency characteristics of precipitation over the Muskingum Basin for 1- to 9-week periods. 1945.
*No. 20. An estimate of maximum possible flood-producing meteorological conditions in the Missouri River Basin above Garrison Dam site. 1945.
*No. 21. A hydrometeorological study of the Los Angeles area. 1939.
*No. 21A. Preliminary report on maximum possible precipitation, Los Angeles area, California. 1944.
*No. 21B. Revised report on maximum possible precipitation, Los Angeles area, California. 1945.
*No. 22. An estimate of maximum possible flood-producing meteorological conditions in the Missouri River Basin between Garrison and Fort Randall. 1946.
*No. 23. Generalized estimates of maximum possible precipitation over the United States east of the 105th meridian, for areas of 10,200, and 500 square miles. 1947.
*No. 24. Maximum possible precipitation over the San Joaquin Basin, Calif. 1947.
*No. 25. Representative 12-hour dewpoints in major United States storms east of the Continental Divide. 1947.
*No. 25A. Representative 12-hour dewpoints in major United States storms east of the Continental Divide. 2d edition. 1949.
*No. 26. Analysis of winds over Lake Okeechobee during tropical storm of August 26–27, 1949. 1951.
*No. 27. Estimate of maximum possible precipitation, Rio Grande Basin, Fort Quitman to Zapata. 1951.
*No. 28. Generalized estimate of maximum possible precipitation over New England and New York. 1952.
*No. 29. Seasonal variation of the standard project storm for areas of 200 and 1,000 square miles east of 105th meridian. 1953.
*No. 30. Meteorology of floods at St. Louis. 1953. (Unpublished.)
No. 31. Analysis and synthesis of hurricane wind patterns over Lake Okeechobee, Florida. 1954.
No. 32. Characteristics of United States hurricanes pertinent to levee design for Lake Okeechobee, Florida. 1954.
No. 33. Seasonal variation of the probable maximum precipitation east of the 105th meridian for areas from 10 to 1,000 square miles and durations of 6, 12, 24, and 48 hours. 1956.
No. 34. Meteorology of flood-producing storms in the Mississippi River Basin. 1956.
No. 35. Meteorology of hypothetical flood sequences in the Mississippi River Basin. 1959.
No. 36. Interim report—probable maximum precipitation in California. 1961.
No. 37. Meteorology of hydrologically critical storms in California. 1962.
No. 38. Meteorology of flood-producing storms in the Ohio River Basin. 1961.
No. 39. Probable maximum precipitation in the Hawaiian Islands. 1963.
No. 40. Probable maximum precipitation, Susquehanna River drainage above Harrisburg, Pa. 1965.
No. 41. Probable maximum and TVA precipitation over the Tennessee River Basin above Chattanooga. 1965.
No. 42. Meteorological conditions for the probable maximum flood on the Yukon River above Rampart, Alaska. 1966.

*Out of print

U.S. DEPARTMENT OF COMMERCE
ENVIRONMENTAL SCIENCE SERVICES ADMINISTRATION

U.S. DEPARTMENT OF THE ARMY
CORPS OF ENGINEERS

HYDROMETEOROLOGICAL REPORT NO. 43

Probable Maximum Precipitation, Northwest States

REPRINTED WITH REVISION OF APRIL 1981

Prepared by
Hydrometeorological Branch
Office of Hydrology
Weather Bureau

Washington, D.C.
November 1966

For sale by the Superintendent of Documents, U.S. Government Printing Office
Washington, D.C., 20402 - Price $1.75

The probable maximum precipitation estimates presented in this report are currently being reviewed. This review is a cooperative project of the Bureau of Reclamation, Corps of Engineers, National Weather Service, and Soil Conservation Service. The results of these investigations will be published in a future volume of the Hydrometeorological Report series of the National Weather Service. Publication is expected in the spring of 1987.

ERRATA

page		
78	Section 3.48	Last sentence should read, "The May-June depth-area..."
78	Heading, section 3.51	Add "*". Footnote should read, "Please see revision to section 3.51, dated April 1981, which is included at the end of this publication."
82	Figure 3-41	See fig. 3.41 (REV.)
126	Table 4-6	Correct spelling is "Rainier".
133	Table 4-7	Zone "C, 3000 ft." for June should read, "91".
178, 179	Figures 5-12, 5-13	Data for Morgan, Utah is incorrect.
181	Step 3	Should read, "Determine the mean elevation within the basin boundary and limiting thunderstorm area."
185	Step 7	Should read, "Multiply isohyet labels of step 6 by the 1-hr., 1-mi.^{2} value from step 4. This gives ..."
186	Step 8	Last line, the 4th period should read, "0.8".
189	Step N	First line should read, "...lies from figure 4-26."
191	J (3-hr.)	Add J (1-hr.), rest should read, "4.1 in. x 57% = 2.3 in. / 4.1 in. x 31% = 1.3 in. } E x % in fig. 3-41 (REV)"
193	J (3-hr.) J (1-hr.)	Should read, "3.8 in. x 61% = 2.3 in. / 3.8 in. x 34% = 1.3 in. } E x % in fig. 3-41 (REV)"

TABLE OF CONTENTS

FIGURES

FIGURES (Cont'd.)

FIGURES (Cont'd.)

FIGURES (Cont'd.)

Frontispiece. Map of the study area

Chapter I

INTRODUCTION

Purpose of report

1.01. This report presents generalized estimates of probable maximum precipitation (PMP) over basins in the Northwest States. Such estimates have been made for coastal drainages of California (1) and the United States east of the 105th meridian (2). Generalized PMP estimates west of the 105th meridian (3) cover the Northwest but the scope of that study does not give the detail nor the range in basin size required by the Corps of Engineers.

Authorization

1.02. Authorization for this study is contained in a memorandum from the Office of Chief of Engineers, Corps of Engineers, dated September 11, 1962. Additional requirements with regard to date of completion and area to be covered were determined in subsequent conferences.

Scope

1.03. Generalized PMP estimates in this report are for the Columbia River Basin in the United States and coastal river drainages of Washington and Oregon (frontispiece). Thus the states of Oregon, Washington, and Idaho plus portions of Montana, Wyoming, Utah, and Nevada are included. Because of proposed flood-control structures on the Kettle and Okanagan watersheds, the estimates have been extended to include the portions of these basins in Canada.

1.04. General storm PMP estimates are provided for basin sizes from 10 to 5000 square miles west of the Cascade Divide and for 10- to-1000-sq. mi basins east of the Divide. Duration of this PMP is from 1 to 72 hours. Seasonal variation is given from October through June. July, August and September are omitted because general storm PMP in these months is less than in June or October. Although PMP may not be required for all months given, the method of development did require consideration of all months.

East of the Cascade Divide summer local thunderstorm PMP is given for small basins and short durations. This storm type is not pertinent west of the Divide.

Critical high air temperature and wind sequences are provided for determining the contribution of snowmelt to the flood hydrograph. These criteria are for the 3-day PMP storm and for three days prior to it. Complete evaluation of probable maximum flood hydrographs requires upper limits of snowmelt criteria (including solar radiation over many days prior to the

PMP storm) and snowpack available for melt. These data and intervals between storms (to determine antecedent ground conditions) are possible subjects of a future report. They are more important for basins larger than those covered in this report.

Definition of PMP

1.05. PMP over a watershed is the depth of rainfall that approaches the upper limit of what the atmosphere can produce. In mountainous regions it is derived in part by physical methods, in that maximum winds and moisture are input to an orographic storage equation that makes use of several principles of airflow to compute precipitation due to lift by mountain slopes. Involved in the procedure is maximizing storms of record for moisture and indirectly for wind. How much and which storms to maximize is all-important to the resulting estimate of the upper limit. Much of this report is devoted to answering these questions. It is easily shown that if storm transposition were unlimited and if maximum values of winds, moisture and other variables of storms were combined, the results would be unrealistic. Limited transposition and combination of near maximum values of a variable with high but not necessarily highest values of other variables require making judgments at several steps in the procedure. Such judgments are influenced through study of record storms. Additional guidelines come from results of other PMP studies and statistical analyses of extremes in observed variables.

PMP in flat and mountainous regions

1.06. In broad level regions, such as the Central States, relatively uncomplicated techniques have evolved for estimating PMP for moderate-sized basins. Storms are maximized by increasing them to allow for maximum moisture. Because terrain effects are slight, storm experience for a basin can be increased many fold by transposing from any location within a large region of similar climate. Thus sufficient storms are available to permit the assumption that other meteorological factors besides moisture have been observed at their optimum. Full explanation of the procedure is contained in Hydrometeorological Report No. 33, "Seasonal Variation of the Probable Maximum Precipitation East of the 105th Meridian for Areas from 10 to 1,000 Square Miles and Durations of 6, 12, 24 and 48 Hours," (2), referred to hereafter as HMR 33.

1.07. The problem becomes more difficult in mountainous regions where precipitation due to lifting of air by ground slopes, called orographic precipitation, is complemented by precipitation due to meteorological processes which would be present were the mountains not there. This latter component, which we have termed convergence precipitation, is much like that in flat areas of the Central States, for example. Study of major storms in the Pacific Coast States demonstrates that both rain processes normally are present at the same time over the same locality. Chapter II of this report cites examples. It is necessary then, when estimating PMP in mountainous regions, to consider the summed result of the two processes.

Method of this report

1.08. In this report each of the two rain-producing processes is maximized and then summed. The orographic component is estimated from a flow model that is first tested against major orographic storms. This model, explained in chapter IV, consists of first, a dynamic treatment of winds and second, a computation of precipitation by calculating the amount of condensation formed in all parts of the flow and following the paths of precipitation to the ground. Convergence PMP is estimated by (1) moisture maximization of highest observed mid-winter rains where orographic effects are small, and (2) use of storm experience for seasonal variation from mid-winter. The procedure is developed in chapter III.

Development of PMP by this method demands that steps be taken to avoid an unrealistic combination of the two precipitation components. This was controlled in several ways. Convergence PMP to be combined with orographic PMP is based on storms with heavy orographic precipitation in the mountains. The envelope of maximum moisture used in deriving both components is based on dew points representative of storm conditions. In determining seasonal, durational, geographic and areal differences in precipitation, average indices are used rather than envelopes.

1.09. Although separate estimates of convergence and orographic PMP are made and then summed, we do not imply that in actual rains the two components are easily distinguished. In chapter IV where tests of the orographic model are described it is pointed out that test results are dependent to some extent on the ability to distinguish the orographic component of total observed rain. Similarly in several steps of convergence rain development, orographic effects may not have been entirely eliminated. Such contamination has slight bearing on PMP after each component is maximized. Characteristic seasonal, durational, areal, and elevation variations of convergence rain differ from those of orographic rain. Study of extreme rains in areas and situations where one component plays the major role, gives important control to PMP values.

Complexity and accuracy of criteria

1.10. The precipitation regimes of the entire study area, Columbia Basin and coastal Oregon and Washington, are varied and complex. Mean annual precipitation ranges from over 220 inches on the slopes of Mt. Olympus to less than 10 percent of this depth immediately to the northeast and to less than 5 percent on the plains of eastern Washington. Most of the active glaciers within the United States (exclusive of Alaska) are in this region. Forests give way to sagebrush in short distances. The intense very local thunderstorms characteristic of the Great Basin threaten the interior, but not west of the Cascades.

A complexity of criteria is required to assess the probable maximum precipitation over this large region, considering seasonal, durational,

regional and elevation variations for a range in basin sizes; thus the large number of charts, diagrams and tables. It may appear to the reader that charts have been carried into great detail in view of the scanty supporting data. This has been found necessary in order to incorporate into PMP estimates the pertinent climatic variations and to accomplish one of the purposes of generalized charts of PMP, consistency of estimates between basins in a region and between regions.

1.11. There is frequent resort to regional and monthly charts in this report, especially numerous in chapter III. While a high degree of accuracy cannot be claimed for many of these charts (the charts of ratio of 6-hr. rain to 24-hr. rain for example) it is believed that the trends depicted are sound.

Seasonal trends

1.12. Seasonal variation has been explored in this report. In some parts of the United States summer rainfall clearly dominates extreme rainfalls, except over very large basins. In other regions, such as central California, summers are dry and winter rain clearly predominates. Such seasonal domination simplifies estimating PMP. In the Northwest, seasonal trends permit omission of general convergence and orographic PMP in July through September. The logic for this simplification is as follows. West-of-Cascades PMP values decline in midsummer, though to a lesser extent than in California. East-of-Cascades midsummer values are overshadowed by thunderstorm PMP for small areas and short durations. Where midsummer values for large areas and long durations approach snowmelt season values, they result in a relatively lower hydrograph.

Relation of this report to Hydrometeorological Report No. 36 (1)

1.13. The basic methods of determining PMP used in Hydrometeorological Report No. 36, "Interim Report-Probable Maximum Precipitation in California," (HMR 36), are used also in this report, with various refinements. Because of the similarity of basic methods in the two reports there are numerous references to HMR 36 in order to avoid repeating details of some developments.

1.14. HMR 36, chapter II, headed "Appraisal of Probable Maximum Precipitation Problem," contains a general discussion of PMP, covering topics such as maximization, storm sampling, internal consistency and general level of PMP. All of this discussion applies to Pacific Northwest PMP also excepting those sections dealing with statistical estimates of PMP and tropical storms.

Organization

1.15. A meteorological summary of major Northwest storms covering large areas is given in chapter II. Chapter III contains the development of convergence PMP. Chapter IV develops orographic PMP. Chapter V develops thunderstorm PMP criteria for areas east of the Cascades. In chapter VI

the procedure for obtaining PMP for a basin is given with sample computations. Suggested time sequences of 6-hr. PMP increments in the PMP storm are also shown. Chapter VII compares PMP estimates from this report with others and with observed precipitation. Chapter VIII contains highest winds and temperatures which can be realized for several days prior to and during the PMP storm.

Chapter II

METEOROLOGY OF MAJOR PACIFIC NORTHWEST STORMS

2-A. WESTERN WASHINGTON AND OREGON STORMS

2.01. The important storms in western Washington and Oregon occur mostly in winter months; yet there have been occurrences as late as June. Their isohyetal patterns reflect the influence of orography. Hence, discussion of the storms will emphasize topographic effects on strong moist onshore flows and the offshore storm tracks. Convergence precipitation is an important concomitant feature in most storms.

Storm selection and presentation

2.02. Storms selected are those having heavy precipitation for 2-3 days over a large area. Those of longer duration but with a midway lull approaching one day are not included.

2.03. Storms west of the Cascades are divided into three groups with respect to location of precipitation. They are (1) northwest Washington, (2) southwest Washington and northwest Oregon, and (3) southwest Oregon.

1. Northwest Washington Storms

2.04. Predominant features of the six storms that follow are summarized. The outstanding 1935 storm is then discussed in more detail.

Dec. 9-12, 1921	Feb. 8-10, 1951
Feb. 24-27, 1932	Nov. 2-4, 1955
Jan. 21-24, 1935	Dec. 9-10, 1956

Summary of storm features

2.05. Direction of movement of Lows. Lows tend to move northward along the coast or eastward across British Columbia or Washington. The eastward storm track is more frequent. Sometimes a secondary Low breaks off from an offshore northward-moving Low and moves inland. In some storms there is a shift from a northward to an eastward track during the storm sequence.

When Lows move northward offshore, southerly winds bring heaviest rain to south-facing coastal mountain areas; when Lows move eastward, moisture-bearing winds are predominantly SW to W and heavy rain favors the Cascades as well as the coastal mountains.

2.06. Latitude of entry of the Low centers approaching the coast tends to vary with their intensity and size. For example, in the 1932 storm, deep Lows entering the coast far to the north (about lat. 55°N.) permitted a

broad inflow of moisture from the Pacific far to the southwest. In the 1921 and 1956 storms, deep but smaller Low centers entered the coast at latitude 52°N., much nearer the rain area, after previous encroachment of filling Lows; they were accompanied by very strong inflow over Washington. In the 1955 storm, the eastward track of the fairly deep but filling Lows was near latitude 50°N. In the 1951 storm, small waves entered the coast as the main Lows remained offshore; their weak Low centers passed directly over the precipitation centers.

2.07. Blocking. In the record 1935 storm (fig. 2-1), deepening offshore waves did not break through the strong continental ridge of high pressure. To a lesser degree than in the 1935 storm, blocking by high pressure over the western part of the continent was evident in all but the 1932 storm. This blocking to north and south of Washington narrowed the corridor of entry of Lows in the 1956 and 1951 storms, thus in part accounting for the unusually strong north-south gradients as Lows penetrated the coast.

2.08. Gradient. Strong pressure gradients characterized the storms, though for a limited time during the 1921 storm. Whereas in other storms winds held to SW, there was a shift to NW at the end of the 1921, 1955, and 1956 storms as deep Lows were followed by pressure ridges.

2.09. Moisture. Because dew point data are sparse in older storms, mean storm temperature at Tatoosh Island, Wash. weather station was substituted to appraise storm moisture, assuming a near saturated atmosphere. Mean storm temperatures varied from 47° to 59°F. In comparison with normal temperatures it was 2°F. above normal in the 1955 storm, 5°F. in the 1935 storm, and 6-8°F. in other storms.

Description of the January 21-24, 1935 storm

2.10. Figure 2-2 shows isohyets in percent of mean annual for the first two days of the January 21-24, 1935 storm. Precipitation surpasses all precipitation records in the Olympics, both for the particularly intense rain of the 21st and 22d and for four days total precipitation. For example, the 23.5 inches in two days and 35.0 inches in four days at Quinault on the south slopes of the Olympics are 40-yr. records, by a wide margin. In the northern Cascades precipitation was relatively light though comparable to that in other large storms. To the lee of these mountains precipitation was extremely heavy. For example, the 24-hr. value of 4.16 inches (52 in. of snow) on the 21st at Winthrop, Wash. (elev. 1765 ft.), is by far a 60-yr. record. It indicates both the extreme intensity of the storm and that in this lee area downslope motion of the warmer inflowing air was prevented by the presence of very cold air below, trapped there following a previous severe outbreak of polar air. Highest temperature at Winthrop, 24°F. on the 21st and 22d, is evidence of this trapped air.

Flooding was serious on streams flowing into Puget Sound and those on the windward side of the Olympics. Less severe flooding occurred to the lee of the northern Cascades as snowfall early in the storm was later melted.

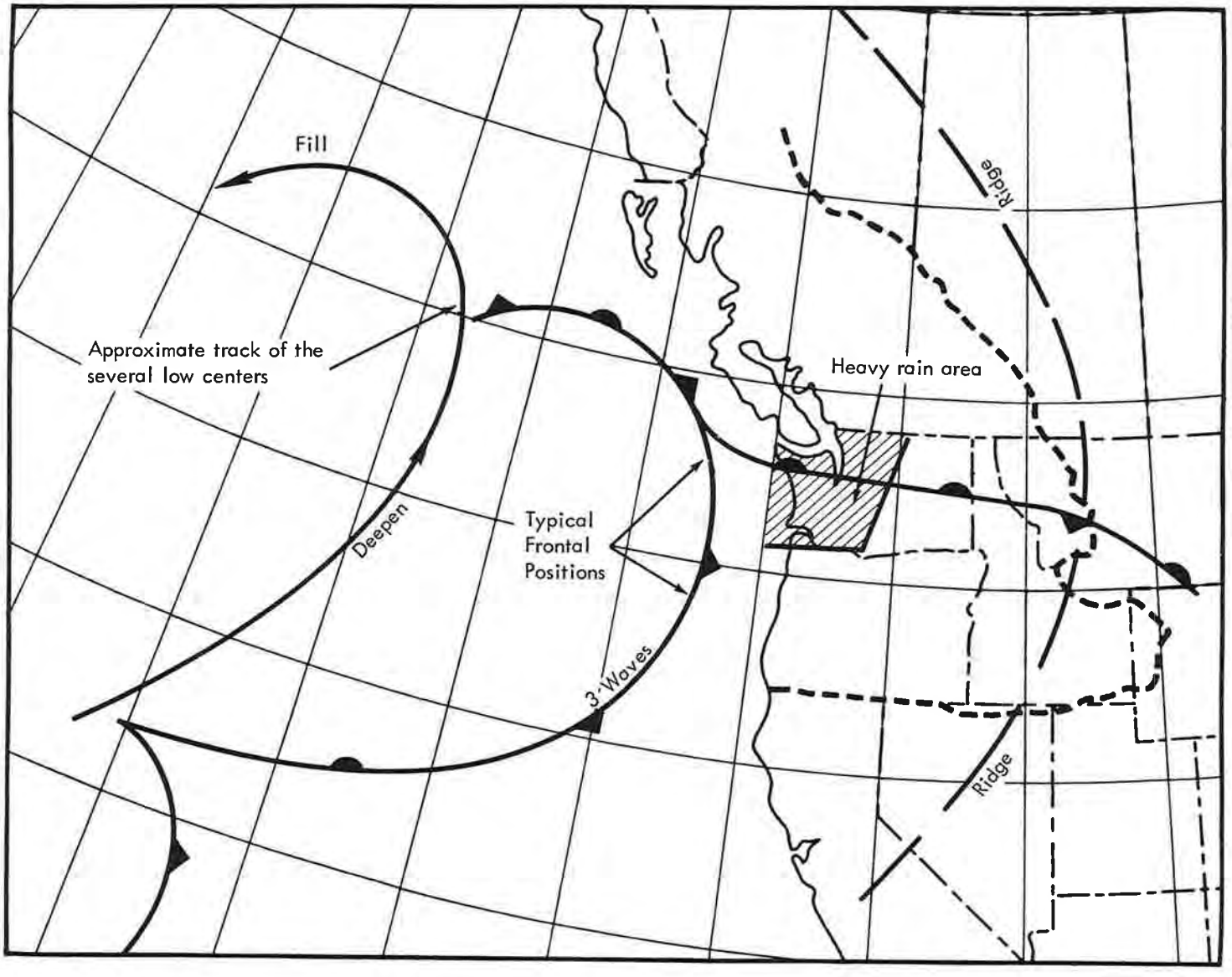

Figure 2-1. Track of Lows in the January 21-24, 1935 storm

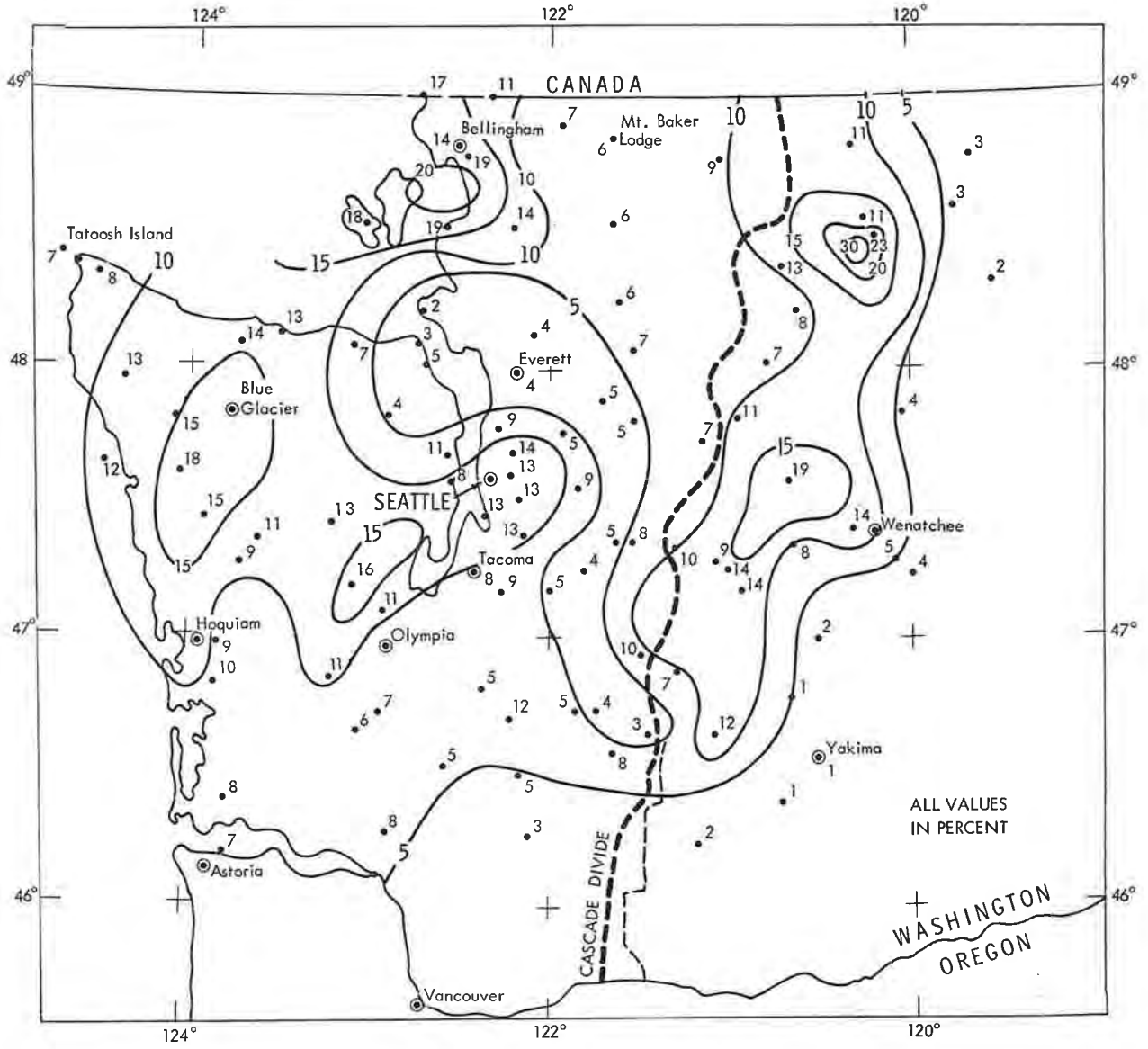

Figure 2-2. Two-day precipitation in the January 21-22, 1935 western Washington storm - in percent of mean annual

2.11. A synoptic review indicates that other factors in addition to high moisture accounted for the extremely heavy rain of the 21st and 22d. The main feature was the repeated approach and blocking of occluding waves at the Washington coast, shown schematically in figure 2-1. These waves developed and moved to the north-northeast in the southerly flow between a deep stationary offshore trough and a strong ridge extending from off the southern California coast northeastward into Idaho and northward into Canada. Failure of the Lows to break down this blocking ridge prevented veering of the flow.

2. Southwest Washington and Northwest Oregon Storms

2.12. Seven large storms since 1900 in southwest Washington and northwest Oregon are:

Nov. 12-14, 1906	Dec. 17-22, 1933
Dec. 17-19, 1917	Dec. 26-28, 1937
Nov. 19-21, 1921	Dec. 14-16, 1939
	Dec. 26-27, 1945

Summary of storm features

2.13. Direction of movement of Lows varied from northerly in the 1917 and 1939 storms to easterly in the 1933 storm. Within storms there was sometimes a shift; in the 1937 storm, it was from easterly to northerly, with the reverse in the 1906 storm.

2.14. Latitude of entry of Low centers at the coast varied from the southeast Alaskan coast for broad, deep, occluded Lows to the latitude of the precipitation area itself in the case of the November 1921 storm when there were flat waves along the polar front between marked continental Highs. This represents variation from no blocking to almost complete blocking of Lows at the coast by an upper-level ridge of high pressure.

2.15. Pressure gradients were high at times in most storms, particularly with those involving repeated entry of deep Lows close to the rain area.

2.16. Moisture. Mean storm temperature at Tatoosh Island was as little as 2°F. above normal in the 1921 storm when no deep Lows reached the coast and 9° to 10°F. above normal in the 1917, 1933, and 1939 storms. The latter storms involved deep Lows with considerable transport of air from southerly latitudes.

2.17. Rain intensity. Three-day rains varied from about 10 to 15 percent of normal annual at the rain centers. Highest percents occurred in the 1921 and 1937 storms. The 1933 storm was unusual for its prolonged heavy rain. The 1939, 1921, and 1937 storm isohyets covered a broad latitudinal width.

November 19-21, 1921 storm

2.18. This storm was the most intense of the group. It featured an east-west trough through the rain area, between ridges of high pressure to north and south. The storm sequence is shown on daily maps in figure 2-3a and schematically in figure 2-3b. Flat waves approached the coast along the frontal boundary in this trough and filled as they moved inland on the 19th and 20th, leaving a deep Low farther offshore. By the 21st this Low was moving eastward, entering the southern British Columbia coast on the 22d. Most of the rain fell on the 19-20th before approach of the Low center and while a sharp shear was present across the frontal zone. Heavy rain at low elevations (Albany, Oreg. had 5.2 in. in 24 hrs.) attests to the large component of convergence rain in storm totals. Rain was especially heavy in the Cascades near the Columbia River, averaging 15 percent of the normal annual; along the coast it averaged 10 to 13 percent from Port Orford in southwest Oregon to Astoria.

The fact that storm temperatures were only slightly above normal indicates less moisture than in most storms reviewed.

3. Southwest Oregon Storms

2.19. Seven of the larger storms in southwest Oregon are:

Nov. 21-23, 1909	Oct. 26-29, 1950
Jan. 17-19, 1911	Dec. 19-21, 1955
June 6-8, 1933	Dec. 25-27, 1955
Dec. 29-31, 1942	

Storm summary

2.20. A variety of storm patterns contributed to these rain periods, ranging from westerly flow with eastward-moving deep Lows (as in the 1909 storm) to south-southwest flow from offshore Lows (as in the 1911 and 1955 storms), and combinations of these contrasting sequences in other storms. Most storms were characterized by strong winds and much above normal temperatures. As with previous storms reviewed, these storms involved several developments in close succession to cause almost continuous rain.

The November 21-23, 1909 storm

2.21. This storm was particularly intense during a two-day period. Three-day amounts were 12 percent or more of normal annual over the southern two-thirds of western Oregon (fig. 2-4 inset).

Prior to entry onshore of two deep Lows shown in figure 2-4, similar Lows entered and moved eastward along the Canadian border on the 18th and

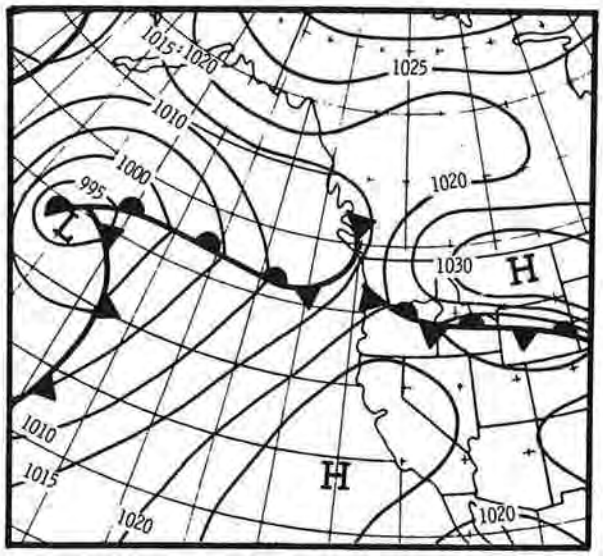

Nov. 19, 1921

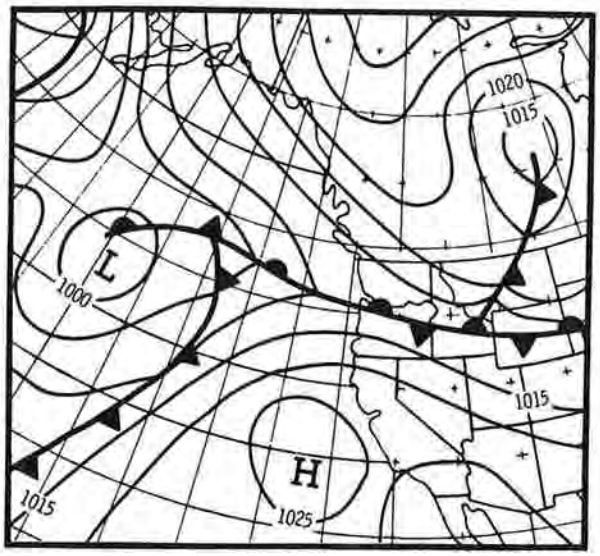

Nov. 20, 1921

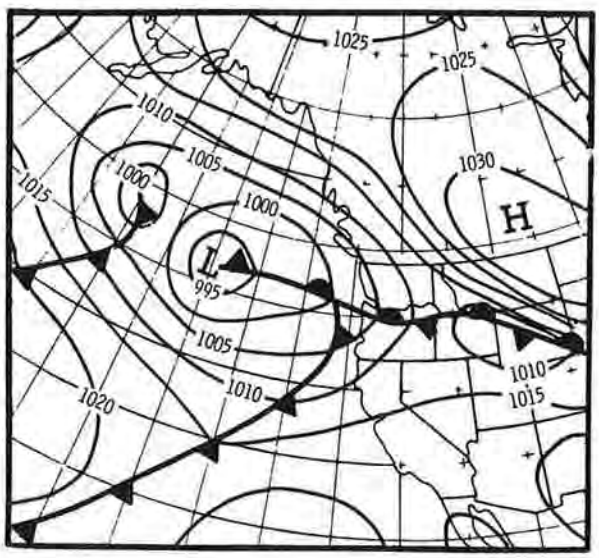

Nov. 21. 1921

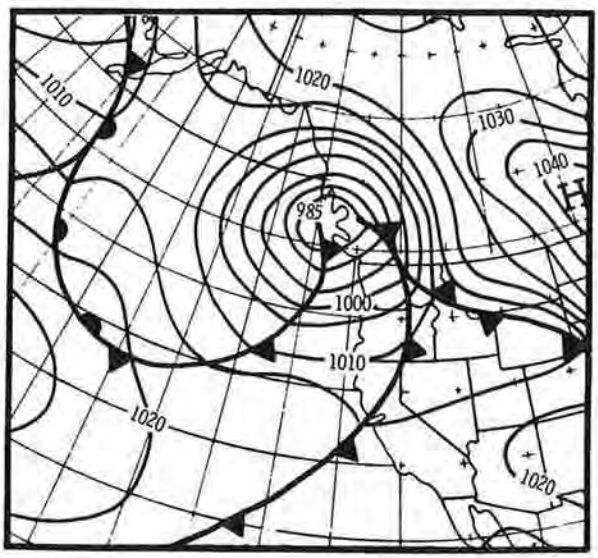

Nov. 22, 1921

Figure 2-3a. Daily surface maps November 19-22, 1921 (0500 PST)

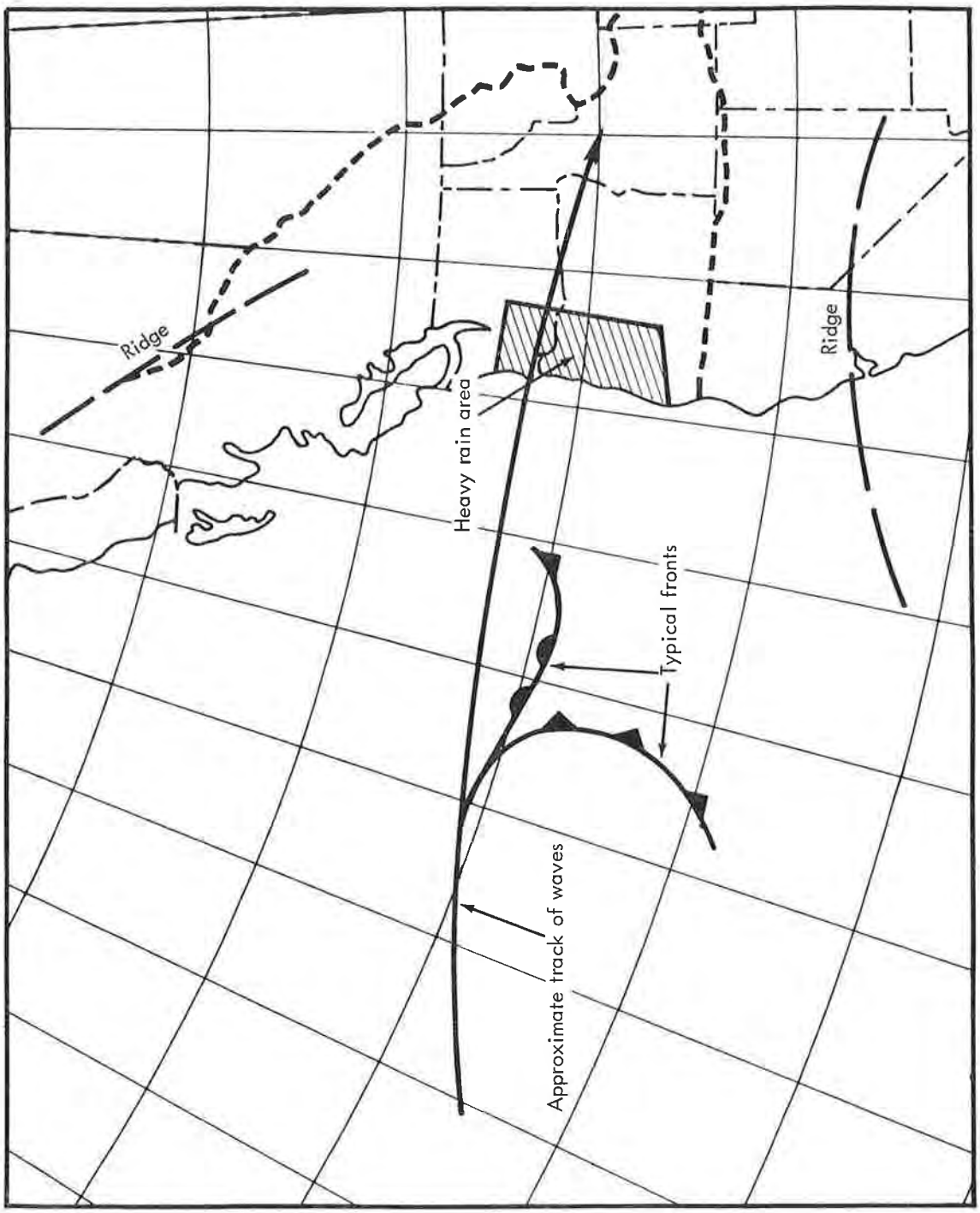

Figure 2-3b. Track of waves in the November 19-21, 1921 storm

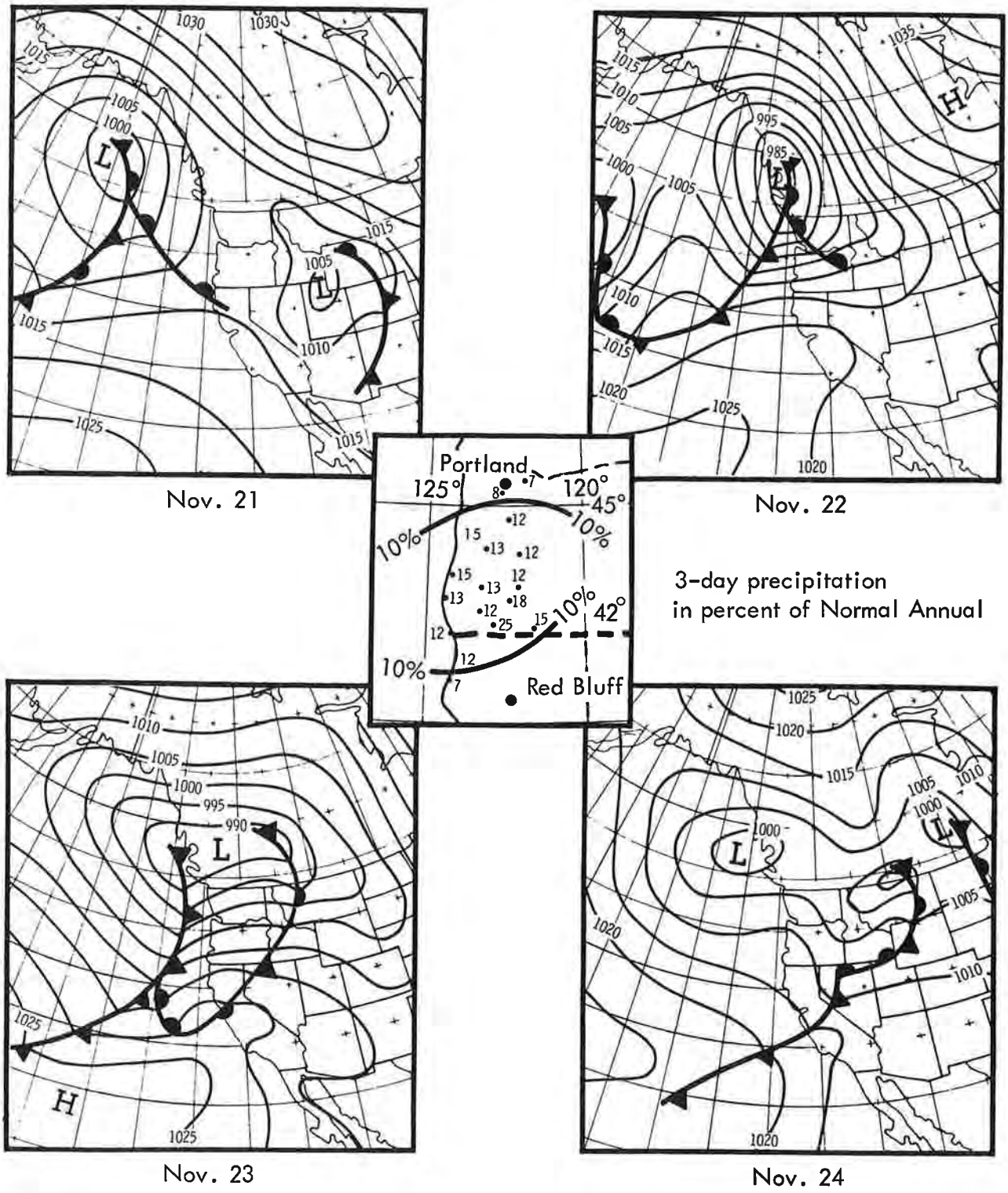

Figure 2-4. Surface maps for November 21-24, 1909 (0500 PST)

evening of the 19th with heaviest rain for this period farther north than in the figure 2-4 inset. By the 21st the first Low of figure 2-4 was deepening and occluding close to the coast before entering southern British Columbia; extreme pressure gradients spread over the Pacific Northwest. On the 22d the second Low, also from the west gained on the first and further deepened, resulting in a single elongated east-west Low center on the 23d. There was no lull in winds or rain between Lows. Possible reasons for the rain center being so far south of the Low tracks are that greater moisture and greater cyclonicity* existed in the occluding portion of the Lows at that latitude. The 3-day mean temperature of 59°F. at Eureka was 5°F. above normal.

2-B. STORMS IN THE CENTRAL INTERIOR COLUMBIA BASIN

2.22. Storms in the central Columbia Basin east of the Cascades were selected on the basis of magnitude and areal coverage of 3-day precipitation expressed as percent of mean annual precipitation. Maps of percents of mean annual precipitation are shown in figures 2-5 and 2-6 for eight large storms here grouped according to place of occurrence.

Group 1	Group 2	Group 3
N Idaho and NE Washington	SE Washington and NE Oregon	SW Idaho
July 2-4, 1902	May 28-30, 1906	Nov. 21-23, 1909
Nov. 17-19, 1946	Mar. 30-Apr. 1, 1931	Nov. 19-21, 1921
		Feb. 19-21, 1927
		Jan. 20-22, 1943

2.23. Two features of these storms are: (1) Location of precipitation centers depends largely on orography in that they are on slopes of fairly steep mountain ranges facing south through west to northwest. (2) The season extends to early summer.

While the above storm grouping is based on location, there is some seasonal grouping also. The two spring storms (Mar.-Apr. 1931 and May 1906) were centered over the northwest-facing slopes of the northern Blue and Wallowa Mountains in extreme southeast Washington and northeast Oregon (fig. 2-5). Four occurring in the months November to February were centered in southwest Idaho on the south- and west-facing slopes north of the Snake River (fig. 2-6).

Two of the storms listed above were of major importance west of the Cascades: the 1909 storm in southwest Oregon (par. 2.21) and the 1921 storm in northwest Oregon and southwest Washington (par. 2.18). The 1943 storm is recognized as a major one in California.

Descriptions of a storm from each of the three groups follow.

---

*A term indicating strength of convergence mechanisms involving shear and/or curvature, or changes thereof.

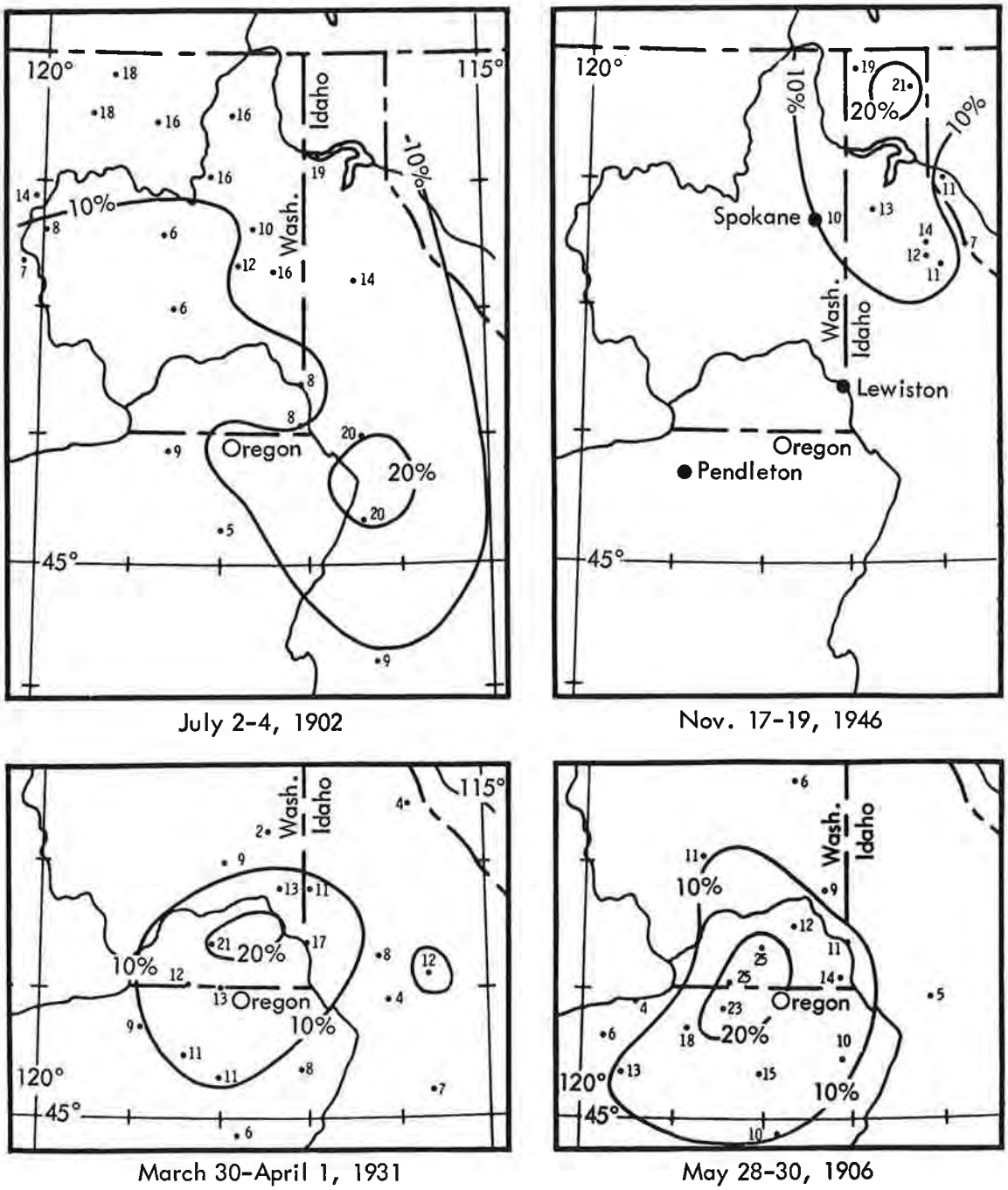

Figure 2-5. Three-day precipitation as percent of mean annual in four storms near the Oregon-Washington-Idaho border

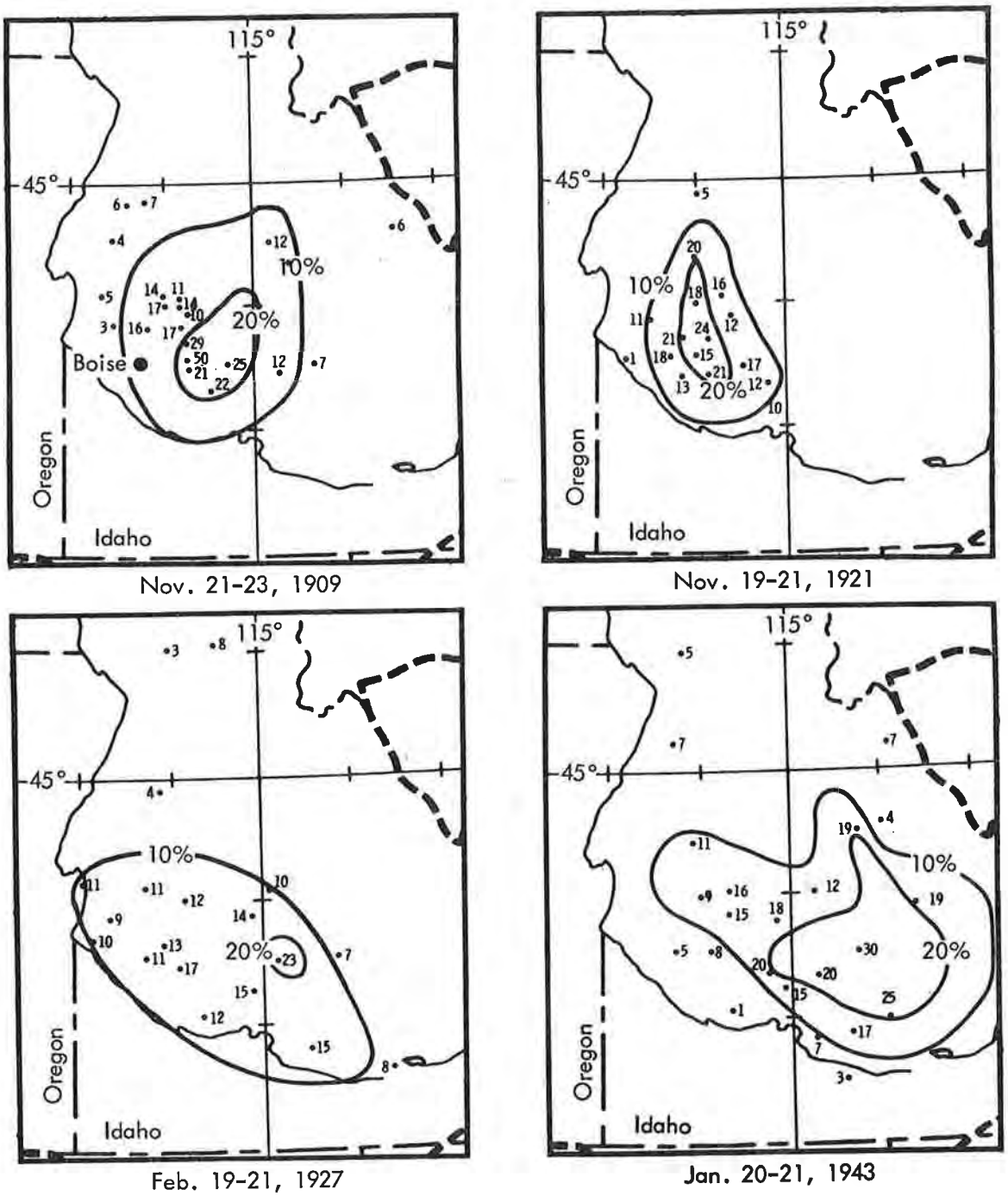

Figure 2-6. Three-day precipitation as percent of mean annual in four southwest Idaho storms

1. Northern Idaho-northeast Washington storm of July 2-4, 1902

2.24. Typical of late spring season storms, Lows in this period approached from the northwest, north of a strong Pacific High. The first Low and associated cold front had moved southeastward across the Pacific Northwest by the 1st; around this front a large area of low pressure had developed by the 2d (fig. 2-7), extending from southern Canada into Utah. It persisted in the north into the 3d, by which time a second Low was reaching the area from the northern Gulf of Alaska, causing renewed deepening through the 4th, centered along the Canadian border. A third weakening Low entered in a similar manner by the 5th, followed by a ridge of high pressure.

Winds were variable during this sequence, including periods of southwest flow favoring rain in northeast Washington and northern Idaho and periods with NW winds favoring rain in the mountains of central Idaho. Convergence in the vicinity of the Low center is evident in the large percentage amounts of rain in figure 2-5 at fairly low-elevation stations subject to little orographic effect. The northerly source of the air and the warm ground at that time of year suggest some instability, though this is not validated by thunderstorms or random large rainfall amounts. The 3-day mean temperature at Spokane was 50°F., or 15°F. below normal.

2. Southeast Washington-northeast Oregon storm of May 28-30, 1906

2.25. A prevailing northwest flow to the rear of a slow-moving Low center was the important feature of this storm (fig. 2-8). Typical of spring storms, the Low entered from west-northwest and deepened over the Northern Plateau as moisture and heat were added to lower levels. The location of heaviest rain was determined by prolonged NW winds being lifted up northwest-facing slopes of the three-state intersection on the 28th and 29th. Rain was especially heavy downwind from Walla Walla where a northwest flow is forced to rise abruptly; 3-day amounts there were as much as 25 percent of normal annual precipitation (fig. 2-5). The few observed thunderstorms occurred outside of the 10 percent line of this figure. The 3-day mean temperature at Walla Walla of 49°F. was 13°F. below normal, indicative of influx of cold maritime air from a higher latitude.

3. Southwest Idaho storm of November 22-23, 1909

2.26. This storm resulted in heavy precipitation both in southwest Idaho and in southwest Oregon (par. 2.21). The 7.17 inches in 18 hours and 10.72 inches in two days at Rattlesnake Creek, about 25 miles east of Boise, are records. The 2-day value is 50 percent of normal annual precipitation, figure 2-6. The terrain around Rattlesnake Creek favors upslope flow for WSW winds. The orographic and general convergence rain was augmented by a thunderstorm on the 23d at Rattlesnake Creek.

The synoptic description of the storm is given in paragraph 2.21. Figure 2-4 shows 0500 PST synoptic maps. Rain began in Idaho on the afternoon

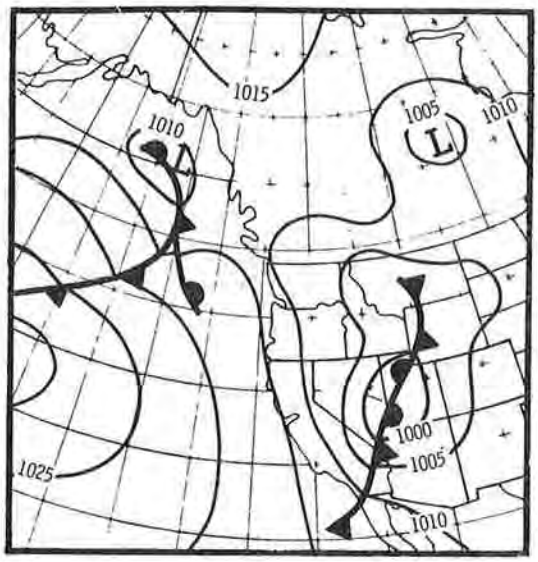

July 2

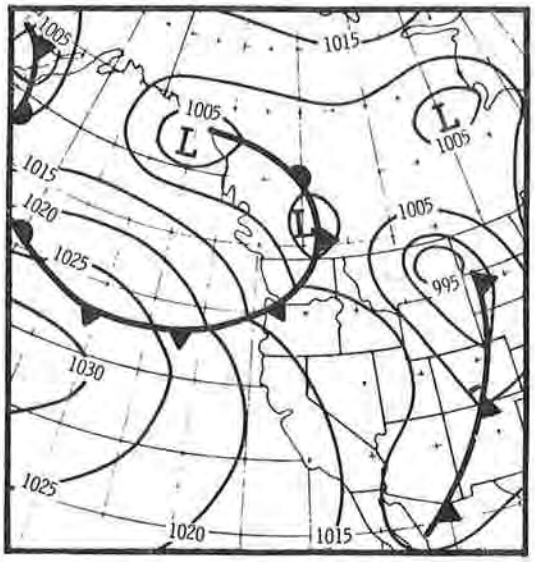

July 3

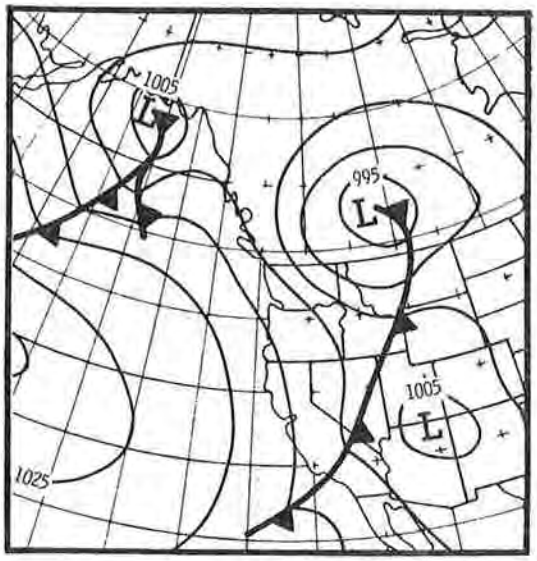

July 4

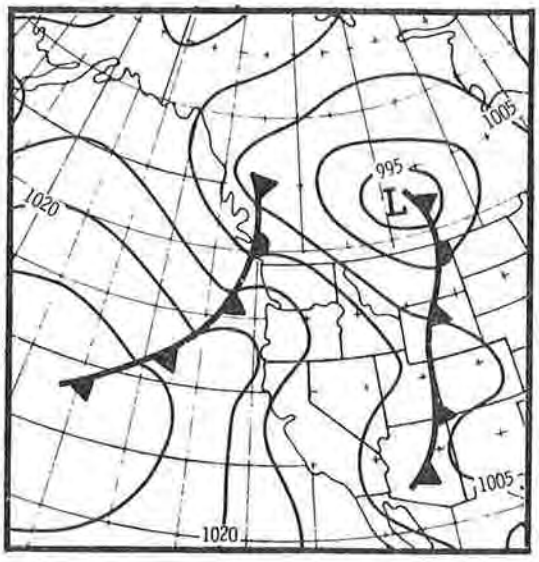

July 5

Figure 2-7. Surface maps for July 2-5, 1902 (0500 PST)

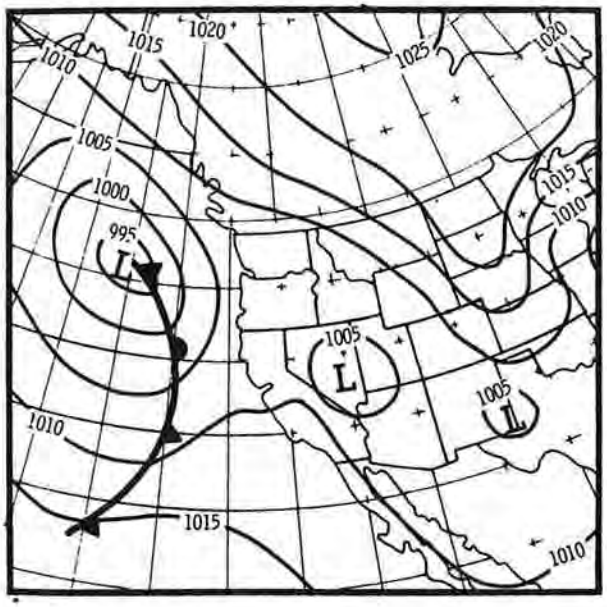

May 27

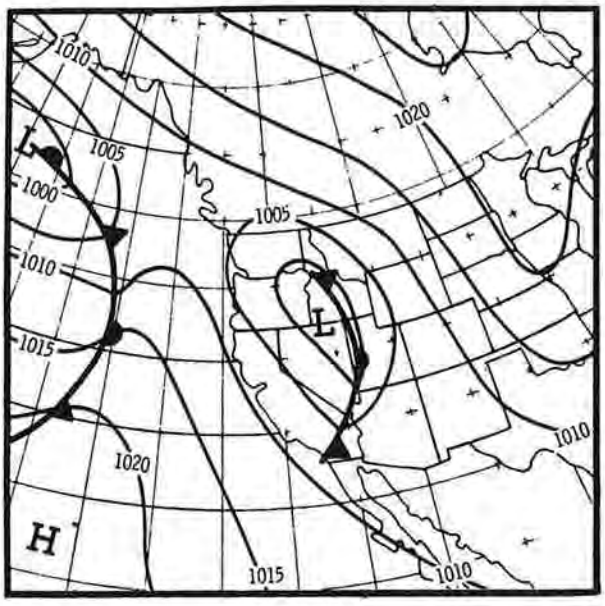

May 28

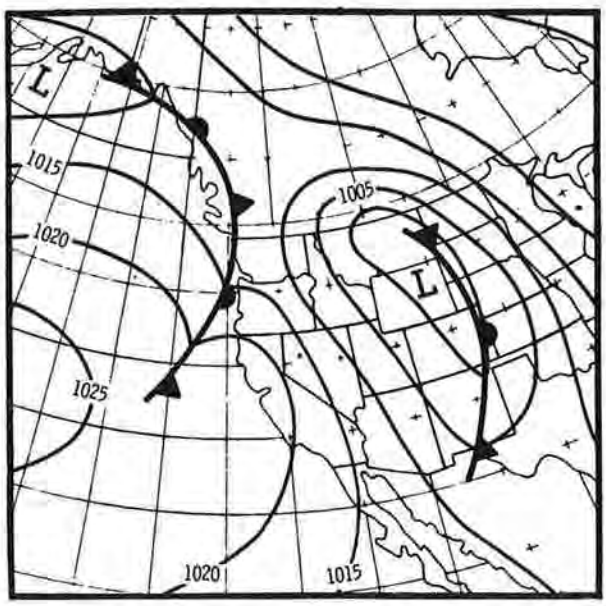

May 29

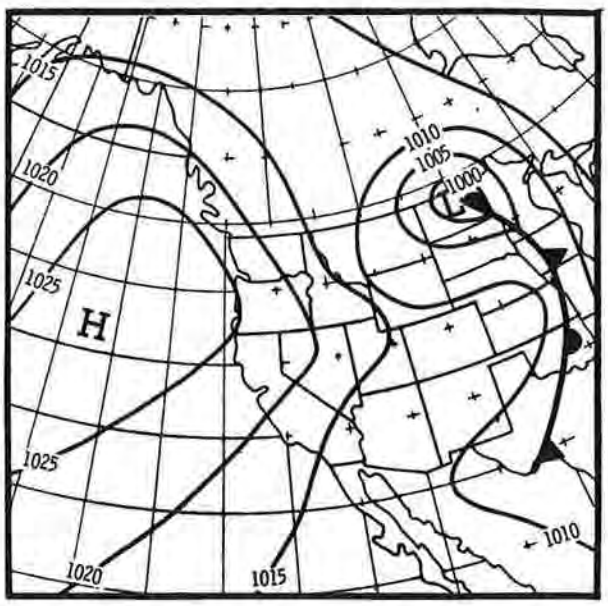

May 30

Figure 2-8. Surface maps for May 27-30, 1906 (0500 PST)

of the 22d with the approach of the first deepening Low. Speedup of the second Low on the 23d brought its passage close behind the first so that, except for a brief lull on the night of the 22d, strong westerly winds and heavy rain continued through the 23d. With nearly west-to-east flow, it is logical that greatest moisture influx and heaviest rain occurred at about the same latitude in Idaho as near the coast. (The 19th-20th also brought heavy rain to southwest Idaho with over 3 in. in 24 hr. at Rattlesnake Creek.)

Southern Idaho - southeast Oregon storm of July 23-26, 1913

2.27. This storm does not fit in the three groups of paragraph 2.22 from the standpoints of location, moisture source (from southeast), and orographic influence. The large area covered by this storm and the large precipitation totals at some locations are evident in figure 2-9, where data are percent of mean annual precipitation.

Storm rainfall was primarily convergence rain, with highest percents favoring normally dry areas (Caldwell 35%), although highest amounts fell on south-facing slopes northeast of Caldwell and Idaho Falls (5.8 in. in 4 days). This predominance of convergence rain follows from the light pressure gradients in the storm area shown by daily maps in figure 2-10.

2.28. The two main factors contributing to high storm totals were high moisture inflow from southeast in the early part of the storm and slow movements of frontal systems. However, the irregular pattern of the percent lines of figure 2-9 and the rather high maximum temperatures indicate that instability contributed to daytime amounts. An example of such contribution is a report of a severe thunderstorm at Morgan, Utah on the 23d, occurring on the eastern edge of the storm area.

The high moisture value in the storm is appraised by 1000-mb. dew point estimates (from 0600M temperatures during rain) averaging 70°F. Its source was obviously the Gulf of Mexico, since from the 18th to the 24th there were the offshore and midcontinent Highs with an intervening northwest-southeast trough through Arizona, Nevada and eastern Oregon, a pattern typical of Gulf air inflow to the Northern Plateau. In this trough rain was reported for several days prior to the storm from El Paso to Reno.

The slow movement of the frontal system is seen in the 0500 PST maps (fig. 2-10) from central Oregon on the 23d to central Wyoming on the 25th. Showers continued under the lagging upper trough on the 26th.

2-C. STORMS NEAR THE CONTINENTAL DIVIDE

2.29. Heaviest precipitation near the Continental Divide falls largely as orographic rain on the eastern slope during warm-season months. High moisture during the warm season reaches these slopes directly from the Gulf

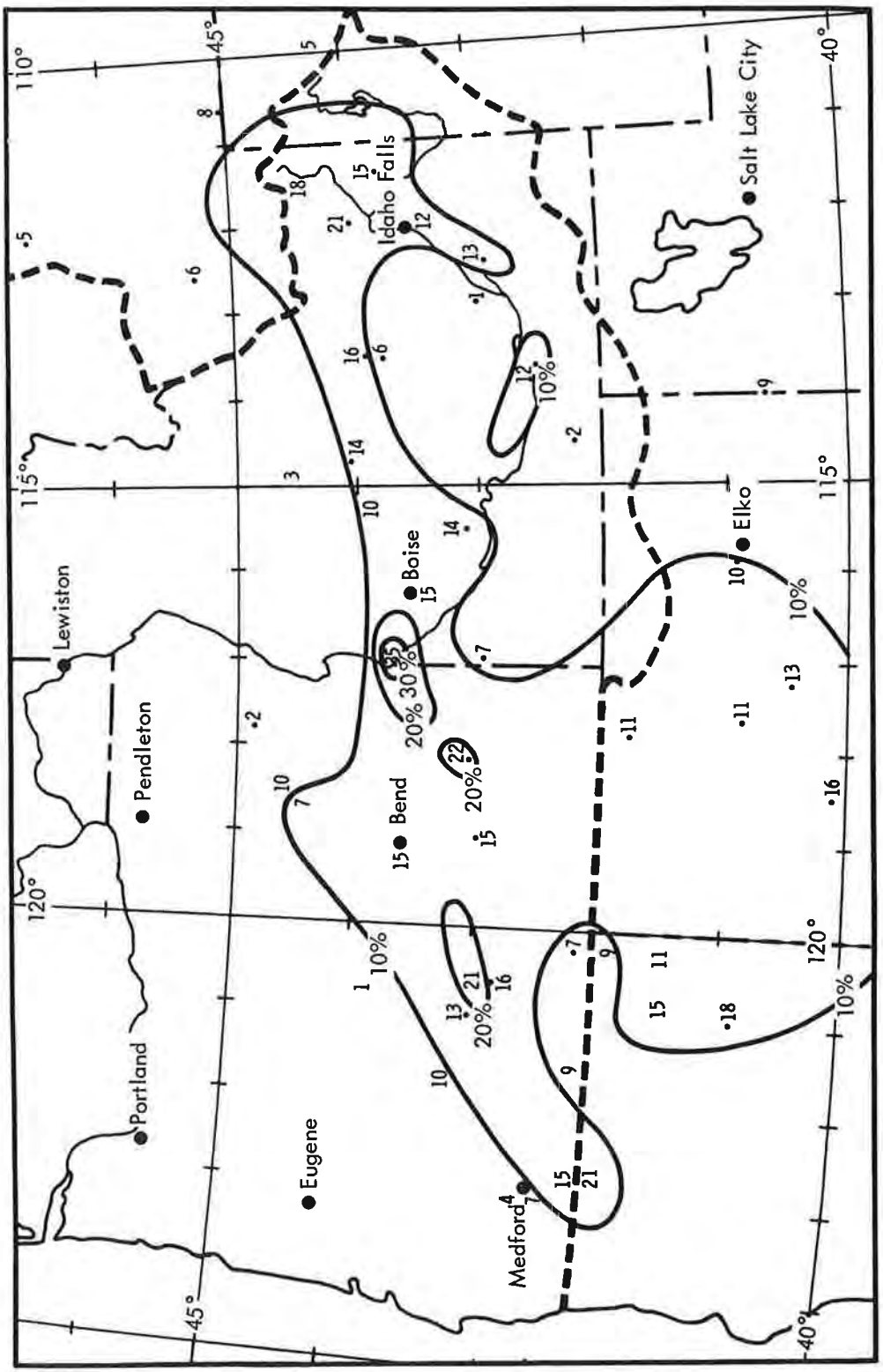

Figure 2-9. Isohyets of percent of mean annual precipitation in the July 23-26, 1913 storm

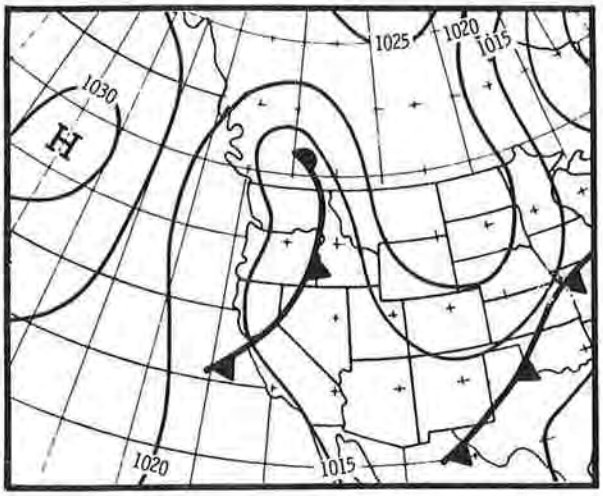

July 23

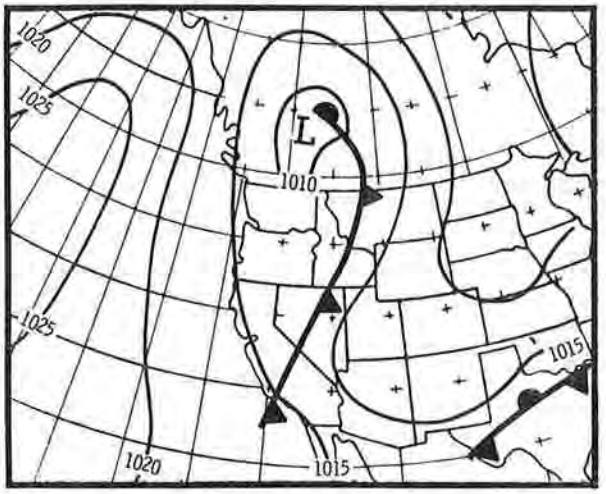

July 24

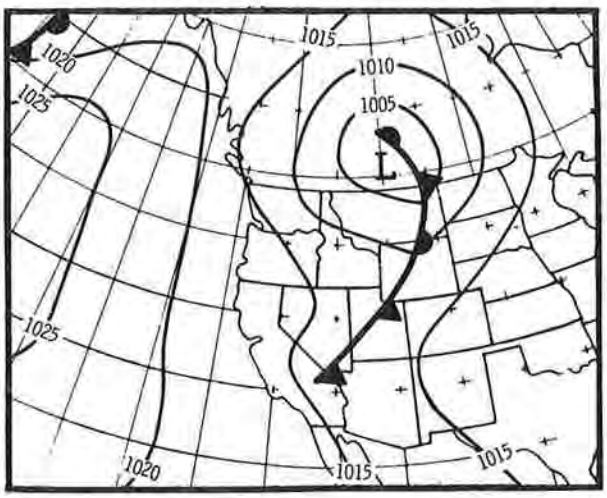

July 25

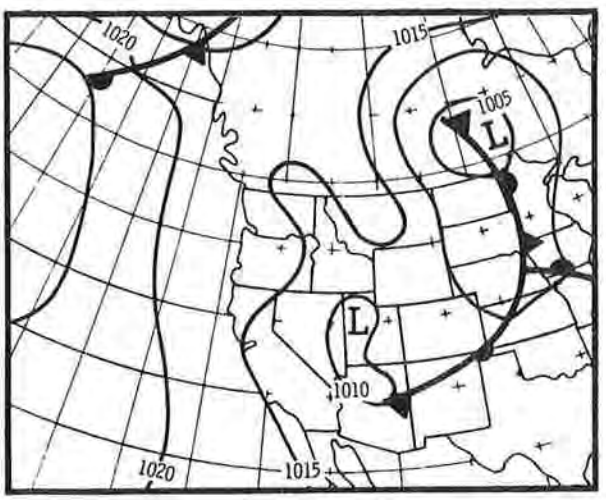

July 26

Figure 2-10. Surface maps for July 23-26, 1913 (0500 PST)

of Mexico without upwind barrier depletion. This requires that a deep Low persists in the northern Great Basin and central Rockies to maintain an easterly upslope flow favorable for maximum lift along the divide in Montana.

The June 7-8, 1964 Montana storm

2.30. An outstanding example is the June 7-8, 1964 storm of about 30 hours duration where amounts up to 14 inches were measured on slopes facing east-northeast (fig. 2-11). A strong southerly flow developed on the 6th (fig. 2-12) extending from the Gulf of Mexico to the Northern Plains. This flow was maintained on the 7th by a deepening Plateau Low which moved from the coast through southern Idaho on the 7th and into Nebraska on the 8th. Because of the northward transport of Gulf air, the 1000-mb. dew point was about 62°F. over central Montana through most of the rain period. During the storm period the Low passed eastward, south of the rain center.

A large convergence component of rain over the area is evident from the high percents of mean annual over fairly flat areas and foothills of central Montana (dashed lines on fig. 2-11). But on the east slope of the divide, the major rain component was orographic. There E and NE winds persisted to high levels around the deep Low to the south and carried moisture up these slopes. A secondary Low trailing the main Low center prolonged the storm by maintaining easterly winds aloft on the 8th. The extremely high percents of mean annual on slopes indicate both the extreme rarity and unusual intensity of this storm.

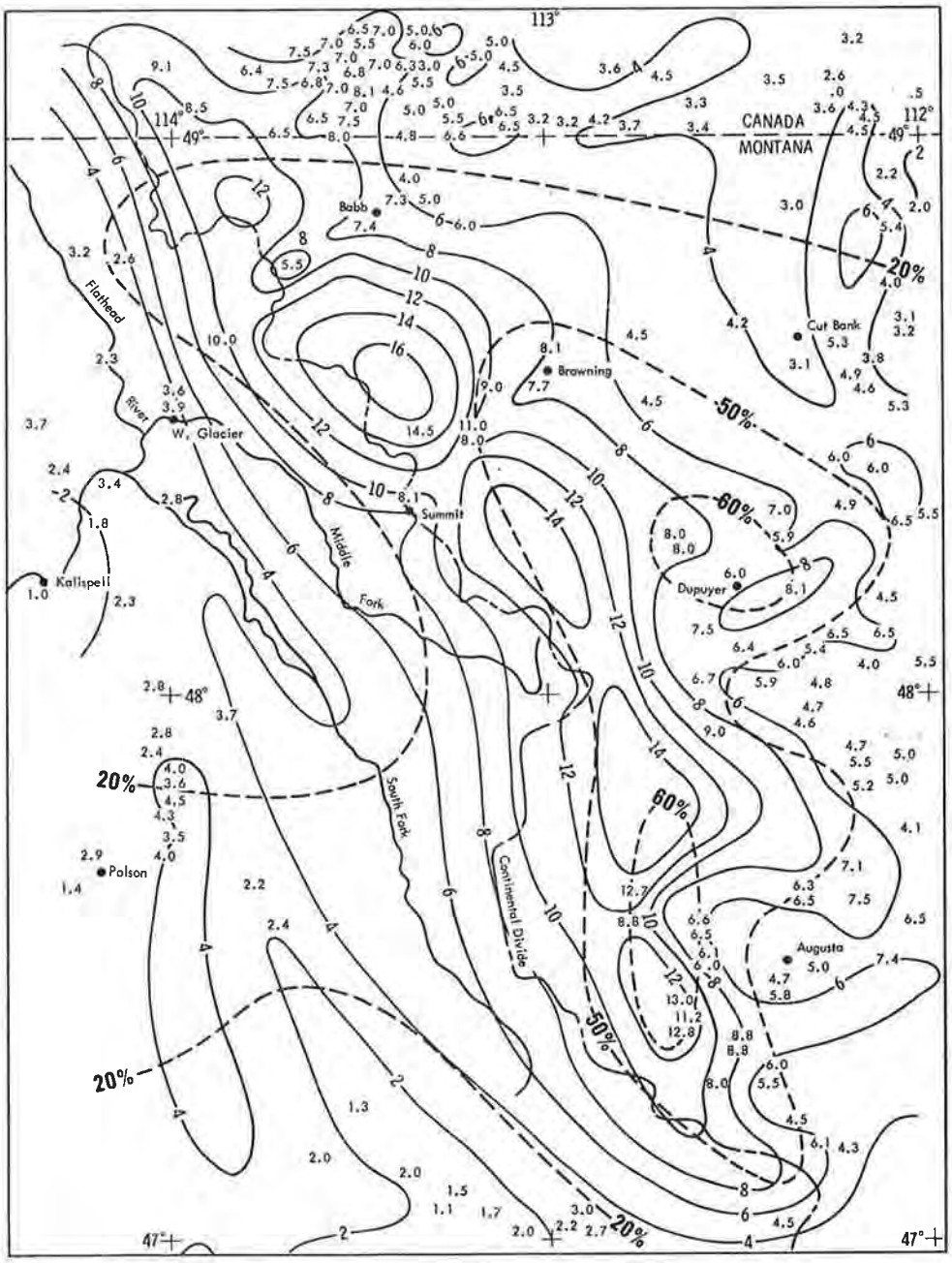

Figure 2-11. Isohyets (in.) in the June 7-8, 1964 Montana storm (Dashed lines are percents of mean annual precipitation)

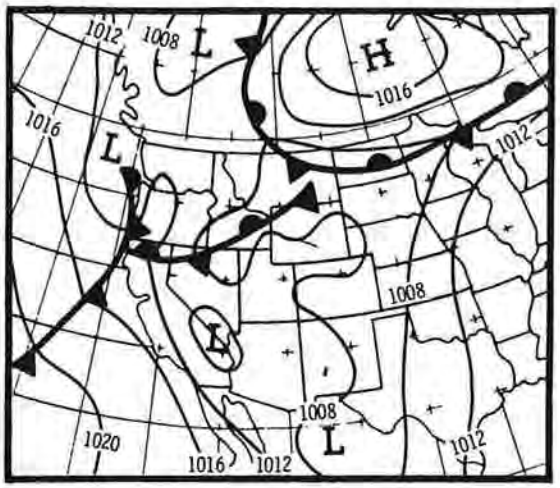

June 6

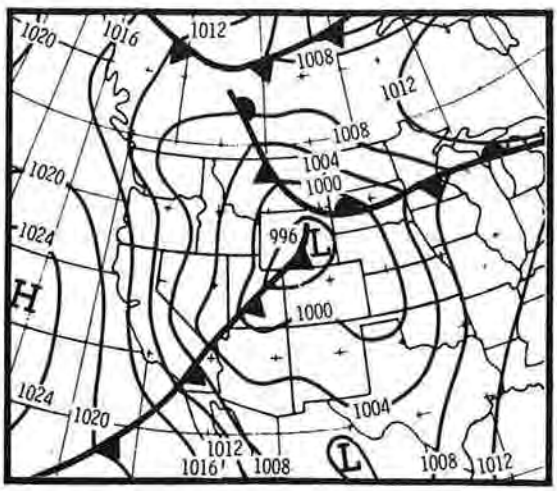

June 7

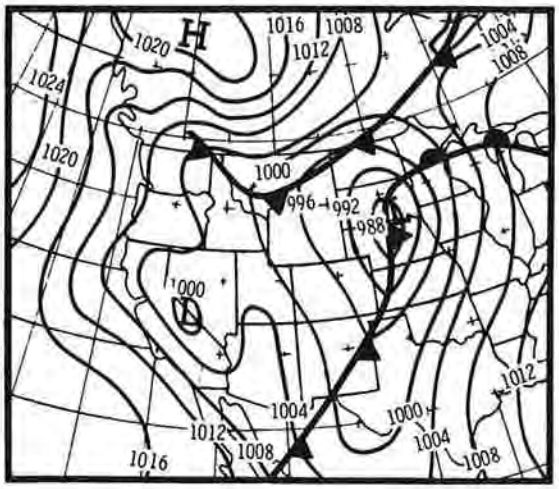

June 8

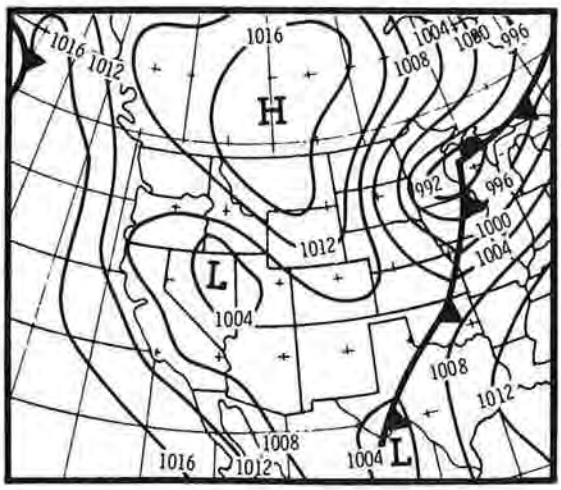

June 9

Figure 2-12. Surface maps for June 6-9, 1964 (1100 MST)

Chapter III

PROBABLE MAXIMUM CONVERGENCE PRECIPITATION

3-A. INTRODUCTION

3.01. Precipitation in flat areas, as well as a portion of that in mountain areas, results from vertical motions associated with convergence processes in the atmosphere. The general storm is a source of broad-scale vertical motions and precipitation, regardless of terrain. In the Northwest, these storms approach from the Pacific Ocean. Within these storms, lines or areas of precipitation exist, often in connection with frontal zones. On a smaller scale, instability release of local showers or thunderstorms is an integral part of many storms. In addition to precipitation from orographic lifting, mountain areas receive and sometimes amplify the precipitation from the general storm. The latter precipitation in its various forms is referred to as convergence precipitation, to distinguish it from that which results from orographic lifting on slopes.

Procedure in maximizing convergence rain

3.02. In this chapter two categories of generalized estimates of convergence PMP are developed. These are:

(1) Estimates for level areas where there is little or no orographic control.

(2) Estimates for mountains, to be combined with estimates of orographic PMP.

The first step in the procedure is to develop maps of January 1000-mb. convergence PMP for 24 hours and 10 square miles, the product of two indices. The first index is enveloping 1000-mb. moisture, M, defined as precipitable water in a column for a given 1000-mb. dew point. The other is enveloping 24-hr. 1000-mb. precipitation/moisture (called P/M) ratios, developed for each of the two categories of convergence PMP. P/M ratios are an index to the highest efficiency of storm processes (exclusive of orographic effects) which convert water vapor to precipitation as explained in paragraph 4.02 of HMR 36 (1). These ratios are determined from record point rainfalls at low elevations in least-orographic areas.

The seasonal, durational and basin-size variation from the 24-hr. 10-sq. mi. 1000-mb. January convergence PMP index maps also are derived from extreme rains in least-orographic areas. Variation with terrain is based largely on empirical rain relations and deductions from study of meteorology of Northwest storms.

A schematic of the procedures, discussed in detail in this chapter, is shown in table 3-1.

Table 3-1

SCHEMATIC OF PROCEDURE FOR DETERMINING CONVERGENCE PMP IN THE NORTHWEST

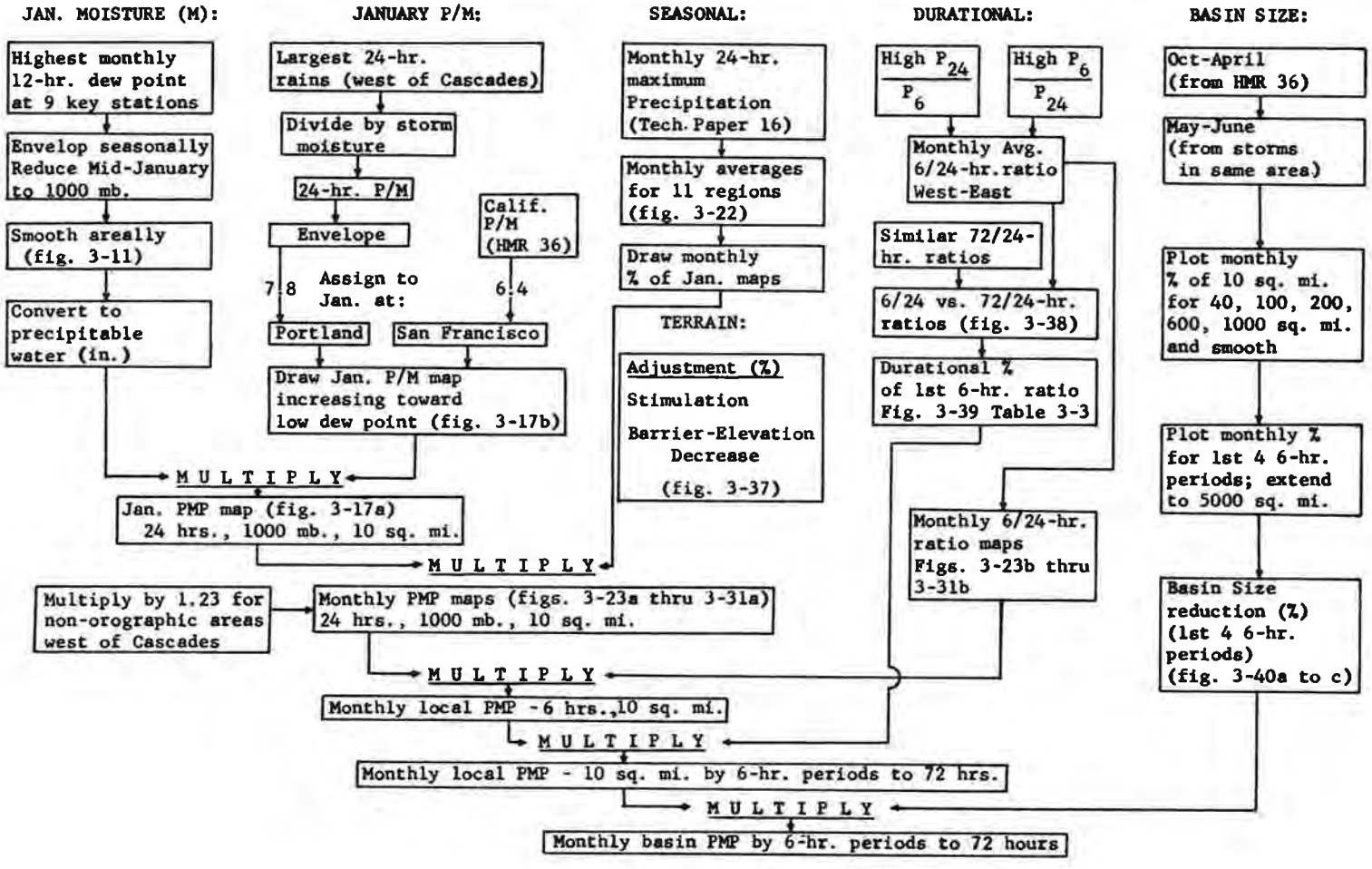

3-B. ENVELOPING DEW POINTS

Summary of procedure

3.03. Representative high 12-hr. persisting dew points at selected stations were used to determine station seasonal envelopes of maximum moisture. These station envelopes were adjusted after areal smoothing of values for each month.

Basic dew point data

3.04. Data sources listed in table 3-2 provide highest persisting 12-hr. dew points. These sources of dew point data are five stations since 1905, Weather Bureau Technical Paper No. 5 (4) updated through December 1961, and four stations surveyed through 1956 in HMR 36.

Table 3-2

STATIONS AND PERTINENT DATA IN NORTHWEST STATES DEW POINT ANALYSIS

Station	Elevation (ft.)	Period of Record	Length of Record (yr.)
Boise, Idaho	2770	1905-1961	57
Kalispell, Mont.	2983	1905-1956	52
Pocatello, Idaho	4503	1905-1956	52
Portland, Oreg.	58	1905-1961	57
Roseburg, Oreg.	510	1905-1956	52
Seattle, Wash.	205	1905-1961	57
Spokane, Wash.	1953	1905-1961	57
Walla Walla, Wash.	976	1905-1939	
		1946-1956	46
Tatoosh Island, Wash.	119	1905-1961	57

Dew points as moisture indices

3.05. Highest 12-hr. persisting surface dew points are satisfactory for determining maximum storm moisture only if they are representative of moisture through depth in the atmosphere. A meteorological analysis is necessary to eliminate, or to rate as to their reliability, those surface dew points which do not adequately estimate moisture in depth during storm conditions. Local influences may make a value unrepresentative. An example is a high dew point, 64° on October 26, 1926, at Roseburg, Oreg., occurring with high pressure to north and with nearest rain in British Columbia. It resulted from residual moisture at low levels from a previous storm. An example of a very high dew point which was considered representative is the 62°F at Seattle in the record storm of October 19, 1940.

Seasonal enveloping 12-hr. persisting station dew point curves

3.06. For each of the nine stations in table 3-2, high 12-hr. dew point values were plotted against date of occurrence in figures 3-1 to 3-9. Those with a degree of unrepresentativeness were marked as being invalid for maximizing purposes. An enveloping seasonal curve of station dew points (not shown) was drawn to these data with over-envelopment in some months to accommodate representative data in nearby months.

Checks on seasonal station dew point envelopes

3.07. The records of the stations shown in table 3-2 were surveyed for the annual series of highest dew points for each month; in spring and fall when the seasonal curves change rapidly, half-month periods were used. These annual maxima for each monthly or half-monthly period were ranked and plotted on normal probability paper, as shown in the example of figure 3-10. Straight lines were fitted to the data by eye from which the 100-yr. return period dew points were read. These 100-yr. values are compared for the nine stations in figures 3-1 to 3-9 with observed 12-hr. dew points on which each seasonal enveloping curve is based and with the midmonth values read from the areally-smoothed 1000-mb. dew point lines of figures 3-11 to 3-13, developed below.

Midmonth 12-hr. persisting 1000-mb. dew point charts

3.08. Midmonth values were read from these nine seasonally-smoothed station envelopes and, after reduction pseudoadiabatically to 1000 mb., plotted by months on maps. Figures 3-11 to 3-13 show the areally smoothed lines drawn to these values. In drawing these lines, both the seasonal nearness of midmonth values to controlling points and the meteorological relevancy (par. 3.05) of those values to storms were considered in the areal smoothing.

Highest persisting dew points as indices of maximum moisture

3.09. Highest persisting 12-hr. dew point values are regarded as indices of maximum moisture appropriate to combine with other parameters of PMP; hence they are referred to as maximum 12-hr. dew points.

Durational variation

3.10. The durational variation of the maximum storm moisture indices are based on observed highest dew points at 12 Northwest stations persisting to 72 hours as listed in Weather Bureau Technical Paper No. 5 (4). The decay rate from 12 to 72 hours was developed from these data in the manner explained in paragraphs 4.21 to 4.25 of HMR 36, with extrapolation to 1 hour. Geographic and seasonal plots of durational variation for the 12 stations indicated that an average durational decay was representative for all months and regions.

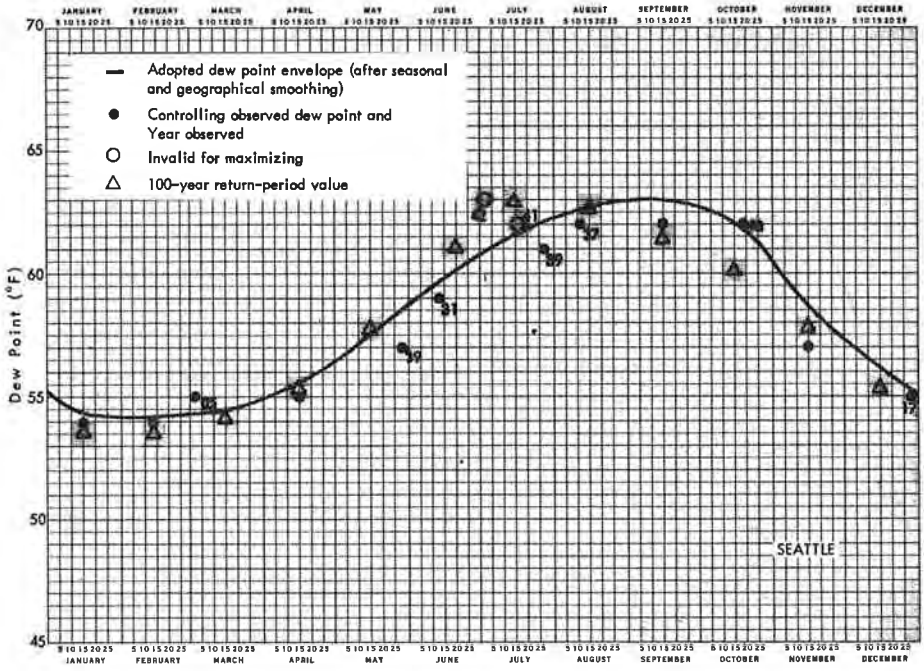

Figure 3-1. Seasonal variation of maximum persisting 12-hr. 1000-mb. dew point - Seattle

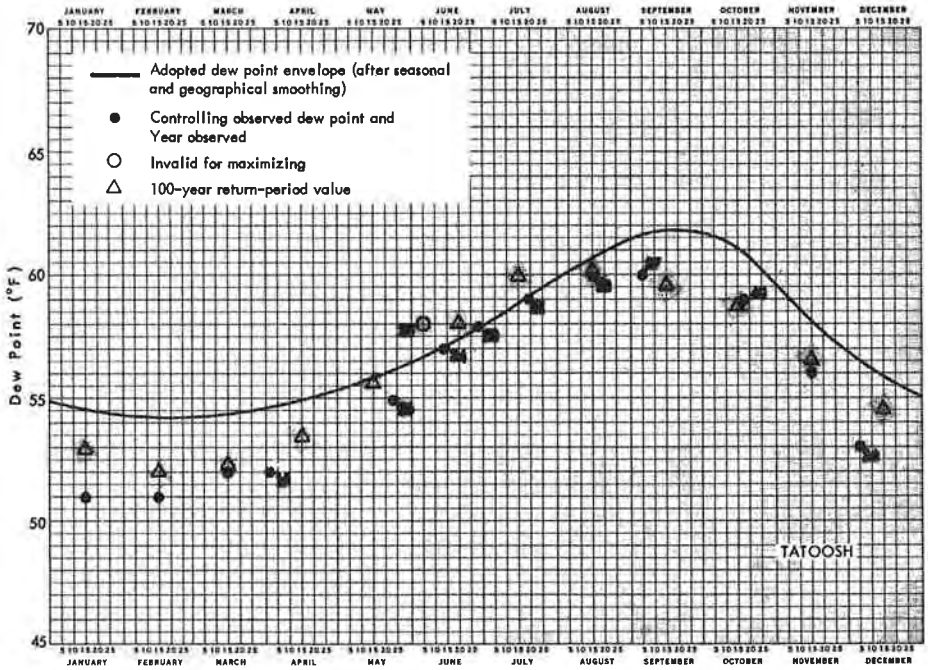

Figure 3-2. Seasonal variation of maximum persisting 12-hr. 1000-mb. dew point - Tatoosh

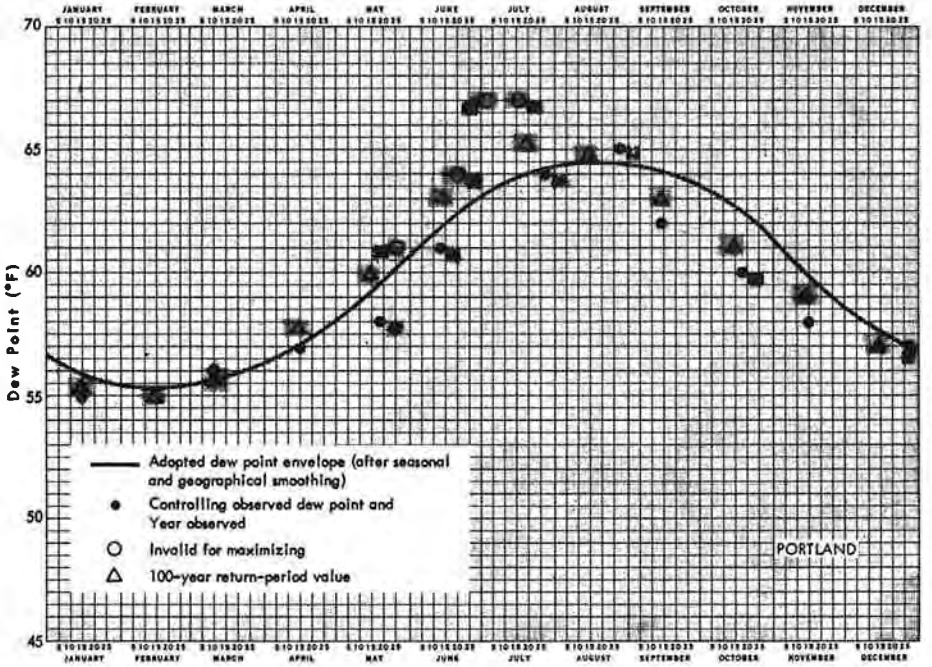

Figure 3-3. Seasonal variation of maximum persisting 12-hr. 1000-mb. dew point - Portland

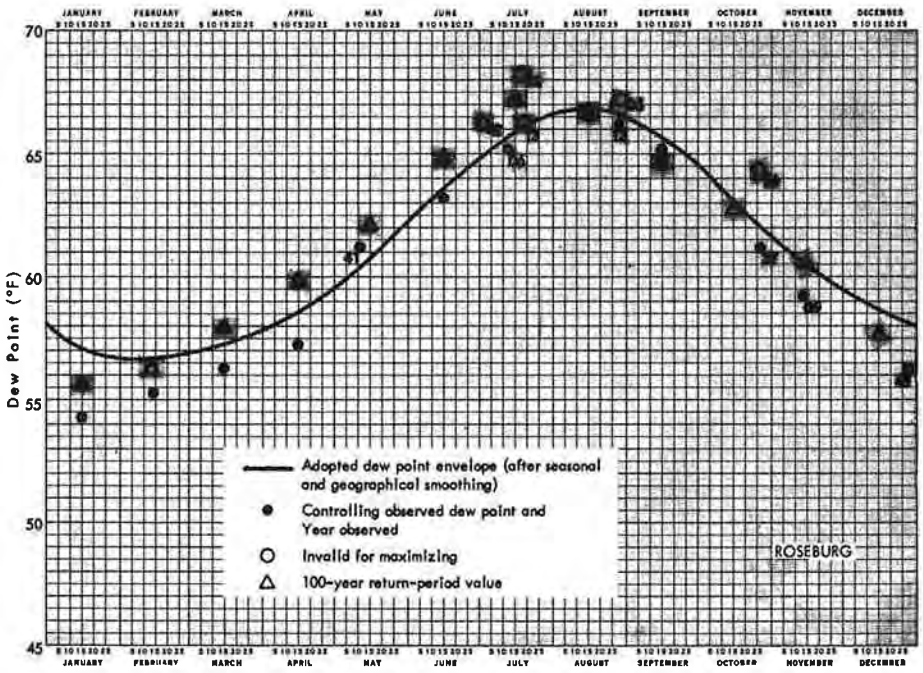

Figure 3-4. Seasonal variation of maximum persisting 12-hr. 1000-mb. dew point - Roseburg

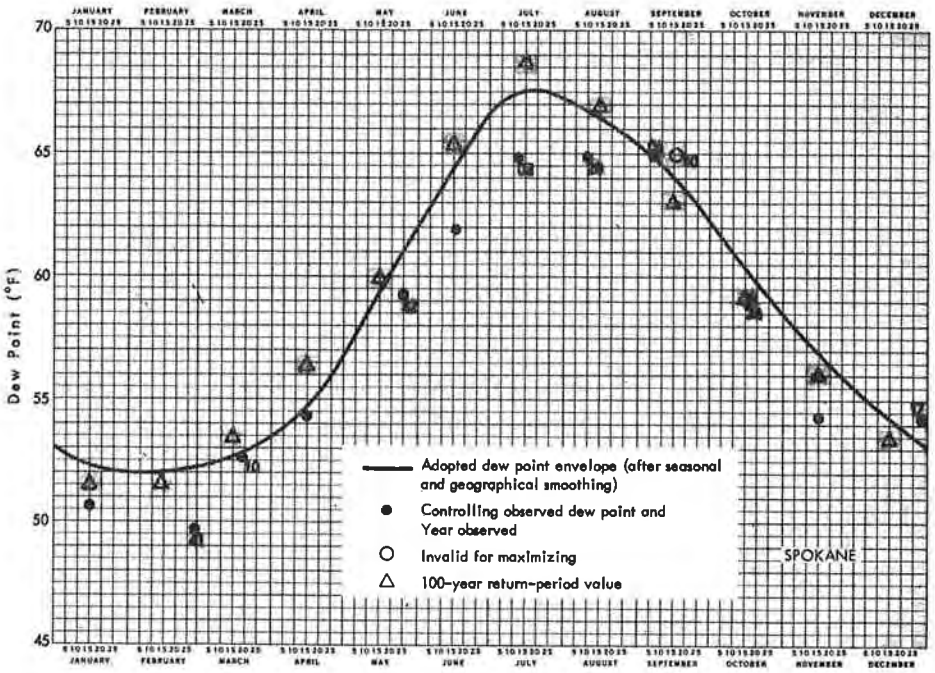

Figure 3-5. Seasonal variation of maximum persisting 12-hr. 1000-mb. dew point - Spokane

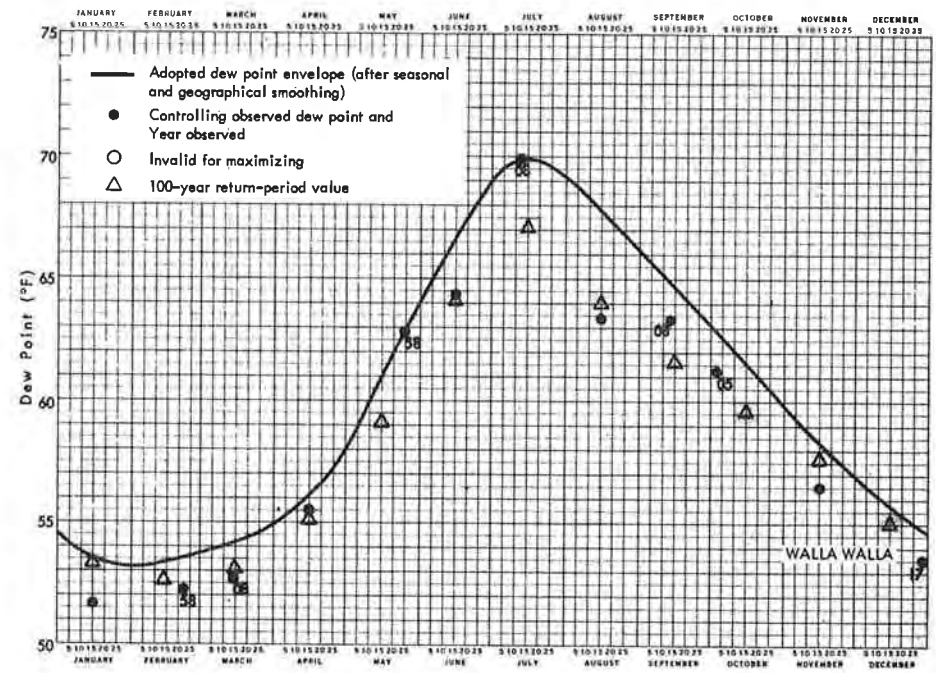

Figure 3-6. Seasonal variation of maximum persisting 12-hr. 1000-mb. dew point - Walla Walla

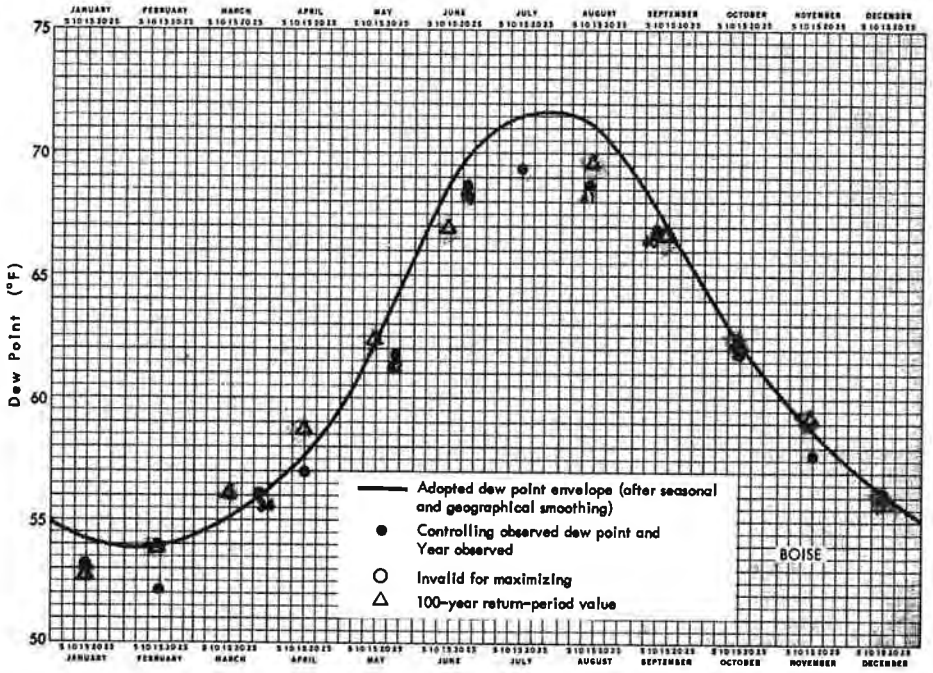

Figure 3-7. Seasonal variation of maximum persisting 12-hr. 1000-mb. dew point - Boise

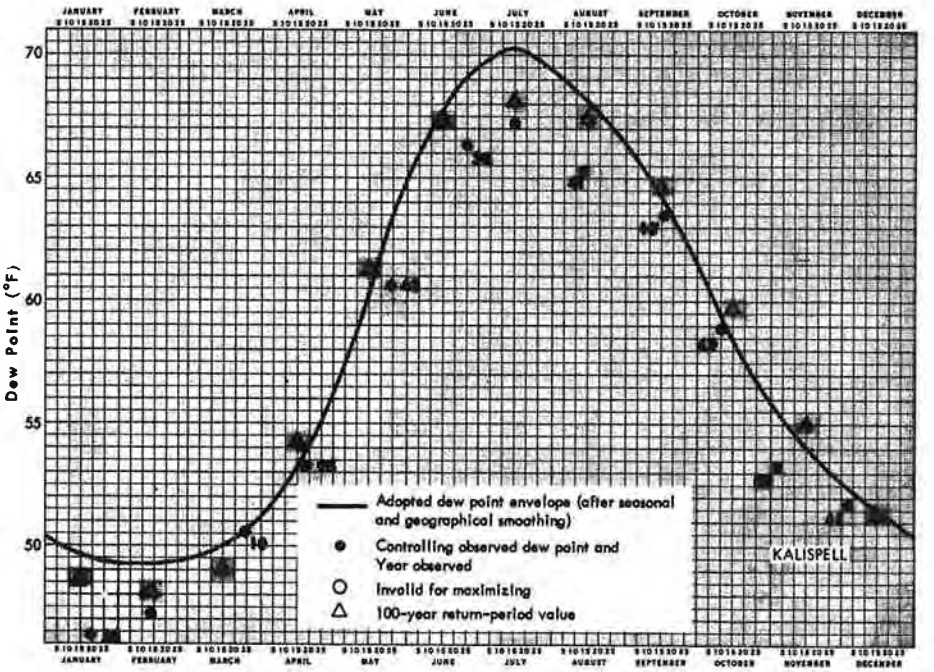

Figure 3-8. Seasonal variation of maximum persisting 12-hr. 1000-mb. dew point - Kalispell

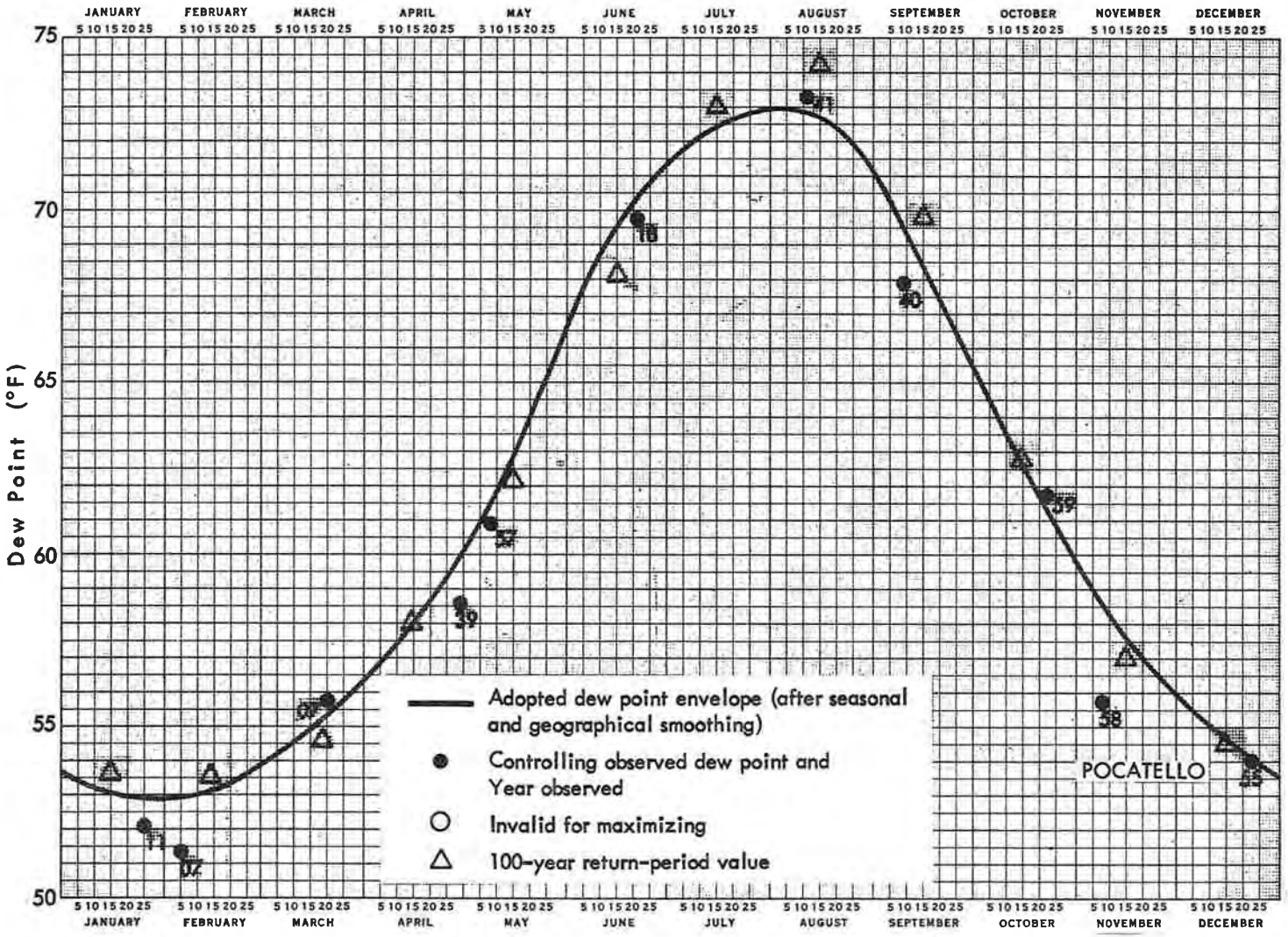

Figure 3-9. Seasonal variation of maximum persisting 12-hr. 1000-mb. dew point - Pocatello

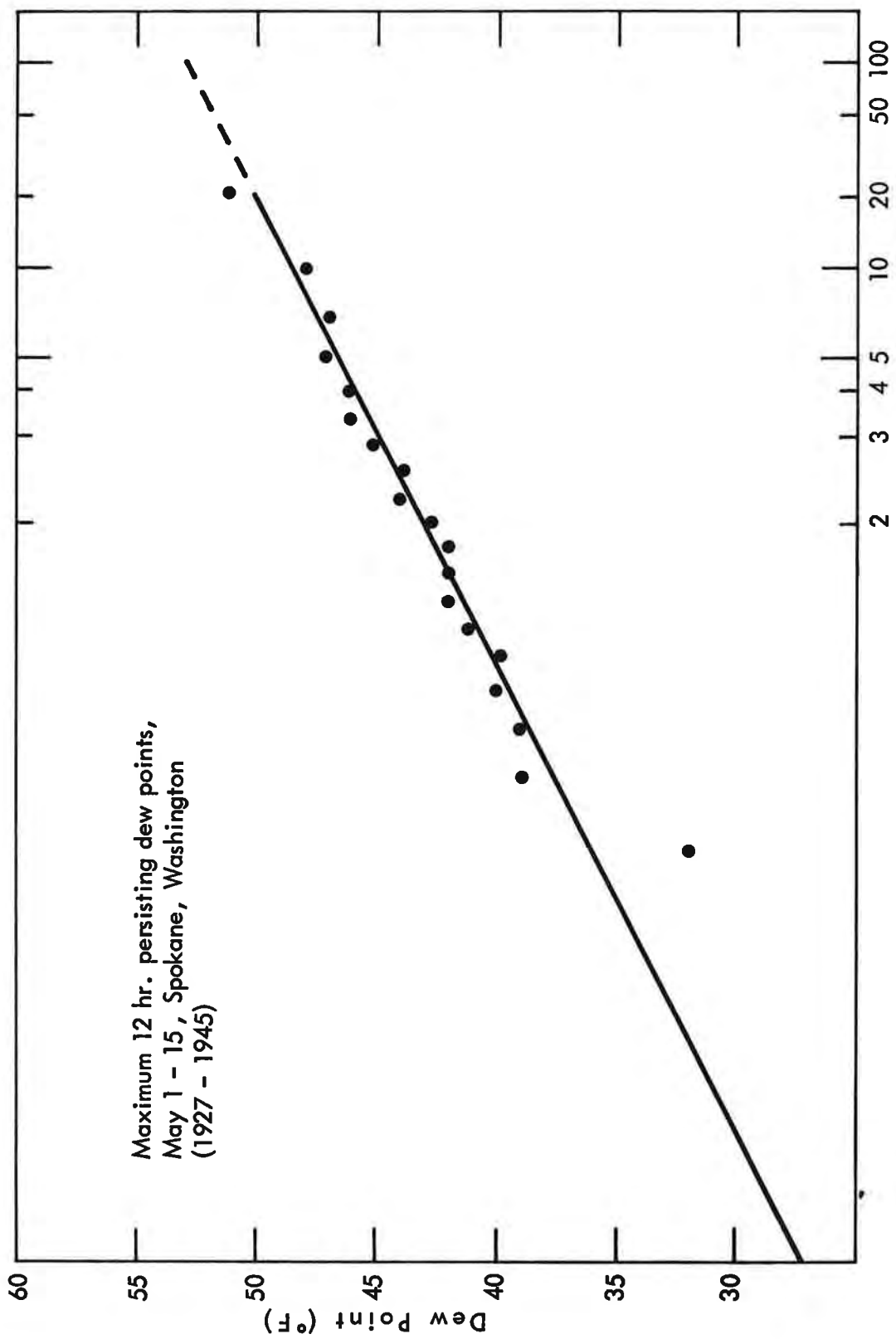

Figure 3-10. Return periods for 12-hr. persisting May 1-15 dew points - Spokane

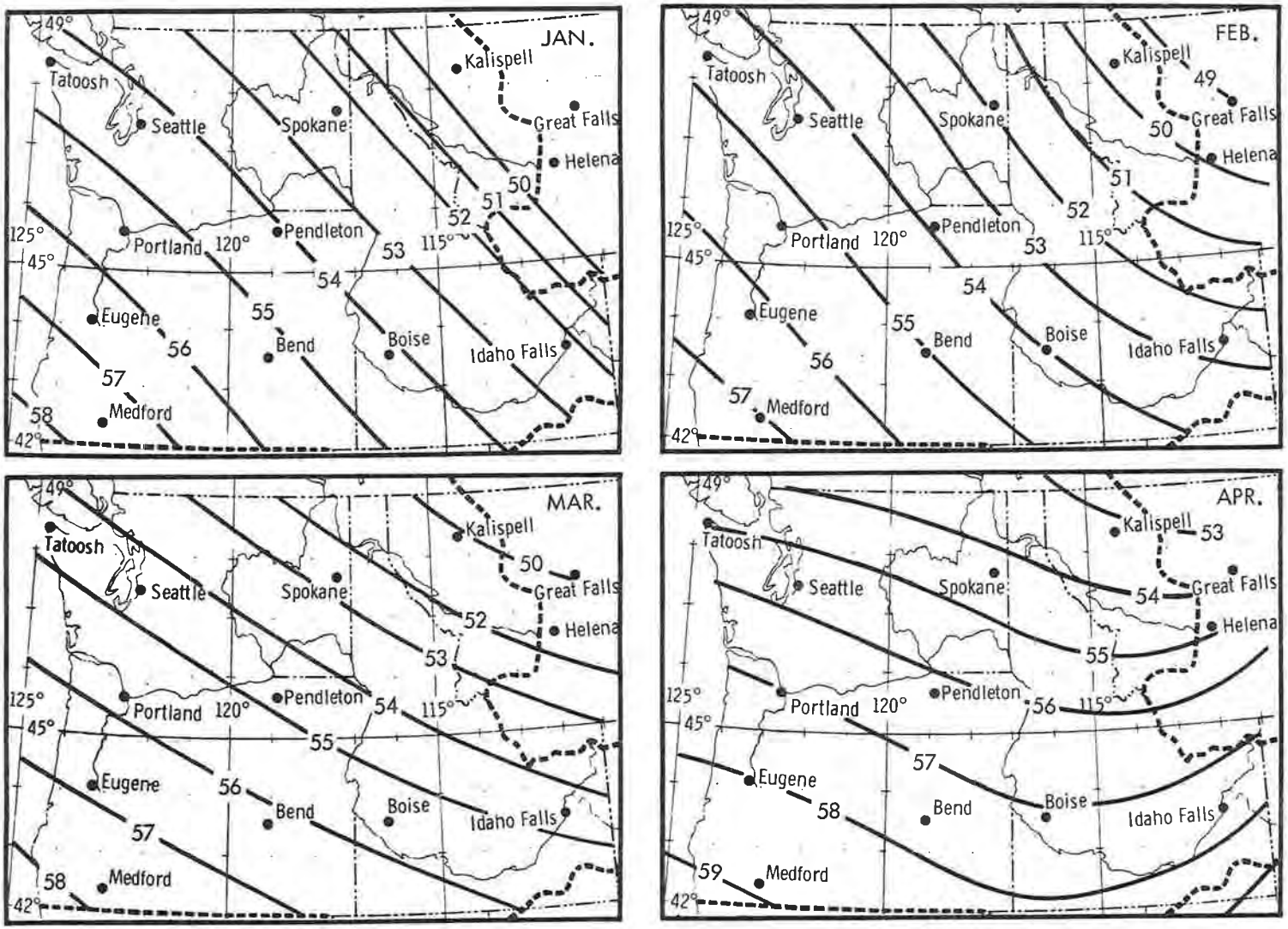

Figure 3-11. Monthly 12-hr. persisting 1000-mb. dew point charts (°F) - January to April

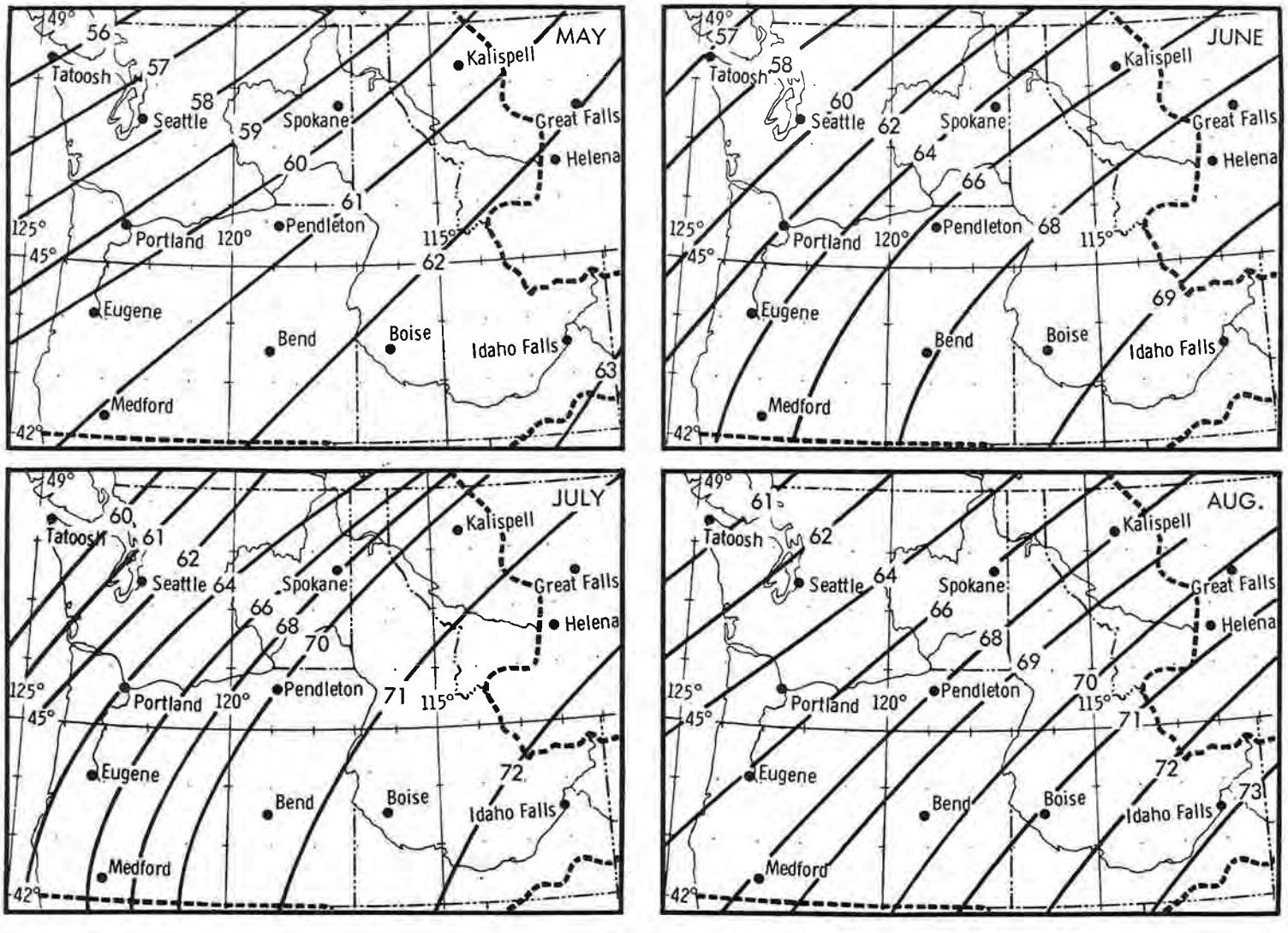

Figure 3-12. Monthly 12-hr. persisting 1000-mb. dew point charts (°F) - May to August

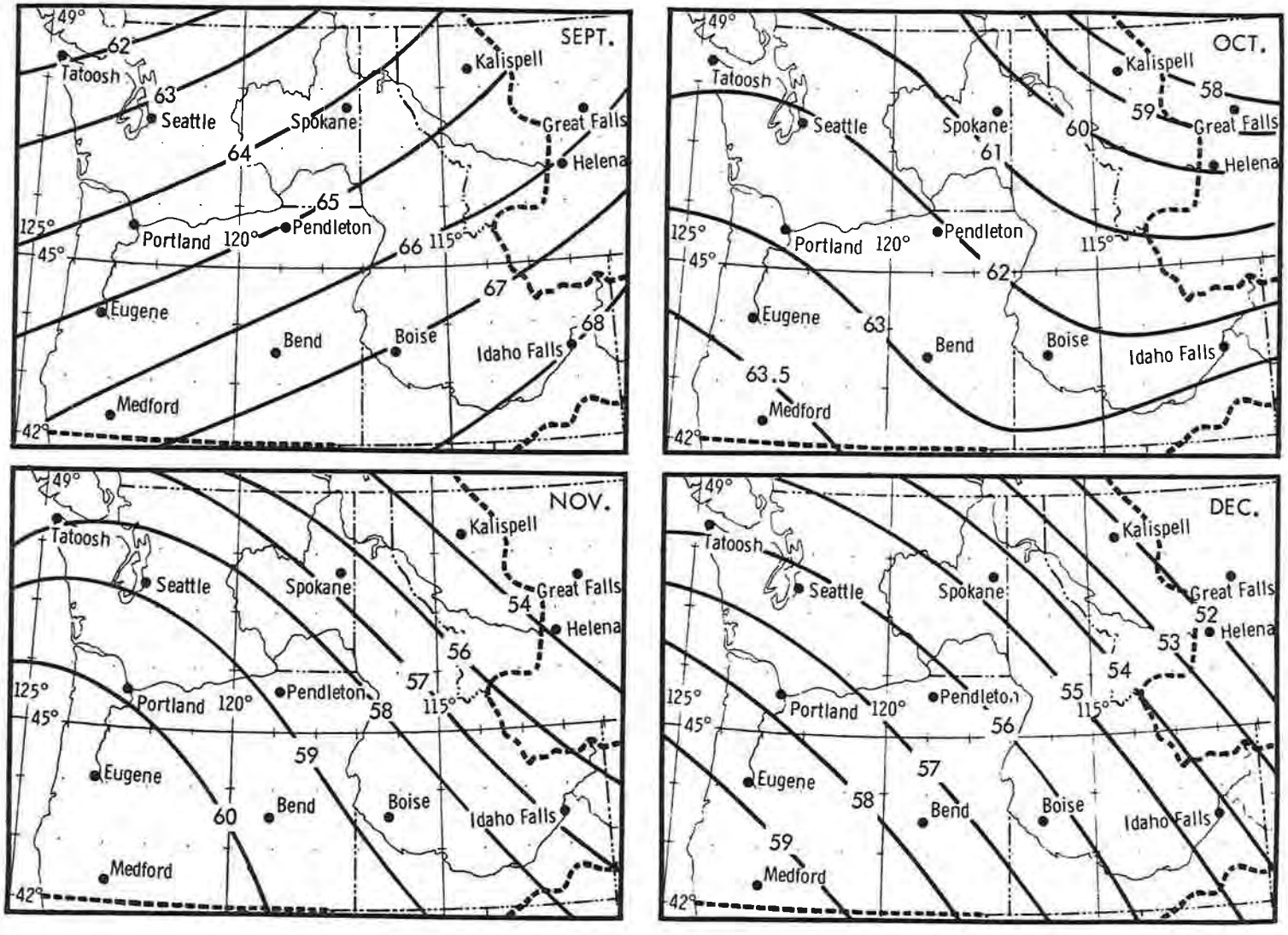

Figure 3-13. Monthly 12-hr. persisting 1000-mb. dew point charts (°F) - September to December

This durational decay rate of observed dew point is compared in figure 3-14 with that for California from figure 4-4 of HMR 36 and with that from Canadian Meteorological Report No. 11 (5).

3-C. DEVELOPMENT OF P/M RATIOS

P/M ratios for 24 hours

3.11. Following the procedure in HMR 36, record precipitation amounts, primarily for 24 hours, were determined in areas near sea level essentially free of orographic effects. There are but few such locations with a long record, most of which are in the Willamette Valley and areas in Washington between the coastal mountains and Cascades. These rain values, in inches, were divided by the precipitable water indicated by the concurrent 12-hr. 1000-mb. dew points, also in inches, to obtain an envelope of highest 24-hr. 1000-mb. P/M ratios.

Reference is made to paragraph 4.29 of HMR 36 where it is reasoned that in storms from the Pacific Ocean highest values of convergence rain depend on a high level of instability. Such instability is not found with highest moisture inflow, which requires a southerly component for a great distance offshore. For this reason, the storms involving the above P/M ratios were put in two groups on the basis of the relative magnitude of the instability contribution, judged by principal inflow direction of moisture in the storm. This grouping gives enveloping P/M ratios compatible with concurrent maximum orographic precipitation (referred to as orographic storm P/M ratios) and ratios not so restricted (referred to as convergence storm P/M ratios).

3.12. P/M ratios compatible with maximum orographic precipitation. Highest P/M ratios shown in figure 3-15 are derived from storms considered appropriate for combination with orographic rain, as follows: A value of 7.4 (fig. 3-15) from the 5.59 inches in 24 hours at Bellingham, Wash. during the record January 1935 storm described in paragraph 2.10. A P/M value of 7.7 from the 5.87 inches at Grapeview, Wash. in the same storm. A value of 8.2 at Portland (city) on December 12-13, 1882, undercut to recognize the effect at Portland (city) of spillover in this storm from hills immediately to southwest. (An average orographic effect at Portland (city) of 12 percent in mean annual precipitation was determined).

These and other data shown in figure 3-15 set the 24-hr. enveloping 1000-mb. point value at 7.8. This value was adopted as a 10-sq. mi. 1000-mb. value near Portland, the mean location of data west of the Cascades. It compares with 6.4 adopted for California in HMR 36, figure 4-7.

3.13. P/M ratios for the maximum convergence storm. Very little data are available to set a 24-hr. P/M level for the maximum convergence storm. Highest value found was 9.5 at Portland in the January 5-6, 1883 storm. Because the orographic component at Portland in this storm was small, no allowance for orographic effect on this Portland value was made. Thus it is not

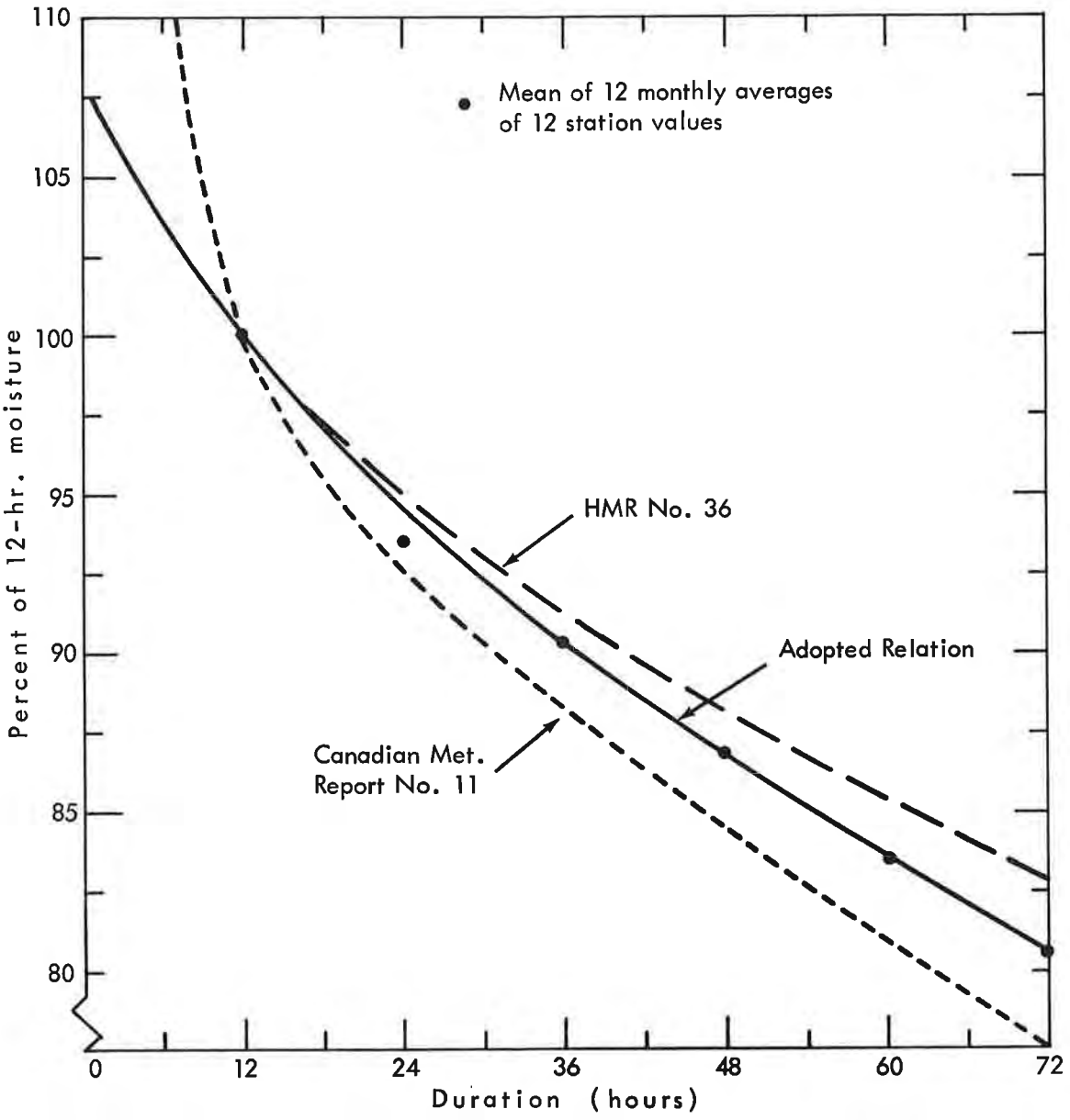

Figure 3-14. Durational variation of maximum moisture

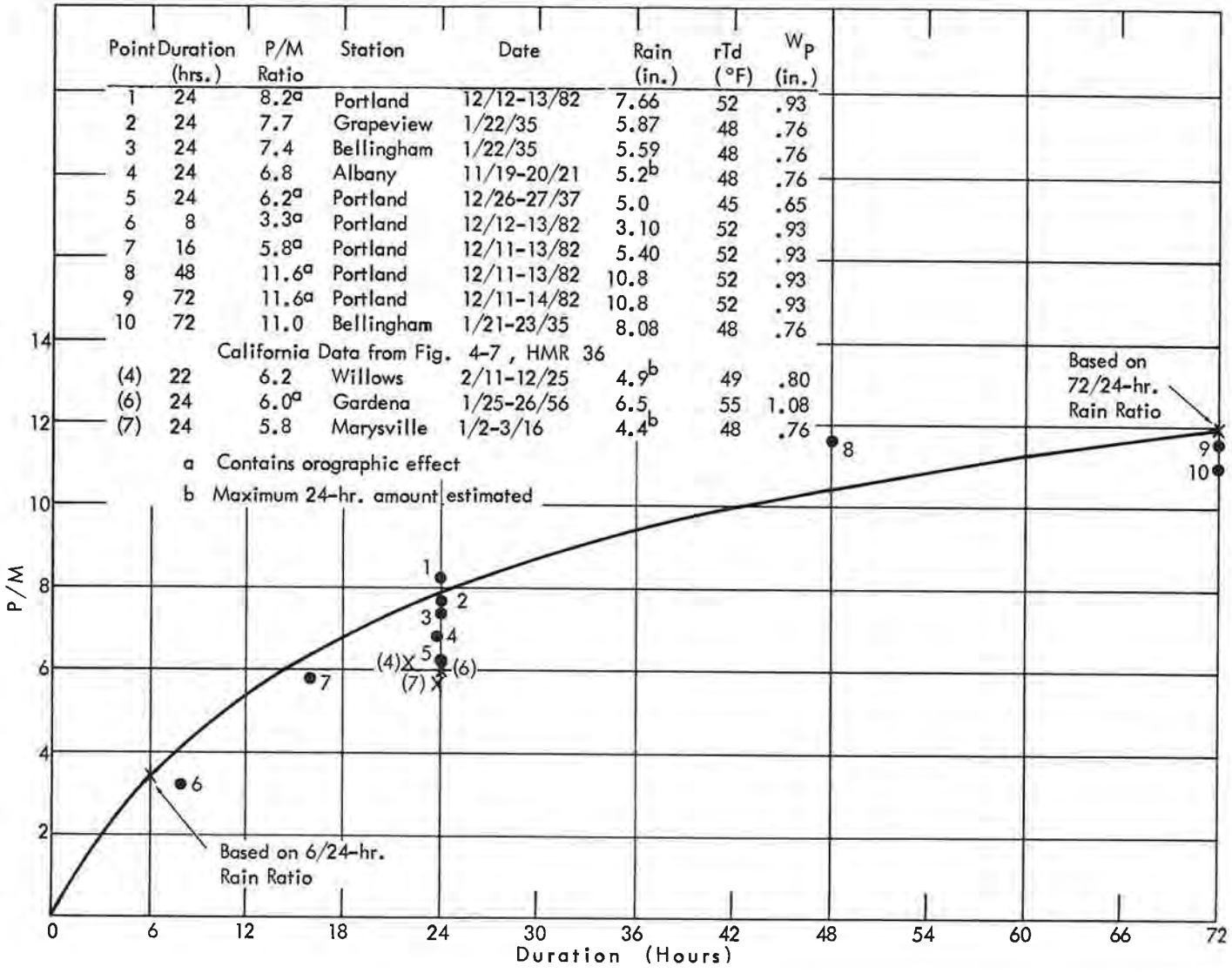

Figure 3-15. Enveloping West of Cascades January P/M ratio curve - convergence component of orographic storm

undercut by the enveloping 24-hr. value of 9.6 shown in figure 3-16. This value is 1.23 times the west-of-Cascades maximum orographic storm 24-hr. value. In California the analogous value is 1.33. The decrease with higher latitude seems reasonable since instability is lessened by shorter trajectory over warmer water of air flowing into the Northwest.

East of the Cascades, no data are available to justify a maximum convergence storm P/M ratio. Further, its role is assumed in summer months by the thunderstorm PMP which controls PMP in non-orographic areas, as will be shown in chapter V. Thus the above concept is limited to west of Cascades in its application in this report.

Map of January 24-hr. 1000-mb. P/M ratio

3.14. Ratio highest in January. The enveloping 24-hr. P/M value is assigned to January. This is justified since the controlling data (pars. 3.12 and 3.13) are primarily from January. January is also the month of lowest moisture. While an inverse relation between trends of P/M and moisture is apparent during cool months in large storms near the coast, it is less apparent in summer months east of the Cascades where some influx of moisture is from south or southeast. In the latter storms the relation between P/M and moisture trends toward that prevailing in intense summer storms east of the Rockies, shown in figure 5-20b of Hydrometeorological Report No. 37 (6), namely, slight increase of P/M with moisture in record 24-hr. convergence rain amounts.

3.15. Geographical variation. A smooth field of 24-hr. P/M (fig. 3-17b) was drawn using a California January value of 6.4 in central California and a west-of-Cascades January value of 7.8 at Portland. The orientation of the lines is parallel to January dew point lines. The rate of increase to northeast is about two-thirds of the rate of decrease in maximum moisture. The concept of seasonal variation of P/M inverse to that of moisture is thus retained in a limited sense in the geographical variation of January P/M.

3.16. Checks on P/M field. A check on January P/M is provided at Cutbank, Mont. With 1.72 inches of precipitation in 24 hours (January 20, 1943) the estimated P/M is 10.8. Dew points at Spokane were used to assess moisture above the barrier level. This value of 10.8 compares with 10.0 extrapolated from the Divide to Cutbank in figure 3-17b.

The November 24-hr. enveloping P/M at Rattlesnake Creek, Idaho (6.7) compares with that in the November 1909 Rattlesnake Creek storm (6.4). Half or 3.6 inches of the 18-hr. total of 7.1 inches was considered convergence rain (see fig. 2-6, upper left) based on the excess of percent of mean annual precipitation over that at nearby stations.

Storm rainfall as clue to monthly durational variation

3.17. The index January P/M ratios west of the Cascades (pars. 3.12 and 3.13) are for 24 hours. Values for durations to 72 hours are desired.

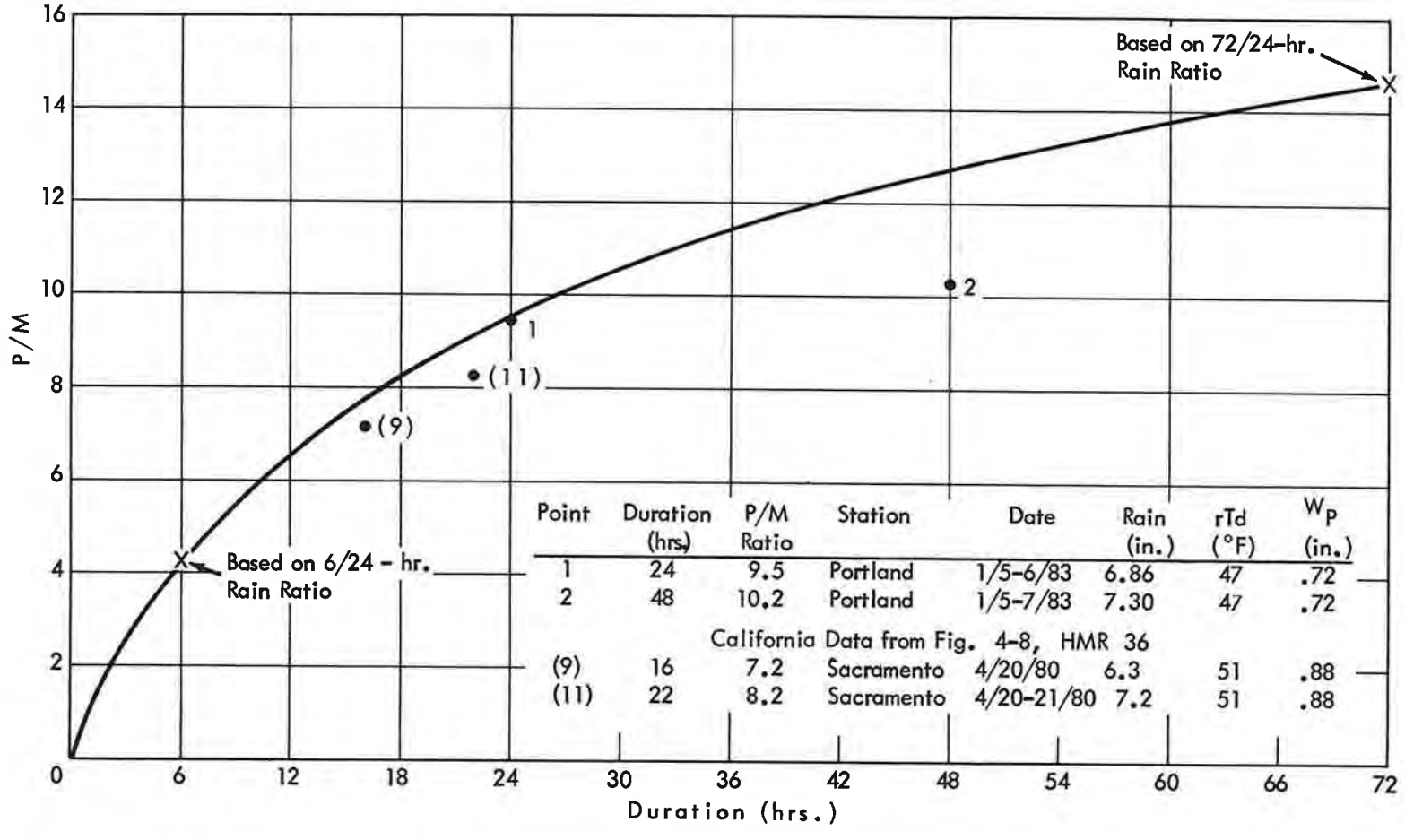

Figure 3-16. Enveloping West of Cascades January P/M ratio curve - convergence storm

For this purpose and for other later uses we will investigate in the following three paragraphs variation of storm rainfall by months, both west and east of the Cascades, for 6 hours and 3 days in relation to 24 hours.

Monthly 6/24-hr. rain ratios

3.18. West of Cascades. The 6/24-hr. rain ratio curve shown in figure 3-18a is based on ratios from highest 6- and highest 24-hr. rains each month (1) at 17 Oregon valley stations for the period 1940-1949 and (2) at Portland for the period 1890-1949. The adopted 6/24-hr. rain ratio curve is slightly higher in winter than the average of the data in winter. The adopted .44 January value compares with .54, the California January value in HMR 36. Summer ratios were undercut considerably to compensate for the very low frequency of storms lasting 24 hours.

3.19. East of Cascades. The 6/24-hr. rain ratios in figure 3-18b depend on a mean of two sets of data: (1) highest 6- and highest 24-hr. rains in each month at eight Oregon and Idaho valley stations for the period 1940-1949 and (2) average of 6/24-hr. ratios for all Boise 24-hr. rains over .5 inch in the period 1946-1960. Here the ratios were only slightly undercut in summer to compensate for slightly lower frequency of 24-hr. summer rains compared to winter.

Monthly 72/24-hr. rain ratios

3.20. The data used to develop the two seasonal variations of 72/24-hr. rain ratios shown in figure 3-19 were averages of within-storm ratios of five highest 3-day and five highest 24-hr. rains for each month for the period 1912-1961. Stations used for the west-of-Cascades relation were Portland and Seattle; for the east-of-Cascades relation, Pocatello, Boise, Baker and Spokane. The adopted curves were smoothed to give a single minimum value in July and a peak in midwinter.

Durational variation of index January P/M ratios

3.21. The 6/24- and 72/24-hr. January rain ratios in paragraphs 3.18 and 3.20 for a mean west-of-Cascades location were multiplied by the index January 24-hr. P/M values of paragraphs 3.12 and 3.13 (7.8 for maximum orographic storm and 9.6 for maximum convergence storm). The resulting 6-, 24-, and 72-hr. P/M values are the basis for the January enveloping curve of P/M shown in figure 3-15 (compatible with the maximum orographic storm) and the curve in figure 3-16 (compatible with the maximum convergence storm). Observed P/M data are entered for 24 hours and for other durations. All data are from west of Cascades except that from large California storms entered in parenthesis for comparison with Northwest data.

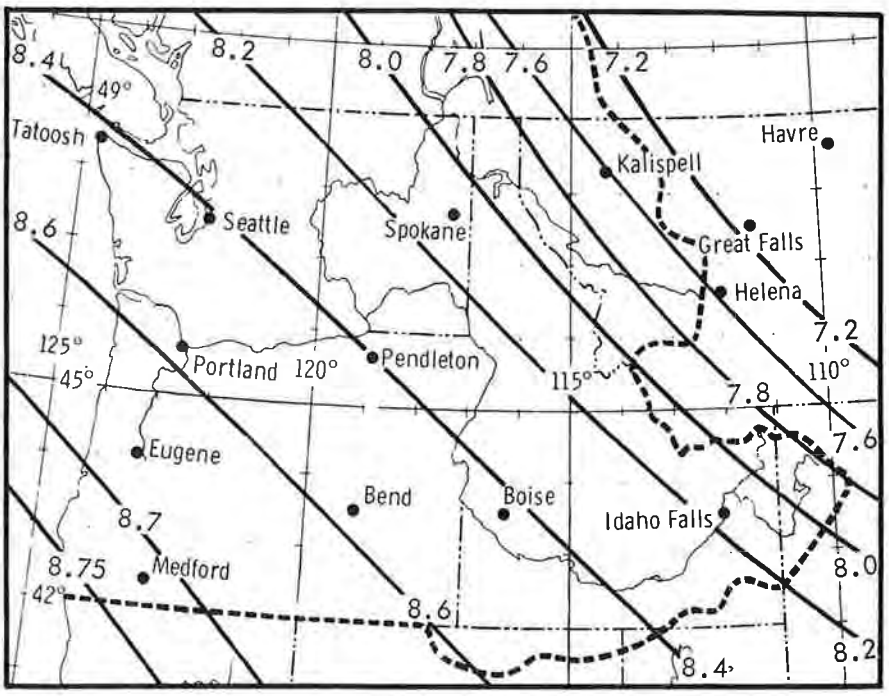

Figure 3-17a. January 24-hr. 10-sq. mi. 1000-mb. orographic storm convergence PMP (in.)

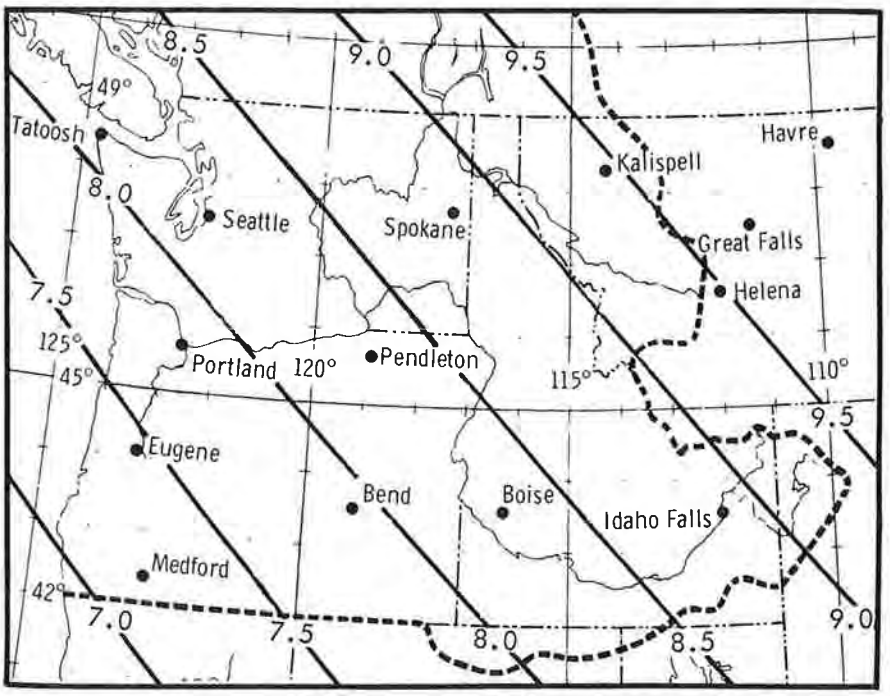

Figure 3-17b. January 24-hr. 1000-mb. orographic storm P/M

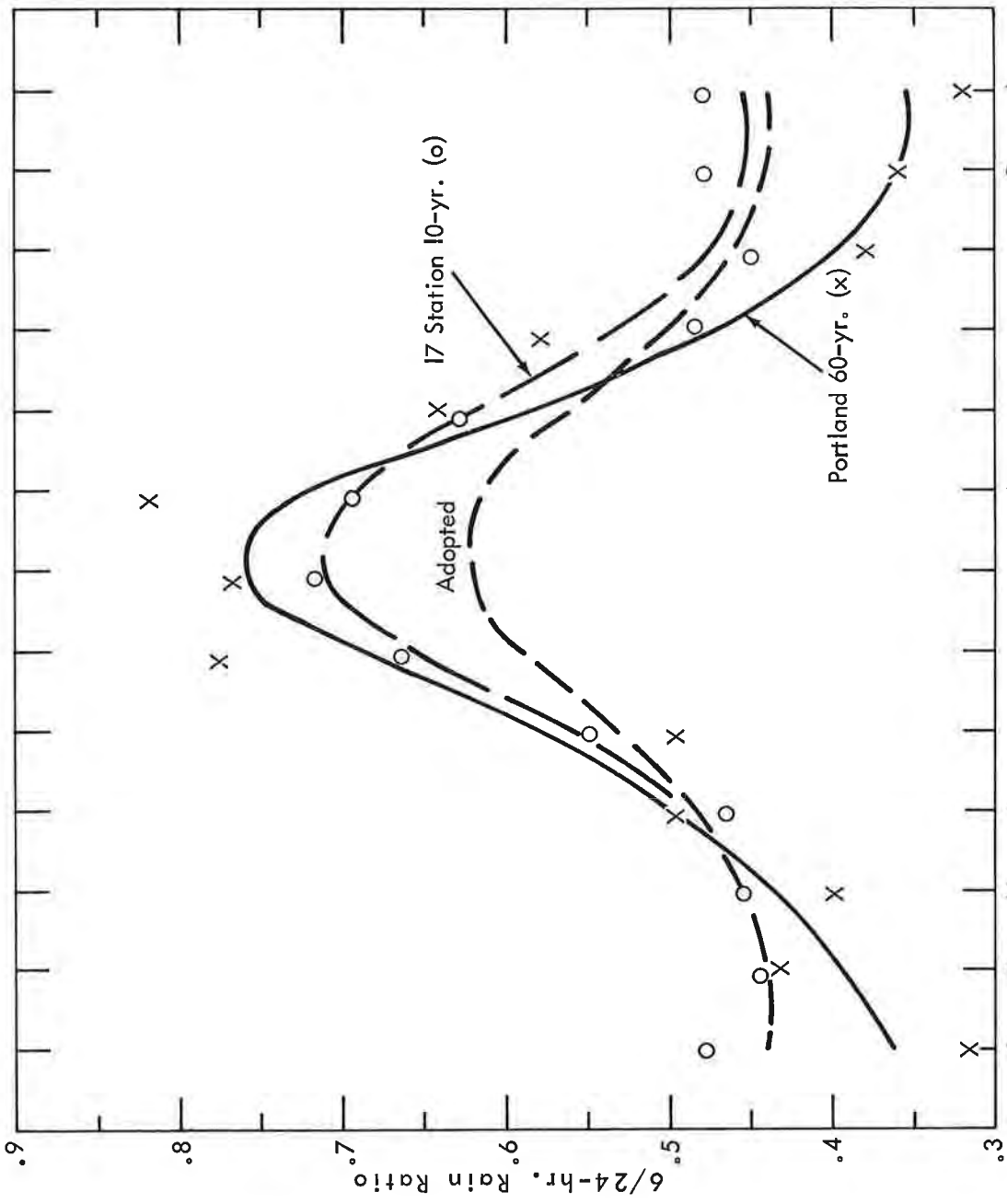

Figure 3-18a. Seasonal trend of 6/24-hr. rain ratios - western Oregon valleys

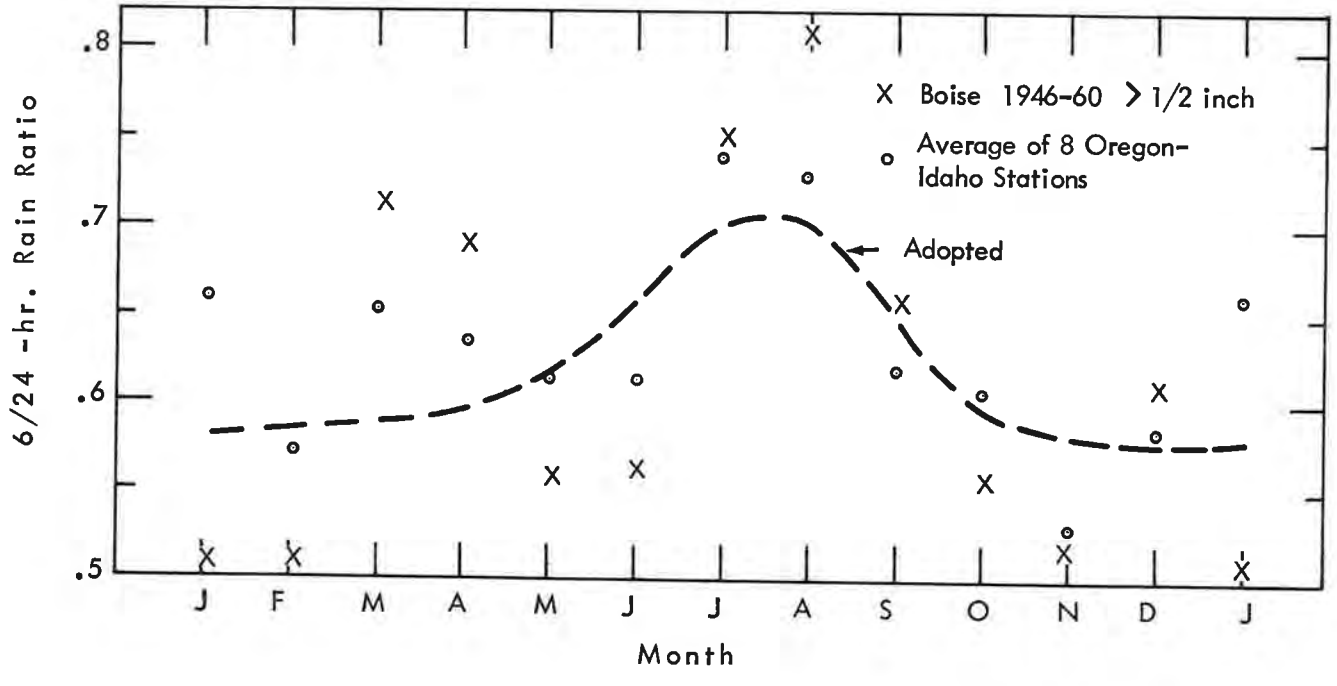

Figure 3-18b. Seasonal trend of 6/24-hr. rain ratios - East of Cascades

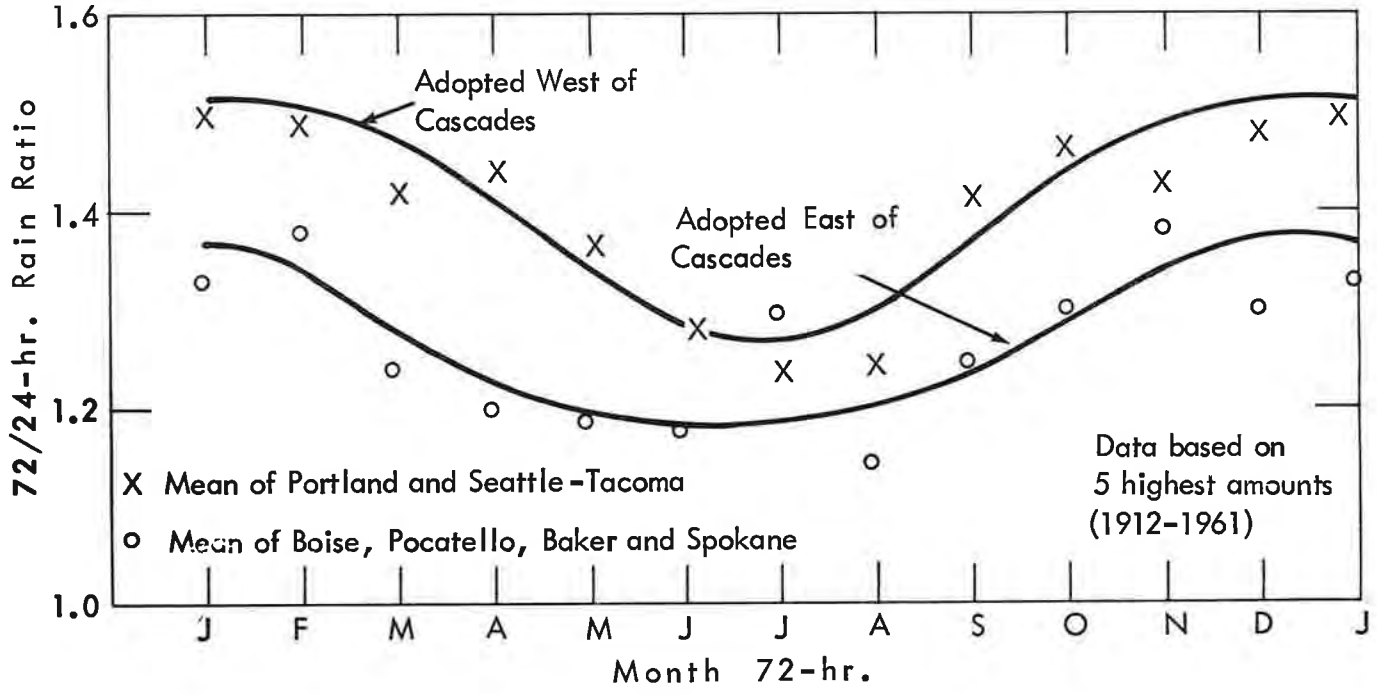

Figure 3-19. Seasonal trend of 72/24-hr. rain ratios West and East of Cascades

3-D. 24-HR. 10-SQ. MI. 1000-MB. CONVERGENCE PMP CHARTS

January 24-hr. 10-sq. mi. 1000-mb. orographic storm convergence PMP index maps

3.22. Values of 24-hr. January 10-sq. mi. 1000-mb. convergence PMP are entered in figure 3-17a. This map is derived by graphical multiplication of the field of moisture represented by the 12-hr. 1000-mb. maximum observed January dew point map of figure 3-11 and the January 24-hr. P/M map derived in paragraph 3.15 and shown in figure 3-17b.

3.23. The next step is to determine the seasonal variation of maximum 24-hr. rains. This variation will then be used to estimate 24-hr. convergence PMP for other months.

Seasonal variation of large 24-hr. rains

3.24. West of Cascades. The summer dropoff in rain along the Pacific Coast is less severe with increasing latitude as storms are shunted to north of the Pacific Ridge, semi-permanent off the California coast. Thus, summer PMP values west of the Cascades are more important than summer values in California. Lighter convergence rain than in winter is suggested by the averages of highest 24-hr. amounts for each month at least - orographic stations, plotted in figure 3-21 for coastal Washington and for coastal Oregon. Also shown by dots are highest station amounts for reference. Technical Paper No. 16, "Maximum 24-Hour Precipitation in the United States" (7), is the source of these data. Station locations are shown in figure 3-20.

While the solid line in each of the two curves of figure 3-21 provides a mean relation, it is necessary to offset the bias of lower storm frequency in other than midwinter months. There is little seasonal variation in these data (and in similar data for California) for the October-April period that is not attributable to frequency bias. This led to use of a nearly constant value from October through April joined by a dashed line paralleling the mean line, as an index to seasonal variation of convergence PMP. This trend was expressed as a percent of January.

3.25. East of Cascades. A summer decrease in highest monthly 24-hr. convergence rain from stations least affected by orography was shown above as typical of the area of summer maritime control in the Pacific Northwest. This trend reverses eastward, with much higher summer than winter values near the Continental Divide.

Seasonal variation of highest 24-hr. amounts for each month, from Technical Paper No. 16 (7), at least-orographic stations was used as a guide to the seasonal variation of convergence PMP. These data were grouped as shown in figure 3-20 and averaged by the following nine geographic regions: central Oregon, eastern Oregon, eastern Washington, southwest Idaho, southeast Idaho, northwest Montana (west and east of Divide), northwest Nevada and northeast Nevada. Averages of five highest 24-hr. amounts for each month from the period of record at Boise, Baker, Pocatello and Lakeview gave

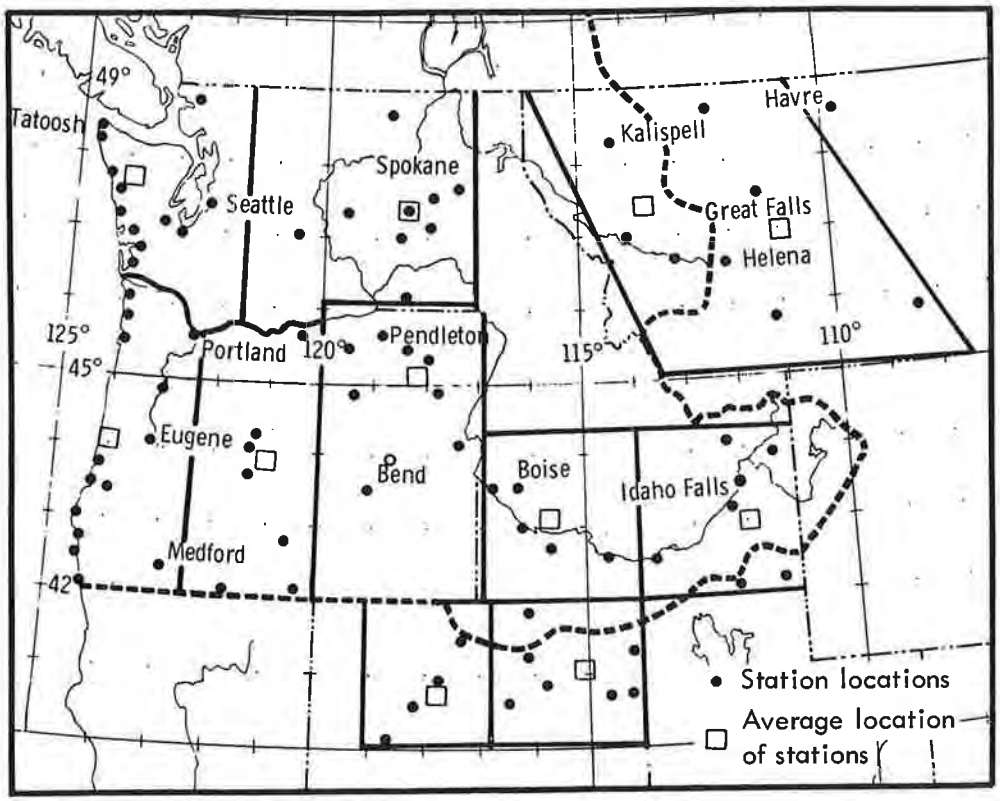

Figure 3-20. Map of data source for figures 3-21 and 3-22

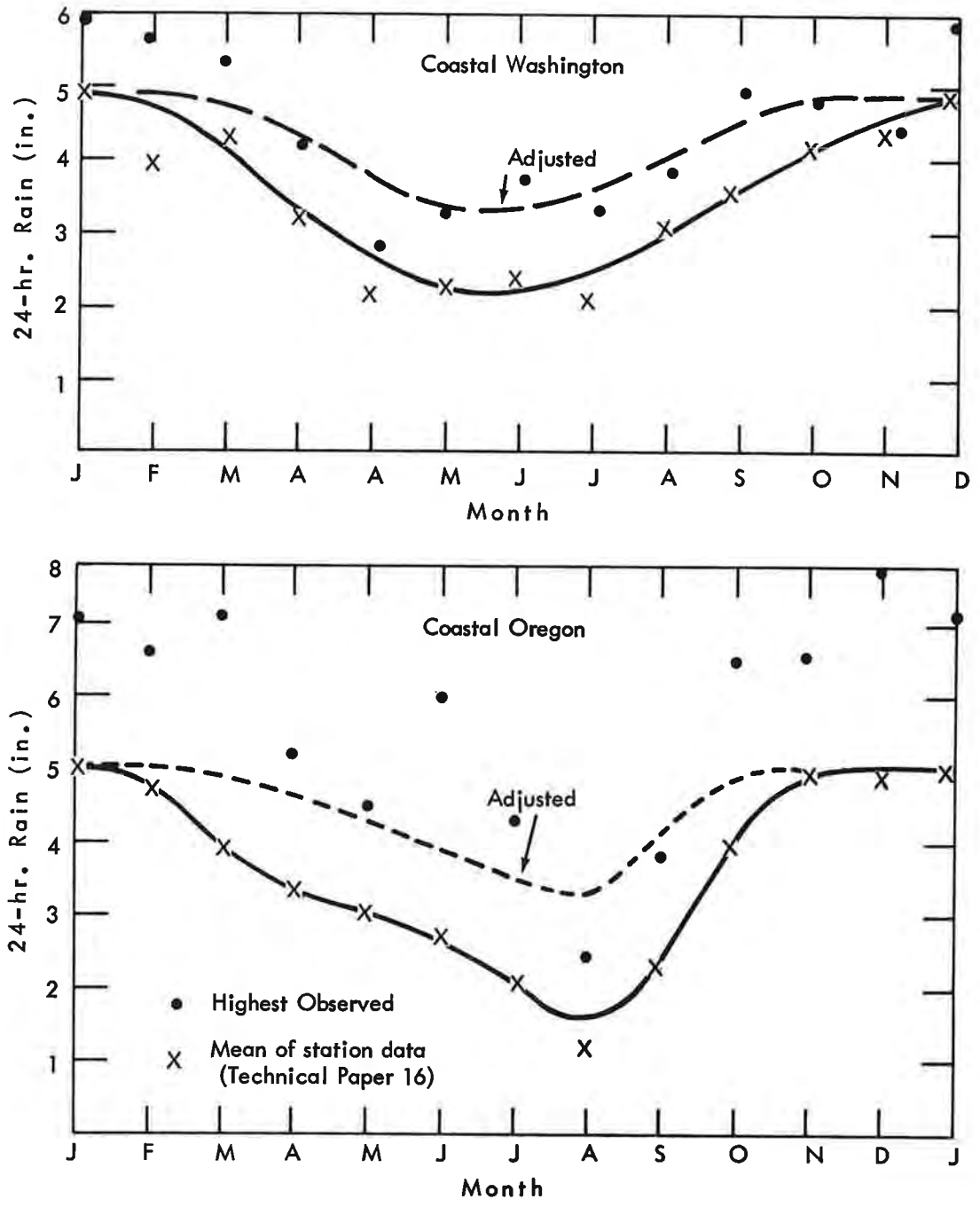

Figure 3-21. Seasonal variation of largest 24-hr. rains at least-orographic coastal stations

further guidance. To obtain broad-scale consistency of seasonal patterns over the entire West, the above procedures were extended through 14 additional regions in the Southwest States and over the western Plains States. In summer months data were examined to eliminate local thunderstorm rains.

Plots were made of averages for each of the nine regions and smooth seasonal curves drawn to the data. These plots, not shown, are similar to those of figure 3-22. The seasonal trend of each plot was expressed in percent of January.

While the coastal seasonal curves of 24-hr. convergence PMP were adjusted for low summer storm frequency (par. 3.24), elsewhere the effect of more frequent summer rains with distance eastward from the Cascades was maintained in the plots.

3.26. Regional and seasonal smoothing. Data centers of geographical regions of paragraphs 3.24 and 3.25 in and adjacent to the basin are shown in figure 3-20. Moisture values from the dew point maps of figures 3-11 to 3-13 were read at each of these centers for each month and expressed as a percent of the January value. The above seasonally smoothed average precipitation for each month at each center (similar to fig. 3-22), in percent of January, was then divided by these moisture percents for each month. The resulting P/M ratios (in percent of January) were smoothed seasonally, then regionally, and multiplied by these same moisture values to give a new set of precipitation values for each month in percent of January. This procedure allows the seasonal and regional variation of moisture to exert a control on the seasonal and regional variation of precipitation.

Multiplication of these precipitation percents for each month by the January 1000-mb. convergence PMP from figure 3-17a gives 1000-mb. convergence PMP for each month for each region (fig. 3-22).

Monthly 24-hr. 1000-mb. convergence PMP maps

3.27. Data from figure 3-22 were plotted on a map for each month and analyzed. These 1000-mb. convergence PMP maps (Oct.-June) are figures 3-23a through 3-31a. Months July to September are not shown. Coastal values are high in winter and low in summer. The reverse is true near the Continental Divide. This difference is an aspect of the difference in severe convergence rain climatology between the two regions. East of the Cascades, summer thunderstorms control PMP for small areas; for larger areas, slightly higher midsummer values in Idaho and eastward result in lower hydrographs than do May or June values combined with orographic PMP and snowmelt.

3.28. The level of convergence PMP in the convergence-only storm relative to the convergence PMP in the orographic storm was set at 1.23 for midwinter by relative P/M ratios (par. 3.13). West of Cascades, this level is considered to apply as well to other months. The concept of a convergence-only storm is not applied east of the Cascades because the thunderstorm PMP assumes that role in non-orographic areas.

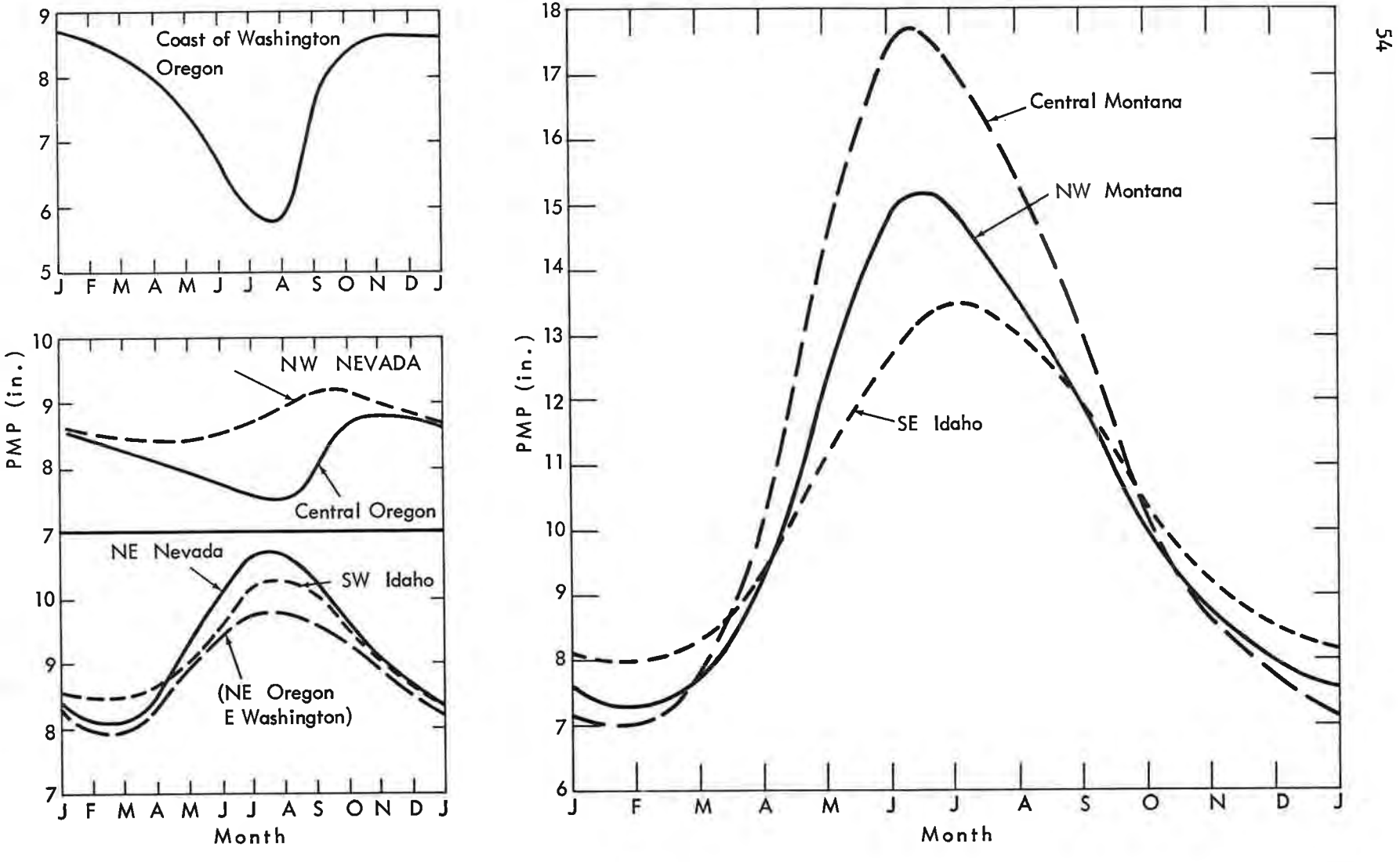

Figure 3-22. Seasonal variation of orographic storm 24-hr. 1000-mb. 10-sq. mi. convergence PMP (in.) by geographic regions

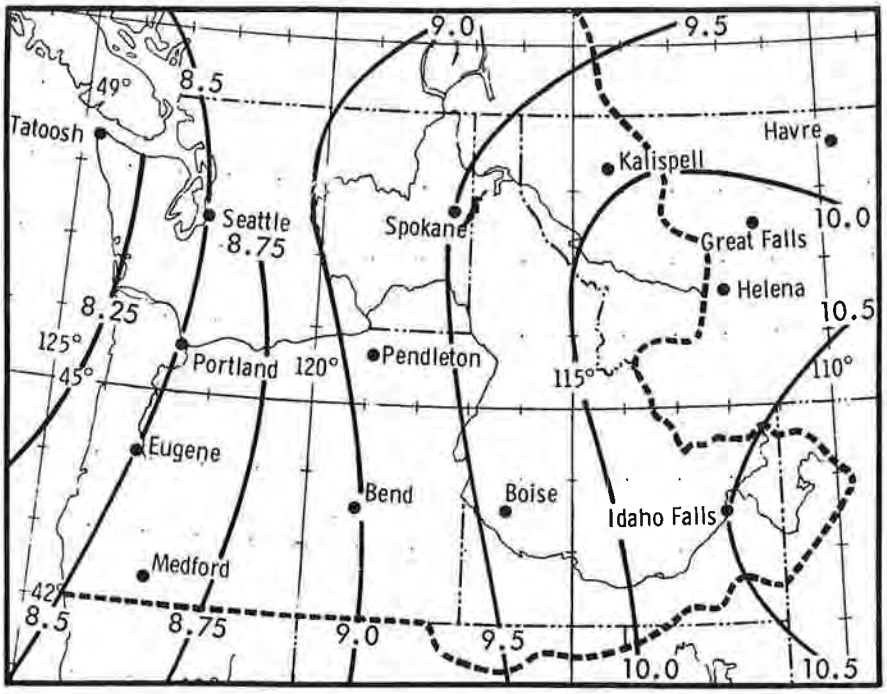

Figure 3-23a. October 24-hr. 10-sq. mi. 1000-mb. orographic storm convergence PMP index chart (in.)

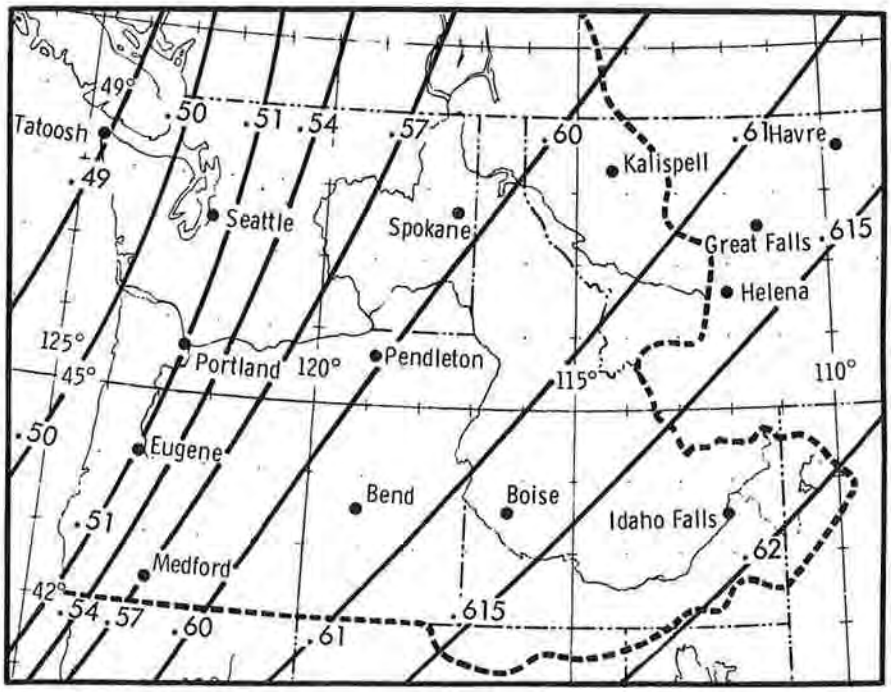

Figure 3-23b. October 6/24-hr. rain ratio map

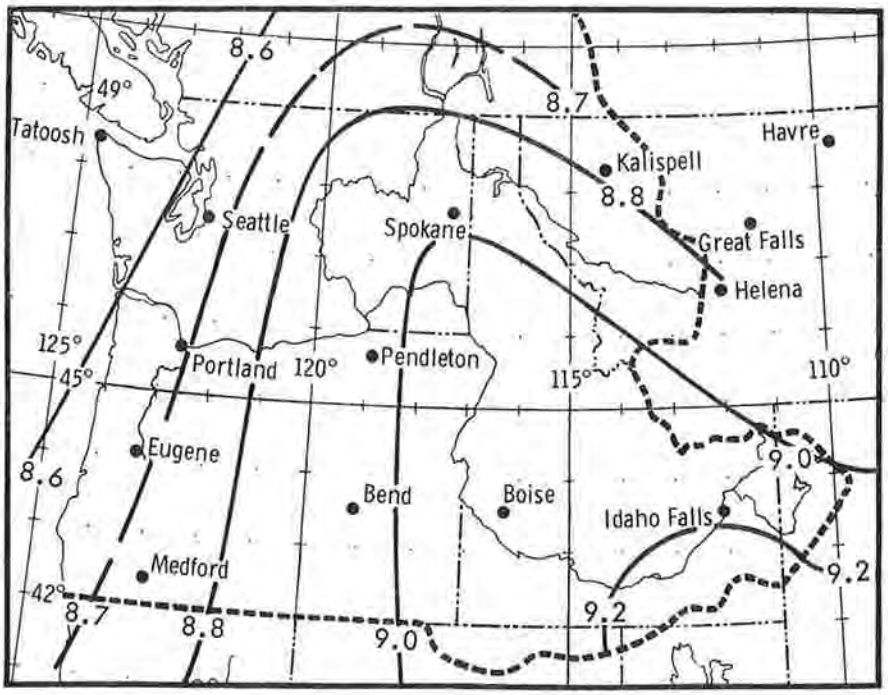

Figure 3-24a. November 24-hr. 10-sq. mi. 1000-mb. orographic storm convergence PMP index chart (in.)

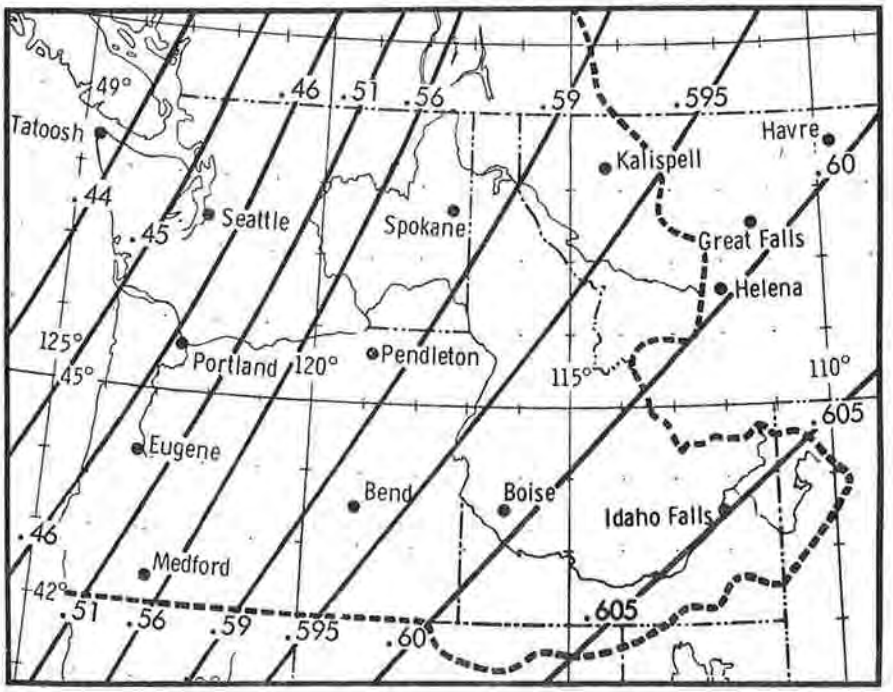

Figure 3-24b. November 6/24-hr. rain ratio map

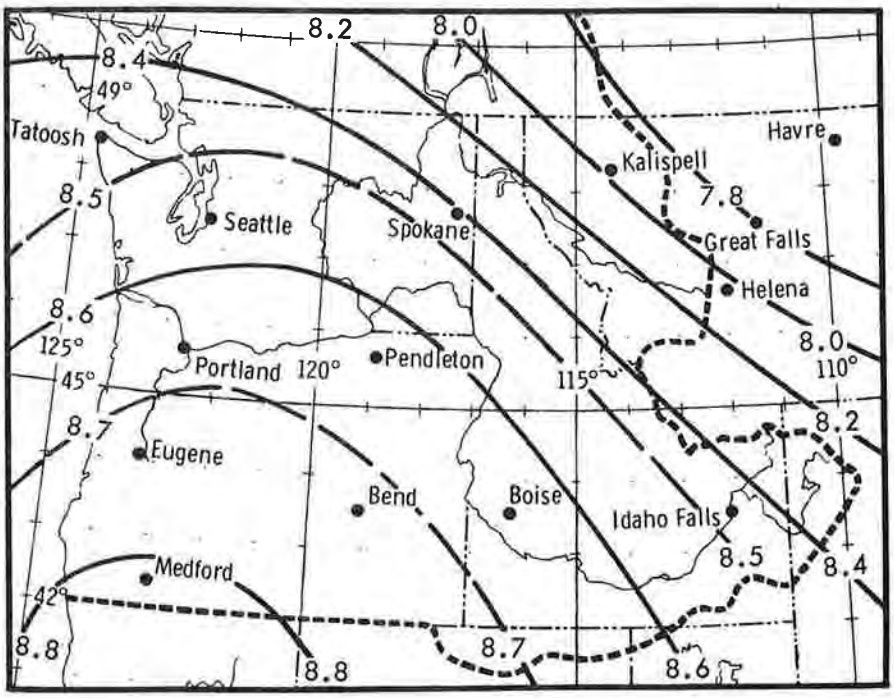

Figure 3-25a. December 24-hr. 10-sq. mi. 1000-mb. orographic storm convergence PMP index chart (in.)

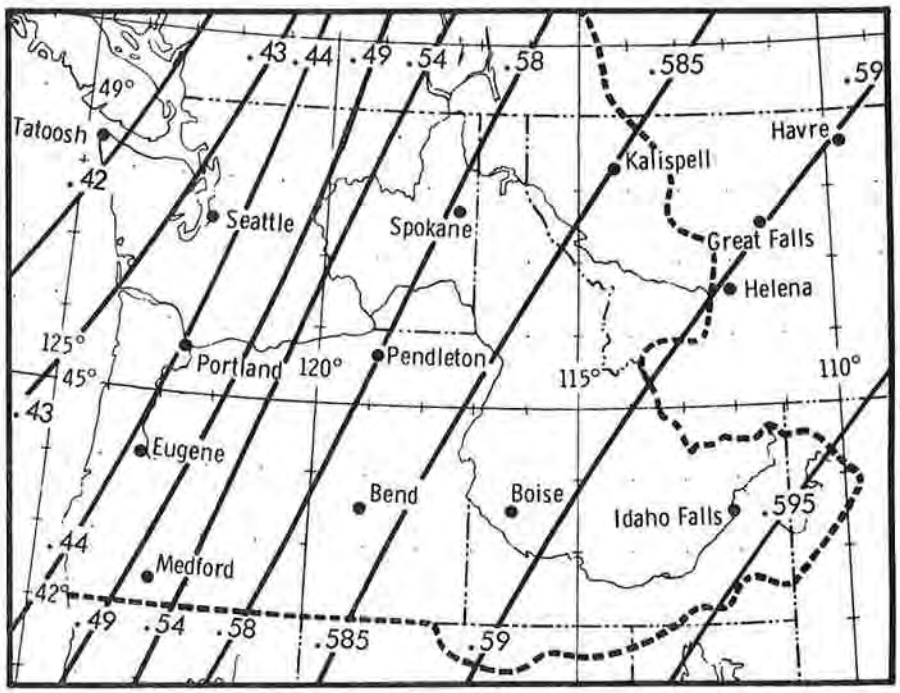

Figure 3-25b. December 6/24-hr. rain ratio map

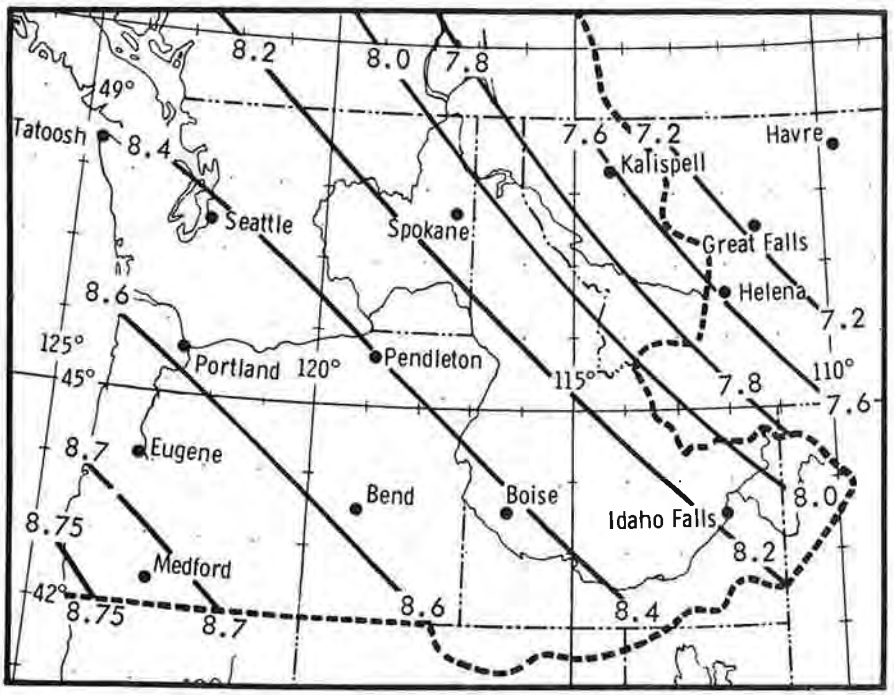

Figure 3-26a. January 24-hr. 10-sq. mi. 1000-mb. orographic storm convergence PMP index chart (in.)

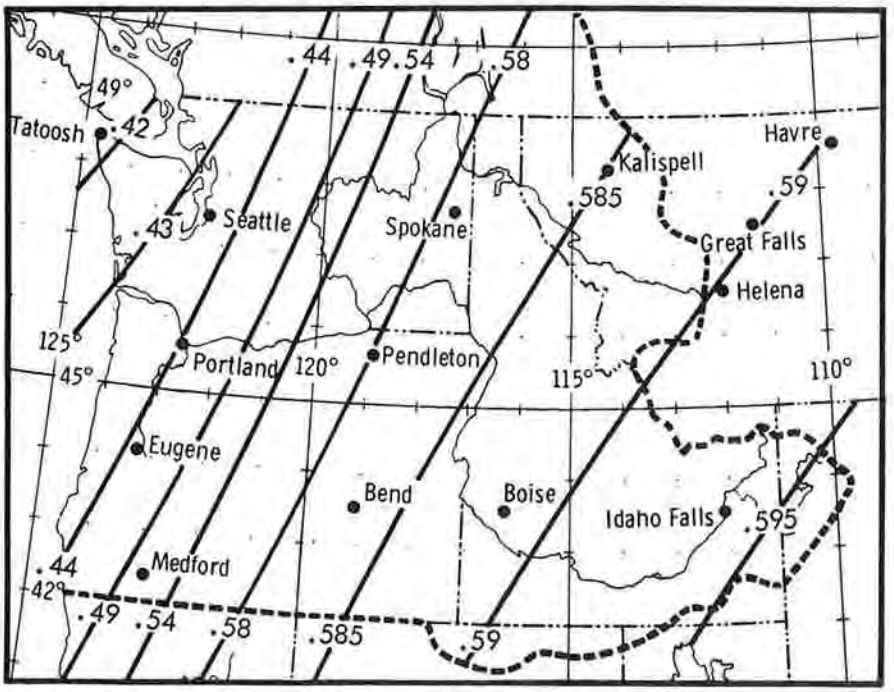

Figure 3-26b. January 6/24-hr. rain ratio map

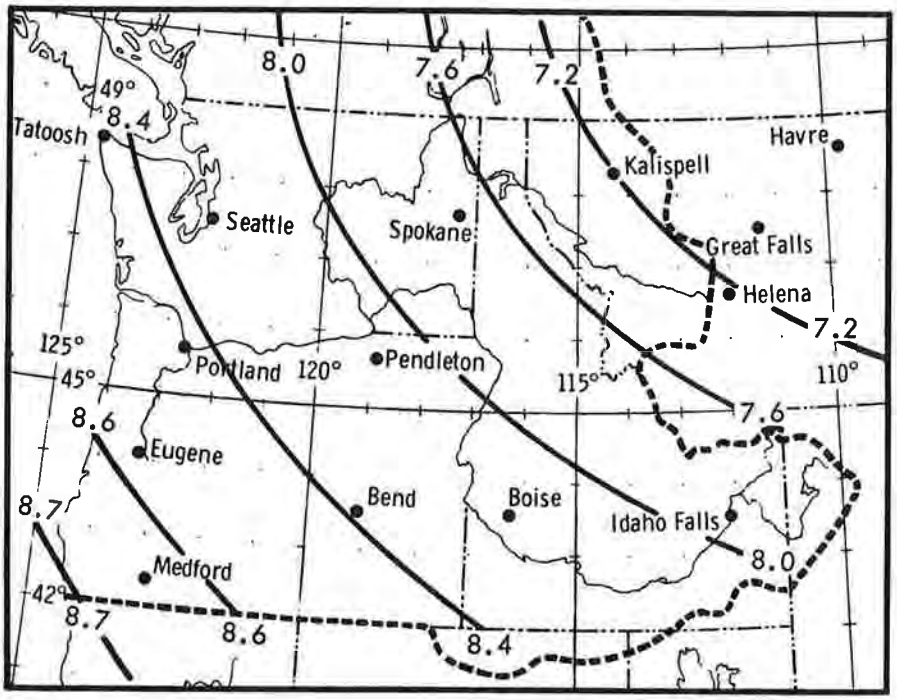

Figure 3-27a. February 24-hr. 10-sq. mi. 1000-mb. orographic storm convergence PMP index chart (in.)

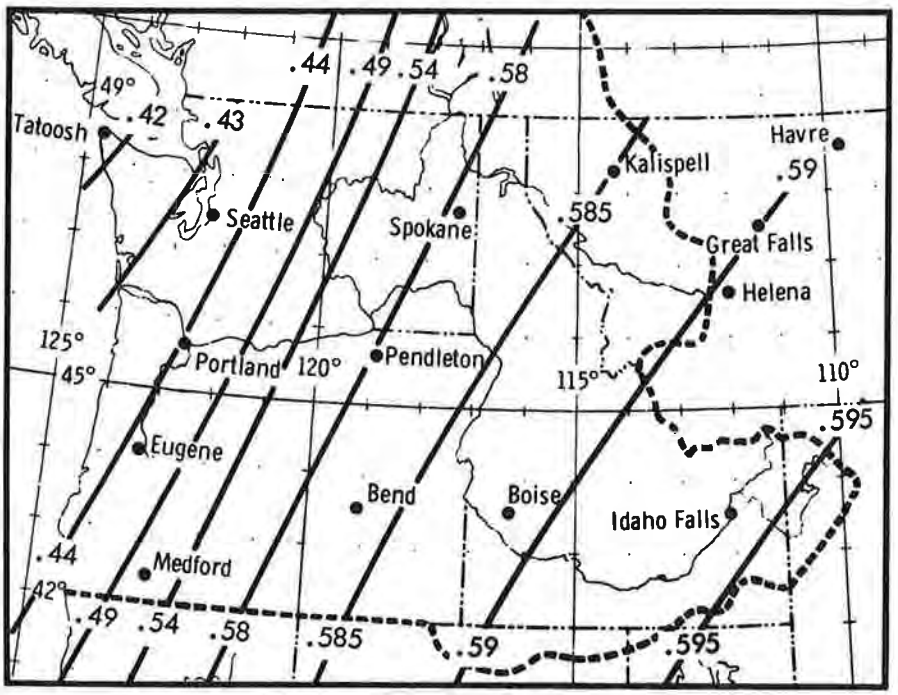

Figure 3-27b. February 6/24-hr. rain ratio map

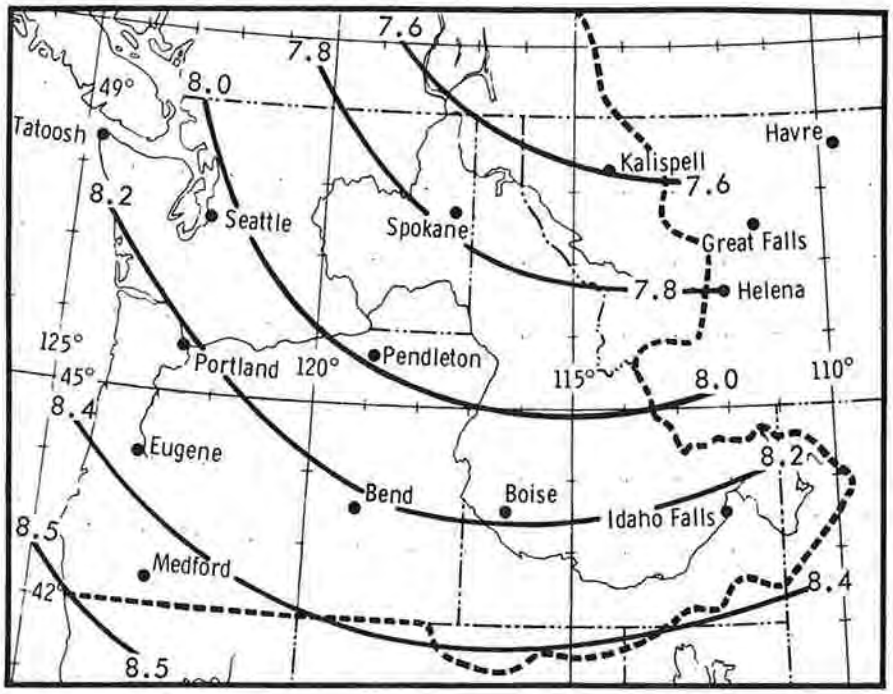

Figure 3-28a. March 24-hr. 10-sq. mi. 1000-mb. orographic storm convergence PMP index chart (in.)

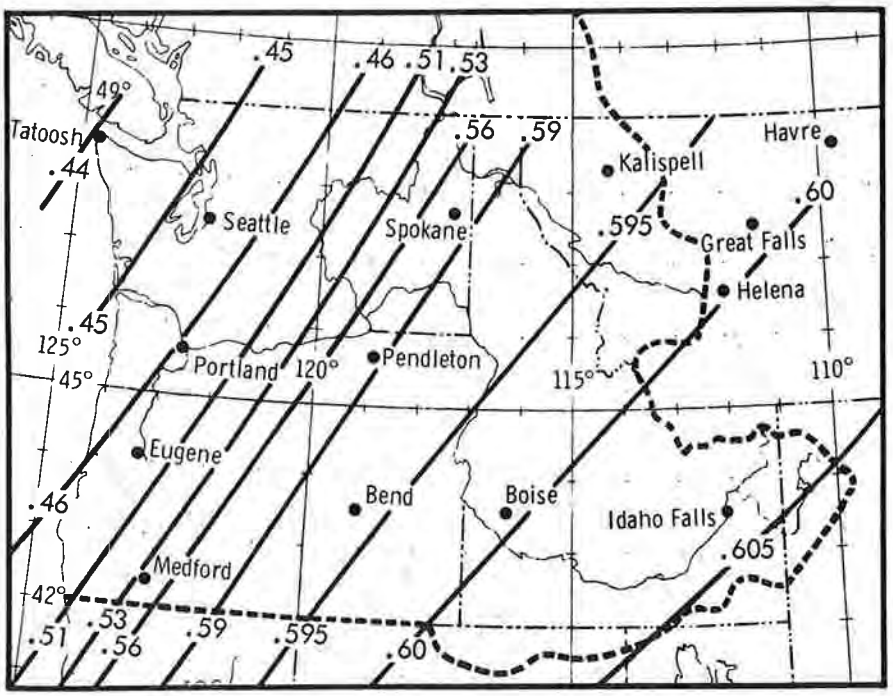

Figure 3-28b. March 6/24-hr. rain ratio map

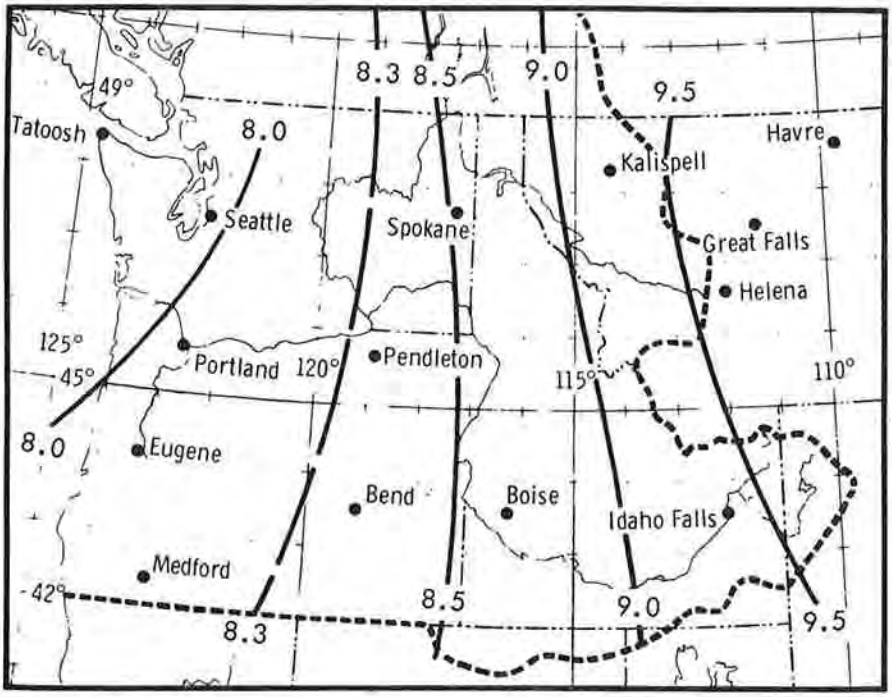

Figure 3-29a. April 24-hr. 10-sq. mi. 1000-mb. orographic storm convergence PMP index chart (in.)

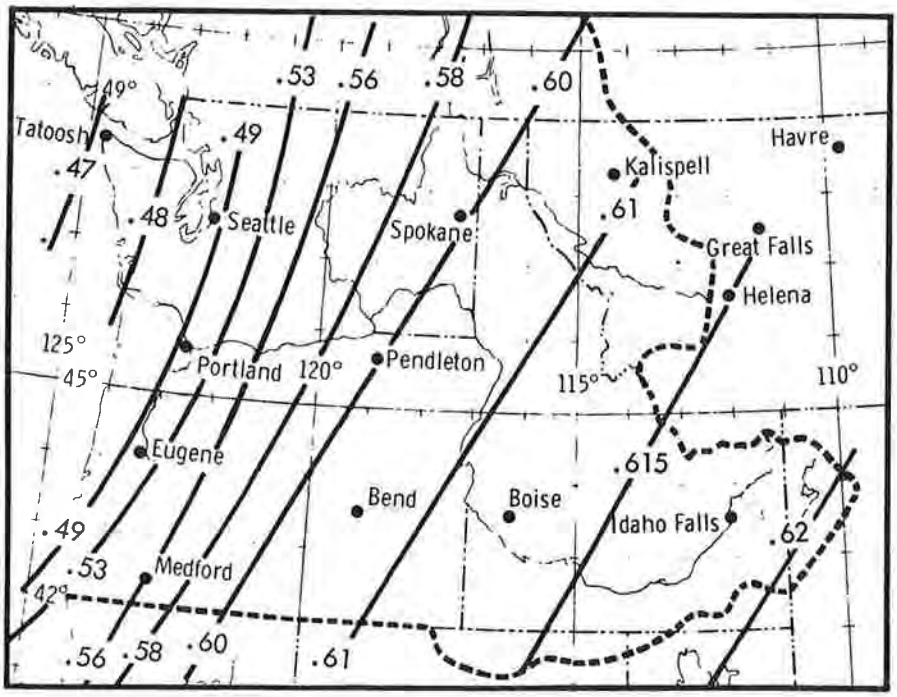

Figure 3-29b. April 6/24-hr. rain ratio map

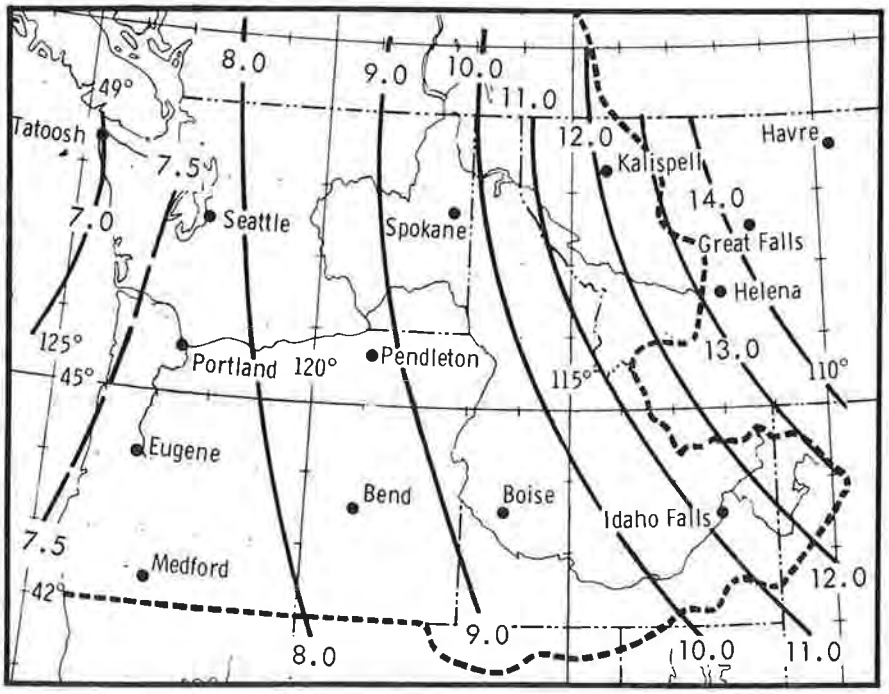

Figure 3-30a. May 24-hr. 10-sq. mi. 1000-mb. orographic storm convergence PMP index chart (in.)

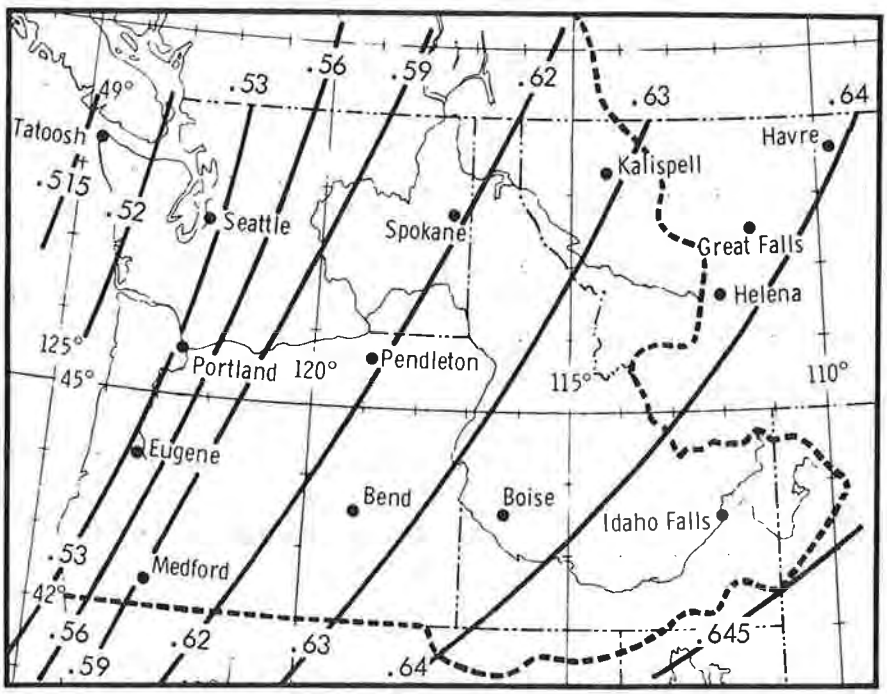

Figure 3-30b. May 6/24-hr. rain ratio map

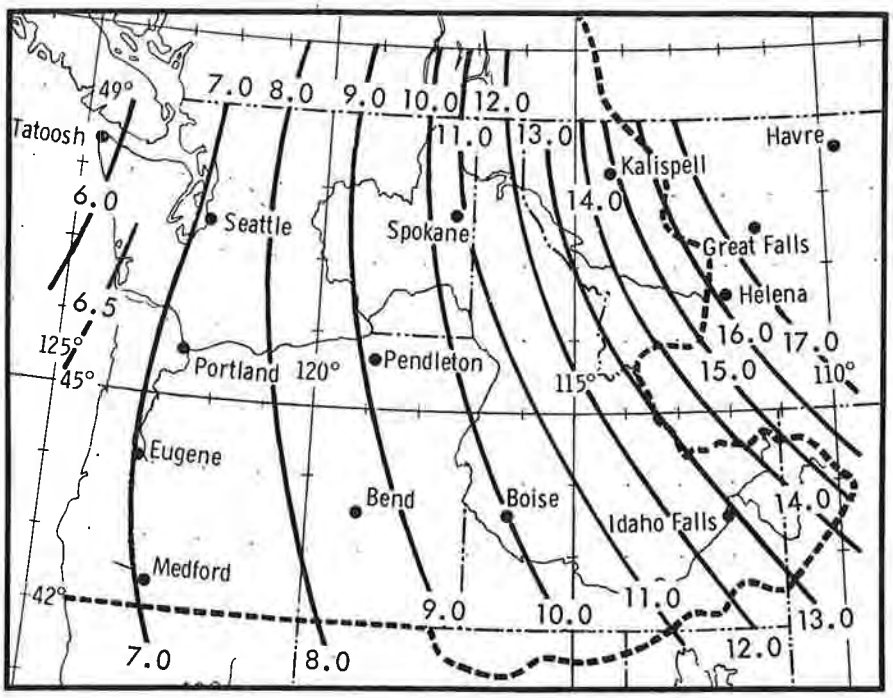

Figure 3-31a. June 24-hr. 10-sq. mi. 1000-mb. orographic storm convergence PMP index chart (in.)

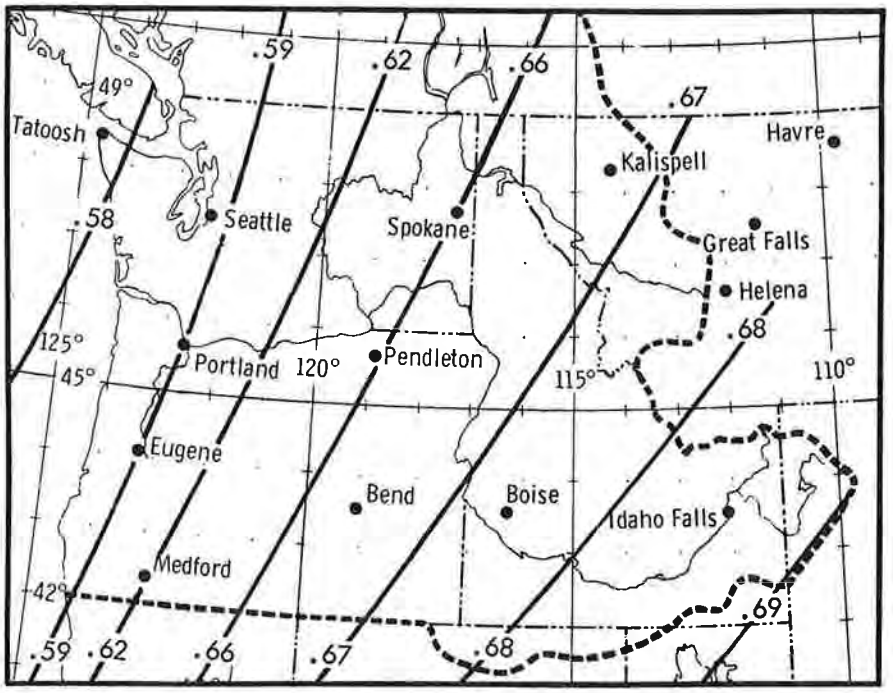

Figure 3-31b. June 6/24-hr. rain ratio map

3.29. Support for monthly 1000-mb. PMP values. The procedure outlined above to obtain monthly 1000-mb. convergence PMP values leans heavily on winter precipitation to the west and on seasonal variation of large rains. To assure that the overall pattern is consistent, checks on PMP are desirable from large storms in other areas during months of high convergence PMP.

After making sure that the following low-elevation observed rains were not augmented appreciably by orography or by local thunderstorms, they were maximized for moisture and adjusted to 1000 mb.

1. Porter, New Mex.: 9.91 inches October 10, 1930 compares with about 11 inches if figure 3-29a is extended to the south-southeast.

2. Circle, Mont.: 13.3 inches over 10 square miles June 20, 1921 adjusts to 14.7 inches at 1000 mb., compared to a June PMP value above 17 inches for that location in eastern Montana (off the edge of fig. 3-31a).

3. Indio, Calif.: 6.45 inches in 7 hours September 24, 1939 adjusts to 7.6 inches at 1000 mb. in 7 hours and about 10 inches in 24 hours, using a California October 7/24-hr. ratio from HMR 36. This value fits the September 24-hr. 10-sq. mi. 1000-mb. map (not shown) extended southward through Nevada.

3.30. Comparison with values for adjacent regions. January orographic storm 24-hr. 1000-mb. convergence PMP is up to 13 percent higher at the California border than corresponding values during cool months given in HMR 36. The difference arises largely from use of geographically constant P/M in HMR 36. Values for the convergence-only storm at the border differ most in April, being 4 percent lower than California values from HMR 36.

Values along the Continental Divide can be compared with HMR 33 (2) extrapolated from longitude 105°W. if allowance is made for elevation in the latter report. The seasonal trend in HMR 33 (2), with relatively low winter values, is greater than that in figure 3-22 for central Montana. Summer values are comparable.

3-E. TERRAIN ADJUSTMENTS ON CONVERGENCE PMP

3.31. Factors which bring about geographic variation in convergence precipitation are difficult to assess because of their mutual interdependence and because of the added orographic component of rainfall. Augmentation of convergence rain near the coast and depletion at upper elevations and to lee of mountains are considered in this section as modifications to 1000-mb. convergence PMP values (figs. 3-23a to 3-31a).

Stimulation

3.32. Particular attention was given to PMP values within a few miles of the coast. Here it is believed that both mean annual and storm

precipitation exceed that over the open sea. The basic "convergence PMP" estimates cover the rainfall associated with general storminess more or less independent of terrain. The "orographic PMP" estimates cover the precipitation associated with the laminar flow of wind up mountain slopes. At the Pacific Coast there is a third effect. Increased friction over the land and low hills and slopes tends to trigger the release of instability in the air. The result is greater lift of the air on the average in the coastal region and more precipitation than is accounted for by the "convergence rain" plus "orographic rain" as treated in this report. This increase we call stimulation.

3.33. Evidence of stimulation is found in the rainfall records of San Francisco by comparison with Farallon Island 25 miles offshore. The overall difference is judged to average about 23 percent in major storms. Similar direct comparisons along the Washington-Oregon coast are not possible because of lack of offshore records near non-orographic coastal locations. One indirect comparison is the considerably lower mean annual precipitation at offshore Tatoosh Island (lat. 48°N.) than at Tillamook, Oreg. (lat. 45.5°N.) where negligible orographic precipitation would be computed.

Evidence of stimulation is found also in the foothills of major mountain ranges, for example the Cascades and Sierra Nevadas.

3.34. Application. To incorporate this effect into the PMP estimates, a stimulation map has been constructed (fig. 3-32). The maximum value shown is 20 percent of the general convergence PMP index. This results in an increase of up to about 1.5 inches/day.

The rules used in drawing coastal percentual isolines on figure 3-32 were to assign 20 percent to coastal areas directly exposed to directions south-southwest, southwest, west-southwest and west; 10 percent or more where there is an upwind barrier from one of these directions; and zero for areas with an upwind barrier in two or more of these directions. The rules for Cascade foothills were to substitute 10 percent for 20 percent and 5 percent for 10 percent in the coastal procedure. This recognizes reduced stimulation in inland areas because of lack of saturation in lower levels and prior discharge of instability. The concept of stimulation was not applied east of the Cascades.

Depletion of 1000-mb. convergence PMP for elevation and barrier

3.35. Effective dew point elevation. In the development of 1000-mb. moisture in section 3-B of this chapter, station moisture (dew point) was normalized to 1000 mb. by use of the moist adiabatic rate of increase from station elevation to 1000 mb. In estimating PMP for higher elevations it is necessary to deplete moisture similarly, namely by the moist adiabatic rate from 1000 mb. up to the elevation where the dew point was observed. This elevation is termed "effective dew point elevation." Figure 3-33 is a map of such elevations based in a general way on elevation of stations used in dew point development in the Northwest and in bordering states. In a

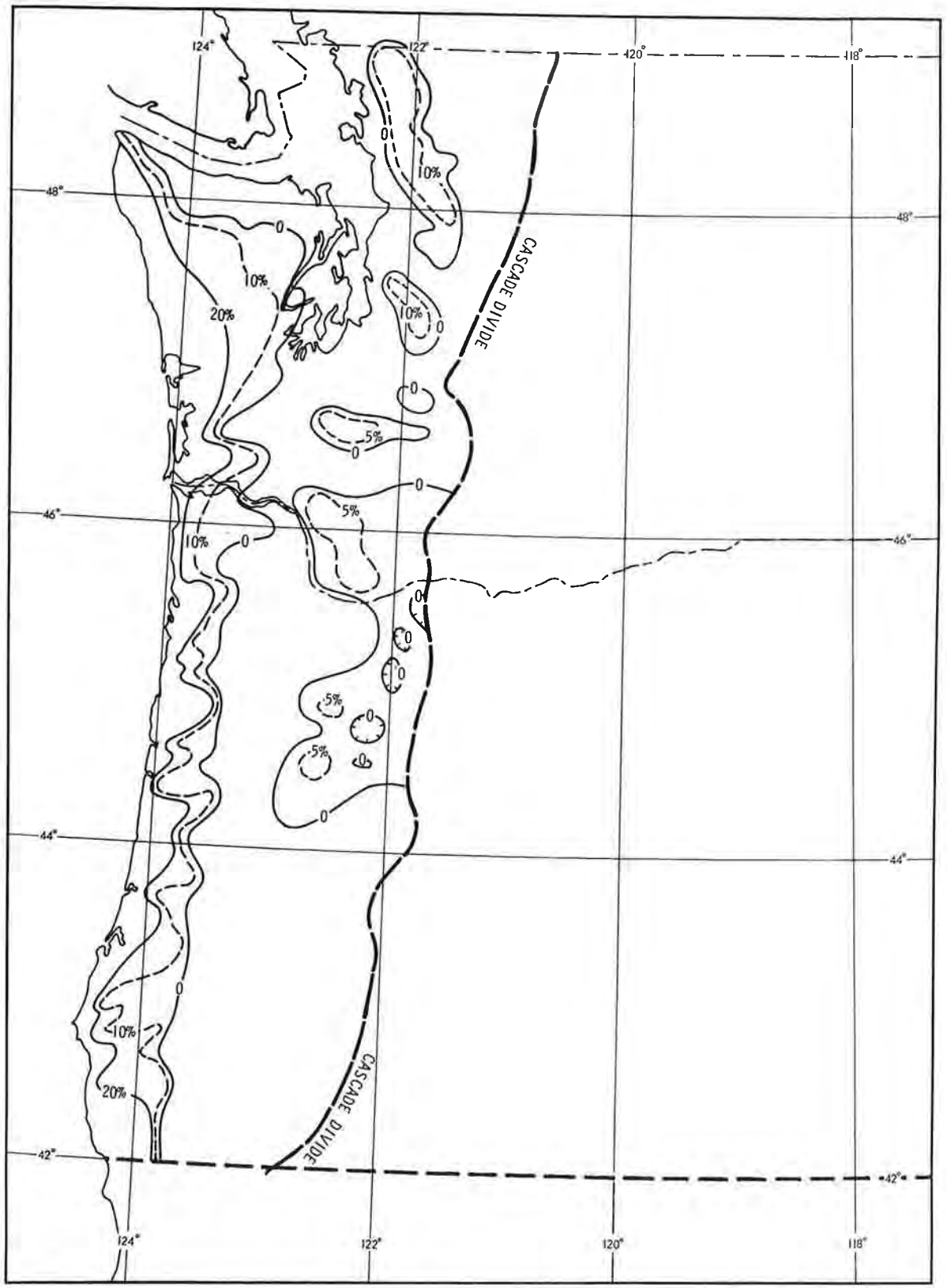

Figure 3-32. Stimulation as a percent of 1000-mb. values of convergence PMP (Values are 20% from coast to 20% line and zero between zero lines.)

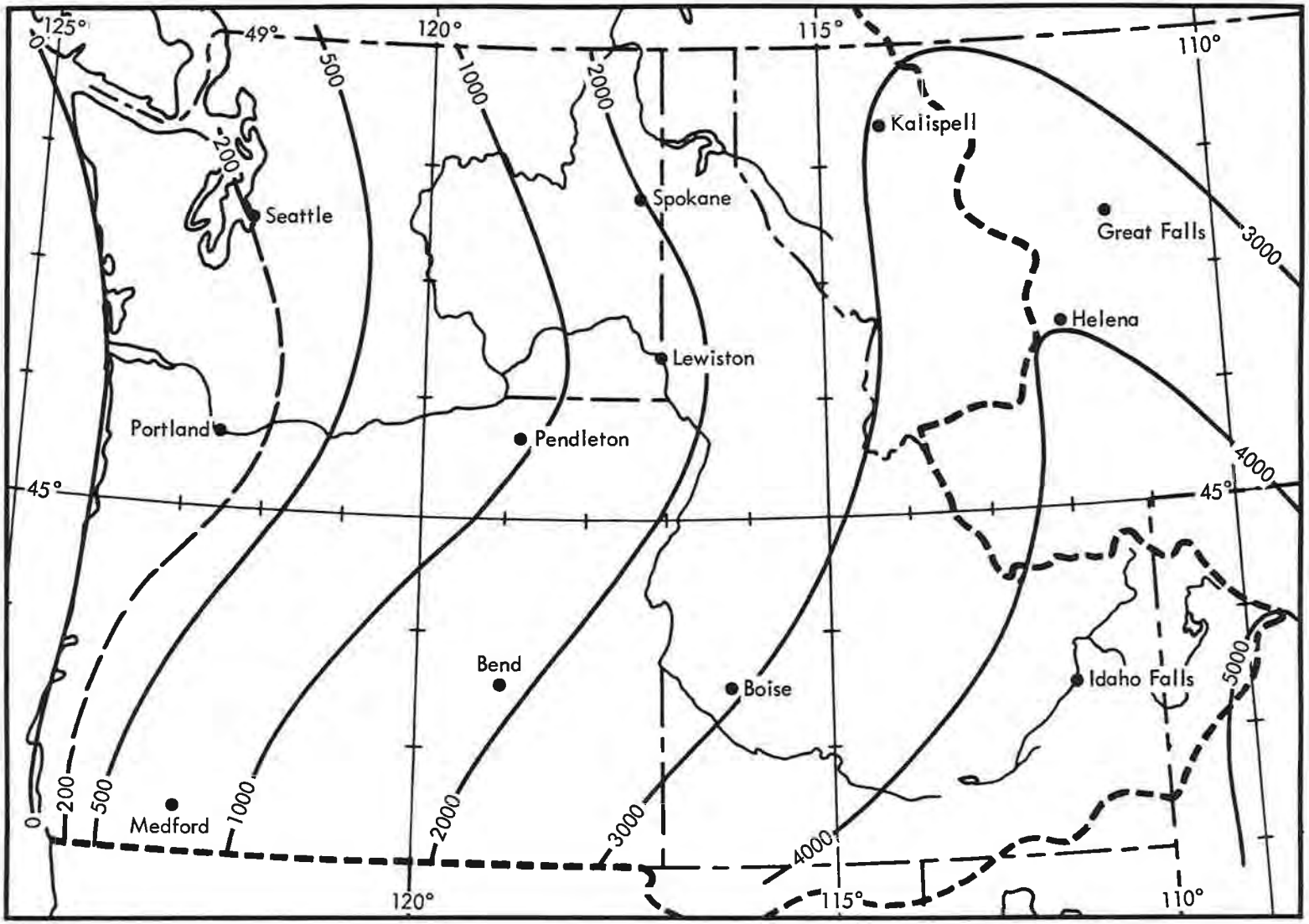

Figure 3-33. Effective dew point elevation map (ft.)

sense, this is an extremely smoothed contour map from the Pacific Ocean to the Continental Divide, ignoring the Cascades from which no dew point data were derived. Convergence PMP at 1000 mb. was reduced by the moist adiabatic rate of decrease up to this effective dew point elevation.

3.36 Rate of depletion above effective dew point elevation. Above the effective dew point elevation, a depletion rate of 5 percent per 1000 feet was used up to ground elevation on windward slopes and to barrier height on lee slopes.

3.37 On windward slopes the main factor considered to alter the reduction of convergence PMP with elevation from the moist adiabatic rate is that convergence mechanisms related to wind tend to increase with elevation in response to wind increase with elevation. This increase is greatest at lowest levels, as is the moist adiabatic rate of decrease of moisture. The net effect leads to the concept of constant decrease of convergence rain with elevation. The rate of decrease adopted, 5 percent per 1000 feet elevation, approximates the adiabatic rate of dropoff of moisture above 8000 feet, as shown in figure 3-34.

3.38 In lee areas, barriers deplete the convergence mechanisms and moisture in the air column below the barrier level. Farther away from the actual barrier the "effective" barrier height is lowered to account for some recharge of both moisture and P/M.

3.39 Support for barrier control of precipitation magnitude and independence from elevation at site of precipitation is found in a study of rain data from stations in western Colorado and eastern Utah. All but the highest are lee stations with respect to nearby or distant barriers. Figure 3-35 is a plot of greatest 3-day May-June rains (1931-1952) in this area. By June, pressure gradients have slackened while instability effects are not yet strong. Then precipitation increase with elevation due to these factors, while present, is at its lowest. The study area elevations vary from 4000 to 9000 ft. While there is evidence of a barrier depletion below 5000 ft. and of considerable orographic increase above 8000 ft., values vary little between 5000 and 8000 ft. (A 3-day duration overcomes effect of fixed observation times on record values.)

Elevation and effective barrier map

3.40 Figures 3-36a and 3-36b show solid lines of elevation and broken lines of effective barrier height used in depleting convergence PMP due to effect of elevation and barrier on moisture and P/M. They show height of barriers to inflow from south-southwest through west, the range of directions involved in storms from the Pacific Ocean when highest moisture can be realized. Although inflow of moisture to the interior may be from the Gulf of Mexico and Gulf of California during May or June, it becomes in most instances a flow from the southwest quadrant by the time it enters storms over the basin. Barriers near the Continental Divide are drawn considering also inflow of Gulf air from an easterly quadrant.

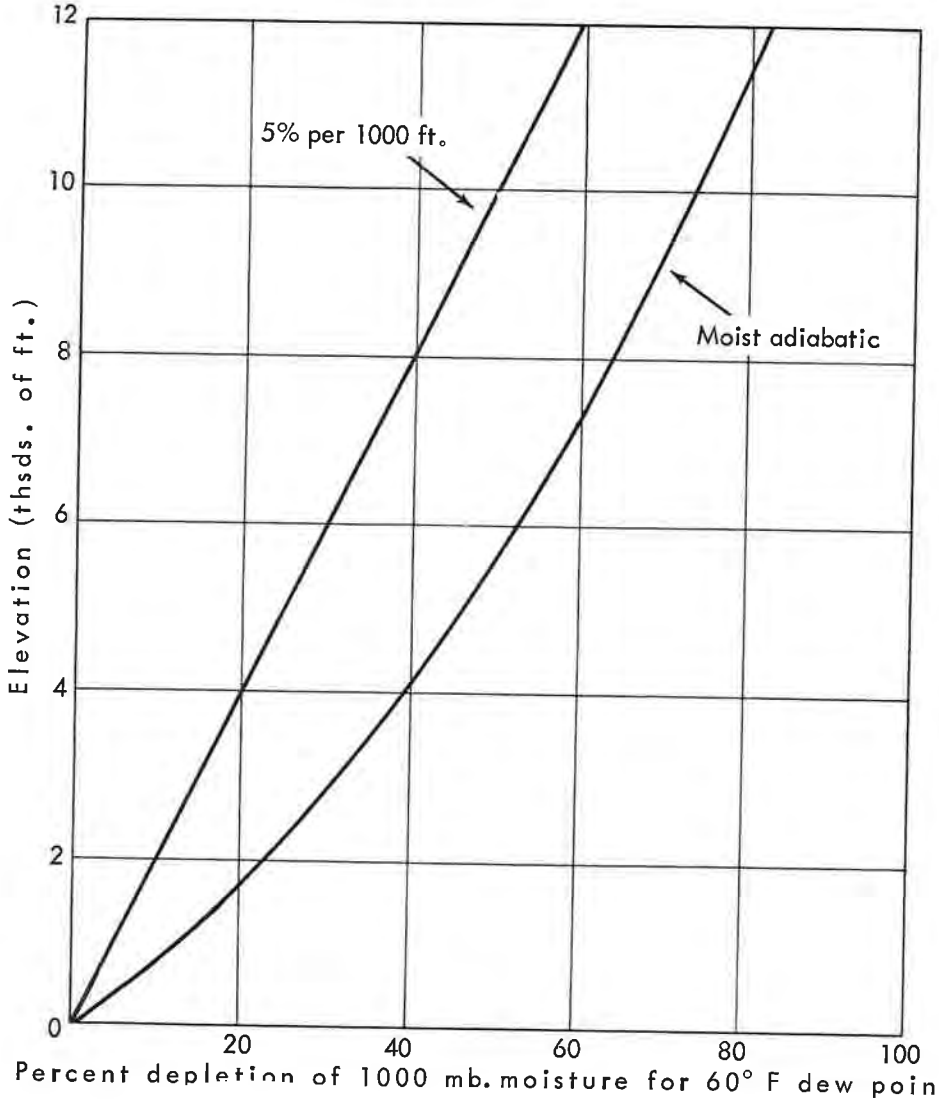

Figure 3-34. Comparison of a 5 percent per 1000-ft. depletion rate with the moist adiabatic rate

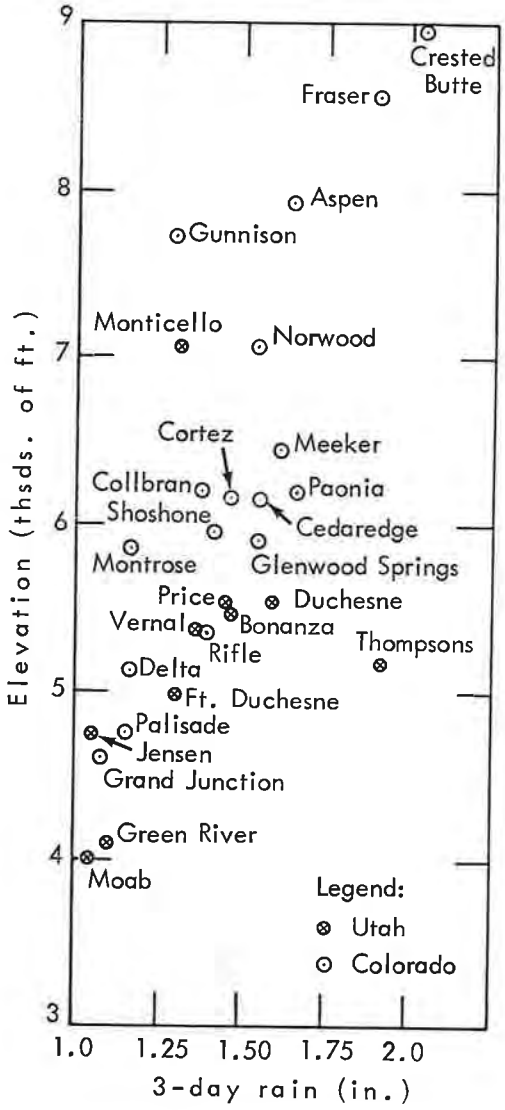

Figure 3-35. Rain-elevation relation for W. Colorado and E. Utah (May and June)

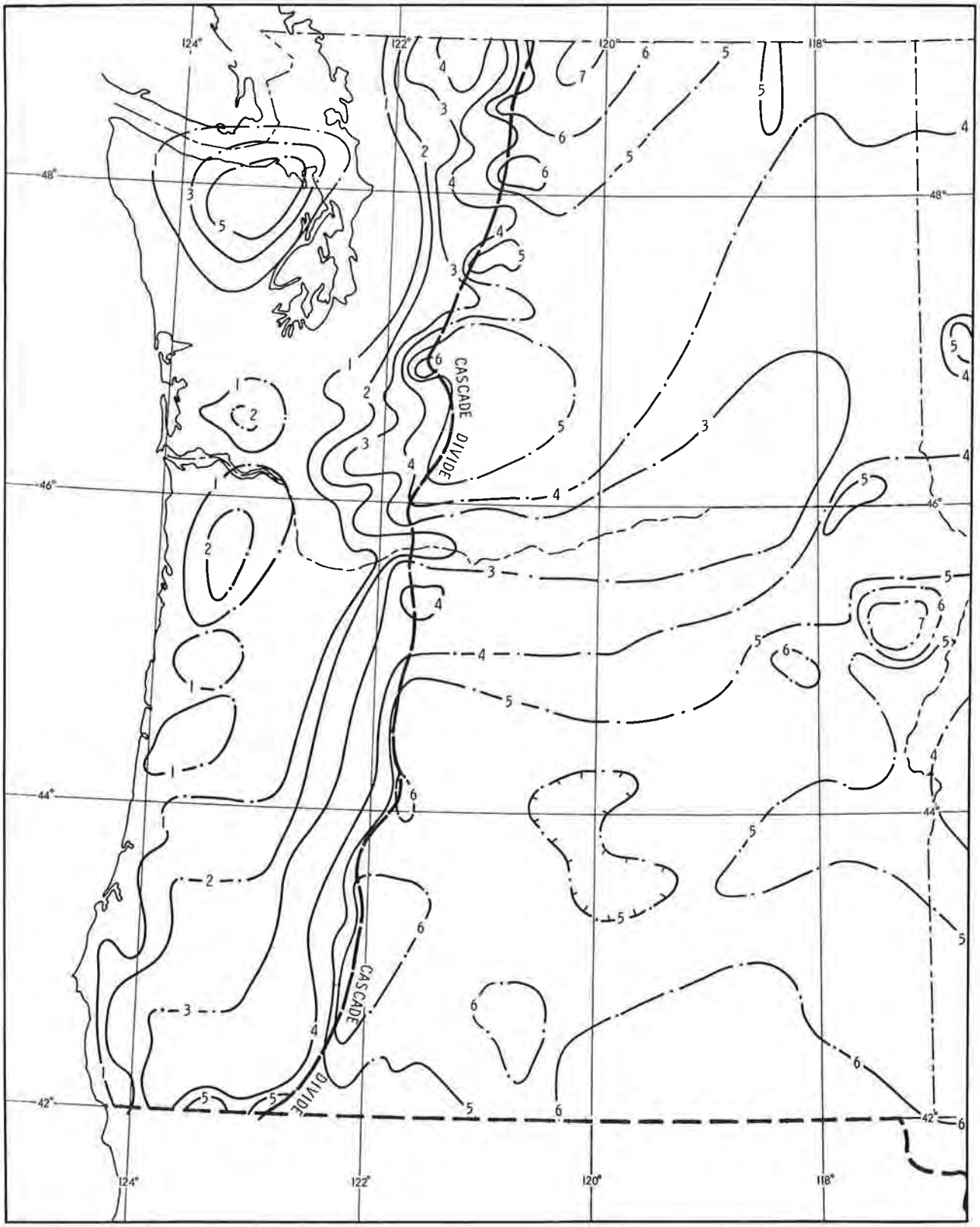

Figure 3-36a. Effective barrier-elevation chart (in thsds. of ft.)

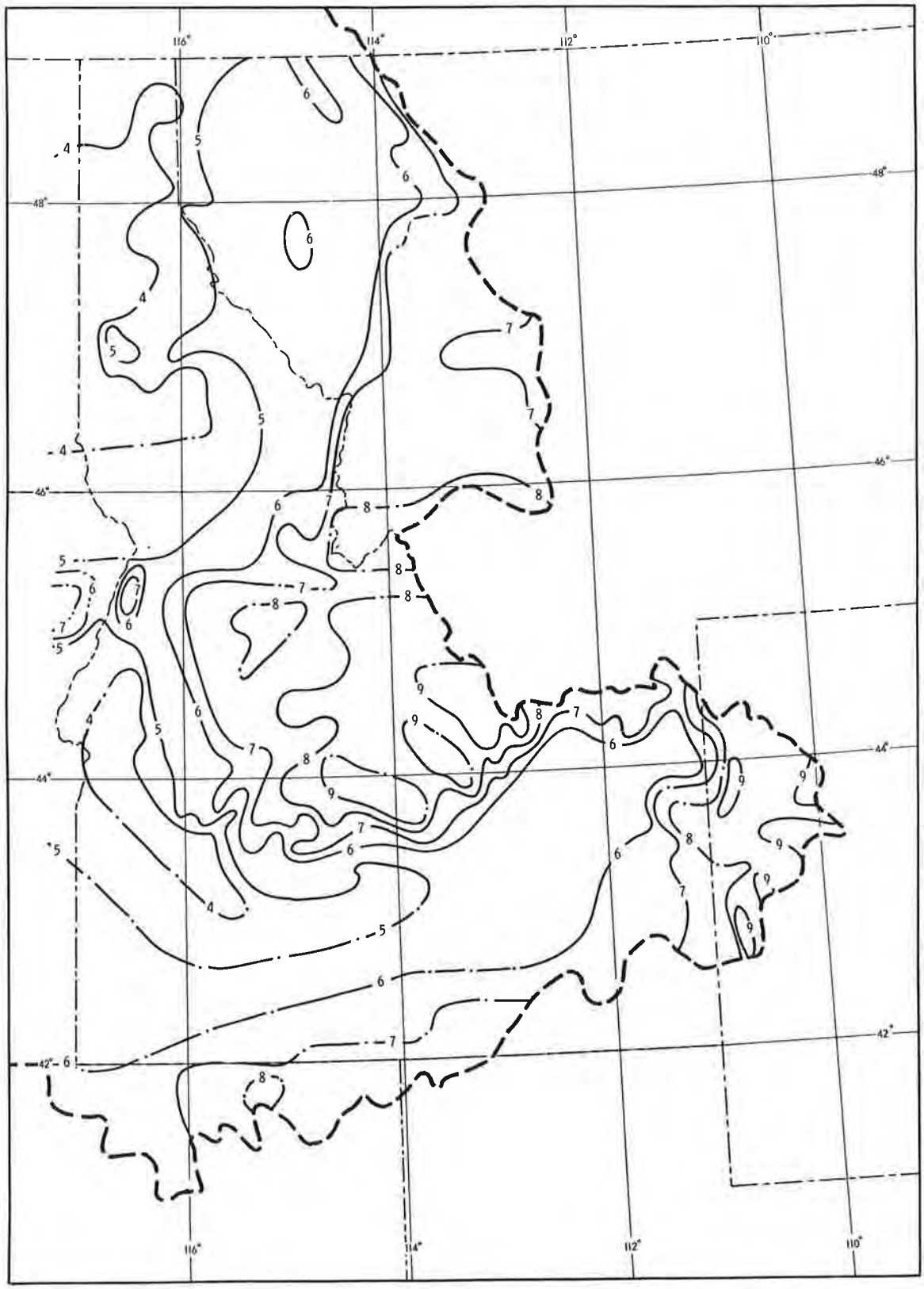

Figure 3-36b. Effective barrier-elevation chart (in thsds. of ft.)

Convergence PMP map in percent of 1000 mb.

3.41. The effects of stimulation, elevation depletion and barrier depletion were combined in a field of percents of 1000-mb. convergence PMP and added to or subtracted therefrom. The adjusted convergence PMP, in percent of 1000-mb. convergence PMP, is shown in figures 3-37a to c.

Monthly 24-hr. 10-sq. mi. convergence PMP basin indices

3.42. Orographic storm. Adjustment of basin October-June 24-hr. 1000-mb. 10-sq. mi. orographic storm convergence PMP values from figures 3-23a through 3-31a for depletion-stimulation effects outlined above is made by multiplying by the basin percent in figures 3-37a to c.

3.43. Convergence storm. Orographic storm values of basin convergence PMP multiplied by the factor 1.23 give corresponding convergence PMP values not to be combined with orographic PMP. These values apply to west of Cascades only (par. 3.28).

3-F. DURATIONAL, GEOGRAPHICAL, AND BASIN SIZE VARIATION OF CONVERGENCE PMP

First 6-hr. 10-sq. mi. convergence PMP

3.44. October-June basin values of 24-hr. 10-sq. mi. convergence PMP (pars. 3.42 and 3.43) are multiplied by basin values of 6/24-hr. rain ratio to obtain first (highest) 6-hr. 10-sq. mi. convergence PMP. These basin 6/24-hr. rain ratios are read from the monthly maps of 6/24-hr. rain ratios shown for October through June in figures 3-23b through 3-31b. The maps are drawn to monthly average 6/24-hr. rain ratios for west and east of Cascades from figures 3-18a and 3-18b, respectively, and for central California from figure 4-9, HMR 36. Use of these fields avoids discontinuities in 6/24-hr. ratios (and thus of 6-hr. convergence PMP) at the Cascade Ridge.

Durational and geographical variation of monthly 10-sq. mi. convergence PMP

3.45. Development. The average 6/24-hr. rain ratios shown on figures 3-18a and 3-18b are plotted by months in figure 3-38 vs. average 72/24-hr. rain ratios (fig. 3-19) for corresponding months and mean locations. A straight-line fit to this monthly 6/24- vs. 72/24-hr. data plot of figure 3-38 is the basis of figure 3-39. It shows a family of incremental depth-duration curves to 72 hours in percent of 1st (highest) 6 hours, for 6/24-hr. ratios ranging from .42 to .69. The above steps provide seasonal and geographical smoothing of incremental 6-hr. rain to 72 hours over the Pacific Northwest. Incremental and cumulative 6-hr. percents of 1st 6-hr. rain read from figure 3-39 are tabulated in table 3-3.

3.46. Use. By entering table 3-3 with a 6/24-hr. ratio for a given basin and month (Oct.-June) from figures 3-23b through 3-31b, incremental

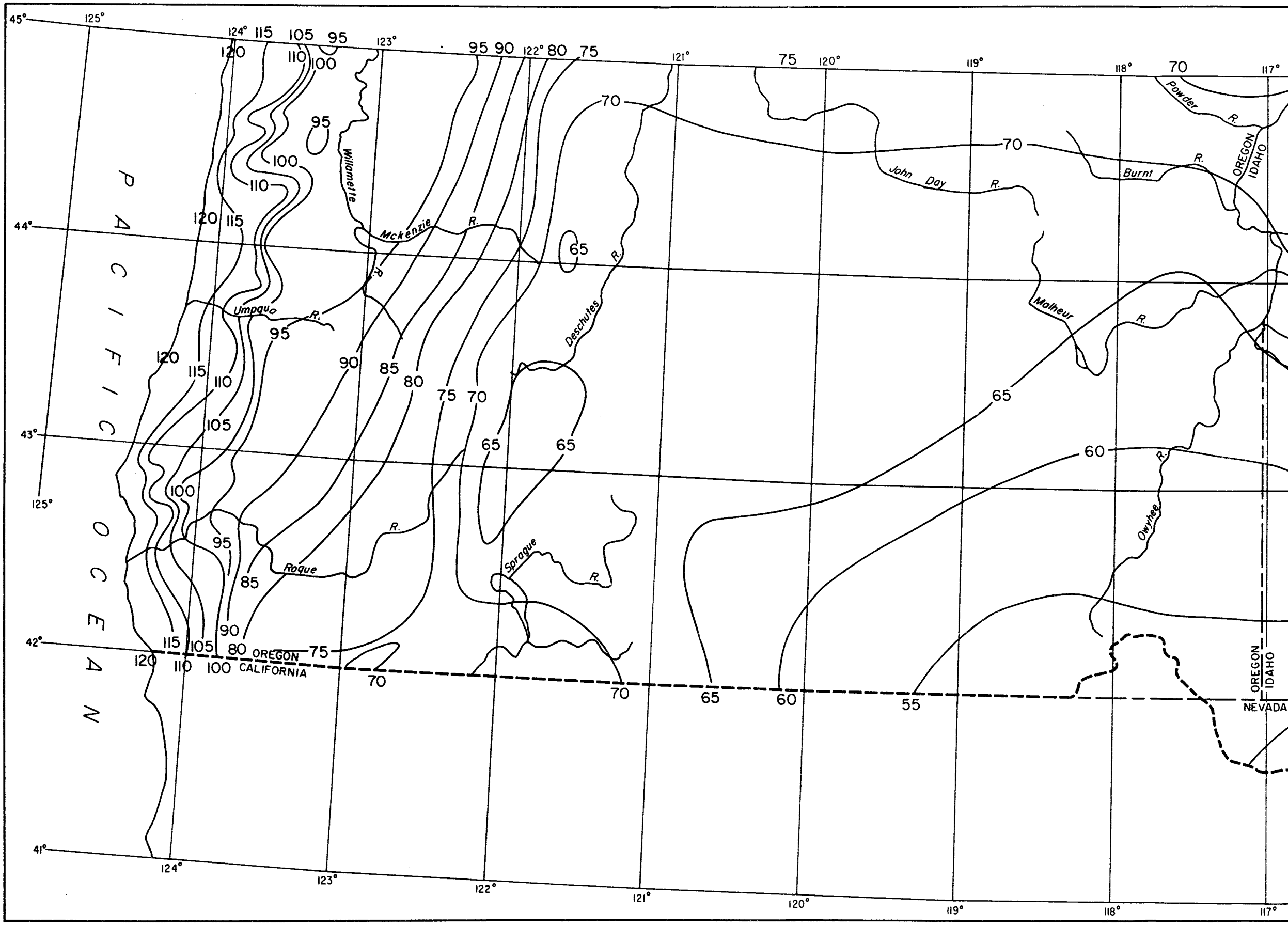
PACIFIC OCEAN
OREGON
CALIFORNIA
IDAHO
NEVADA
Willamette R.
Mckenzie R.
Umpqua R.
Roque R.
Deschutes R.
John Day R.
Powder R.
Burnt R.
Malheur R.
Owyhee R.
Sprague R.
45°
44°
43°
42°
41°
125°
124°
123°
122°
121°
120°
119°
118°
117°

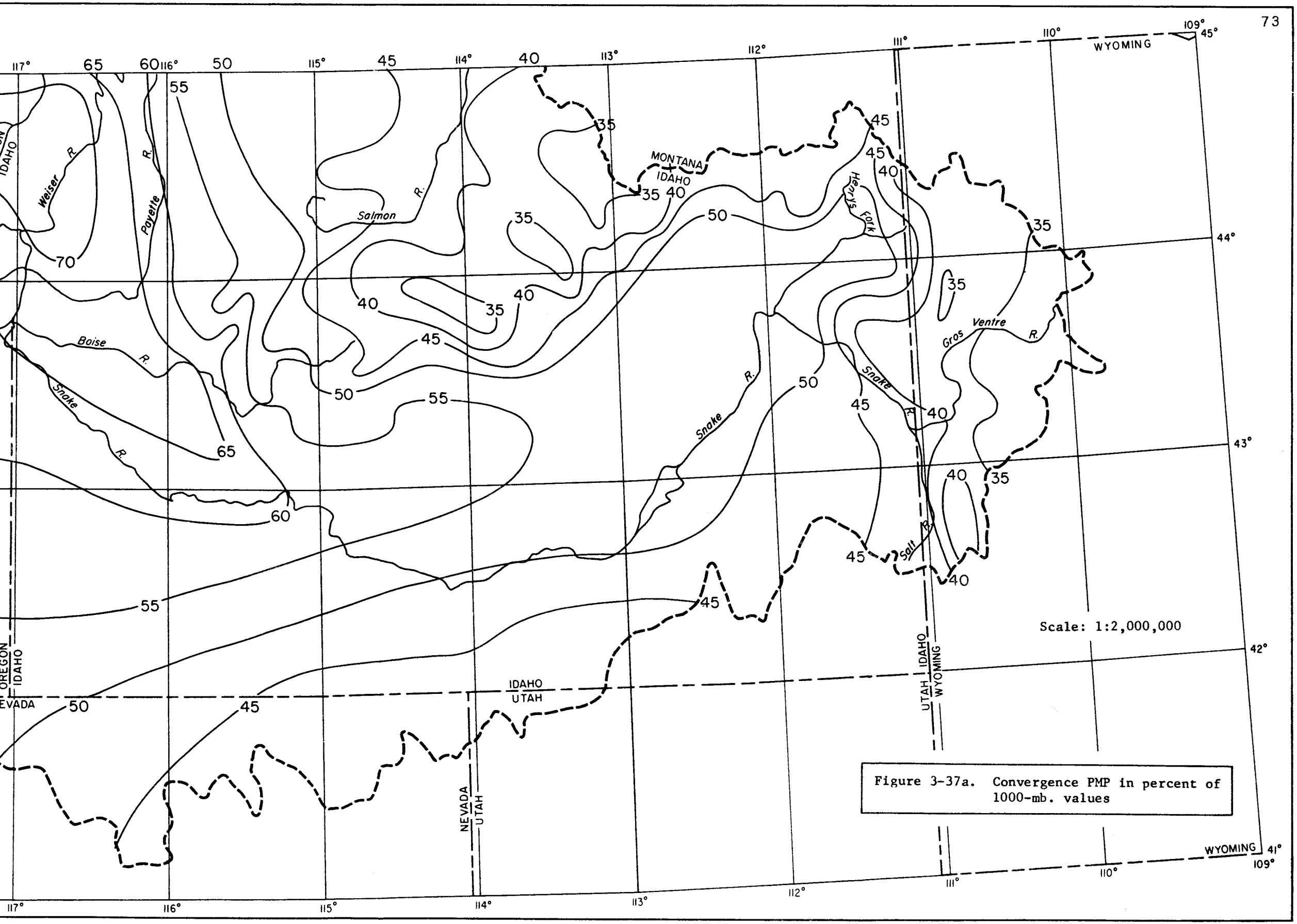

Scale: 1:2,000,000

Figure 3-37a. Convergence PMP in percent of 1000-mb. values

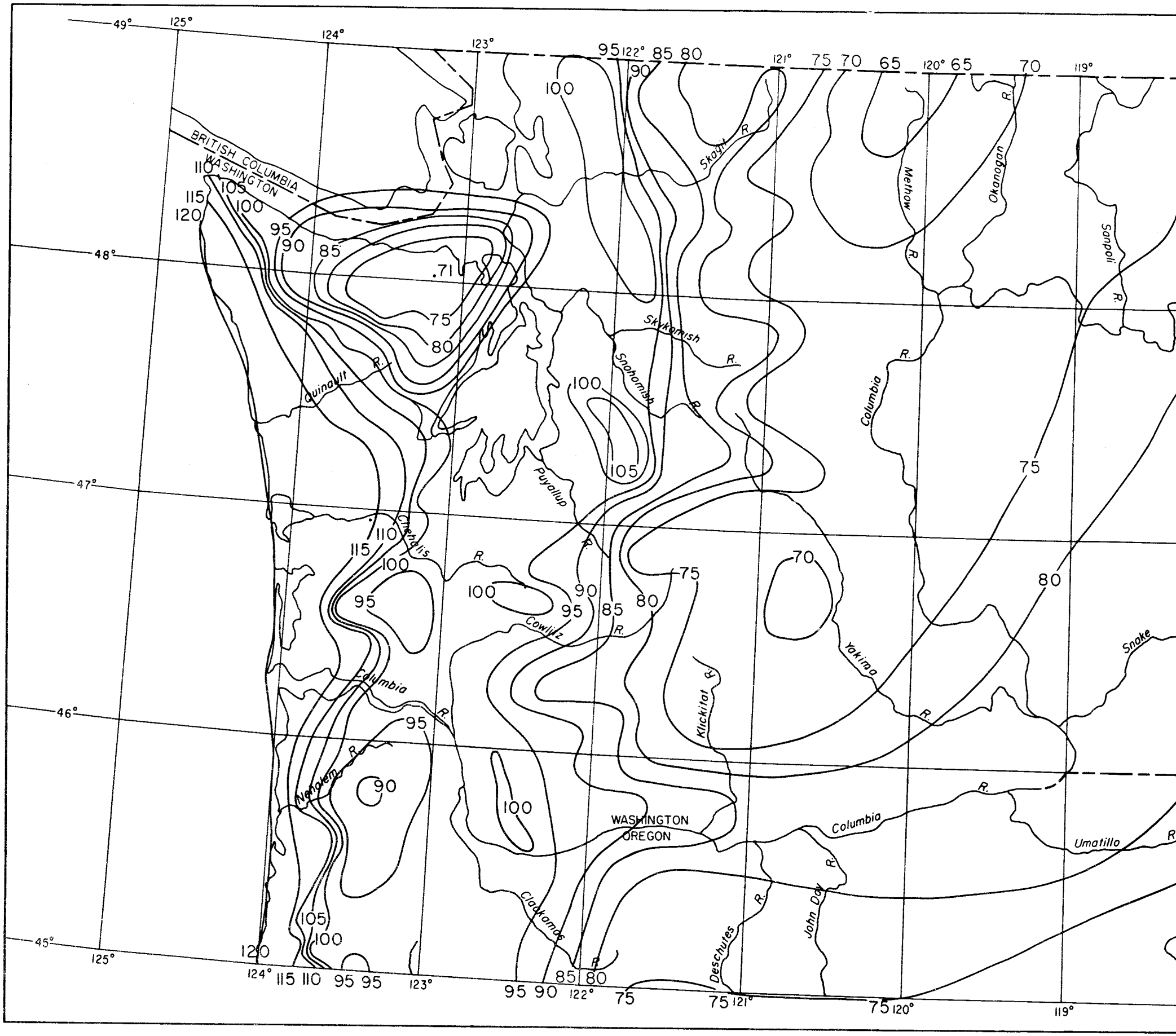
BRITISH COLUMBIA
WASHINGTON
WASHINGTON
OREGON
Quinault R.
Chehalis R.
Cowlitz R.
Columbia R.
Nehalem R.
Clackamas R.
Puyallup R.
Snohomish R.
Skykomish R.
Skagit R.
Methow R.
Okanogan R.
Sanpoil R.
Klickitat R.
Yakima R.
Deschutes R.
John Day R.
Umatilla R.
Snake R.
Columbia R.
49°
48°
47°
46°
45°
125°
124°
123°
122°
121°
120°
119°

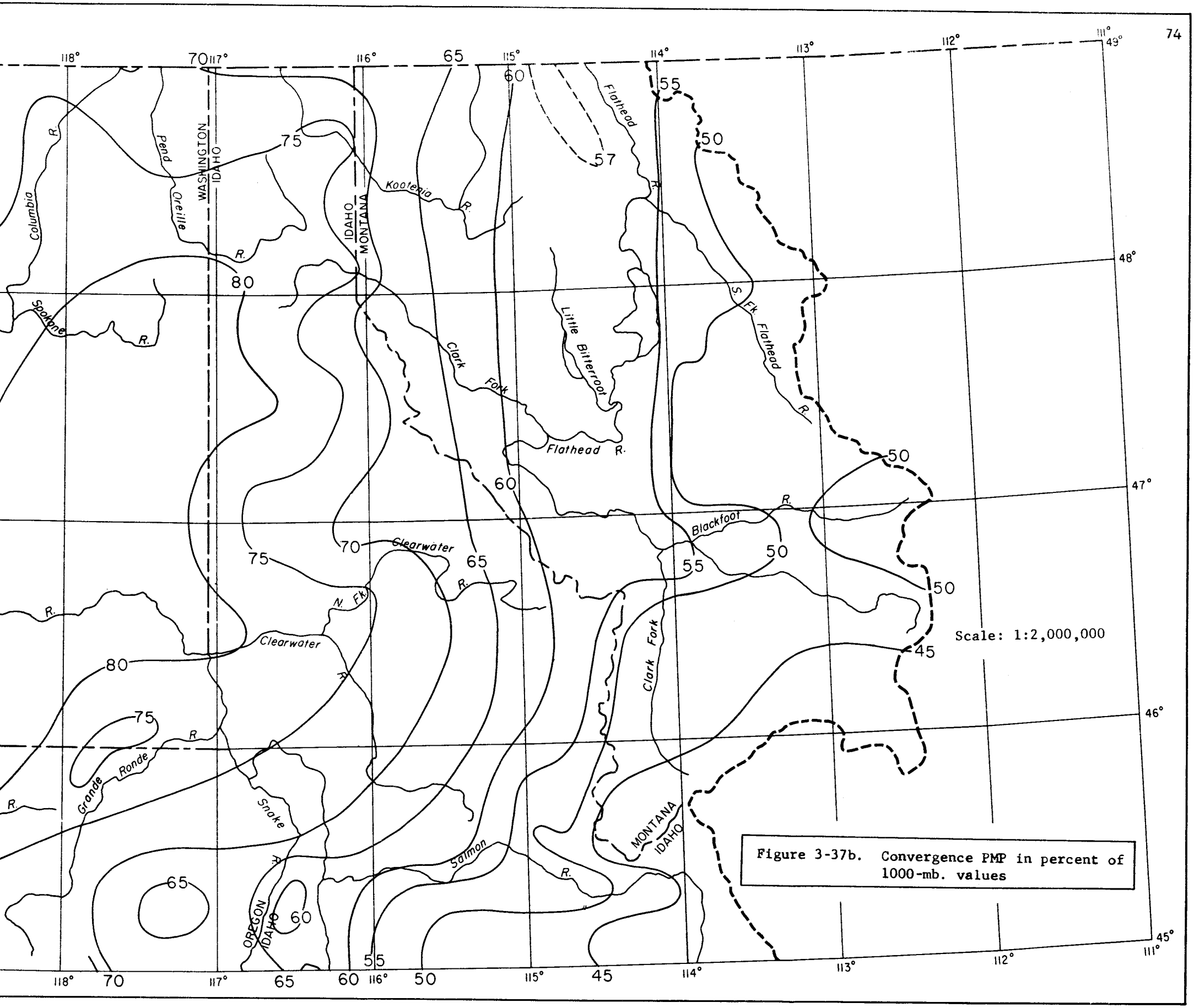

Figure 3-37b. Convergence PMP in percent of 1000-mb. values

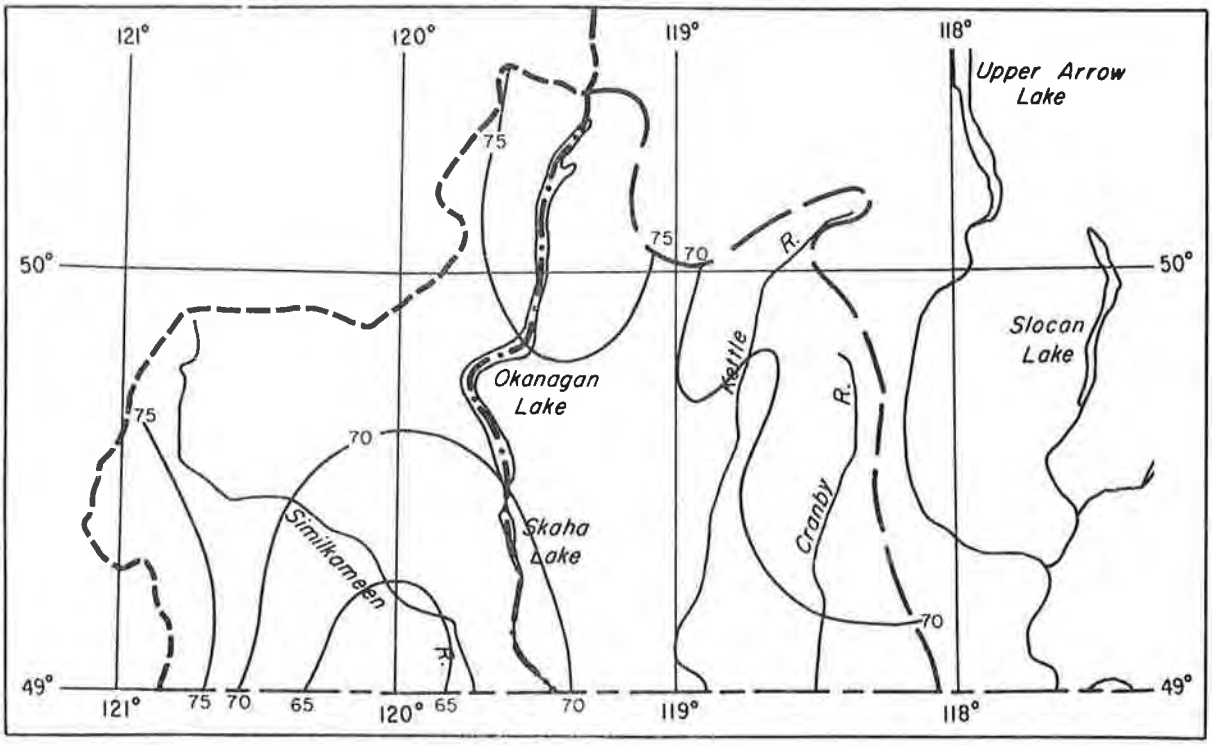

Scale: 1:2,000,000

Figure 3-37c. Convergence PMP in percent of 1000-mb. values

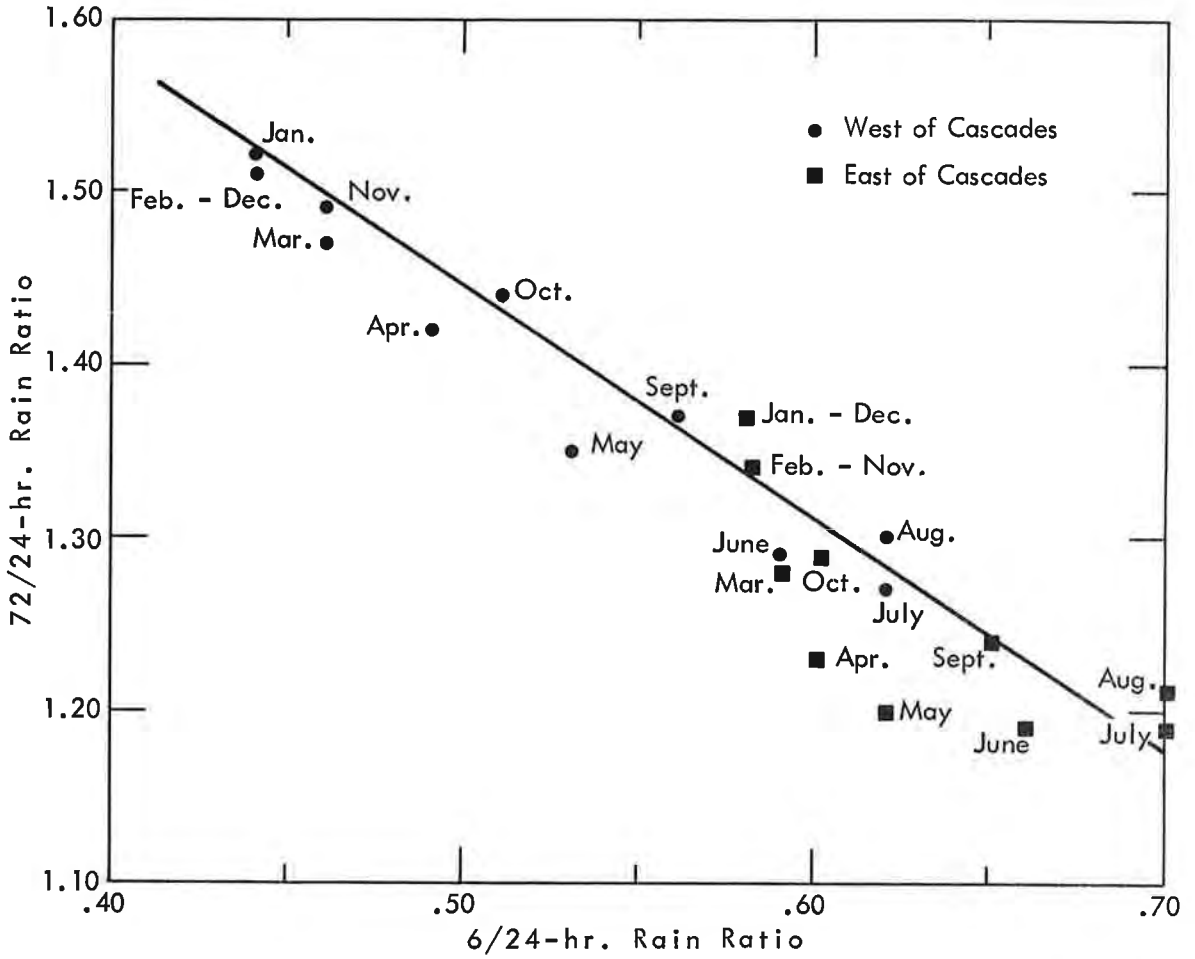

Figure 3-38. Variation of 72/24-hr. rain ratio with 6/24-hr. rain ratio

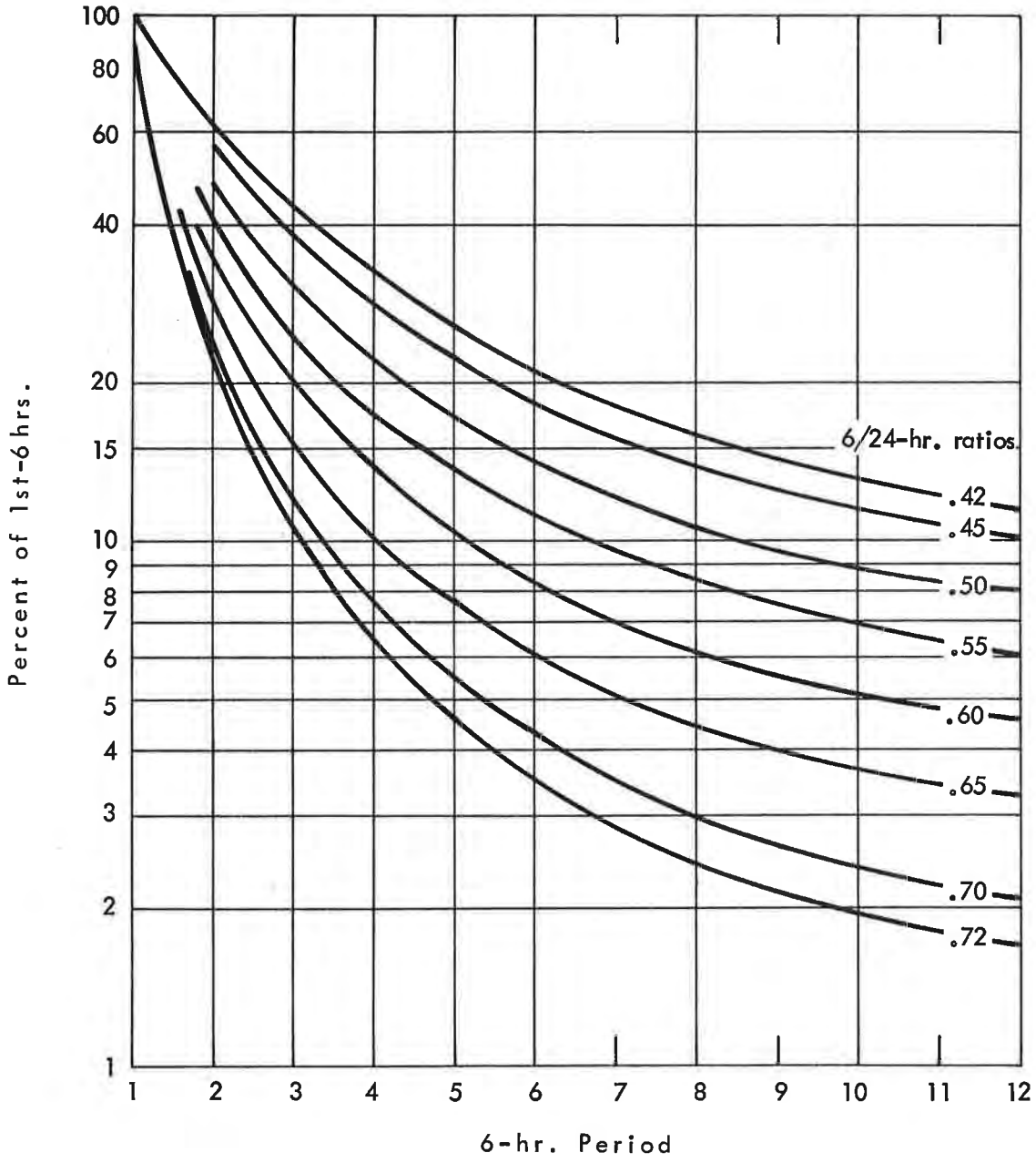

Figure 3-39. Durational decay of 10-sq. mi. convergence PMP with 6/24-hr. rain ratio

and/or cumulative percents of 1st 6-hr. 10-sq. mi. convergence PMP are obtained. These percents multiplied by 1st 6-hr. convergence PMP (par. 3.44) give PMP values for other 6-hr. periods or other durations. Note that accumulated percents in table 3-3 are to be used in computing 10-sq. mi. convergence PMP only.

Depth-area relations

3.47. The depth-area relations that reduce 10-sq. mi. convergence PMP for basin size to 5000 square miles are given in graphical form by months October-June in figures 3-40a and 3-40b for the first four 6-hr. periods.

3.48. Development. The 6-hr. incremental areal reduction factors were derived from October-April Eastern United States storm depth-area relations described in paragraph 4.48, HMR 36. The May-September depth-area relations were obtained in a similar manner.

3.49. The procedure followed to obtain the percents in figures 3-40a and 3-40b is outlined below:

(1) Plot and smooth seasonally the 1st 6-hr. rain percents of each month for 10, 40, 100, 200, 600 and 1000 square miles.

(2) Smooth similar plots of 2d, 3d and 4th periods for areal, seasonal and durational consistency.

(3) Plot smoothed percents against basin size for successive 6-hr. periods (figs. 3-40a and 3-40b) and draw percent lines.

(4) Extend to 5000 miles by extrapolation.

3.50. Use. The first three or four incremental 6-hr. PMP values obtained from table 3-3 are reduced for basin size by multiplying by October-June per cents in figures 3-40a and 3-40b. No decrease for basin size is required for other 6-hr. increments of PMP.

Depth-duration relations for 1 and 3 hours*

3.51. Seasonal 1/6-hr. and 3/6-hr. rain ratios developed in a manner similar to that of 6/24-hr. ratios proved unreliable. Because of predominance of low-intensity rain in the limited data and the wide scatter in the relations, they are considered inferior to 1/6- and 3/6-hr. ratios interpolated from a greatly expanded version of the 1st 24-hr. portion of figures 3-42a and 3-42b. The latter are cumulative depth-duration curves drawn through the monthly 24- and 72-hr. percents of 6 hours, at a mean west- and mean east-of-Cascades location, respectively. (The percents for 72 hours come from the 72/24-hr. value read along the straight-line relation of figure 3-38 for each monthly average 6/24-hr. rain ratio). From these interpolations, October-June 3-hr. percents of 6 hours for east- and west-of-Cascades are plotted at 10 square miles in figure 3-41. For 1 hour, similar

*Please see revision of section 3.51, dated April 1981, which is included at the end of this publication.

percents are shown. Curve A applies for October-April and curve B for June. May percents may be interpolated. The areal decay shown is adopted from table 4-3 of HMR 36. No geographical smoothing at the Cascade Ridge line of the west and east percents is attempted.

Table 3-3

INCREMENTAL AND ACCUMULATED PERCENTS OF 1ST 6-HR. 10-SQ. MI. CONVERGENCE PMP, TO 72 HOURS FOR VARIOUS 6/24-HR. RATIOS (FROM FIG. 3-39)

6/24-hr. Ratio	Percent of 1st 6-hr. period							
	1st	2d	3d	4th	5+6	7+8	9+10	11+12
.42	100	62	43	33	46	34	27	23
	100	162	205	238	284	318	345	368
.43	100	60	41	31	44	32	25	22
	100	160	201	232	276	308	333	355
.44	100	58	39	30	42	31	24	21
	100	158	197	227	269	300	324	345
.45	100	56	38	28	40	30	23	21
	100	156	194	222	262	292	315	336
.46	100	54	36	26	38	29	22	20
	100	154	190	216	254	283	305	325
.47	100	52	34	25	36	27	21	19
	100	152	186	211	247	274	295	314
.48	100	50	32	24	34	26	20	18
	100	150	182	206	240	266	286	304
.49	100	49	31	23	32	24	19	17
	100	149	180	203	235	259	278	295
.50	100	48	30	22	30	23	18	16
	100	148	178	200	230	253	271	287
.51	100	46	28	21	29	22	18	15
	100	146	174	195	224	246	264	279
.52	100	44	27	20	28	21	17	14
	100	144	171	191	219	240	257	271
.53	100	43	26	19	27	20	16	13
	100	143	169	188	215	235	251	264
.54	100	42	25	18	26	19	15	12
	100	142	167	185	211	230	245	257
.55	100	41	24	17	25	18	14	12
	100	141	165	182	207	225	239	251

Table 3-3 (Cont'd.)

INCREMENTAL AND ACCUMULATED PERCENTS OF 1ST 6-HR. 10-SQ. MI. CONVERGENCE PMP, TO 72 HOURS FOR VARIOUS 6/24-HR. RATIOS (FROM FIG 3-39)

6/24-hr. Ratio	Percent of 1st 6-hr. period							
	1st	2d	3d	4th	5+6	7+8	9+10	11+12
.56	100	39	23	16	23	17	13	11
	100	139	162	178	201	218	231	244
.57	100	38	22	16	22	16	12	10
	100	138	160	176	198	214	226	236
.58	100	36	21	15	21	15	12	10
	100	136	157	172	193	208	220	230
.59	100	35	20	15	20	14	11	9
	100	135	155	170	190	204	215	224
.60	100	34	20	14	19	13	10	9
	100	134	154	168	187	200	210	219
.61	100	33	19	13	18	12	10	8
	100	133	152	165	183	195	205	213
.62	100	32	18	12	17	11	10	8
	100	132	150	162	179	190	200	208
.63	100	31	17	12	16	10	9	8
	100	131	148	160	176	186	195	203
.64	100	30	16	11	15	10	9	7
	100	130	146	157	172	182	191	198
.65	100	29	15	10	14	9	8	7
	100	129	144	154	168	177	185	192
.66	100	27	14	10	13	9	8	6
	100	127	141	151	164	173	181	187
.67	100	26	14	9	12	8	7	6
	100	126	140	149	161	169	176	182
.68	100	25	13	9	11	8	6	6
	100	125	138	147	158	166	174	178
.69	100	24	12	9	10	7	6	5
	100	124	136	145	155	162	168	173

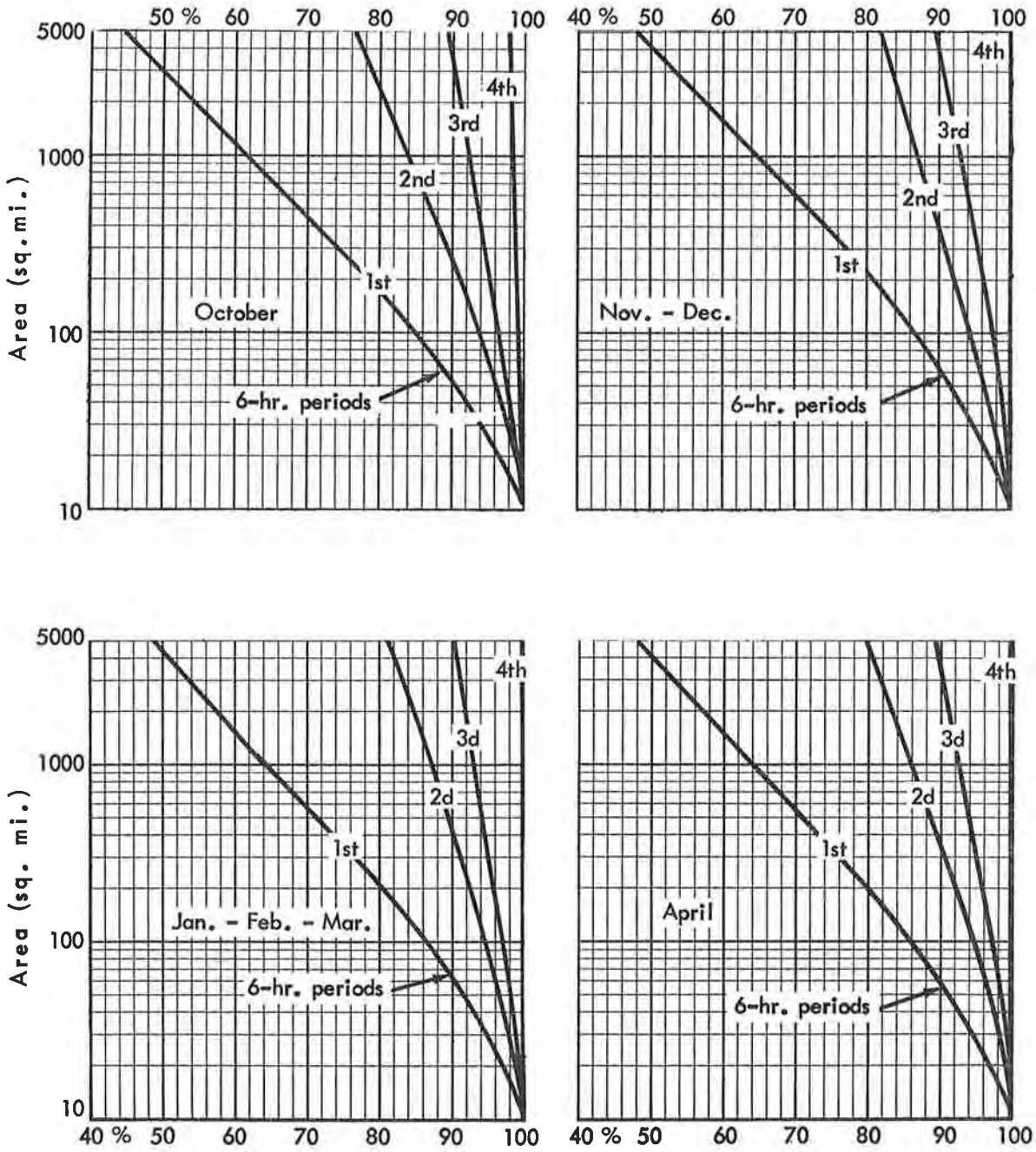

Figure 3-40a. Variation of convergence PMP with basin size (Oct.-April)

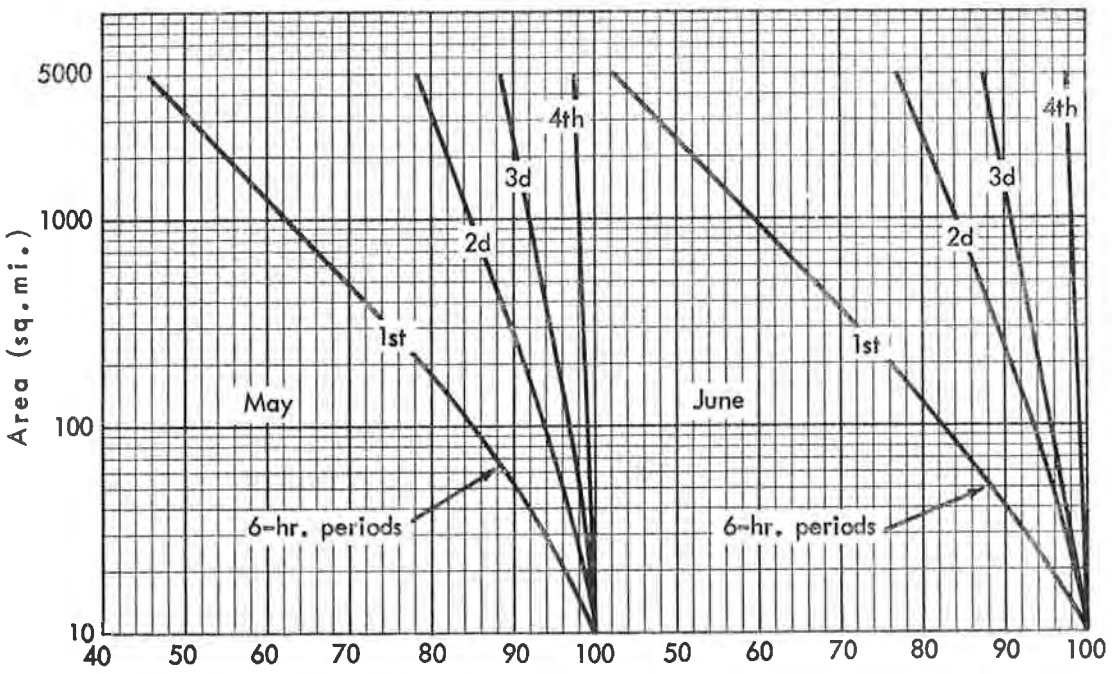

Figure 3-40b. Variation of convergence PMP with basin size (May-June)

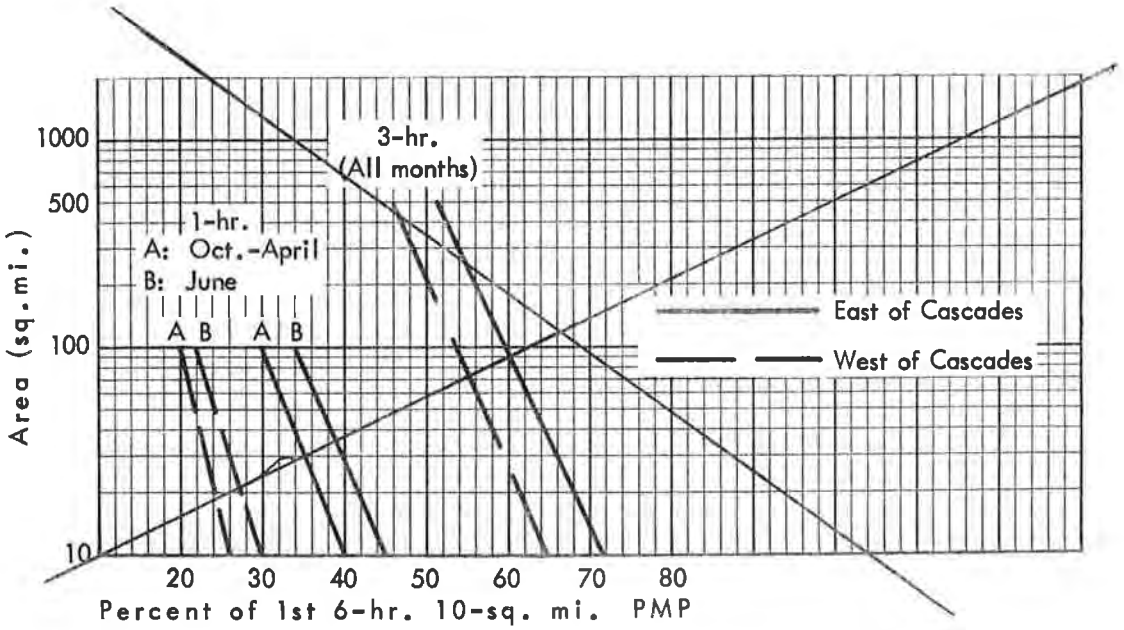

PLEASE SEE REVISION OF THIS FIGURE, DATED APRIL 1981, WHICH IS INCLUDED AT THE END OF THIS PUBLICATION.

Figure 3-41. October-June variation of short duration PMP in percent of 1st 6 hour

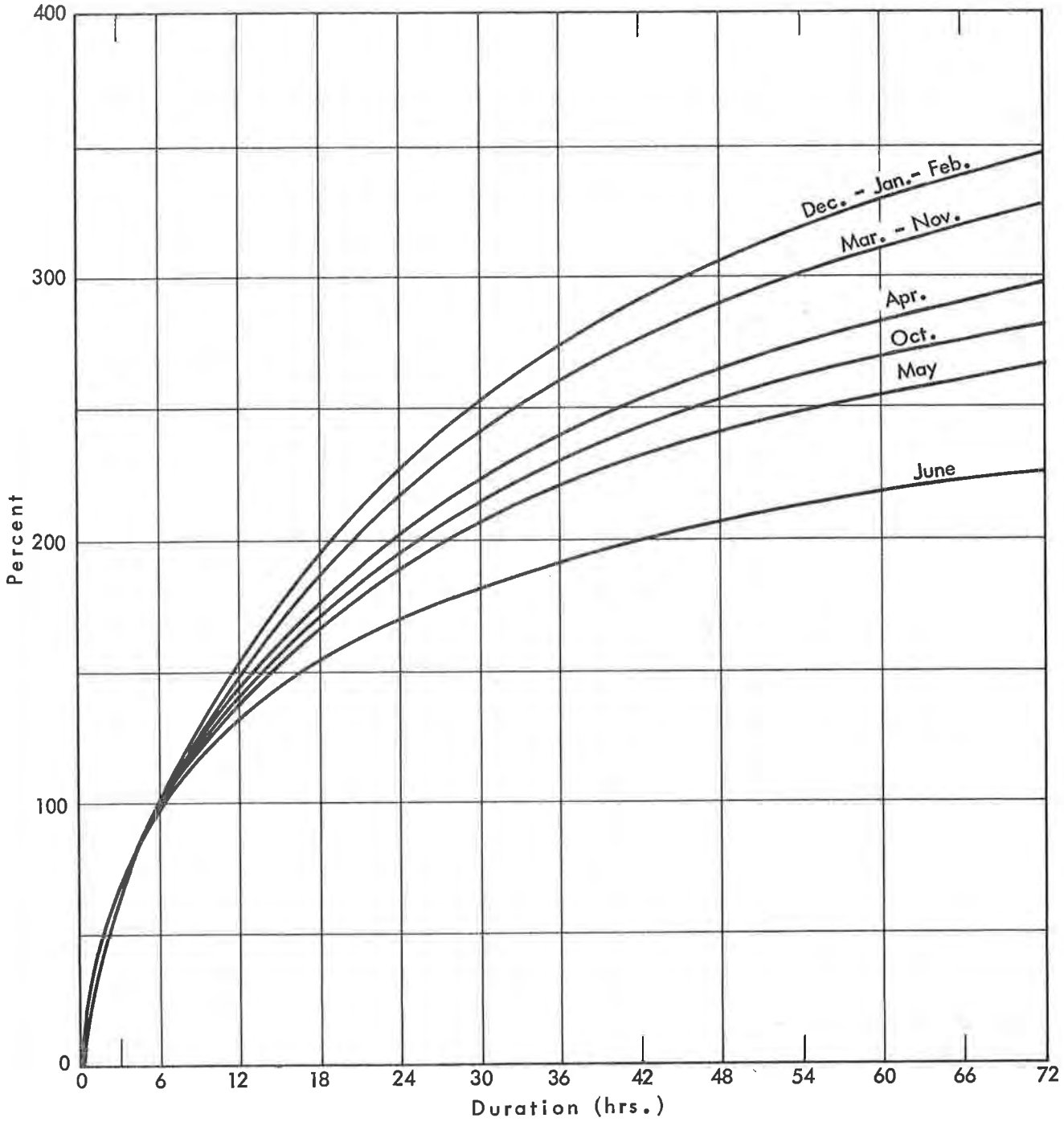

Figure 3-42a. Durational variation by months of convergence PMP as percent of 1st 6 hour - West of Cascades

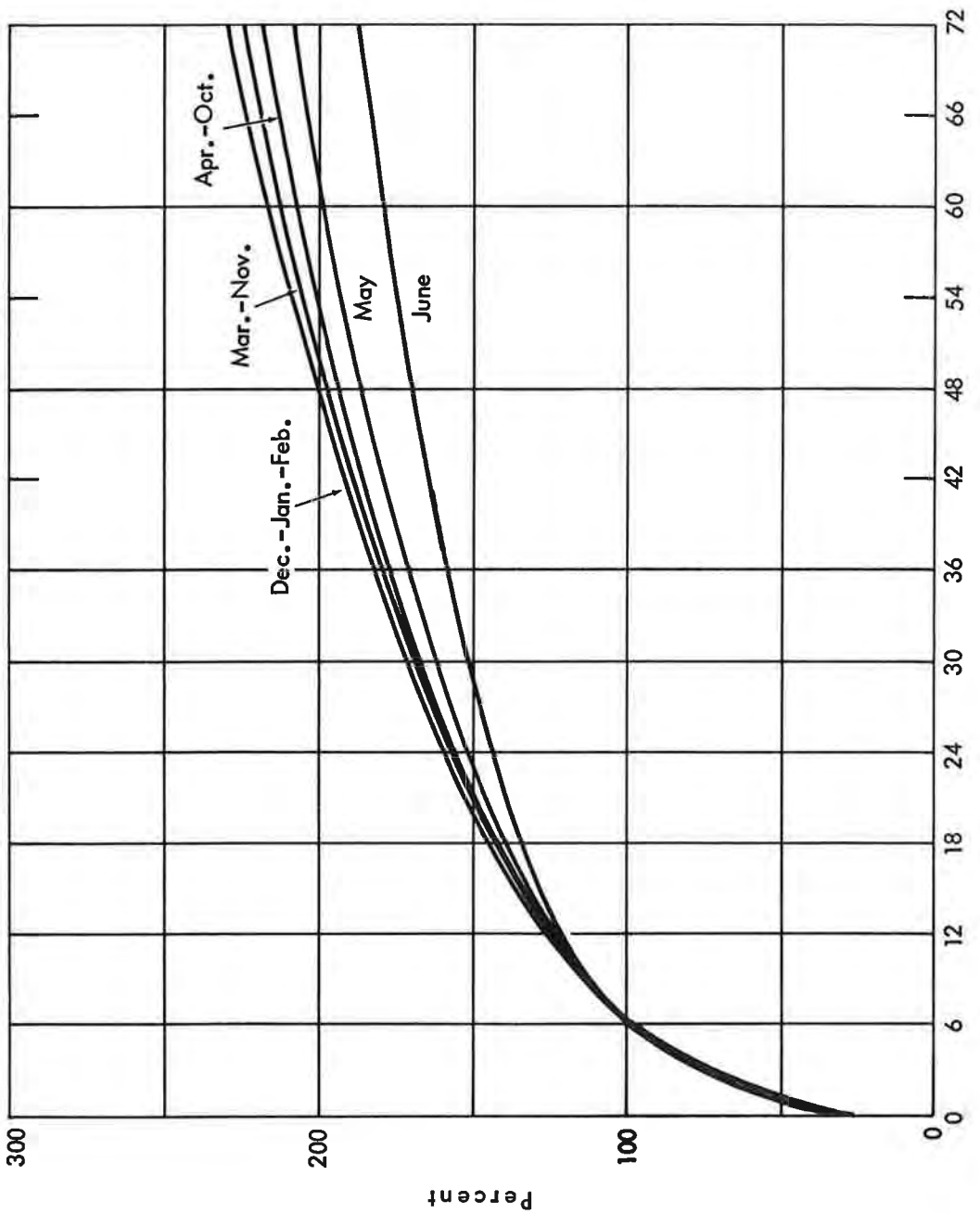

Figure 3-42b. Durational variation by months of convergence PMP as percent of 1st 6 hour - East of Cascades

Chapter IV

PROBABLE MAXIMUM OROGRAPHIC PRECIPITATION

4-A. INTRODUCTION

4.01. Inspection of mean seasonal precipitation maps over the Northwest shows highest values on steep slopes or crests of mountains. Storm isohyetal maps often have similar patterns. Slopes lift inflowing moist air, causing adiabatic cooling. The capacity of the air to hold water vapor is reduced and precipitation results. The slopes in this way provide an always present precipitation mechanism. Other processes in the atmosphere that contribute to total observed mountain precipitation, are described in paragraphs 3.01 and 3.32.

First slopes encountered by moist air currents are the most effective in precipitation formation. However secondary ridges become more important as the distance between ridges increases. Where ridges are not parallel, rain patterns are complicated. During passage of a single storm, inflow moisture from several directions can produce precipitation, depending on the direction the slopes face. Some areas, east of the Cascade Divide in particular, can utilize moisture inflow from southeast to northwest.

Synopsis of procedure

4.02. An orographic model is used for computing precipitation formed by lifting of air up slopes and for following raindrops or snowflakes to the ground. Tests of this model against observed orographic precipitation in storms were made on a slope in California and on four slopes in the Northwest, using observed moisture and wind values as input data and generalized terrain profiles for the most critical inflow directions, constructed from topographic maps. Results of the tests are within acceptable limits, considering that terrain has to be simplified to carry out computations, that observed precipitation may not be representative of the actual precipitation over an area, and that the manner in which convergence rain is estimated and subtracted from the observed may be over-simplified.

4.03. Maximum moisture (estimated from maximum observed surface dew points discussed in chapter III) is combined with maximum windspeeds as input to the orographic precipitation computation model. Adjustment is made for non-saturation in regions where moisture is reduced by upwind barriers. Results of these computations using the most critical inflow directions are then generalized to allow for other pertinent directions. This involves sample computations on selected slopes, analyses over topographic maps, and guidance from distribution of a rainfall frequency map.

4.04. Seasonal variation was derived from a combination of model computations of PMP values for each month and observed seasonal variation of

maximum precipitation. Qualitative judgment based on streamflow variation and on experience gained in study of the orographic precipitation problem also entered into the adopted seasonal variations.

4.05. Durational variation of orographic PMP was determined from model calculations, with durational variations of wind and moisture as parameters.

4.06. Because of the direction-enveloping method used in defining the orographic PMP index and limitations on the lateral extent of highest moisture inflow, a basin size reduction factor is introduced. This for the most part was based on observed storm depth-areal relations.

4-B. THE OROGRAPHIC MODEL

4.07. The precipitation model used in this report is the one developed by Showalter (8). The equation representing this model is:

$$I = \frac{.4\ \overline{V}_1\ \Delta P_1\ (\overline{w}_1 - \overline{w}_2)}{Y} \qquad (1)$$

"I" is the intensity in inches per hour of condensation or sublimation of water vapor to rain or snow in a layer bounded by an upper air streamline and a lower streamline.

The other factors are:

$.4$ = Constant for units. Dimensions of constant are in./mb.

$\overline{V}_1$ = Average windspeed in layer at inflow (kts.)

ΔP_1 = Thickness of layer at inflow (mb.)

$\overline{w}_1$ = Mean mixing ratio at inflow (gm./gm.)

$\overline{w}_2$ = Mean mixing ratio at outflow (gm./gm.)

Y = Horizontal distance from inflow to outflow (n. mi.)

Subscript 1 variables are inflow parameters at the foot of the mountain slope. The value of $\overline{w}_2$ (outflow moisture) is obtained by computation from outflow pressures and temperatures, which are derived by theory discussed in HMR 36. From equation (1) it is seen that the decrease in w along a streamline is an important factor in the quantity of orographic precipitation. Other elements that determine the intensity are 1) the inflow windspeed (V_1), which sets the length of the airstream to be processed in an hour; 2) the depth of the layer (ΔP_1); and 3) the distance over which the

precipitation is dispersed (Y). Figure 4-1 illustrates the application of equation (1) to a layer. In order that the model give a realistic representation of the atmosphere in which the precipitation forms, the equation is applied to a number of layers, as many as 20 to 25. Computation is carried up to where level flow is attained (200 mb. in fig. 4-1) or where the precipitation trajectory crosses the entrance line (370 mb. in fig. 4-1).

4.08. Precipitation trajectories. Equation (1) accounts for the rate of formation of raindrops or snowflakes. The next step is to trace the path of the falling precipitation to the ground. This path is the vector sum of the wind and the terminal vertical velocity of the precipitation element in still air. The terminal velocity of rain and snow was set at 36 and 7.5 mb. per minute, respectively. These rates correspond to approximately 6 m./sec. for the raindrops and 1.5 m./sec. for snowflakes and were taken from HMR 36, paragraphs 5.20 and 5.21. The rate for snow is an estimated average value for the two hundred millibar layer above the freezing level.

4-C. TEST OF MODEL ON OBSERVED STORMS

1. Tests in California

Test area and storm period selection

4.09. The most reliable test of the orographic model employed in this report was conducted along the slopes of the Sierra Nevada Range of California. The area chosen has a good distribution of observing stations along the face of the upslope. Figure 4-2 shows the location of the California test area and rainfall recorder stations while figure 4-3 gives the ground profile of the test area and the elevation of all rainfall stations (recorders and non-recorders) relative to the ground profile.

4.10. Heavy precipitation periods in the December 1955 and November 1950 storms over this area were chosen for the test. Six 6-hr. and one 24-hr. periods (not overlapping) in the 1955 storm and one 24-hr. period in the 1950 storm were studied. These test periods are listed in table 4-1.

Table 4-1

STORM TEST PERIODS FOR CALIFORNIA SLOPE

0000-0600 PST Dec. 21, 1955
0600-1200 PST Dec. 21, 1955
1200-1800 PST Dec. 21, 1955
1800-2400 PST Dec. 21, 1955
0600-1200 PST Dec. 22, 1955
1200-1800 PST Dec. 22, 1955
1800-1800 PST Dec. 22-23, 1955
0000-2400 PST Nov. 18, 1950

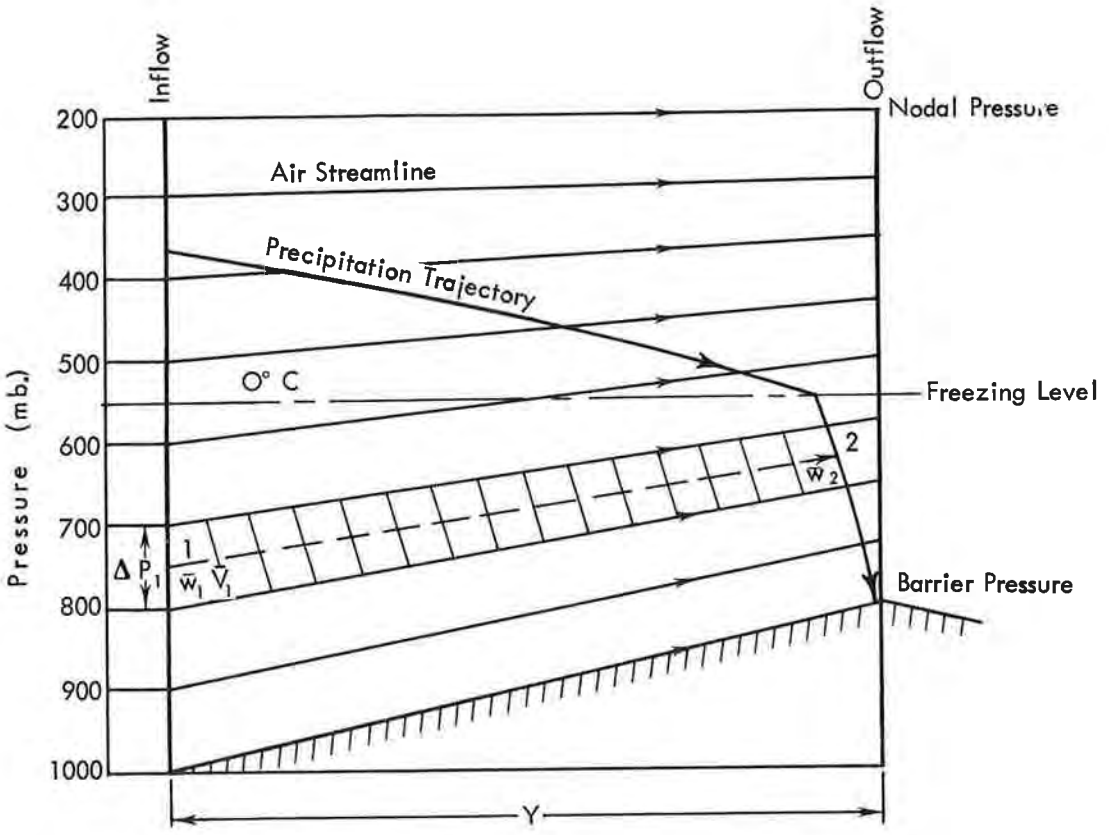

FIGURE 4-1. Orographic precipitation model (schematic)

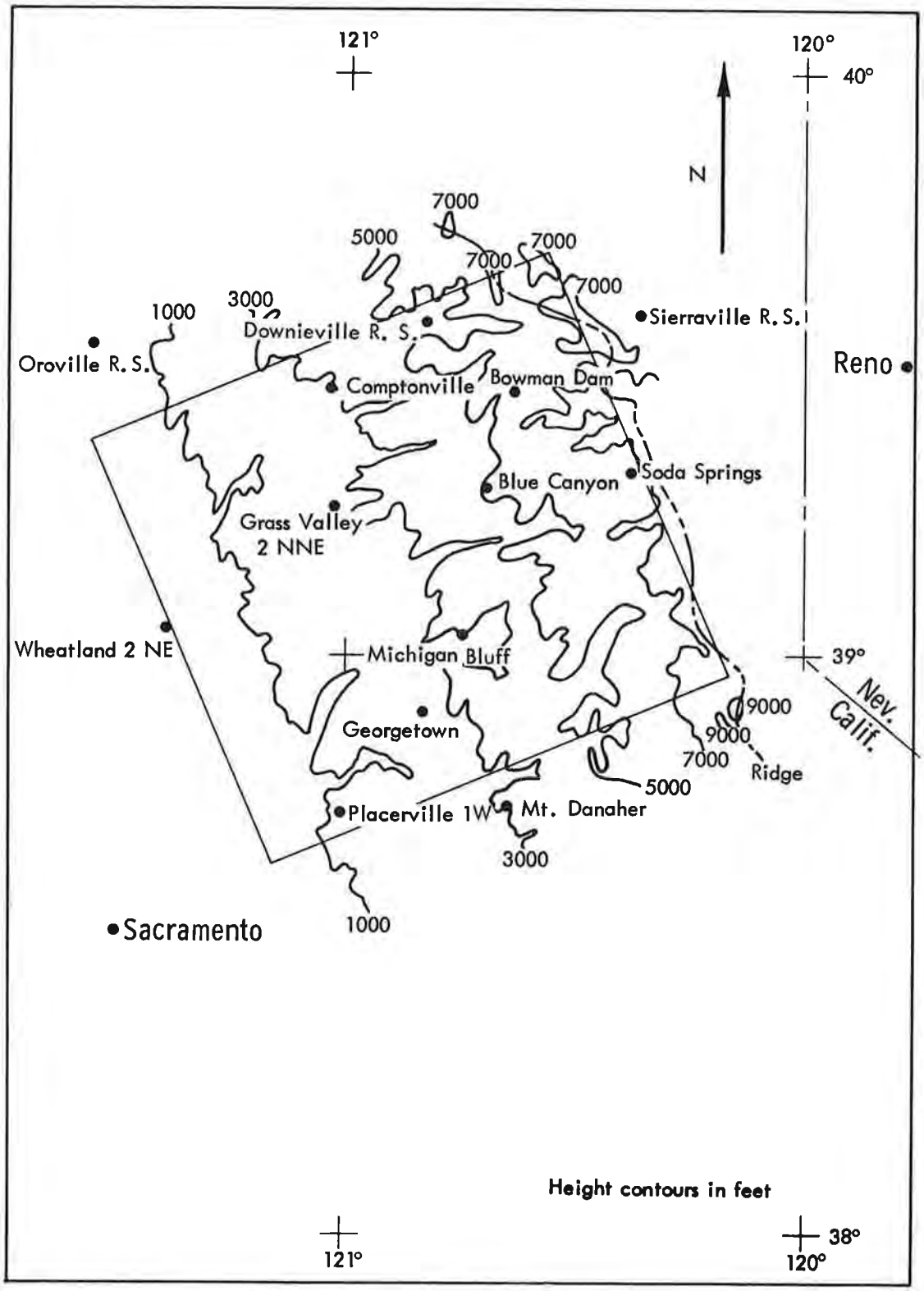

Figure 4-2. Model - test area in California

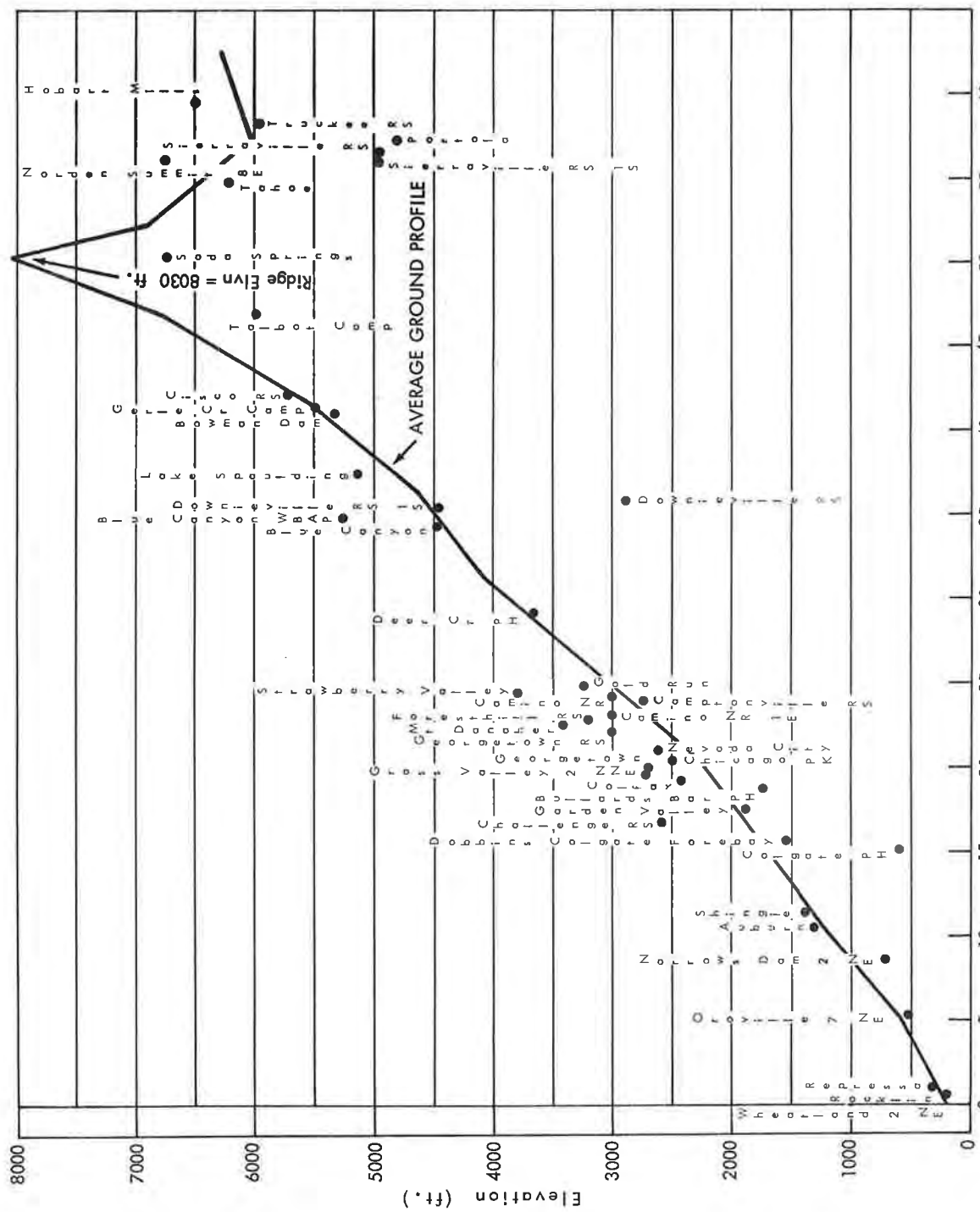

Figure 4-3. Elevations of stations relative to adopted ground profile in California test area

Inflow winds and moisture

4.11. Storm inflow winds and moisture were derived primarily from the Oakland, Calif. upper-air sounding which is about 85 nautical miles from the entrance to the test area. The pilot balloon observation at Sacramento, Calif., and the radiosonde at Merced, Calif., provided auxiliary information. Sacramento was given precedence, when available, since it is the closest wind measurement to the test area. Merced was substituted only when the Oakland sounding was missing. In a few cases the upper portion of the Merced sounding was used when a short run was made at Oakland.

The component of the wind against the Sierra barrier was used in all cases, since the model is in two dimensions. The moisture was taken directly from the radiosonde report. The low-level temperature inversion found on many of the Oakland soundings was eliminated since it is due to the cold water offshore and either would not be present on the east side of the Sacramento Valley at the entrance to the test area or the cold air beneath it would not ascend the mountain. A few adjustments were made to the upper-level temperatures by way of smoothing out small irregularities.

Computation of orographic precipitation

4.12. Storm orographic precipitation is computed by electronic computer. First, the wind, temperature, pressure and moisture values are computed for the region vertically above the crest of the barrier (outflow). This is based on the minimum energy theory explained in HMR 36, paragraphs 5.10-5.15 and more fully in (9). Second, the values of the four parameters are obtained at all significant points between entrance and outflow. These significant points are generally determined by the intersection of air streamlines with the verticals above breaks in the ground profile or else by the intersection of the air streamlines with the freezing level. Finally, from equation (1) the precipitation formed in each part of the flow is computed. These products of condensation are then followed down and accumulated at the ground. In areas of spillover, i.e., to lee of significant barriers, the air is assumed to flow horizontally and the precipitation accumulation is computed on this basis.

Estimation of observed orographic precipitation

4.13. There are about 40 observing stations in or very near the test area including about a dozen recorders in the 1950 and 1955 storms. The non-recorder daily amounts were divided into the time periods listed in table 4-1 by reference to the recorders, using an isopercental technique.

During intense rains over slopes, significant amounts are usually observed over the flat valley areas upwind of the slope where there is no possibility for orographic lift. This precipitation, attributed to convergence processes, is assumed to decrease 5 percent per thousand feet with elevation over the nearby slope. (See pars. 3.36 and 3.37.) The estimated observed orographic precipitation over the slope, or a portion of

it, is the difference between the observed total and the convergence precipitation component estimated in this manner.

Comparison of precipitation volumes over total slope

4.14. The first test compares computed with observed orographic precipitation over the total slope or area extending to the generalized ridge line (8030 ft.). Figure 4-4 shows this relation. Despite necessary approximations, such as assuming that the Oakland sounding is representative of conditions at the entrance of the slope, the mean relationship is good. The correlation coefficient is 0.95 and the regression line is quite close to 45 degrees.

Comparison of distributions of precipitation up the slope

4.15. In order to study the distribution of precipitation up the slope, orographic precipitation was computed by elevation bands six miles wide, roughly paralleling the ground contours. Figure 4-5 shows the comparison, computed vs. observed orographic, for each elevation band in the 6-hr. test period 0600-1200 PST, December 22, 1955. The ground profile is also given in the figure. For this period the estimated convergence precipitation is negligible, so that the observed total is also the observed orographic component.

It will be noted that computed and observed orographic precipitation both increase with increasing elevation; the highest observed is in the ninth elevation band and the highest computed is in the tenth. In general, too much has been computed on the lower slopes, but there is close agreement between computed and observed on the upper portion of the slope.

In the 24-hr. period 0000-2400 PST November 18, 1950 the computed exceeds the observed orographic for all elevation bands, with the greatest exceedance near the ridge line. These comparisons are shown in figure 4-6. The computed precipitation over the total slope is about 38 percent higher than the observed orographic precipitation.

2. Tests in Northwest States

Test area and storm period selection

4.16. Several tests were made to determine how well the model reproduces storm precipitation in the Northwest. Test areas selected should be near and downwind from meteorological stations with upper-air soundings, should have significant slopes, and should have enough precipitation stations to define storm precipitation. Four areas which come closest to meeting these requirements are the Cascade slopes east of Salem, Oreg. and east of Seattle, Wash., the mountain slopes northeast of Boise, Idaho, and the slopes of the Continental Divide west of Great Falls, Mont. There is an upper-air sounding at each of these four stations.

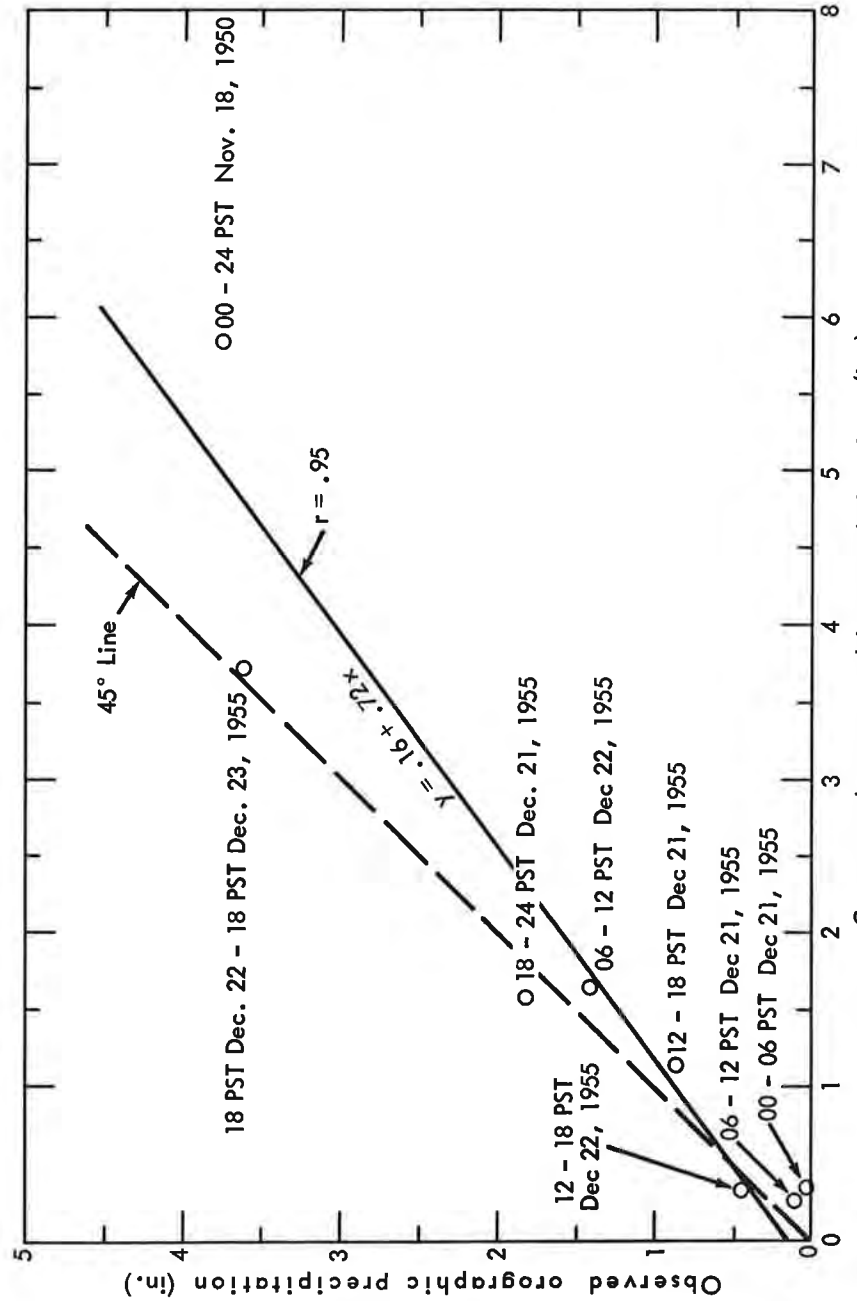

Figure 4-4. Relation between observed and computed orographic precipitation over California test area

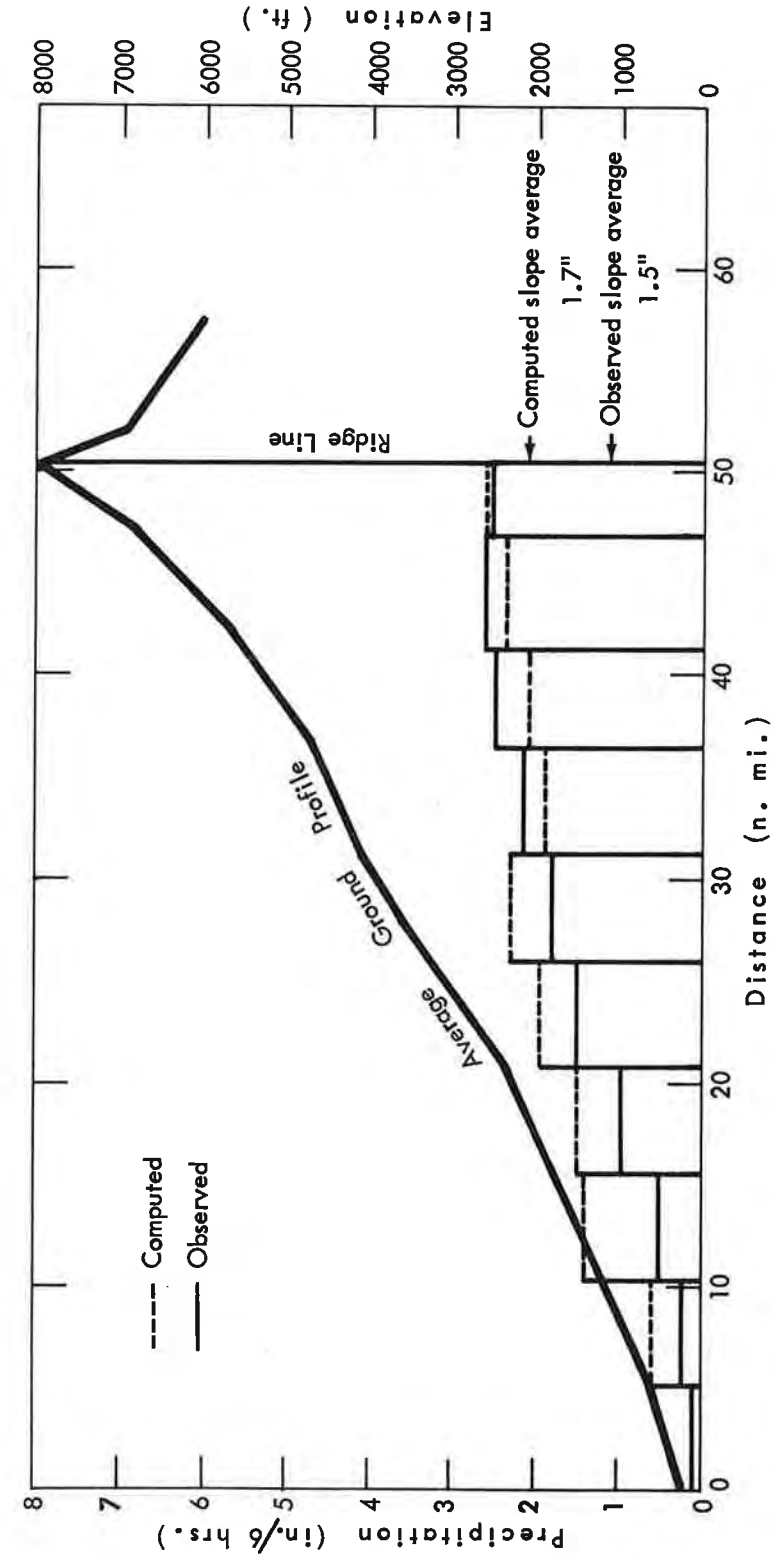

Figure 4-5. Computed and observed orographic precipitation distribution 06-12 PST Dec. 22, 1955 along California test area slope

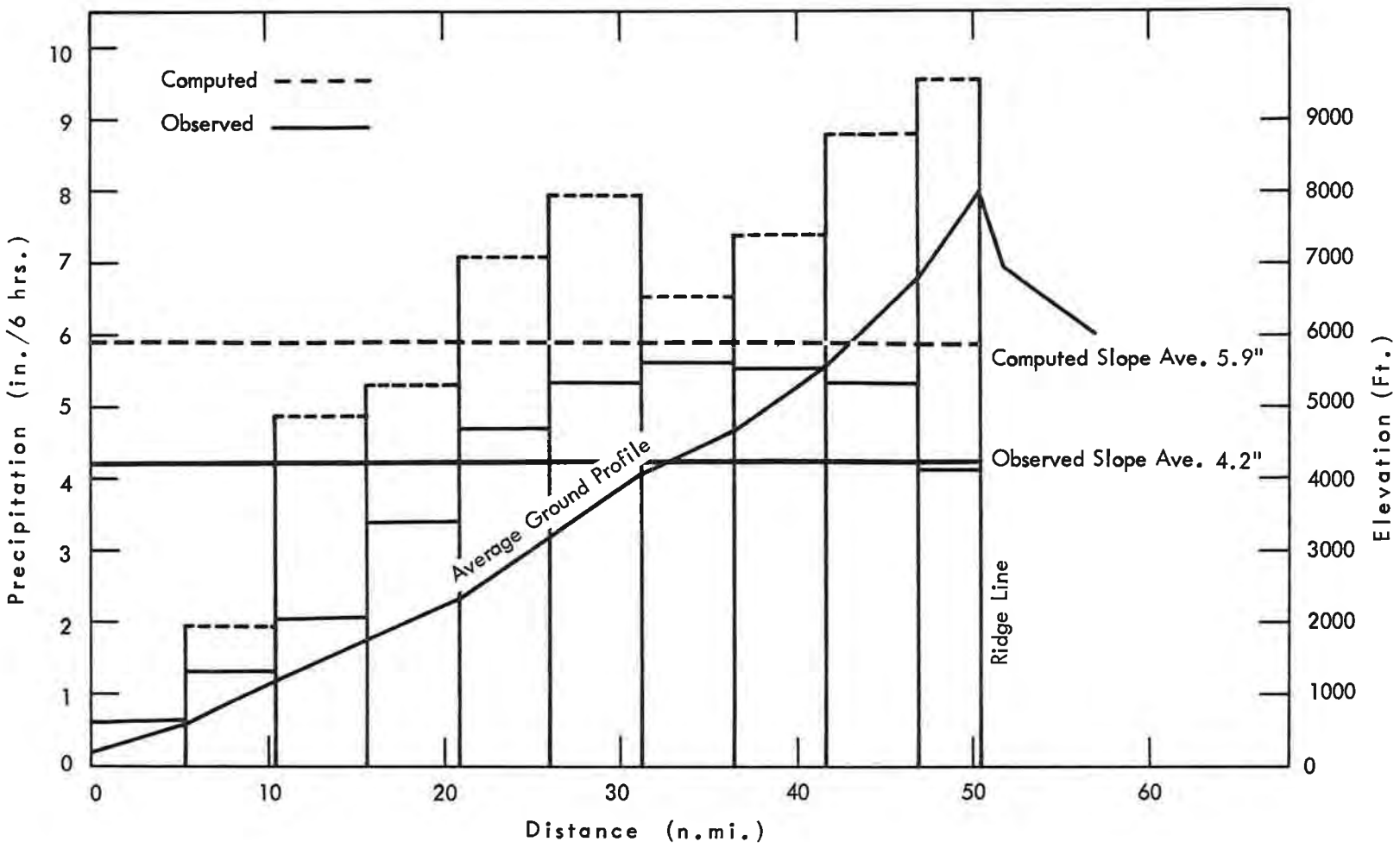

Figure 4-6. Computed and observed orographic precipitation distribution 00-24 PST Nov. 18, 1950 along California test area slope

4.17. Storms on which to test the model must be recent enough that upper-air data are available to determine moisture and wind input. This eliminates some of the major storms, such as the January 1935 which otherwise would be an excellent choice. The storm periods chosen should show rains of unusual magnitude. It would have been desirable to test only storm periods with a small convergence contribution over the slopes if this condition did not impose a severe restriction on the number of available storms. The storms selected for testing are listed in table 4-2.

Table 4-2

TEST STORMS IN NORTHWEST

Seattle test area:	Nov. 20-23, 1959; Sept. 4-6, 1959
Salem test area:	Nov. 24-25, 1960; Feb. 9-11, 1961; Nov. 22, 1961
Boise test area:	Dec. 18-23, 1955
Great Falls test area:	June 7-8, 1964

Most intense 6-hr. periods within these storms were chosen unless upper-air data were not available for these periods. The periods are listed in table 4-3 for all but the Great Falls test area.

Determination of storm inflow winds and moisture

4.18. Storm inflow winds were derived primarily from rawins* and pilot balloon observations at the four stations. In cases of short soundings, the winds at upper levels were estimated by means of constant pressure charts from the National Weather Analysis Center. Corrections were applied to the geostrophic windspeeds to reduce them to actual windspeeds. The corrections were derived by an independent comparison of actual winds with the geostrophic. The geostrophic wind direction was assumed to approximate the true wind direction.

Moisture and temperatures also were derived directly from radiosonde measurement or by interpolations for the hour midway between successive 12-hr. radiosondes. Such interpolations were especially numerous in reconstructing the December 1955 Boise area data.

Average terrain profiles

4.19. Tests were made with inflow from two directions for the Seattle and Salem areas: from the west, the direction that produces the greatest lift to moisture inflow; and from the southwest, the average inflow direction during the test storm periods. One direction only, southwest, was used for the Boise area since this direction presents greatest lift by slopes and was the average direction of inflow during the test storm. Inflow from northeast was used in the June 1964 Continental Divide storm.

*A method of determining windspeeds and directions in the atmosphere by tracking a target with radar or equivalent means.

4.20. Average terrain profiles were constructed for each of the test areas parallel to the inflow directions. Figures 4-7 and 4-8 show the location, average width, and boundary elevations of the west-east Seattle and Salem test areas and the average profiles and elevations of the precipitation stations available for the storms that were tested.

Figure 4-9 gives the location and stations used for the southwest-northeast oriented test area for Seattle. The area was divided into three strips labeled A, B and C. Profiles for these strips, which cut across the contours, are shown in figure 4-10. The Salem area was handled similarly for southwest-northeast inflow. Figure 4-11 shows location of strips and stations while figure 4-12 gives profiles of the strips.

The Boise test area location, boundary elevations, precipitation stations and average profile are shown in figure 4-13.

4.21. The Rocky Mountain area in northern Montana is a series of more or less parallel ridges, as seen in figure 4-14. The Divide (—) and an assumed western limit to possible spillover from an easterly flow (--) are outlined. For this easterly flow, the most critical precipitation areas just west of the divide are where the divide is on the front (most easterly) range. This is the case from 47° to 50°N. latitude except between 47.5° and 48°N. There the divide is on the second parallel ridge. Slopes of the front range are steep just east of the ridge. Highest elevations are mostly along the divide 48°-49.5°N., but are on ridge lines to west or east 47°-48°N. Farther south the front range is 75 miles or more east of the divide, with the Missouri headwater area in between. Here a flow from north to northeast may cross the divide 46°-47°N. without much upwind barrier. The divide is fairly low west of Helena with some higher mountains to northeast.

Location of three sample strips for northeast flow is shown in figure 4-14, along with elevation of the box boundaries or of the upwind barrier.

Computation of orographic precipitation

4.22. Storm orographic precipitation was computed by 6-hr. periods in the same manner as for the California test area (par. 4.12) over each total slope and for each straight-line segment of the slope.

Estimation of observed orographic precipitation

4.23. Observed precipitation for a 6-hr. period averaged over an elevation band of a test area was determined by expressing 6-hr. precipitation values at each station as a ratio to the mean annual precipitation at that station. An average of these station ratios was then multiplied by the mean annual precipitation of the selected area to obtain 6-hr. area-averaged precipitation. To verify the adequacy of this procedure in areas where station

Table 4-3

AVERAGE OBSERVED AND COMPUTED OROGRAPHIC PRECIPITATION (IN.)

Date	Case No.	Center of 6-hr. Period (GMT)	Elevation Band I Obs. Total	I Obs. Oro.	I Comp.	II Obs. Total	II Obs. Oro.	II Comp.	III Obs. Total	III Obs. Oro.	III Comp.	IV Obs. Total	IV Obs. Oro.	IV Comp.	Total Slope Obs. Total	Total Slope Obs. Oro.	Total Slope Comp.
Seattle Test Area																	
9/4/59	1	18	.21	.03	0	.37	.20	0	1.03	.88	.20				.62	.46	.10
9/5/59	2	00	.27	.02	.08	.48	.25	.74	.79	.59	.45				.55	.22	.37
	3	06	.19	.04	.05	.34	.20	.85	.29	.07	.47				.27	.14	.39
	4	12	.03	0	0	.20	.17	.52	.17	.15	.30				.12	.09	.24
	5	18	.17	.05	0	.39	.28	.76	.64	.54	.44				.41	.30	.34
9/6/59	6	00	.10	0	.03	.30	.21	.60	.47	.39	.43				.32	.22	.33
	7	06	.06	0	.02	.36	.30	.66	.62	.57	.39				.38	.33	.31
	8	12	.06	0	.19	.29	.23	1.40	.53	.48	.81				.32	.27	.70
11/20/59	9	00	.05	.01	.02	.06	.02	.32	.12	.09	.32				.08	.05	.22
	10	06	.35	.05	0	.57	.29	.21	.99	.74	.38				.70	.42	.22
	11	12	.68	.18	.06	.71	.25	.98	1.67	1.26	.63				1.16	.70	.49
	12	18	.86	.21	.02	.97	.37	.84	1.31	.78	.58				1.09	.51	.43
11/21/59	13	00	.94	.14	.01	1.30	.56	.12	1.47	.81	.05				1.27	.54	.05
	14	06	.81	.06	0	.74	.14	0	.90	.40	0				.84	.24	0
11/22/59	15	06	.03	0	0	.10	.07	0	.11	.09	0				.08	.05	0
	16	12	.20	.05	0	.39	.25	0	.73	.61	.22				.49	.36	.10
	17	18	.19	.01	0	.67	.50	.58	1.97	1.82	.55				1.13	.97	.36
11/23/59	18	00	.23	.03	0	.58	.39	1.84	2.40	2.24	1.75				1.34	1.16	1.16
	19	06	.05	0	.02	.43	.38	.92	1.25	1.21	.77				.69	.64	.53
Average			.29	.05	.03	.49	.27	.60	.87	.72	.46				.62	.40	.33
Salem Test Area																	
11/24/60	1	12	.86	.16	0	.85	.20	.19	1.28	.68	.44	1.68	1.12	.56	1.10	.47	.28
11/25/60	2	00	.95	.10	.04	1.33	.54	.36	1.42	.69	.48	1.22	.54	.46	1.26	.49	.34
	3	12	.08	.03	0	.27	.22	0	.41	.37	.08	.15	.11	.16	.27	.22	.05
2/9/61	4	12	.28	.03	0	.35	.12	0	.47	.25	0	.68	.48	.23	.41	.17	.02
2/10/61	5	00	.66	.04	0	1.07	.42	.37	1.10	.50	.33	1.46	.96	.42	1.03	.40	.27

Table 4-3 (Cont'd.)

AVERAGE OBSERVED AND COMPUTED OROGRAPHIC PRECIPITATION (IN.)

Date	Case No.	Center of 6-hr. Period (GMT)	Elevation Band I Obs. Total	I Obs. Oro.	I Comp.	II Obs. Total	II Obs. Oro.	II Comp.	III Obs. Total	III Obs. Oro.	III Comp.	IV Obs. Total	IV Obs. Oro.	IV Comp.	Total Slope Obs. Total	Total Slope Obs. Oro.	Total Slope Comp.
2/10/61	6	12	.76	.01	0	1.24	.54	.31	1.26	.61	.36	1.42	.82	.48	1.15	.47	.27
2/11/61	7	00	.63	.03	0	1.12	.47	.16	.89	.29	.24	1.16	.60	.26	.90	.27	.16
11/22/61	8	00	.54	.04	0	.60	.13	0	.89	.46	.37	1.06	.56	.71	.75	.19	.22
	9	12	.66	.14	0	1.09	.54	.60	1.47	.78	.67	1.44	.80	.67	1.16	.42	.49
Average			.60	.06	.01	.88	.35	.22	1.02	.51	.33	1.14	.67	.44	.90	.34	.23
								Boise Test Area									
12/18/55	1	03	0	0	0	0	0	0	0	0	.02	0	0	.06	0	0	.02
	2	09	0	0	0	0	0	0	0	0	.06	.04	.04	.06	.01	.01	.03
	3	15	.04	.01	0	.11	.08	0	.18	.15	.01	.04	.02	.02	.09	.06	.01
12/19/55	4	03	.04	.01	0	.27	.24	0	.56	.53	0	.48	.46	.03	.35	.32	.01
	5	15	.02	0	0	.19	.17	0	.32	.30	.04	.04	.02	.08	.15	.13	.02
	6	21	.12	.02	0	.43	.34	.07	.84	.75	.24	.26	.18	.45	.42	.33	.16
12/20/55	7	03	.09	.02	.02	.27	.21	.11	.46	.40	.24	.30	.24	.49	.27	.21	.18
	8	09	.04	.01	0	.16	.13	.01	.21	.18	.14	.30	.28	.21	.16	.13	.08
	9	15	.05	.02	0	.19	.16	.02	.25	.22	.12	.43	.41	.17	.18	.15	.07
12/21/55	10	03	.00	0	0	.05	.05	0	.07	.07	.03	.13	.13	.11	.06	.06	.03
	11	15	.02	0	0	.08	.06	.01	.32	.30	.08	.13	.11	.22	.13	.11	.06
	12	22	.12	.02	0	.33	.24	0	.70	.61	.08	.78	.70	.29	.44	.35	.07
12/22/55	13	04	.12	.02	.06	.43	.34	.41	.63	.54	.43	1.12	1.04	.68	.51	.42	.35
12/23/55	14	03	.12	.02	.08	.52	.43	.14	.35	.26	.27	0.56	.48	.40	.36	.27	.20
	15	15	.36	.06	.03	.57	.30	.11	.39	.13	.16	.69	.45	.15	.48	.21	.11
Average			.08	.01	.01	.24	.18	.06	.35	.30	.13	.36	.30	.23	.24	.18	.09

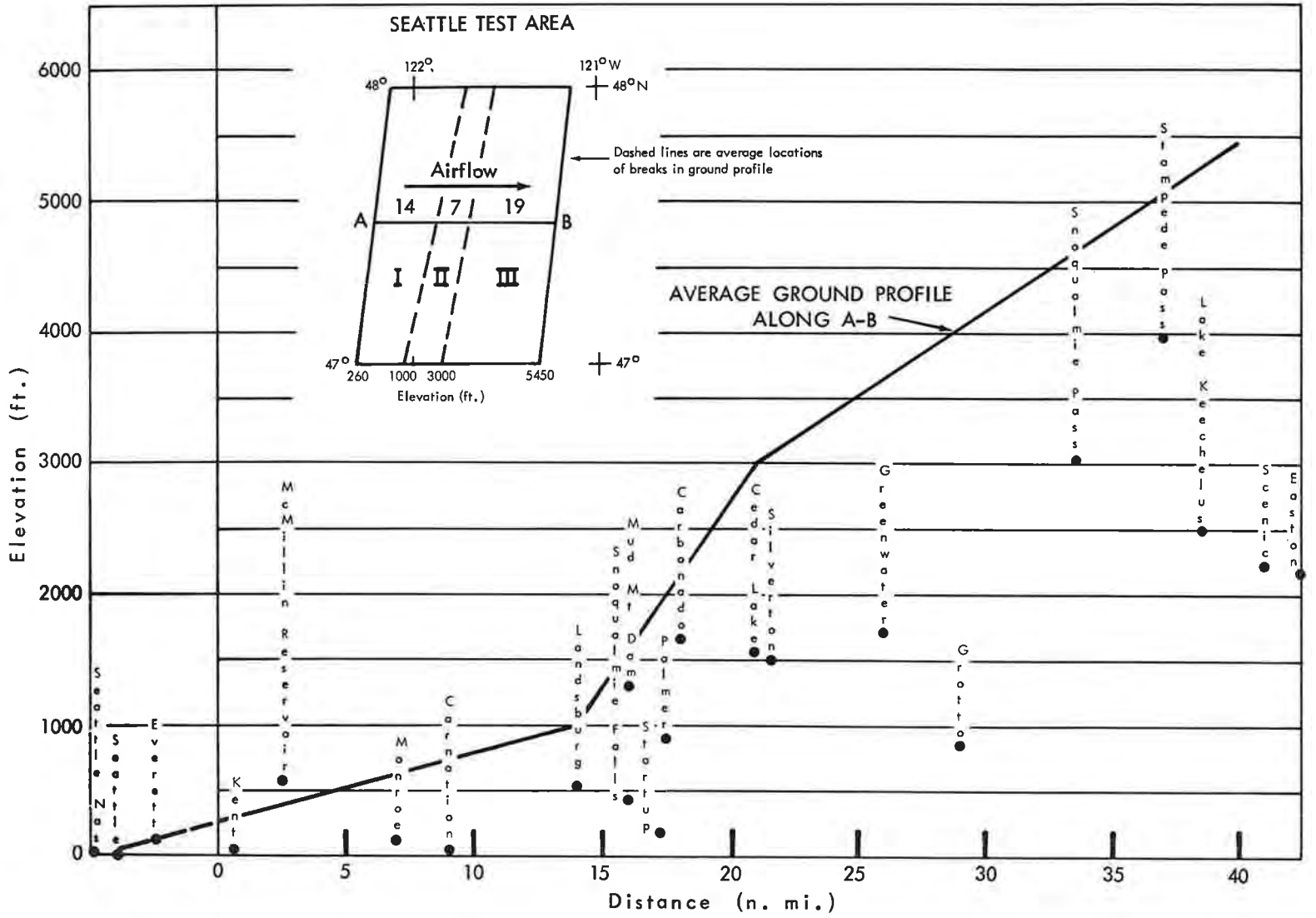

Figure 4-7. Elevations of stations relative to adopted ground profile in Seattle, Wash. test area (west inflow)

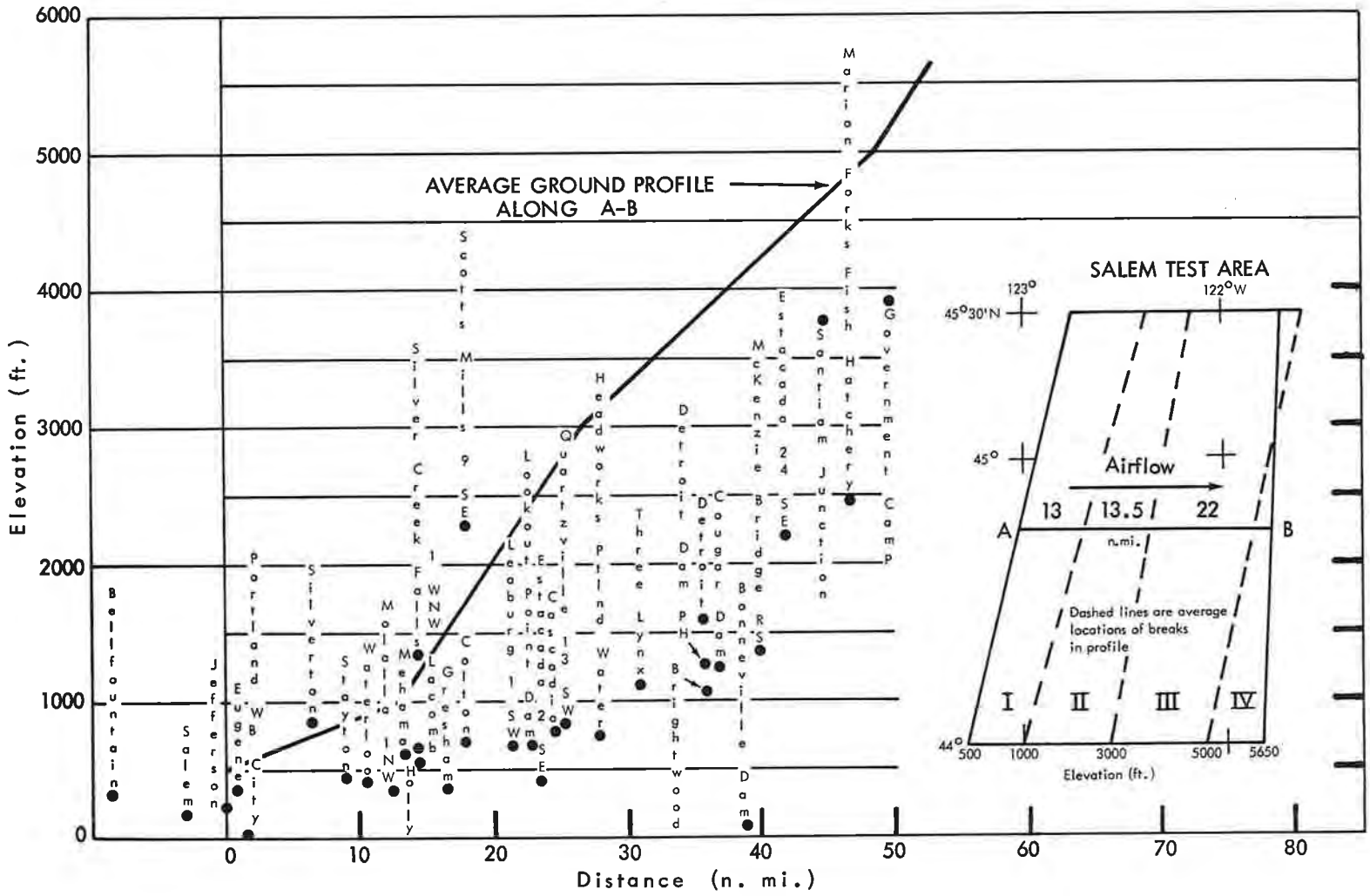

Figure 4-8. Elevations of stations relative to adopted ground profile in Salem, Ore. test area (west inflow)

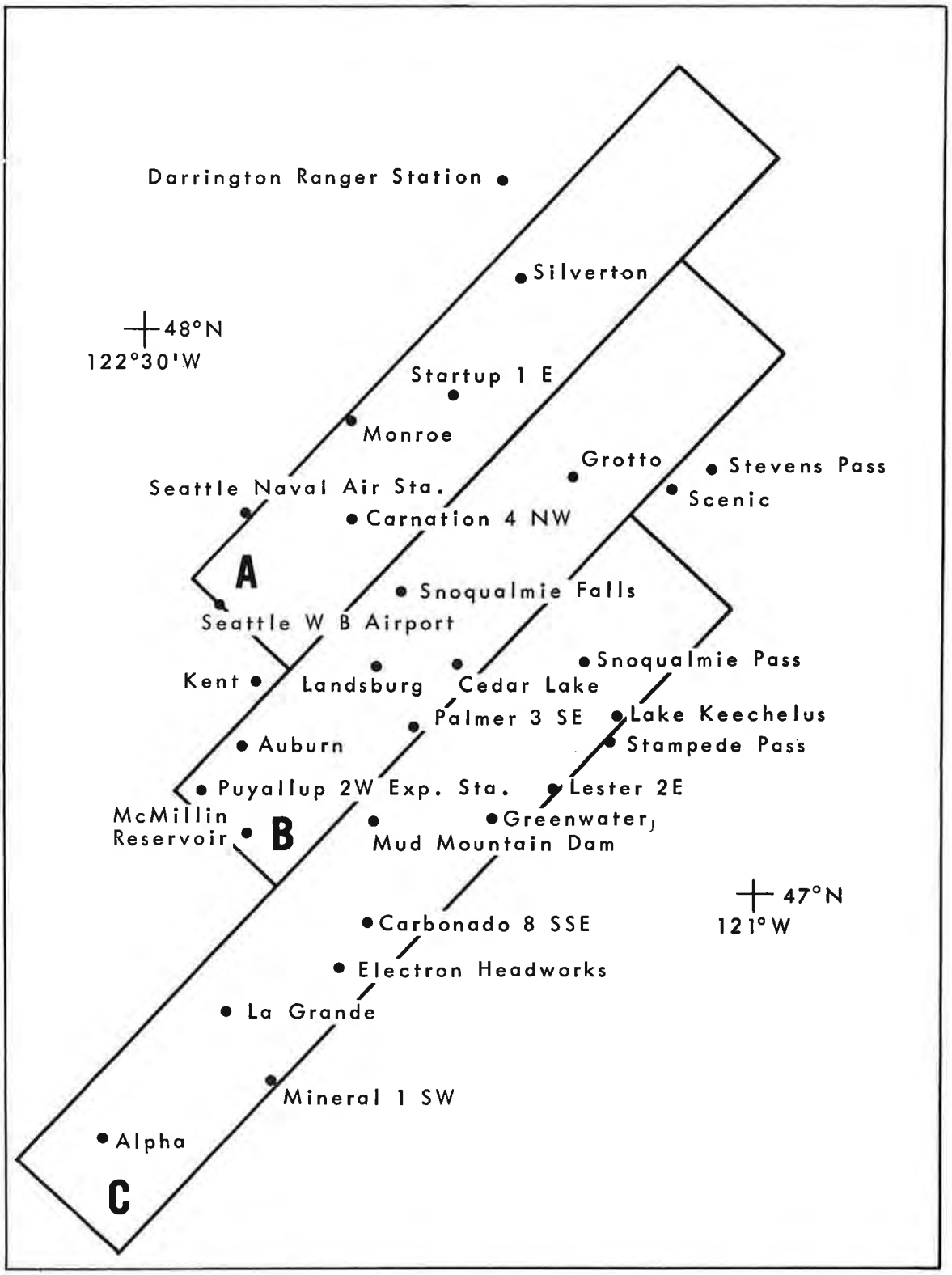

Figure 4-9. Seattle SW-NE test area and station location

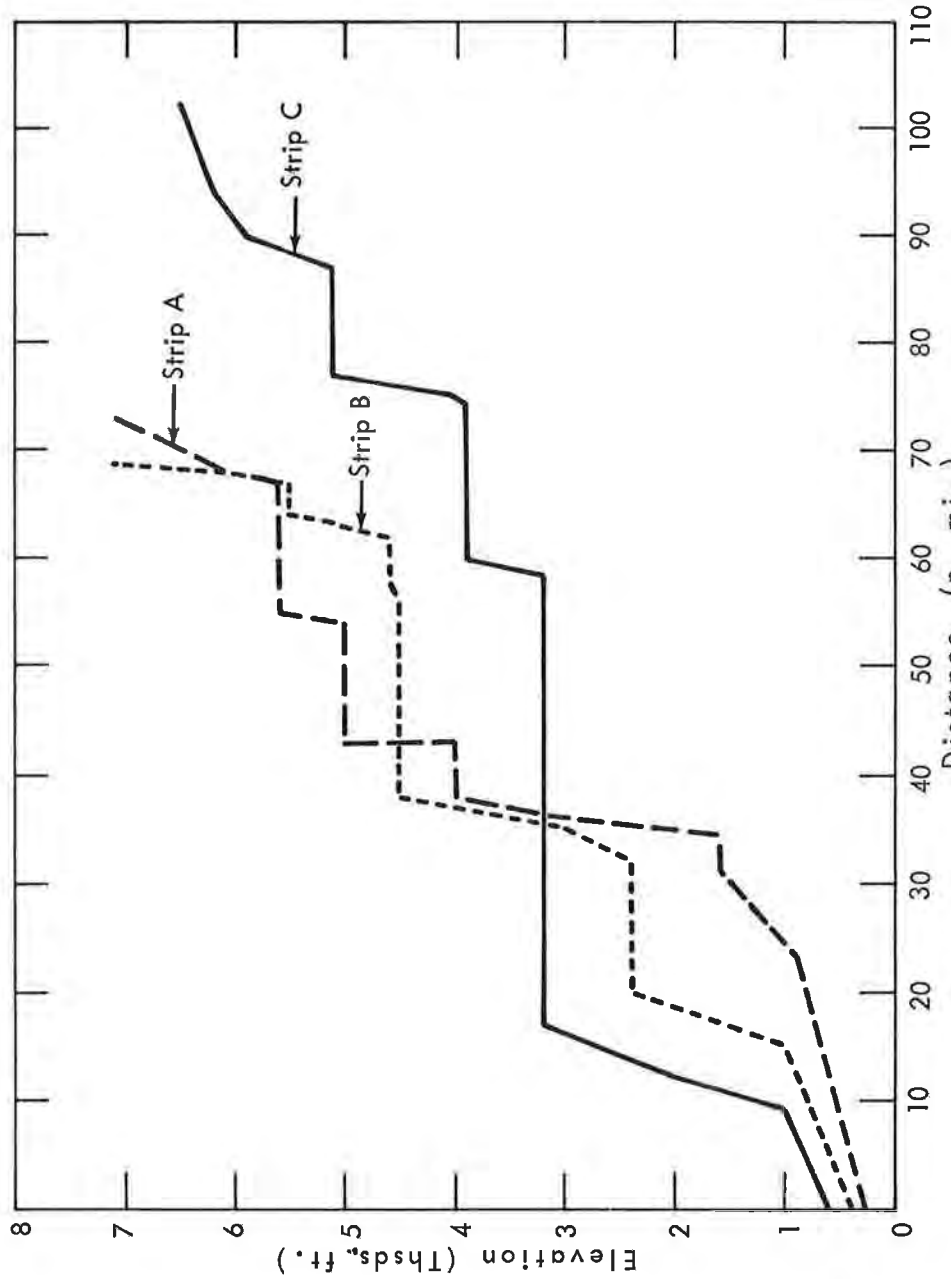

Figure 4-10. Seattle test area profiles (SW inflow)

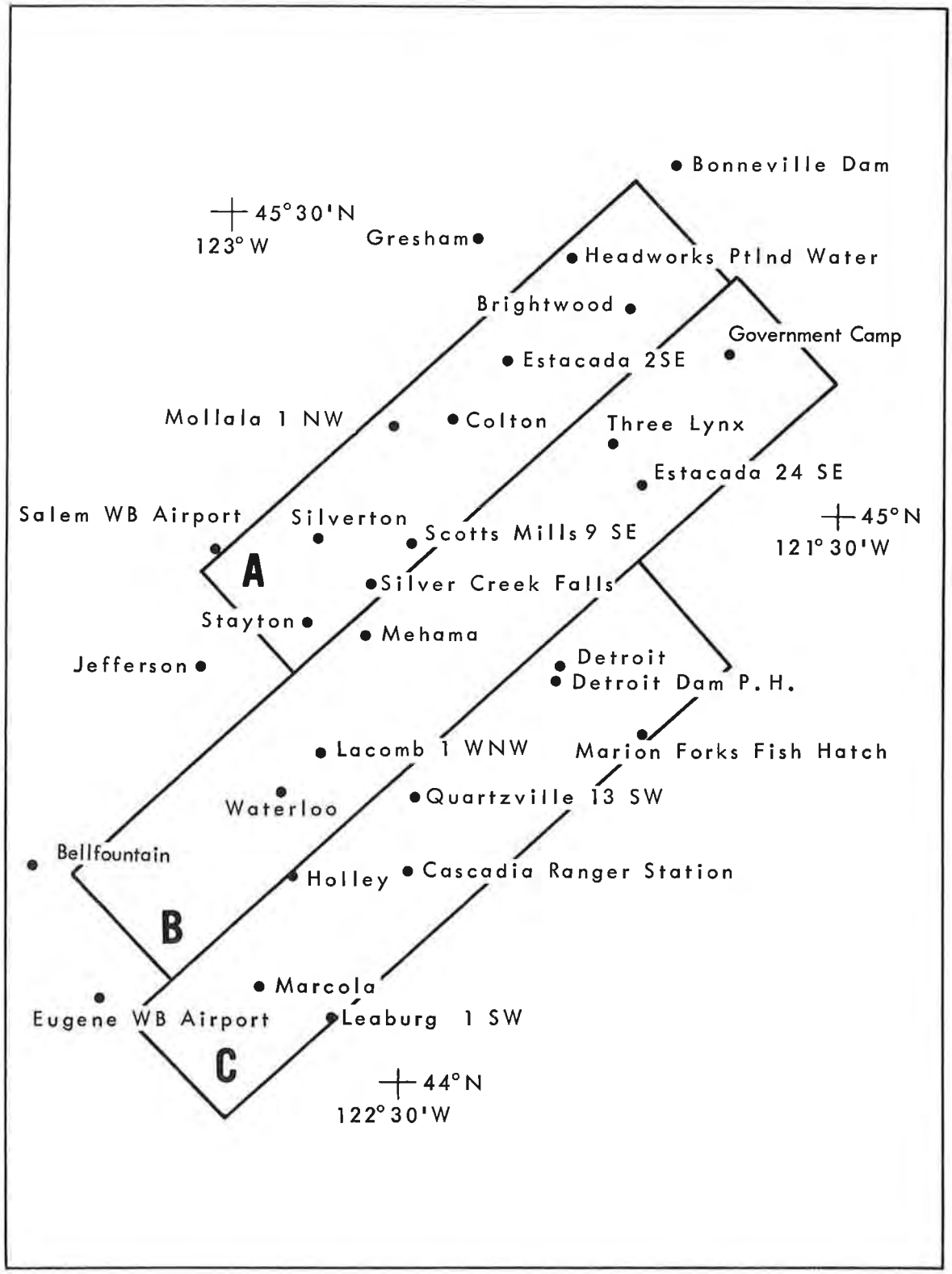

Figure 4-11. Salem SW-NE test area and station locations

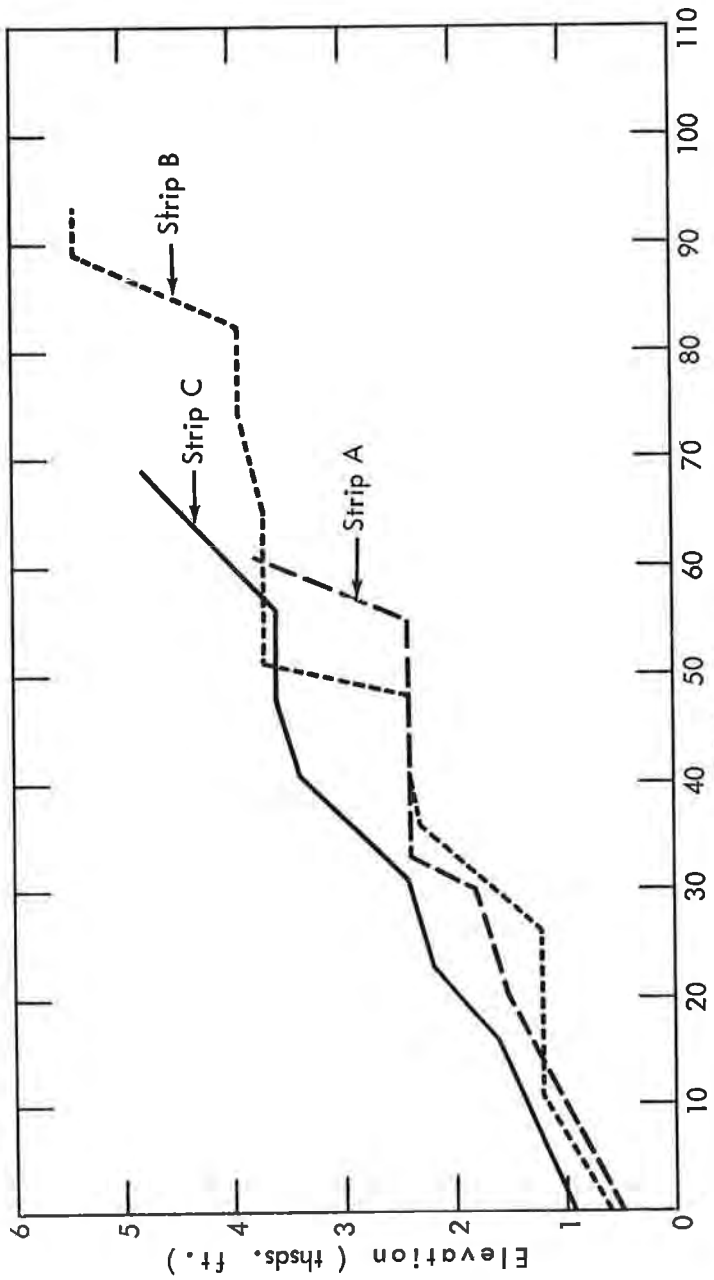

Figure 4-12. Salem test area profiles (SW inflow)

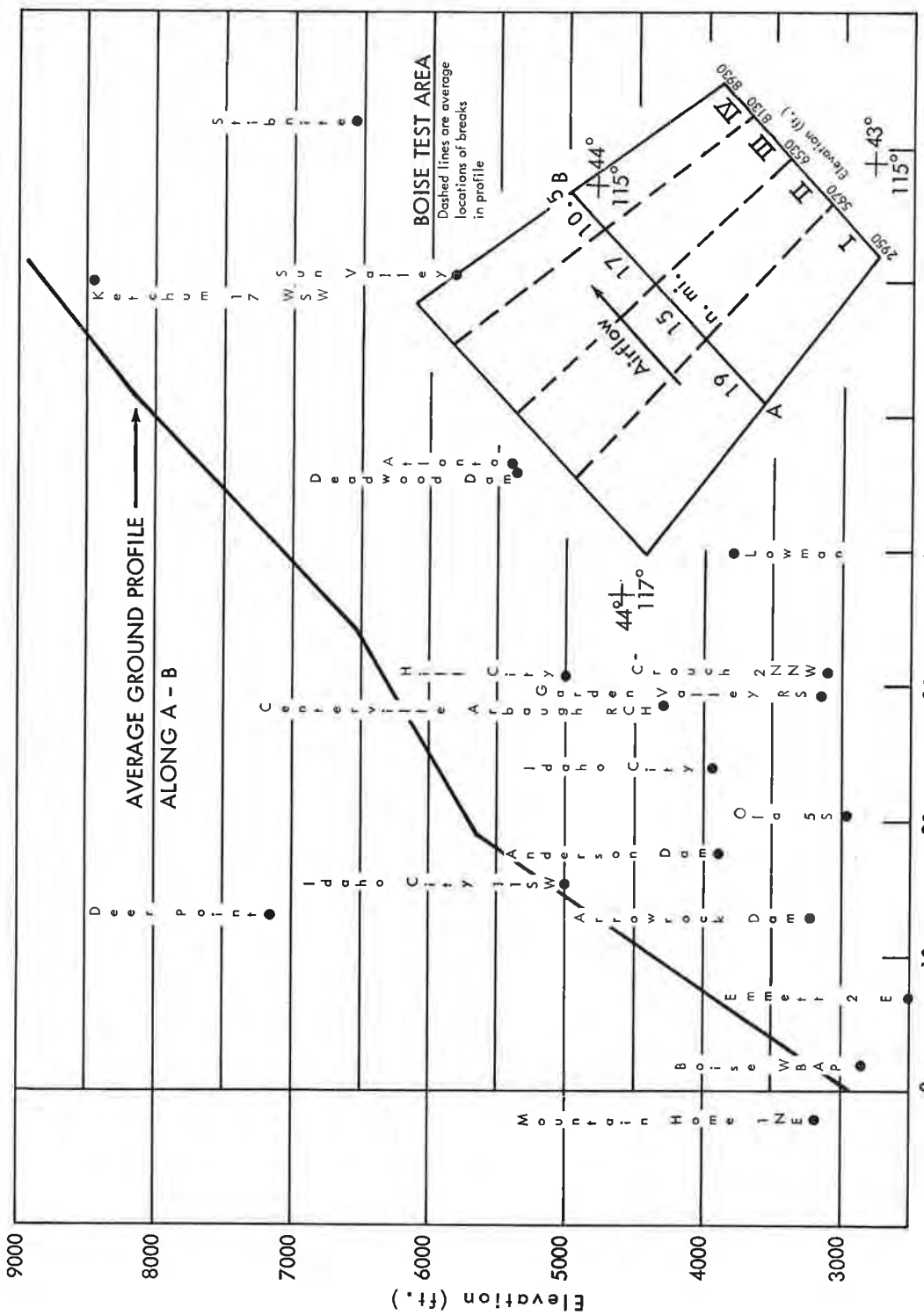

Figure 4-13. Elevations of stations relative to adopted ground profile in Boise, Idaho test area

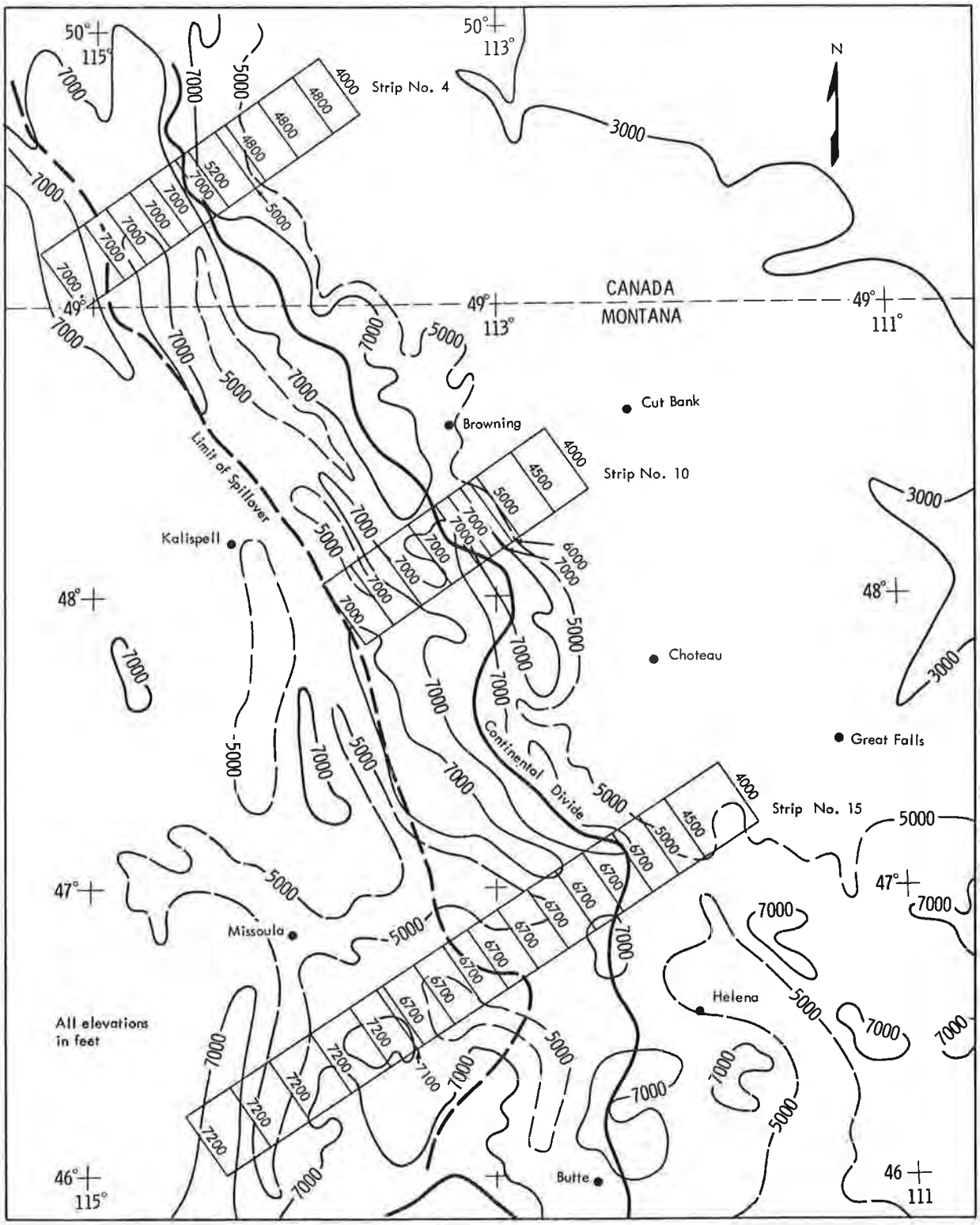

Figure 4-14. Orographic spillover area for easterly flow over Continental Divide (Sample computation strips are divided by assumed average elevations or upwind barrier shown in ft.)

distribution is not uniform, similar estimates were made for a random sample of periods and areas by weighting the station values by means of Thiessen polygons. Results differed from the above normalized estimates by only a few percent.

Observed area-averaged precipitation was then reduced by the convergence precipitation in each elevation band, estimated as described in paragraph 4.13.

Comparisons of observed and computed orographic precipitation

4.24. Over total slope. In general the relation between computed and observed orographic values averaged over entire test area is better than that over individual elevation bands or strips. Figures 4-15a and 4-15b show these average relations for the Seattle and Salem west inflow tests, respectively. Comparisons over the Seattle and Salem test areas for southwest inflow are shown in figures 4-16a and 4-16b, respectively. For the Seattle test, ten of the highest rain periods were selected for southwest inflow computations. Some of the differences between figures 4-15a (Seattle west inflow) and 4-16a (Seattle southwest inflow), and between figures 4-15b (Salem west inflow) and 4-16b (Salem southwest inflow), are due to using a slightly different test area when inflow direction changes. The computed precipitation for southwest inflow was that which approximately covered the west inflow test areas. Figure 4-17 shows computed and observed precipitation for the Boise test area.

Data on the five figures indicate average relations with slopes slightly greater than 45°, except considerably greater for the Boise test area. Differences between west and southwest profile computations for the Seattle and Salem tests are small. For Salem, west inflow gave slightly better correlation between computed and observed precipitation.

4.25. In the June 1964 test storm on the Continental Divide in Montana involving slow-moving cold Lows, lapse rates were near the moist adiabatic. Both high temperatures in the lower level flow from the Gulf of Mexico and gradual lifting to near the 3000-ft. elevation of the foothills steepened lapse rates. Thus a significant part of the rainfall on east slopes was due to influence of instability, referred to in chapter III as stimulation. Rain amounts averaged higher on steep upper slopes than the sum of computed orographic rain and the assumed convergence rain (that over foothills downwind). It was found however that if northeast winds of 30 to 40 knots are assumed during the most severe part of the storm, they would yield a computed rain volume equal to the "observed" orographic rainfall and that winds of this speed would yield rain volumes exceeding the "observed" during lesser parts of the storm. Thus it is indicated that the model does not exaggerate the storm rainfall. The sensitivity of computed spillover into the Lakehead River Basin to wind increase is illustrated. At 25 knots, computed rain spillover of .8 inches in 6 hours just west of the ridge extends to only about 10 n. mi.; with a 40-kt. wind it increases to 1.4 inches just west of the ridge and extends to about 30 n. mi.

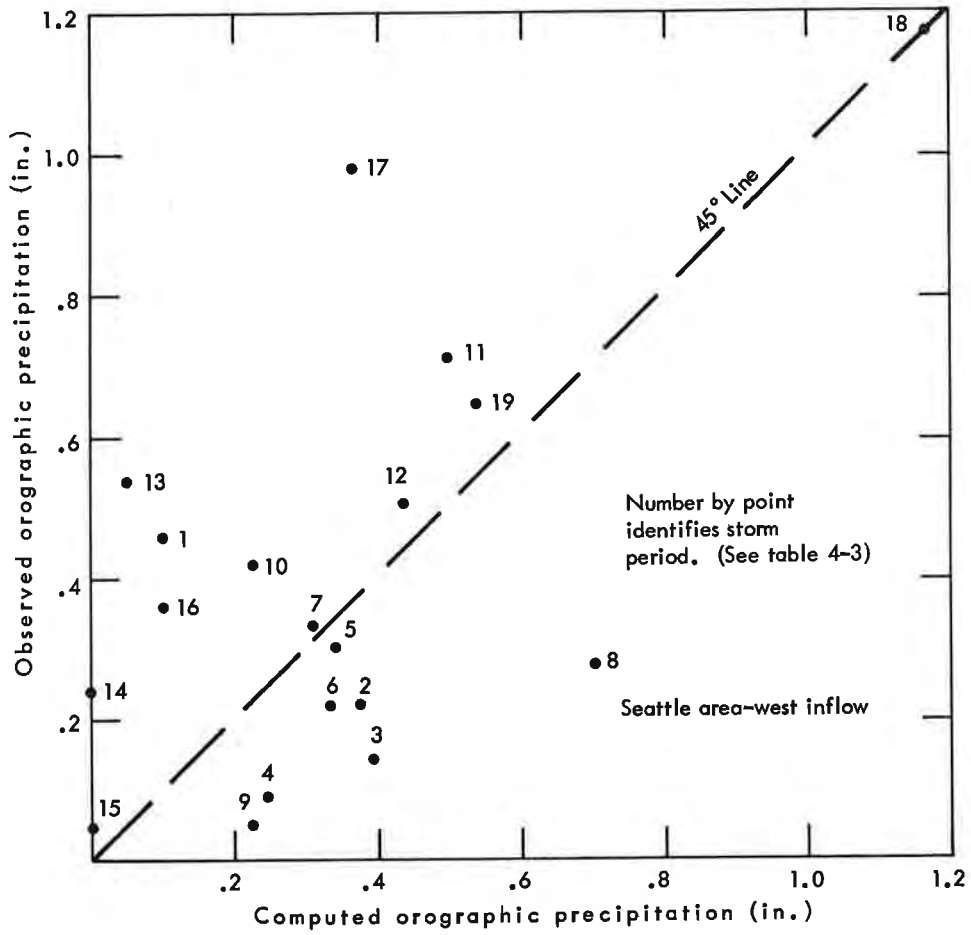

Figure 4-15a. Computed and observed orographic precipitation - Seattle area (west inflow)

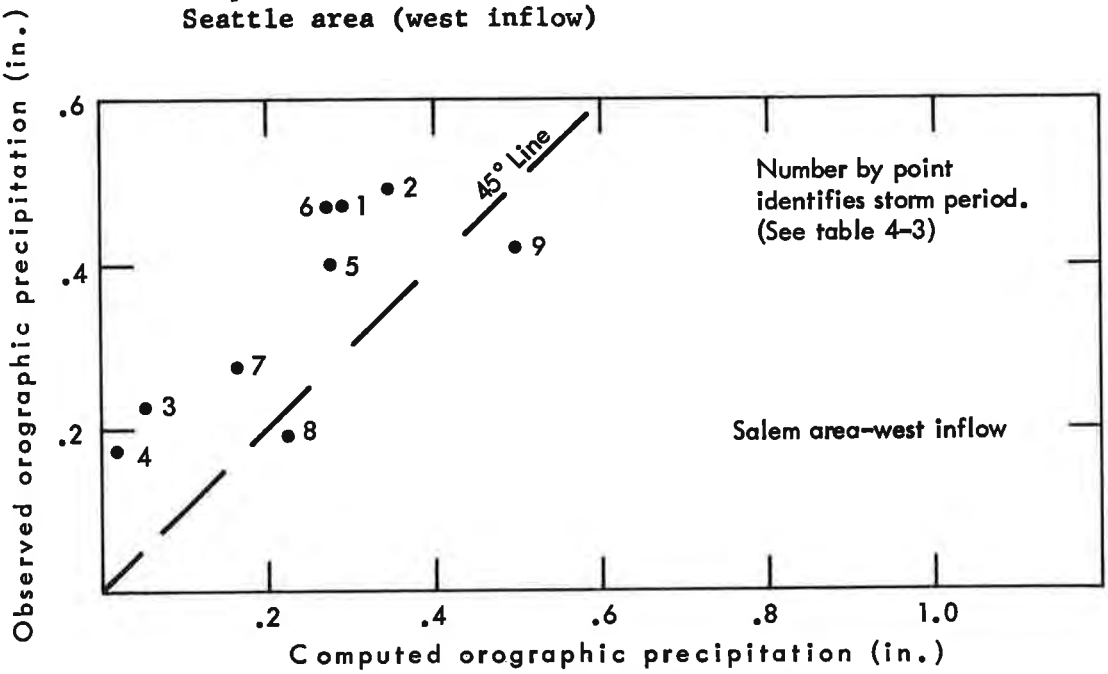

Figure 4-15b. Computed and observed orographic precipitation - Salem area (west inflow)

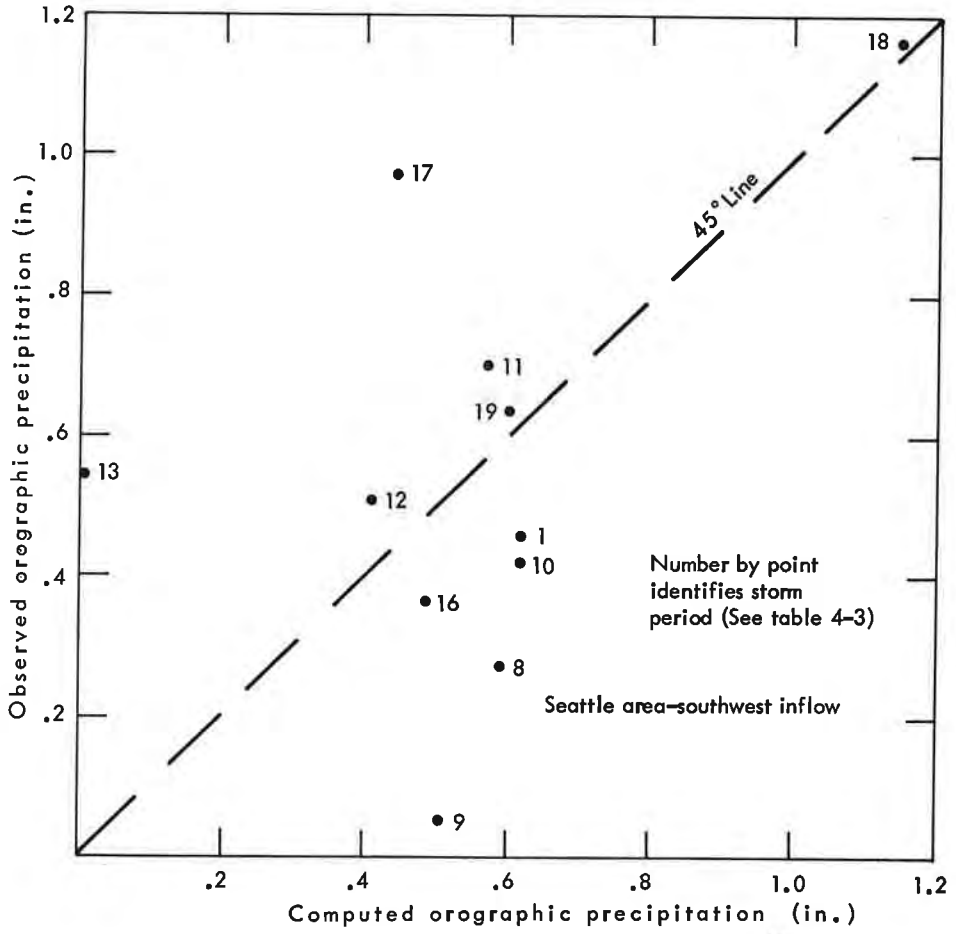

Figure 4-16a. Computed and observed orographic precipitation - Seattle area (southwest inflow)

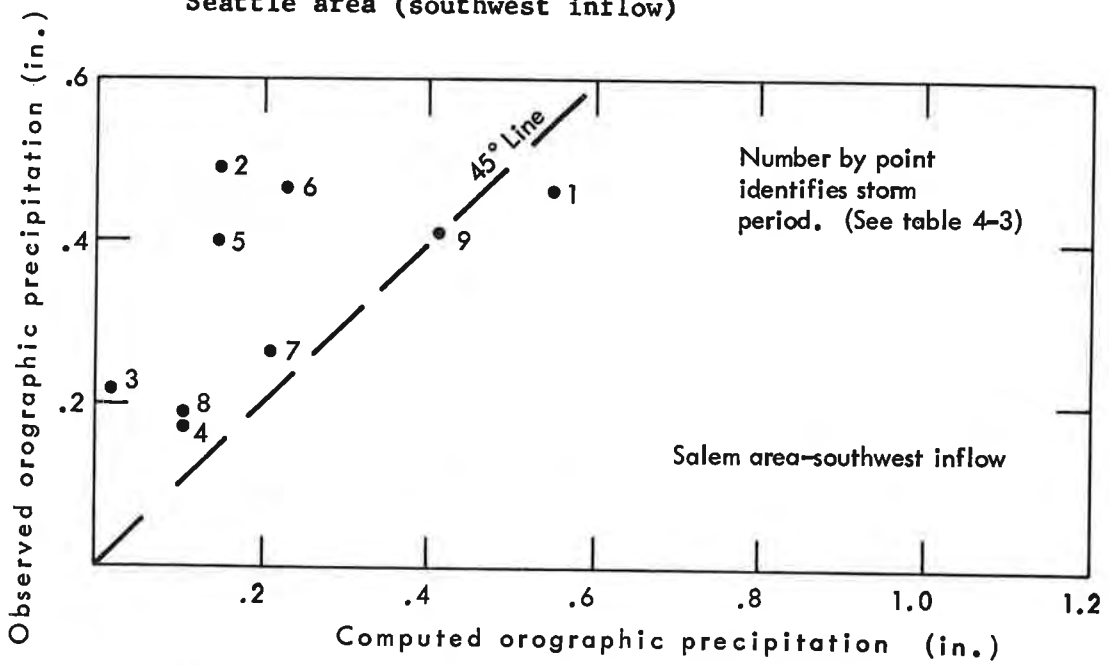

Figure 4-16b. Computed and observed orographic precipitation - Salem area (southwest inflow)

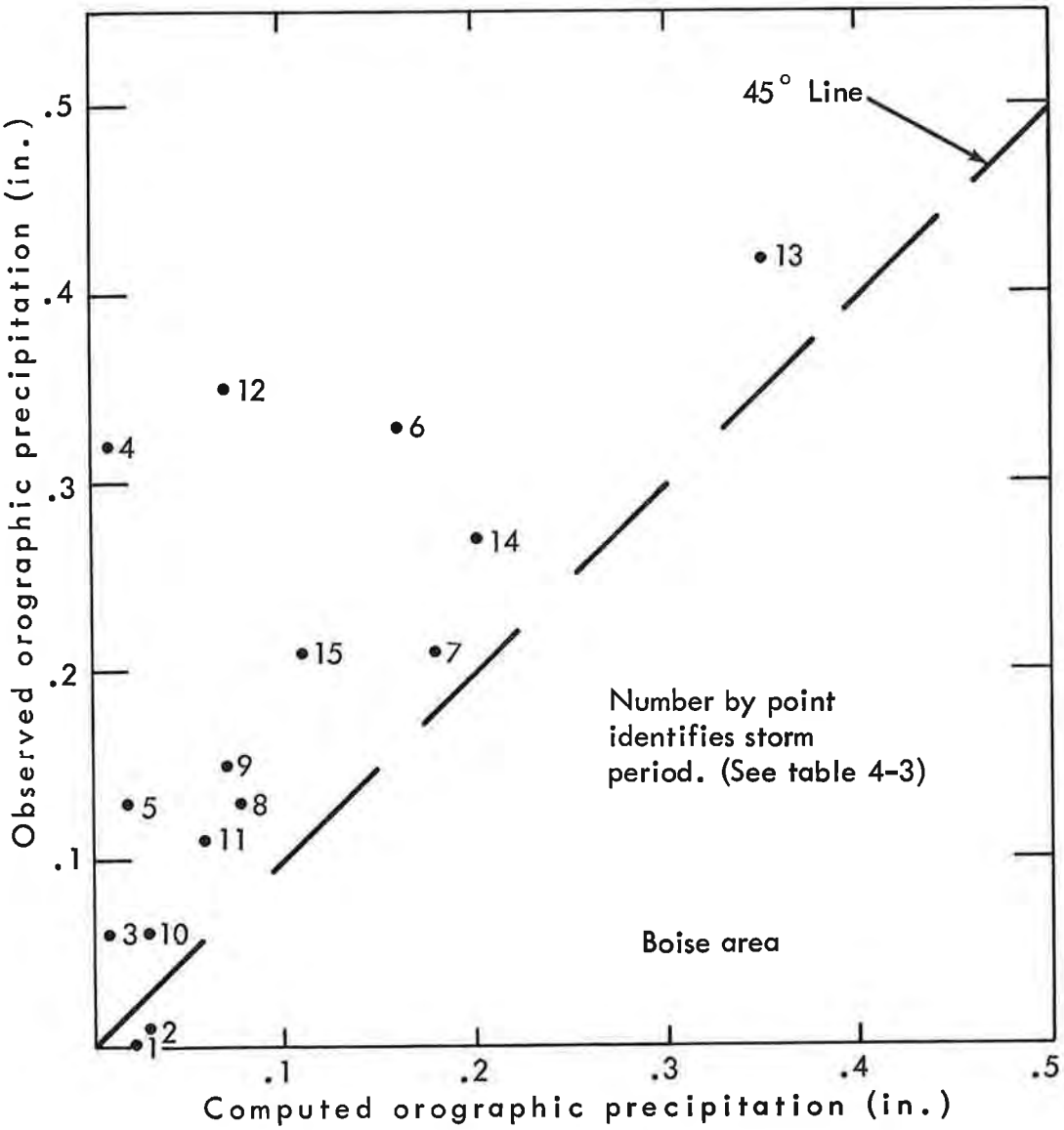

Figure 4-17. Computed and observed orographic precipitation - Boise area

4.26. Over elevation bands. Table 4-3 contains both total and orographic component of the observed precipitation, and the computed orographic precipitation, averaged for each 6-hr. period over each elevation band and over the total slopes for west-east Seattle and Salem test areas and the Boise test area.

The degree of agreement between observed orographic and computed orographic differs from elevation to elevation and from one test area to the other. For example over the first elevation band, observed orographic is a little higher than computed in each area. For the second band, the observed orographic is less than computed in the Seattle area, but higher than computed in the Salem area.

The largest excess of computed over the observed orographic precipitation occurs in the middle elevation band of the Seattle area. The rise in its computational profile from 1000 feet to 3000 feet in a distance of seven miles, by far the sharpest slope in the area, accounts for the high computed values. Most of the precipitation stations in this elevation band are in valleys or canyons near the entrance to the band at elevations mostly below 1000 feet. This suggests that their rainfall underestimates the average over the band. The observed orographic values further downwind in the third band, however, are higher than the computed. Also over the Salem area, they are higher in each band. Observed on the average are double the computed over the Boise area.

4.27. Causes of disparity. Lee depletion effects on valley rain upwind of the Boise test area probably results in too small slope convergence precipitation estimates, using the procedure of paragraph 4-13. That is, mountains to the southwest of the test area reduce the valley rain such that too little convergence precipitation is subtracted from slope total precipitation. This accounts for some of the much greater observed orographic precipitation (total minus convergence) compared to computed. Another cause of disparity between observed and computed precipitation is low elevation of observed precipitation amounts relative to the average terrain profile that determines the computed precipitation, as mentioned above with respect to the middle band of the Seattle test area. In band III of the Seattle test area, for example, all observations are more than 1000 feet below the mean elevation. An additional shortcoming is use of a mean annual precipitation map to obtain areal depths in a 6-hr. storm period, which often has a much different pattern.

In the June 1964 storm, much of the orographic effect was in the nature of stimulation (see par. 3.32) of convection by triggering. Also good wind observations were not available along the axis of the heavy rain.

3. Conclusions and Application

Conclusions

4.28. The results of the California test are considerably better than for the tests in the Northwest. One reason for this is the much better

sampling of observed rain amounts, especially on higher slopes, in the California area. Also, the elevations of stations in the California test correspond more closely to the elevation of the terrain profile used in the computations. Comparison of terrain profiles and station elevations in figure 4-3 with those in figures 4-7, 4-8, and 4-13 show the differences.

In the Northwest, computed averages over total slopes are somewhat less than observed. In California the reverse is true. Some of this difference may be due to over- or underestimation of convergence to subtract from total observed. Estimation of convergence rain is difficult. A consistent procedure, used in this report, leads to oversimplification. But alternative independent decisions on the convergence component for each storm period would lead to excessive subjectivity.

The overall results of the tests are considered good in spite of uncertainty of the actual precipitation and its breakdown into components and approximations in the model and in the input.

Application

4.29. In view of the above conclusions, the model is used directly to compute orographic PMP for slopes in the Northwest without calibration or adjustment. Input to it are maximum winds and moisture, the subject of the next section.

4-D. MAXIMIZATION OF WIND AND MOISTURE

Intensity of orographic precipitation is set by the terrain configuration and by the rate of inflow of moist air. Winds and moisture that determine the latter for orographic PMP are developed in this section.

Maximum wind

4.30. West of Cascade Divide. The maximum 1-hr. (single observation) winds used for the area west of the Cascade Divide are the coastal maximum 1-hr. winds adopted for California in HMR 36 (fig. 5-23 curve C). In summary, these winds are based on 1) a combination of maximum observed winds along the entire West Coast, using the 5 to 12 years of rawins available at the time the report was prepared, and 2) maximum geostrophic winds. The latter winds were derived from surface pressure gradients along or near the Pacific Coast from about 60 years of record and converted to actual winds by various empirical means. Figure 4-18 shows these winds. Also given are the adopted maximum 6-hr. winds. Winds for this duration are compared because it is the basic wind used in most of the orographic computations. Reduction to 6 hours duration is by the durational variation of winds, paragraph 4.78.

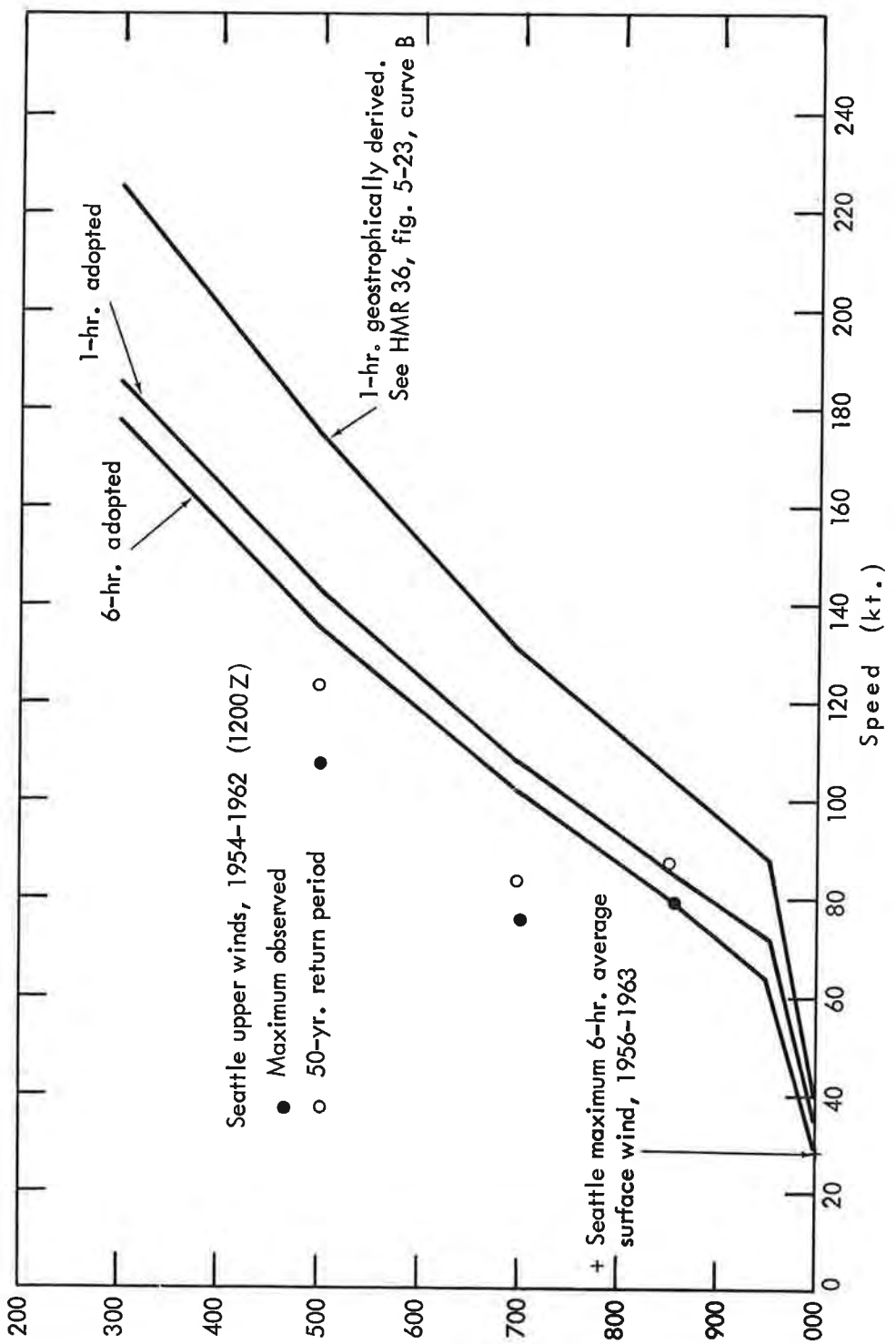

Figure 4-18. Maximum winds West of Cascade Divide

Recent upper-air winds at Seattle were used to judge the magnitude of the adopted winds. Using 1200Z observations for the period 1954 to 1962 at 500-, 700-, and 850-mb. levels, the highest winds from the south through west were selected for each year. Estimates of the 50-yr. return-period windspeeds were obtained from plots of the annual extremes. These 50-yr. return-period and the maximum observed values are shown in figure 4-18.

The highest 6-hr. average wind at the surface (1000 mb.) was determined from maximum hourly south through west winds for the period July 1956 through May 1963. The adopted 6-hr. surface wind is equal to the highest value in the period.

4.31. East of Cascade Divide. Above 500 mb., maximum winds east of the divide are equal to those on the west side. Statistical analysis of the upper-air winds used for seasonal variation at Seattle, Wash., Medford, Oreg., Boise, Idaho, Kalispell, Mont., and Ely, Nev. (par. 4.55) showed no significant difference in maximum winds above 500 mb.

The adopted curve of figure 4-19 is drawn for east-of-Cascades values above 500 mb. and for the 700-mb. west-of-Cascades value (fig. 4-18) reduced by 10 percent for effect of upwind barrier.

Surface winds at Walla Walla, Wash., Spokane, Wash., Boise, Idaho, Pocatello, Idaho, and Ely, Nev., were utilized to define the maximum wind at the surface elevations. Maximum annual 24-hr. average winds from the southwest quadrant were found at each station for 12-14 years of record and the 50-yr. return-period winds were computed. These were converted to 6-hr. 50-yr. return-period winds by the durational variation of paragraph 4.78. They are shown in figure 4-19 by x's at the appropriate pressure elevation. A smooth variation of windspeed with surface elevation was drawn to these data (dashed curve). Points along this curve at 1000, 900, and 800 mbs. were then smoothed into the adopted 700-mb. wind.

A check on the derived winds is once-a-day upper-air winds at Boise from 1951 to 1962. The maximum observed and 50-yr. return-period values based on this period are plotted on figure 4-19. At 850 and 500 mb. the single observation 50-yr. values for Boise are quite near to the adopted 6-hr. winds.

4.32. Near the Continental Divide. The typical weather pattern of spring storms near the Continental Divide involves a Low at the surface and aloft, centered in the northern Rocky Mountain area. In the more severe storms moisture is drawn from the Gulf of Mexico into Montana. In the recent storm of June 7-8, 1964 (fig. 2-12) this moist flow to high levels was oriented mainly up slopes facing east or northeast, accounting in part for the extreme precipitation amounts (fig. 2-11). Use was made of all available rawin data along the northern Rockies for maximum wind analysis. Figure 4-20 shows the stations and years of record used and the highest wind at standard levels from directions 20° to 130°. Also plotted is the average

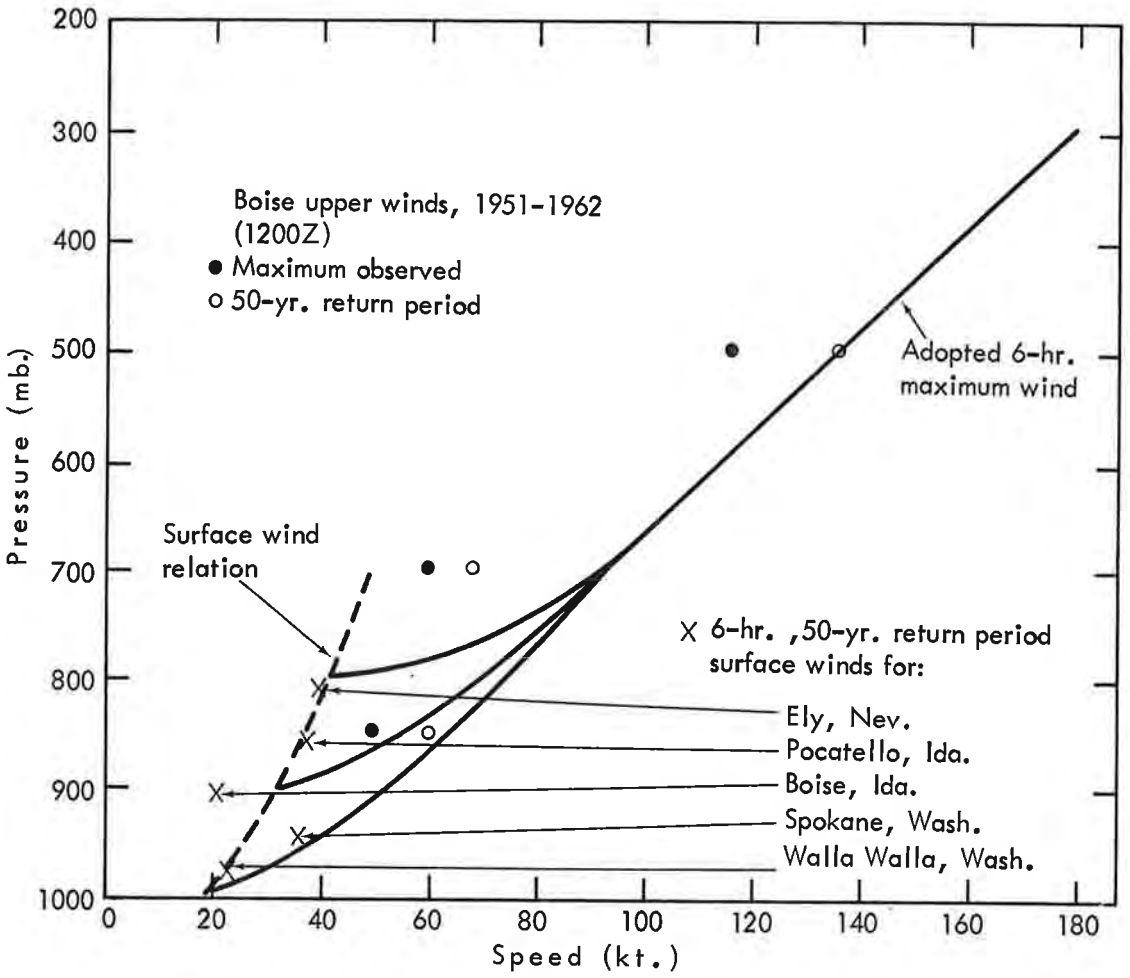

Figure 4-19. Maximum winds East of Cascade Divide

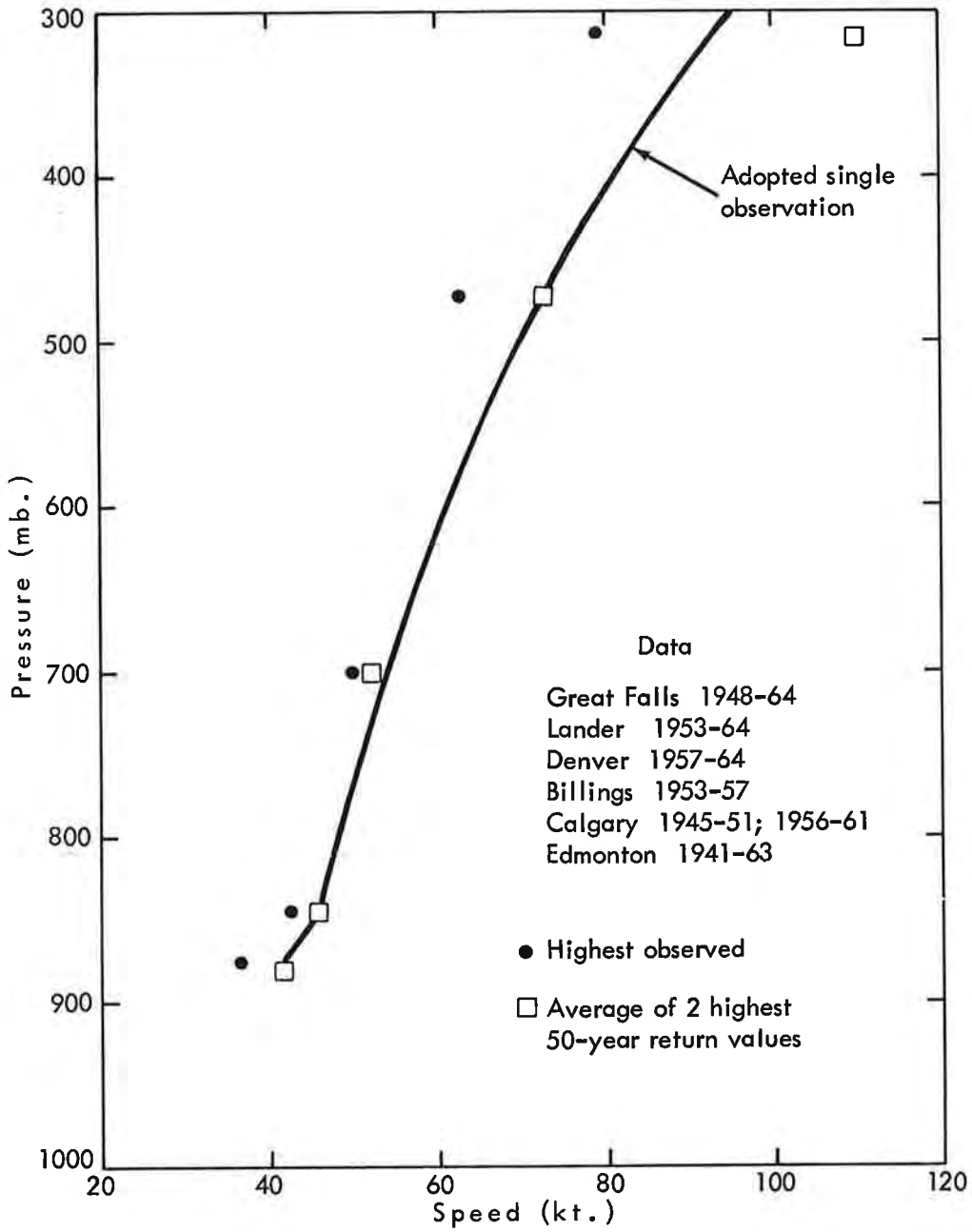

Figure 4-20. Adopted maximum winds 020-130°, May-July East of Continental Divide

of the two highest station 50-yr. values at each level. The adopted curve envelops all but the 300 mb. 50-yr. average, considered less reliable because of scarcity of data at that level. Compared with the adopted wind curve west of Cascades (fig. 4-18) for prevailing wind directions, this plot for opposite to prevailing direction shows comparable surface speeds (little retardation by friction and upwind barrier) but speeds about half at all other levels.

These maximum windspeeds, obtained from a range of directions, are considered upslope components in Continental Divide orographic PMP computations. East and northeast directions were common in the controlling speeds, especially above levels where terrain affects direction.

Maximum moisture

4.33. West of Cascade Divide. Maximum 1000-mb. dew points discussed in chapter III provide the basis for maximum moisture. Saturation of the air column is assumed with a lapse rate slightly more stable than the moist adiabatic lapse rate. The degree of stability adopted in the maximum case was derived from a study of lapse rates in large storms of the region. The incremental difference between a moist adiabatic lapse rate and that adopted is given in table 4-4.

4.34. East of Cascade Divide. Maximum 1000-mb. dew points again were the starting place for maximum moisture. These were reduced to the elevation of the beginning of slopes along a moist adiabatic lapse rate. Above this surface elevation, temperature lapse rates were again patterned after storms in the region. The adopted rate for southwest flow is given in table 4-5 relative to the moist adiabatic rate.

Near the Continental Divide the June 1964 Montana flood is the principal prototype of lapse rates. Strong upslope flows from the east will be provided primarily by deep slow-moving cold Lows. For maximum rainfall the lower levels must carry high moisture brought up in the southerly current from the Gulf of Mexico. Upper-level air would in the optimum rainfall situation be relatively colder. These factors suggest a moist adiabatic lapse rate. With moist adiabatic inflow in neutral equilibrium and energy areas in two-dimensional computations zero, a 300-mb. nodal surface was assumed and outflow pressures and winds were computed by proportionate spacing of streamlines, rather than as outlined in paragraph 4.07.

4.35. In interior cool-season storms, the air is generally unsaturated below the height of upwind barriers. To take this into account in the PMP storm, a procedure was devised that relates relative humidity to upwind barrier height. The most nearly saturated sounding at Boise during the December 1955 storm was selected as a prototype of conditions during the PMP storm. In this sounding, plotted as X's in figure 4-21, relative humidity is 80 percent at 875 mb., increasing to 92 percent at 700 mb. In the

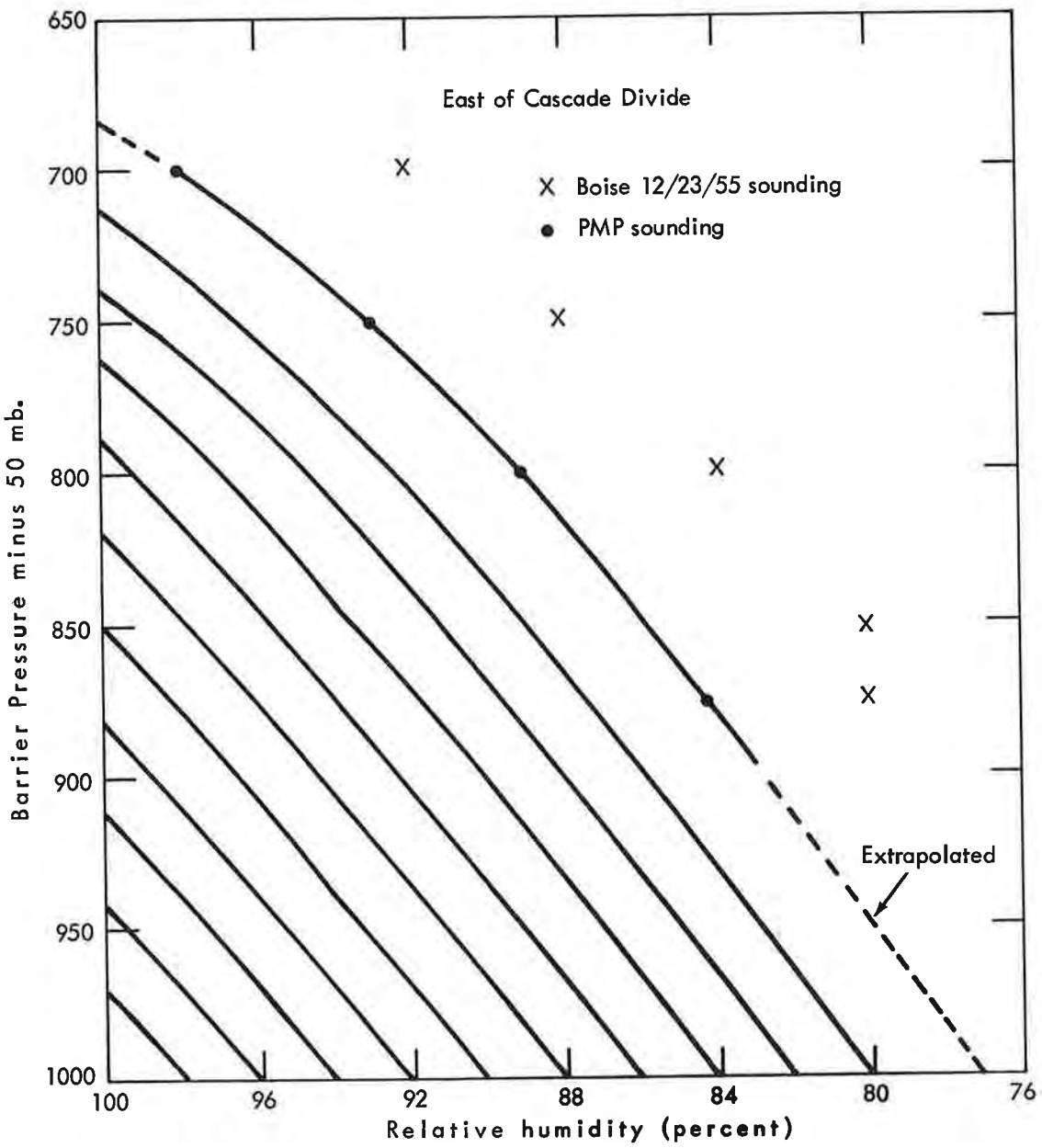

Figure 4-21. Variation of relative humidity with inflow barrier height (East of Cascade Divide)

Table 4-4

DIFFERENCE BETWEEN MOIST ADIABATIC LAPSE RATE AND ADOPTED
(WEST OF CASCADE DIVIDE)

Layer (mb.)	°C*
1000-900	+0.2
900-800	+0.2
800-700	+1.0
700-600	+1.0
600-500	+1.0
500-400	+1.4
400-300	+1.4

Table 4-5

DIFFERENCE BETWEEN MOIST ADIABATIC LAPSE RATE AND ADOPTED
(EAST OF CASCADE DIVIDE)

Layer (mb.)	°C*
1000-900	+0.5
900-800	+0.5
800-700	+0.5
700-600	+1.0
600-500	+1.5
500-400	+1.0
400-300	+1.0

*More stable than moist adiabatic lapse rate.

adopted relation (joining the circles), relative humidity is 84 percent at 875 mb. and increases to 98 percent at 700 mb. This is a slight maximization for the PMP storm. For lower barriers, lines parallel to this line were constructed.

Relative humidities for entrance points to lee of barriers were determined from the nomogram just described in the following manner. Barrier elevation pressure was obtained from figures 3-36a and 3-36b and 50 mb. was subtracted. This last step allows 100 percent relative humidity at 50 mb. above the barrier height. From figure 4-21 relative humidities were obtained by entering the vertical axis with barrier pressure minus 50 mb., then proceeding down the sloping lines to read relative humidities on the

horizontal scale for various pressure levels, usually at 25-mb. intervals. The purpose of assigning relative humidities of less than 100 percent at low levels to the lee of barriers is to indicate lack of saturation characteristic of the region. It is not to reduce the specific humidity of air. This lack of saturation calls for a higher cloud base and less orographic precipitation in foothill areas than saturation would provide. These requirements are met by assuming the temperatures determined in paragraph 4.34 are wet-bulb temperatures. The assigned relative humidity is then used to calculate the concurrent dry-bulb temperatures.

4.36. With a northeast low-level inflow across the Continental Divide directly from the Gulf of Mexico, and with a gradual lifting of lower levels to approximately 3000-ft. elevation with no upwind barrier, saturation is a logical assumption for conditions prior to lifting up the east face of the Continental Divide. Hence saturation is assumed for critical periods in PMP computations there.

4-E. SEASONAL VARIATION OF OROGRAPHIC PMP

4.37. The intensity of major storms over the Columbia and Coastal Basins varies with the season. Seasonal trends in PMP are similar to, but not identical with, the trends shown by observed storms. The seasonal variation, then, of the orographic component of the PMP in various subregions of the Pacific Northwest is determined by combining indications from observed precipitation and from theoretical calculations.

Importance of seasonal variation

4.38. The maximum flood hydrograph for all large basins and many small ones in the Pacific Northwest results from a combination of snowmelt and rainfall. Both the amount of snow available for melting and the rate at which it can melt varies with season, To find the most severe combination of concurrent rainfall and snowmelt, it is necessary to define the PMP seasonally.

Seasonal trend of orographic storm intensity

4.39. West of the Cascade Divide winter storms dominate the records. Moving to the mountains of Idaho, the predominance of winter storms disappears and there is a more even seasonal distribution. Continuing eastward to the east slope of the Rockies, we find the potential for storms in late spring clearly exceeding that in winter.

4.40. These trends are reflected in the major storms selected for discussion in chapter II without particular regard to their season. Of the 20 west of the Cascade Divide (pars. 2.04, 2.12, and 2.19), the dates all range from November to February except for one each in June and October.

The storms for the interior Columbia Basin (par. 2.22) are spread out from November to July. The record-breaking Montana storm of June 7-8, 1964 (par. 2.30) is the principal example near the Continental Divide.

Factors in seasonal variation

4.41. The progressive decrease in intensity of winter orographic storms relative to spring and early summer from the Pacific Coast to the Continental Divide is in part a trend from a maritime to a continental climate.

4.42. Cyclonic intensity. The coastal regions west of the Cascades are affected by very intense cyclones (Lows) which form at sea, and do so most readily in midwinter. In contrast, winter storms reaching the eastern part of the Columbia Basin are weakened in lower levels in passing inland over mountain barriers while spring storms often intensify there with increased moisture supply.

4.43. Moisture supply. On the coast, dew points are closely related to East Pacific Ocean sea-surface temperatures, remain high into fall, and recover slowly in spring. The annual cycle of sea-surface temperatures lags behind the sun. In the interior the annual range in maximum dew points (figs. 3-11 to 3-13) is larger than on the coast. In the fall the dew points decrease earlier, faster, and to lower values than on the coast. In the spring, however, there is a more abrupt recovery in the interior in late April and May as Gulf of California and Gulf of Mexico air begin to find their way northward across the Great Basin and contribute to precipitation intensity.

4.44. Combined effect of moisture and cyclonic activity. On the coast, midwinter predominance of observed storms coincides with the maximum cyclonic activity at sea. However, the combined effect of seasonal trends results in the largest potential for precipitation in the fall, when intense cyclonic activity can be expected occasionally while dew points are still high.

In most of the interior the combined seasonal trends (spring cyclogenesis and rapid increase in moisture) allow the maximum orographic storm to coincide with the peak of the snowmelt season, quite in contrast to the entire area between the Pacific Coast and the Cascade-Sierra Nevada Divide.

4.45. Effect of melting level. Another factor important to month-to-month variation of PMP over some basins is the height of the melting level in the atmosphere. If the 0°C isotherm is low, the orographic precipitation remains in the form of snowflakes until close to the ground and is carried by the high winds necessary to produce the orographic PMP a great distance from the point of formation before reaching the ground. The melting level does not of itself have much effect on the total volume of PMP formed along a lengthy profile parallel to the wind, but it greatly

affects the maximum amount that may be collected on a short steep slope. The snow that forms drifts on by. Thus, low melting level is a factor tending to limit winter PMP on steep slopes in regions that are cold by virtue of latitude, location, or elevation as compared to the precipitation potential at the same spots in a warmer season. The higher elevations, steeper slopes, and colder temperatures in winter subject some portions of the interior of the Columbia Basin to the influence of this "melting level depression" much more than most of the Cascade Range. The PMP is more sensitive to melting level than average storm precipitation because of the high winds.

This melting level effect accounts for much of the difference in seasonal trend at low elevations and high elevations prescribed for "Zone C" (defined in par. 4.59).

Seasonal variation of PMP appraised by station data

4.46. The seasonal trend in the orographic component of PMP on exposed slopes should be reflected in part by the precipitation records at higher elevation stations.

4.47. Western Washington. Twenty-two stations were chosen on the west slope of the Cascades, in Washington, and five stations in the Olympic Mountains. The stations and their elevations are listed in table 4-6. Highest observed one-day precipitation for each month was tabulated for the period of record through 1961 for each station and averaged within each of the two groups. The resulting seasonal variation of daily precipitation is plotted at the bottom of figure 4-22, expressed as a percent of January.

4.48. As another measure of seasonal variation, precipitation differences between Snoqualmie Pass, Wash. and Seattle were summarized. The five highest three-day totals at Snoqualmie Pass in January, in February, etc., were averaged for the years 1916-1961. Then, to approximate removal of the convergence rain component, the average contemporaneous rain at Seattle was subtracted from each Snoqualmie average. (This adjustment is only approximate because of elevation differences and a distance of 40 miles between the two stations.) The Snoqualmie Pass-Seattle difference for each month, expressed as a percent of the January difference, is shown by another seasonal curve at the bottom of figure 4-22.

4.49. Idaho and Upper Snake Basin. Similar seasonal curves were constructed for three groups of high-elevation mountain stations: in the extreme Upper Snake Basin, to the east of Boise, and in northern Idaho. Maximum daily precipitation published in Weather Bureau Technical Paper No. 16 (7) was averaged for each group of stations for each month. The percent-of-January plots are found in figure 4-23 and a list of stations in table 4-6. The curves are irregular because of too few stations in each group. However, the much smaller decrease from January to summer compared to western Washington is evident, and also the tendency toward maximum values in fall and early winter.

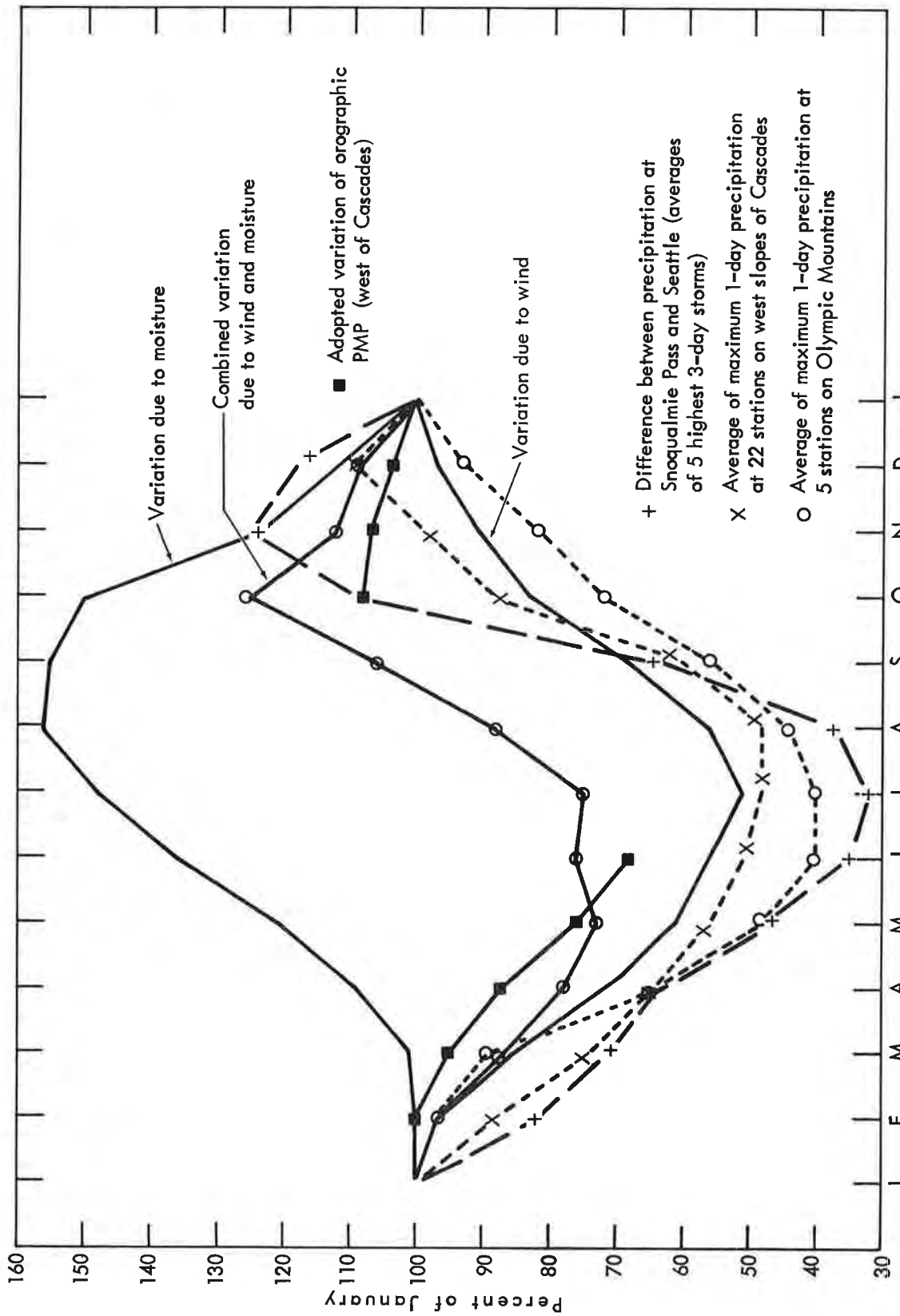

Figure 4-22. Seasonal variation of orographic PMP (West of Cascades)

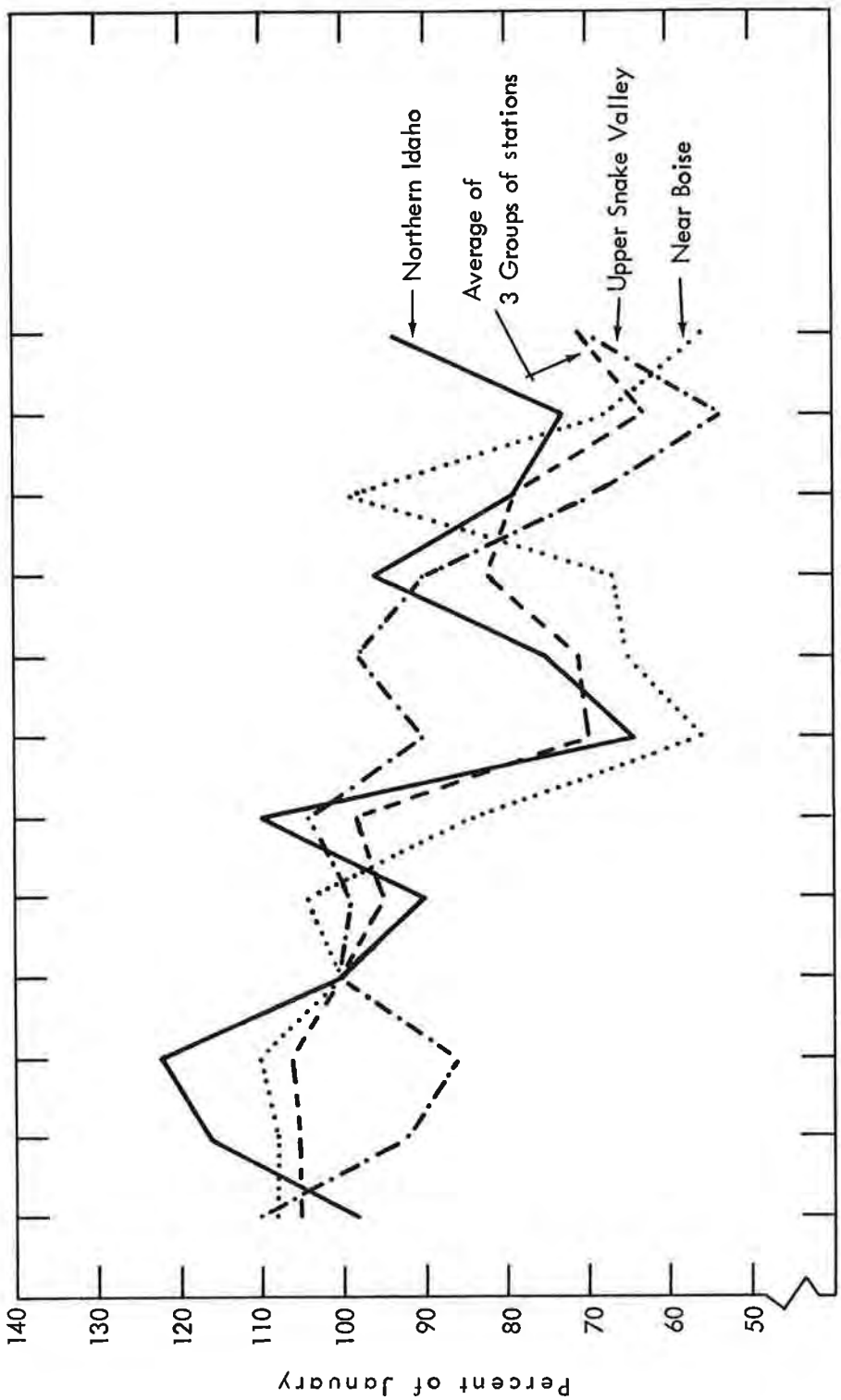

Figure 4-23. Seasonal variation of maximum daily precipitation at high elevations (East of Cascade Divide)

Table 4-6

SOURCE OF MAXIMUM DAILY RAINFALL USED TO EVALUATE SEASONAL VARIATION OF OROGRAPHIC PMP

Olympic Mountains

Station	Elevation (ft.)
Aberdeen-Wishkah	435
Cushman Dam	760
Quinault	220
Spruce	400
Wynoochee-Oxbow	670

Cascade Slopes in Washington

Station	Elev. (ft.)	Station	Elev. (ft.)
Alder Dam Camp	1301	Packwood	1060
Buckley	685	Palmer	895
Cedar Lake	1560	Randle	940
Goat Lake	2900	Ranier - Carbon River	1716
Greenwater	1708	Ranier - Longmire	2762
Headworks	985	Ranier - Ohanapecosh	1925
Index	532	Ranier - Paradise R. S.	5550
Lake Kachess	2270	Scenic	2224
Lester	1626	Silverton	1511
Mineral	1500	Snoqualmie Pass	3020
Mud Mountain Dam	1308	Startup	170

Northern Idaho

Station	Elevation (ft.)
Wallace	2770
Roland West Portal	4150
Pierce R. S.	3175

Upper Snake River

Island Park Dam, Idaho	6300
Bechler R., Wyo.	6300
Snake River, Wyo.	6882

Mountains Northeast of Boise

Idaho City	3940
Idaho City 11 SW	5000
Atlanta	5500
Solder Creek	5755
Deadwood Dam	5375

4.50. Near the Continental Divide. General storms in Montana near the Continental Divide occur mainly in spring, corresponding with months of peak snowmelt and prior to the season of extreme local storms. June is the month of most frequent extreme 24-hr. rains at stations in Montana west of 110° longitude. This is shown by listing record daily rain at such stations above 3500-ft. elevation in Weather Bureau Technical Paper No. 16 (7) by month of occurrence. This tabulation follows. Forty stations had their heaviest rain in June, far more than in any other month. Also, June record daily rains are heavier than in other months. Some of these stations, however, have little orographic rain.

Month:	Jan.	Feb.	Mar.	Apr.	May	June	July	Aug.	Sept.	Oct.	Nov.	Dec.
No. of stations:	1	0	1	3	13	28	5	7	5	4	3	5

4.51. Other areas. Similar plots of station data were attempted for other areas, including the Cascades of Oregon and the slopes north and northwest of Spokane. The station locations in these regions, however, are less satisfactory. From the similarity to the plots for low-elevation stations (figs. 3-21 and 3-22), it is concluded that convergence precipitation predominates enough to mask orographic trends.

4.52. Limitations of method. The correspondence of station seasonal variation to that for orographic PMP will be far from exact for several reasons. First, the station data are affected by frequency of storms in the various months more than is the PMP. Second, the convergence component of the precipitation is only minimized, not eliminated, by station selection. Third, the stations do not lie on exposed slopes, but in valleys. The failure of existing precipitation stations to sample exposed slopes throughout the Columbia Basin is noted in the discussion of tests of the orographic model, paragraph 4.27.

Seasonal variation calculated from orographic precipitation model

4.53. A theoretical seasonal variation of orographic PMP at any one place is attained by computation from the laminar flow model described in paragraphs 4.07 and 4.08, and tested in subsequent paragraphs. This model is employed to compute the orographic index map (described in the next section of this chapter). The seasonal variation is a prelude.

4.54. Model calculations. The precipitation calculated by the laminar flow model approximates the orographic component of PMP when the input data above the foot of the mountain range are the maximum moisture and maximum wind. The calculated precipitation varies from month to month as the moisture rises and the wind decreases (spring) or conversely (fall). These opposing trends do not exactly cancel, nor is their interaction the same at different elevations and steepness of slope. Maximum moisture at each level derives from the maximum dew point envelopes of figures 3-11 to 3-13. These values are extrapolated to upper levels approximately along a moist adiabat

(par. 4.33). Maximum winds derive from an envelope of wind data. Presentation of midwinter wind envelopes for orographic storms is found in section 4-D. Month-to-month ratios to these values, determined independently, are described in the next paragraph.

4.55. Seasonal variation of winds. Once-a-day winds at upper levels for Ely, Nev.; Great Falls, Mont.; Boise, Idaho; Medford, Oreg., and Tatoosh (or Seattle), Wash. were available for analyses for the period 1951-1958. This is a short record but adequate for seasonal variation. The highest average windspeeds persisting from the southwest quadrant for 1, 2, 3, 5, 7 and 10 days were selected from these data for the 950-, 850-, 700-, 500-, and 300-mb. levels for each station and each month (the maximum January value from the record, etc.). Further differentiation was made on the basis of wind direction. Seasonal envelopes of these highest winds for each station, level and duration were then drawn. These curves (not shown) indicated differences from month to month and from station to station which could be explained only as random occurrence of high windspeeds at a particular station. Grouping them gave consistent seasonal curves among the various levels. The higher the level the less seasonal variation exists. Expressed in percent of January, the resulting adopted seasonal variation is shown in figure 4-24.

As a check a differing analysis was made at Boise and Seattle, with a few additional years of record (Boise 1952-61, Seattle 1954-61). The highest wind for each month (highest January each year, etc.) was selected for 500, 700 and 850 mb. The seasonal variation of the mean of the monthly maxima was then determined. Results verified that the adopted seasonal curves (fig. 4-24) are adequate. Most difference was found in summer months, indicating that at 500 mb. the adopted speeds may be somewhat low. The contribution to precipitation from this height is small compared to lower levels, therefore no changes were made in the adopted curve.

4.56. West of Cascade Divide. One typical calculated seasonal variation of 6-hr. orographic PMP on the windward side of the Cascade Range is marked on figure 4-22 by circles. This calculation is for a west wind impinging on a representative cross-section of the range with the crest at 5000 feet. The average of the dew points at Tatoosh, Portland and Seattle, Wash. and Roseburg, Oreg. was the index of inflow moisture. The winds are from the west-of-Cascades curve of figure 4-18, modified by the seasonal variation of figure 4-24. An analysis of seasonal variation of elevation bands of 1000 feet showed the following: The annual range of values decreases with elevation. The decrease is modest from 2000 feet to 5000 feet. Below 1000 feet the exceedance of winter over summer is much more marked. A separate seasonal variation of the low orographic component at these low elevations (with lower warm-season values) would be of little practical significance. A single seasonal variation is adopted for all elevations west of the Cascades (par. 4.60), based on the 0 - 5000 ft. total to which the higher elevation bands contribute most of the volume.

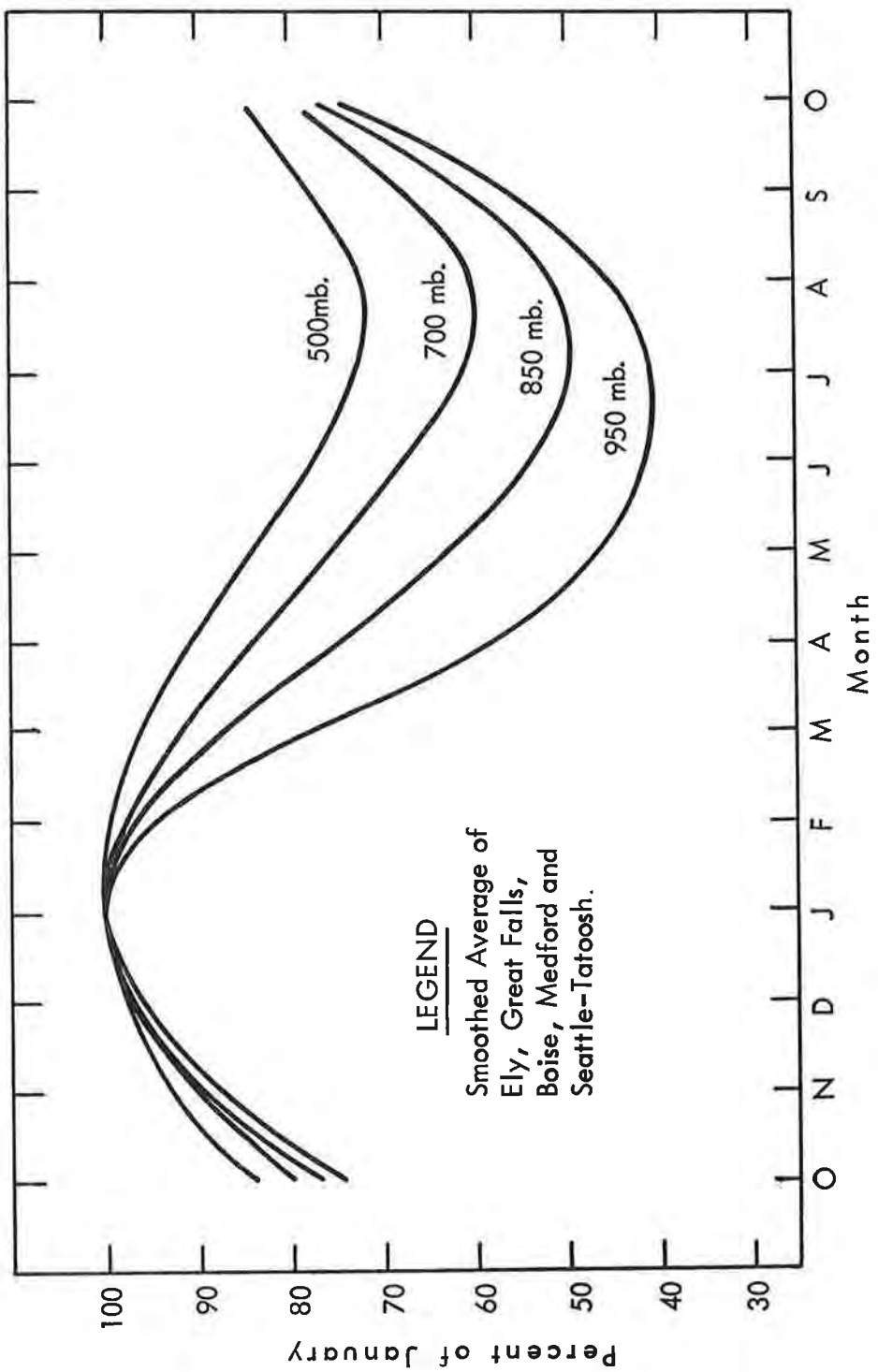

Figure 4-24. Seasonal variation of maximum wind speed

4.57. Interior of Columbia Basin. The seasonal variation of calculated orographic PMP in different topographic situations in the Columbia Basin is illustrated in figure 4-25. Curve S is for very steep slopes, curve M for intermediate slopes and the remaining curve, G, for gentle slopes. Curve S is calculated from airflow up the steep slopes rising northeastward from the Owyhee River in eastern Oregon at about 42°30'N., with the upwind mountains to the southwest ignored. Curve M is for the slopes rising northeastward from the Snake River at about 43°N., 116°W. (in the vicinity of Mountain Home, Idaho). Curve G is for a generalized version of the gentle slope from the Columbia River just above Pasco, Wash., northeastward to the Pend Oreille Lake region. The values plotted on figure 4-25 are ratios of the entire 6-hr. precipitation volume computed to fall along the strip 12 miles wide extending from smoothed valley floor to smoothed ridge crest.

4.58. Limitations on method. It is not appropriate to use the calculated seasonal variation of the orographic PMP exactly as computed without adjustment for several reasons. First, the computational model cannot replicate all of the effects in the real storms. A second problem is the necessity for generalizing the rather rugged terrain into simplified terrain profiles. A third factor is a seasonal effect on the storm mechanism. The computational model assumes laminar flow, a good assumption for midwinter storms. In warmer seasons, a strong topographic effect on the precipitation distribution is evident but generally takes on more of the characteristics of "stimulation," that is, setting off of convection in favorable locations and less true laminar flow. Since methods have not been devised for incorporating these stimulation effects into a flow model, all calculations are made with a pure laminar flow. A compromise between the seasonal variation of station rainfall and computed seasonal variation is believed to give the best indication of the real seasonal variation of extreme orographic storms.

Adopted seasonal variation by zones

4.59. Zones. By weighting all factors it is found that the predominant seasonal trends in the orographic PMP can be classified into four zones. These are shown in figure 4-26. Zone A is the principal orographic region of the west and extends from the coast to the Cascade Divide. Zone D is the principal orographic region of the east and extends from a generalized 6000-ft. elevation contour in Idaho eastward. This zone includes valleys that are at lower elevations than 6000 feet. Zones B and C are separated along a line of lower orographic index as follows: Along Okanagan Lake and River to Columbia River, along Columbia River to 46°N., 119°W., along line segments shown in figure 4-26 to Snake River, along Snake River to near Nampa, Idaho, and along eastern edge of Owyhee River drainage to southern periphery of Columbia Basin. The four zones minimize discontinuities of transition from zone to zone as follows: A and B have same seasonal variation in fall and winter, but not in spring; B and C have same seasonal variation at low elevations; C and D have same seasonal variations at 6000 feet.

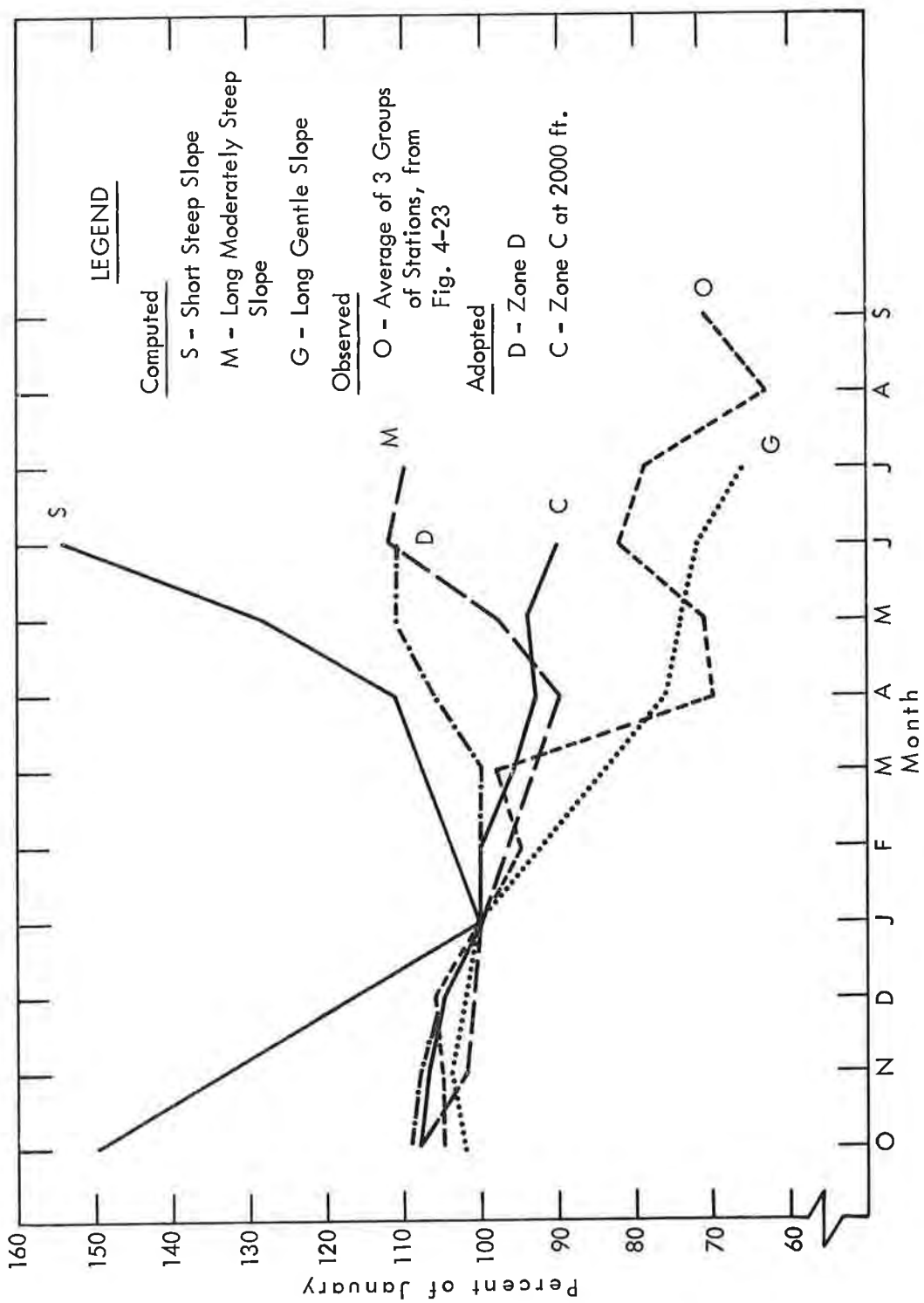

Figure 4-25. Computed and observed seasonal variations of orographic PMP (East of Cascade Divide)

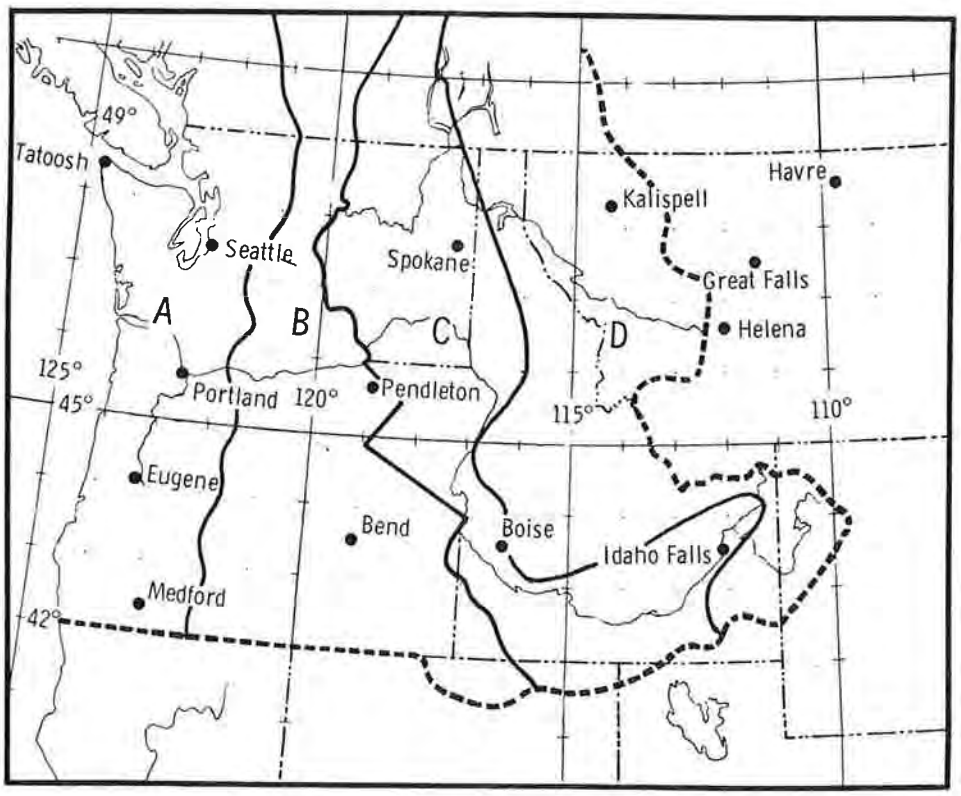

Figure 4-26. Zones for seasonal variation of orographic PMP

4.60. Adopted variation. The final adopted seasonal variation is shown in figure 4-27. Percents from figure 4-27 are given in table 4-7. In zone A, and also B, 100 percent is assigned to midwinter and the orographic index chart is constructed accordingly (par. 4.69). In zone D 100 percent is assigned to the critical snowmelt season and the orographic PMP index chart in that region is constructed accordingly. For these zones, elevation effects have been averaged out (see par. 4.59) and the adopted curves apply to all elevations. In zone C the elevation variation of the seasonal variation is maintained, with fall maximum at the low elevations (primarily near Columbia River in eastern Washington and near Snake River in southern Idaho), shifting to a spring snowmelt season maximum at 6000 feet.

For convenience, the zonal boundaries A, B, C and D are given on the orographic PMP index maps, figure 4-33a to c.

Table 4-7

SEASONAL VARIATION OF OROGRAPHIC PMP

	Midmonth								
	Oct.	Nov.	Dec.	Jan.	Feb.	Mar.	Apr.	May	June
Zone and elevation	% of orographic PMP index (figs. 4-33a to c)								
A, all elevations	108	107	104	100	100	95	87	76	68
B, all elevations									
C, 1000 ft. or less	108	107	104	100	100	95	90	90	85
C, 2000 ft.	106	105	102	98	98	94	91	92	88
C, 3000 ft.	104	103	100	96	96	93	92	94	71
C, 4000 ft.	102	101	98	94	94	92	93	96	94
C, 5000 ft.	100	99	96	92	92	91	94	98	97
C, 6000 ft. or more and D, all elevations	98	97	94	90	90	90	95	100	100

4.61. Summer excluded. Orographic storms are cool-season storms. Occasionally in July through September circulations are set up that are similar to those of spring or fall -- for example, the July 1913 storm, paragraphs 2.27 and 2.28. But the July intensity is less than June and September less than October. No specific seasonal variation ratios have been developed for these summer months. East of the Cascade Divide, summer thunderstorms provide the controlling PMP in summer up to basin sizes close to the maximum considered there in this report, 1000 square miles. West of the Cascade Divide it is well known that summer intensities are low.

4.62. Use of seasonal variation graph. The seasonal variation zone boundaries necessarily split a few basins. The whole of such basins, up to 1000 square miles, should be assigned to the zone in which more than half of the basin lies. For zone C basins, enter figure 4-27 (or table 4-7) with the average elevation of the basin. For basins of 1000 square miles or less, a differing seasonal variation within the basin is normally an unwarranted refinement.

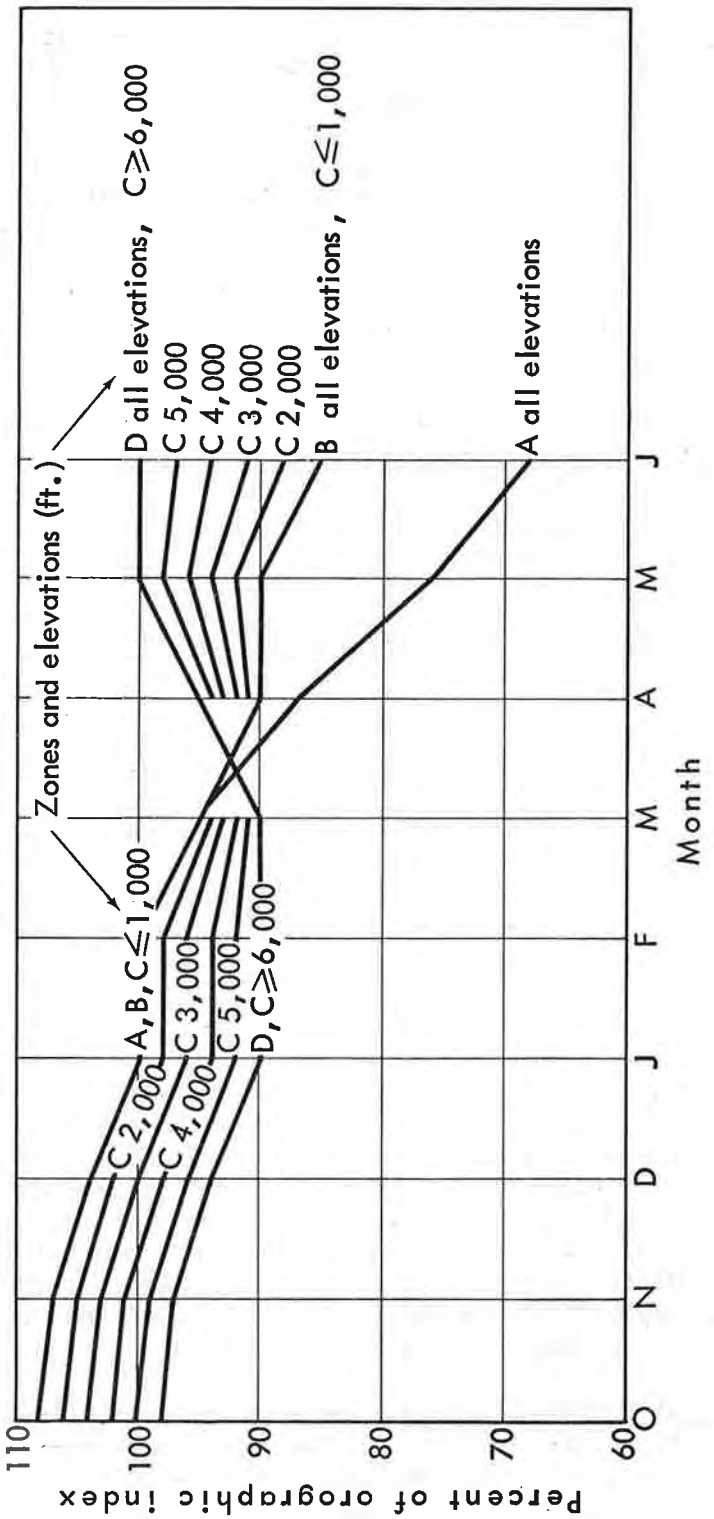

Figure 4-27. Adopted seasonal variation of orographic PMP by zones of figure 4-26

4.63. Floods as a check. Maximum annual discharges and other flood peaks for a number of selected basins in the Pacific Northwest (USGS Water Supply papers) were examined as a check on the seasonal variation of the PMP. (The seasonal variation of flood peaks, of course differs from the seasonal variation of PMP because of snowmelt contributions and other reasons. However, if a number of annual maximum discharges on a medium size or small basin occur in a particular month, that month is at least suspect as having a relatively high potential for high precipitation. Conversely, if no maximum annual peak discharges appear in a particular month, or season, then it is doubtful if the potential for precipitation is as high in that month as in some other month.) The discharge data show general agreement with the adopted seasonal variations. West of the Cascades, peak discharges predominate in winter while near the Continental Divide late spring is the most critical flood season. Immediately to the east of the Cascades the majority of peak flows are either in winter or spring. Near the west border of Idaho there is marked variation in peak flows between basins and from year to year, with the majority between December and May. Higher elevations tend to have peak flows later in the season.

4-F. OROGRAPHIC PMP INDEX

4.64. Orographic PMP for a basin is computed from an index map. This map, figures 4-33a to c, envelops the effects of lifting of air by slopes facing critical directions. Method of developing the index map is the main subject of this section.

Development

4.65. Maximum winds and moisture values, defined in section 4-D, were input to the orographic precipitation computation model discussed in section 4-B. The terrain was generalized and profiles were constructed parallel to critical moisture inflow directions. Elevations for these profiles were taken from 1:1,000,000 aeronautical charts. Slopes were generalized by smoothing over deep valleys, since air tends to flow over or along such valleys rather than down into them and up again. Precipitation was computed in a manner similar to that for the tests of the orographic model along segments of each profile (par. 4.12).

4.66. Terrain profiles. The entire study area was covered by terrain profiles oriented from at least one direction.

West-east profiles 5 nautical miles wide were constructed for the region from the coast to the 120th meridian (lee slope of Cascades). This orientation was chosen because most of the steepest slopes face west, thus giving the greatest lift to moisture inflow. That part of the basin east of the 120th meridian was divided into strips 12 nautical miles wide oriented southwest-northeast. This direction is usual for inflow in major storms, such as the December 1955 case. It also is normal to many of the

steeper slopes. Profiles began either near the 120th meridian or near the southern boundary of the basin. The exact entrance for each profile was at the beginning of upslope, at the foot of the mountains if there is a coastal plain, or in a broad valley such as the Willamette or Snake.

Examples of terrain profiles are shown in figure 4-28 (west-east at 46°35'N.) and figure 4-29 (southwest-northeast from close to Boise). Here the solid lines are the profiles as read from a generalized aeronautical chart, while the dashed lines are the smoothed profiles used for computational purposes. Figure 4-30 shows a sample of the outcome of generalizing the topography in this manner. It gives the computational contours between latitudes 48° - 49°N. in the northern Cascades, and can be compared with the actual topography. The high point or computational ridge is indicated on the figure. This may not correspond exactly with the drainage divide. Also shown is the entrance contour where computations were started for each profile.

4.67. West of Cascades, the primary west-east profiles were supplemented by profiles from two other directions, south-north with southwest-northeast over two quadrangles to provide a sample of the influences of various directions in this region. In selected areas east of the Cascades additional terrain profiles with other orientations were constructed. South-north profiles covered the quadrangles located by longitude and latitude 116°, 42°; 113°, 42°; 116°, 47°; 113°, 47° and 120°, 46°; 117°, 46°; 120°, 50°; 117°, 50°, these being areas of most prominent south-facing slopes east of the Cascades. Near the Continental Divide, in addition to southwest-northeast profiles, northeast-southwest profiles were drawn from about 3000-ft. elevation up the east slopes of the Divide and over the western slopes where spillover is important.

The use of the overlapping profiles from different directions is covered in paragraph 4.71.

4.68. PMP computation. Maximum moisture determined from 12-hr. dew points, figures 3-11 to 3-13, was combined in the orographic model with maximum winds, figures 4-18 to 4-20 and appropriate relative humidity to compute 6-hr. orographic PMP. Relative humidity is assumed 100 percent west of Cascades and east of the Continental Divide and is dependent on height of inflow barrier elsewhere east of Cascades, figure 4-21. These values were used at the entrance point of each profile. Computations were made for segments along the profile, called "boxes," determined by either breaks in the profile slope or at 10-mi. intervals if there were no breaks.

4.69. January maximum input winds and moisture were used for all profiles west of Cascades and both January and May east of Cascades. In the latter region, on shallow slopes, January gave the highest PMP except near the Continental Divide; for steep slopes May gave the highest computed PMP, partially because maximum January precipitation is in the form of snow which is carried beyond steep slopes. Distribution along the slopes was therefore patterned after May computations.

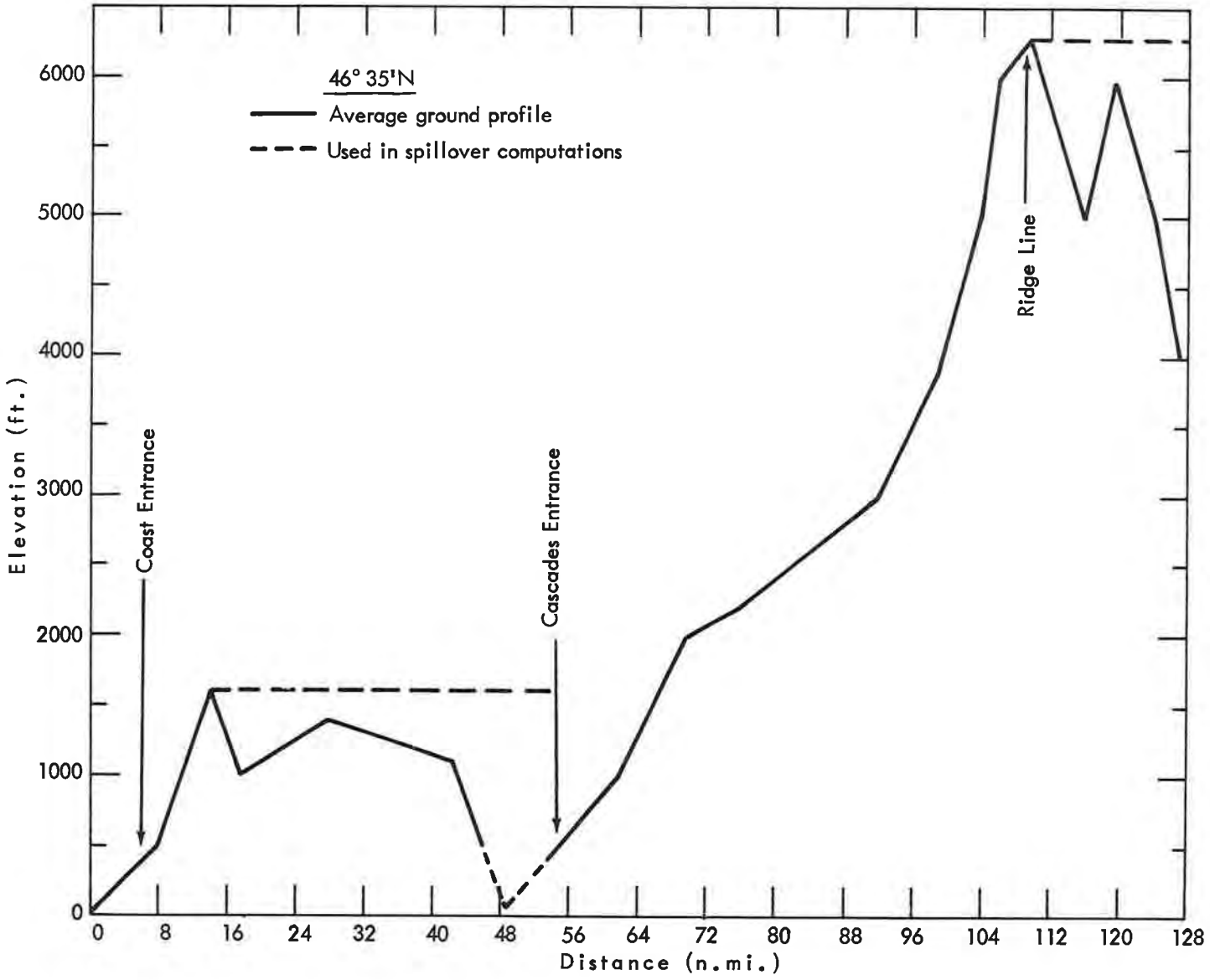

Figure 4-28. Sample of ground and computational profiles (West of Cascade Divide)

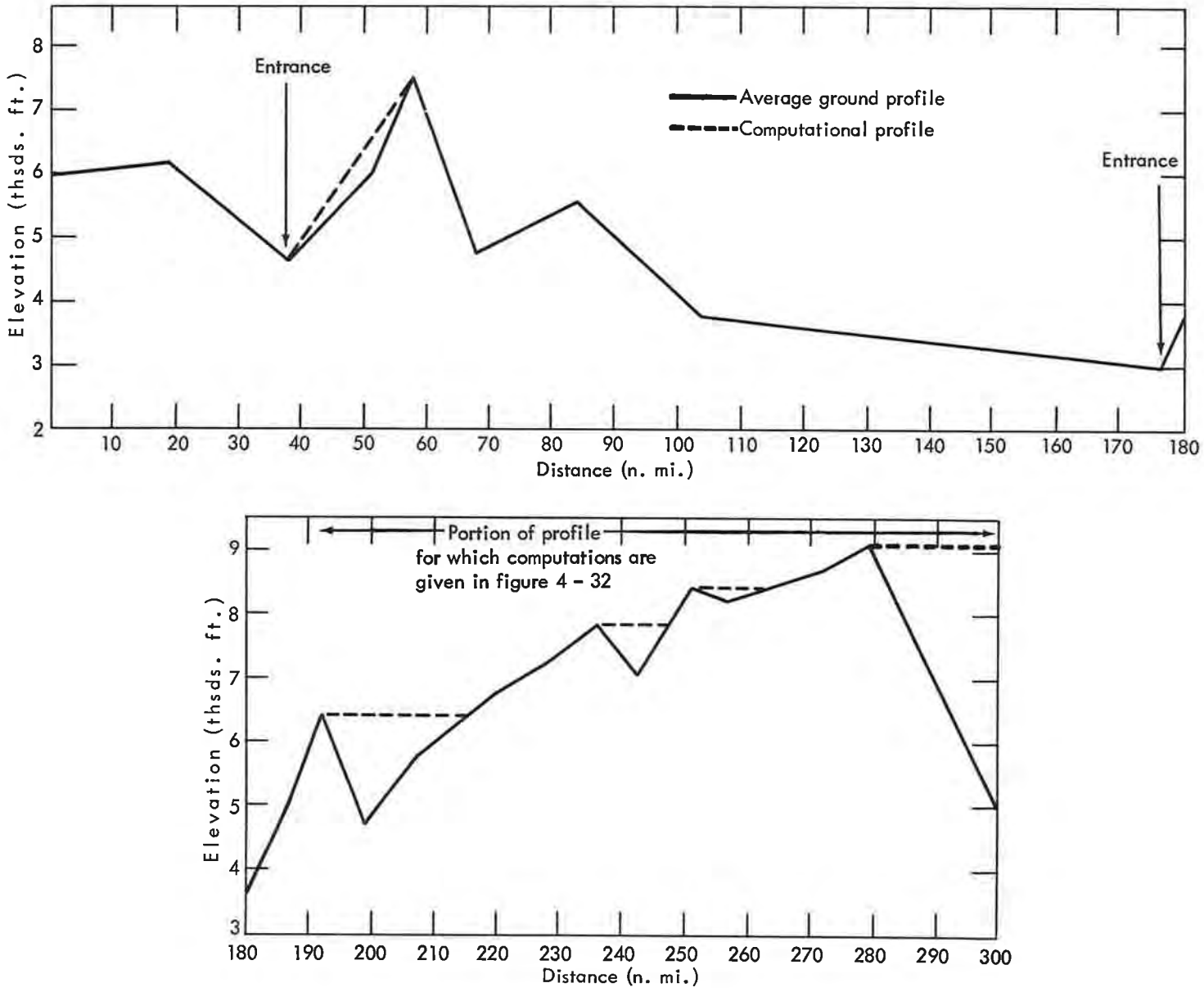

Figure 4-29. Sample of ground and computational profiles (East of Cascade Divide)

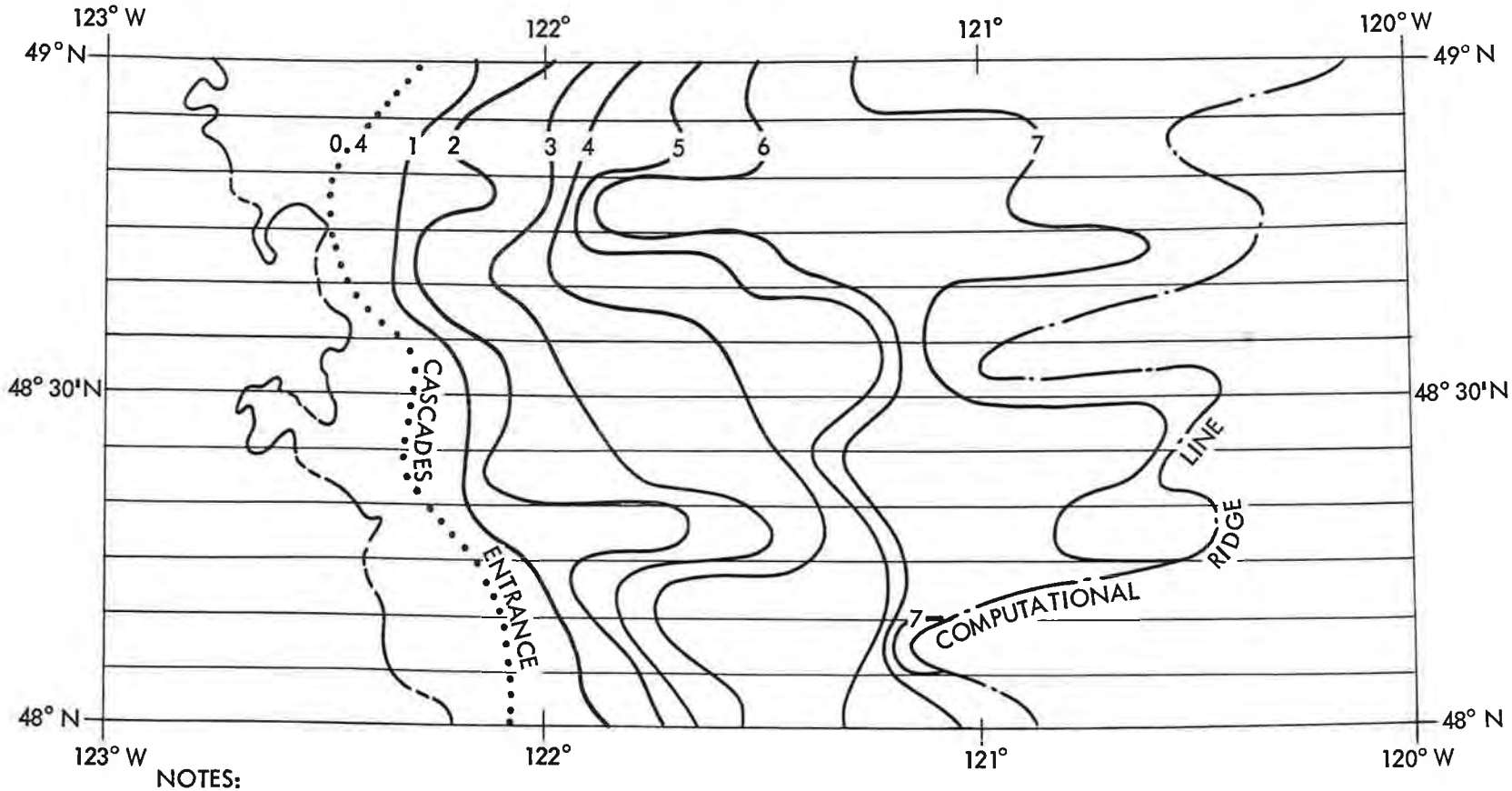

NOTES:

1. Isolines are drawn through mean elevations of 5-min. lat. strips at 1000-ft. intervals and are not actual contours from map.
2. Ridge line connects mean barriers used for orographic precipitation computation in each 5-min. lat. strip.

Figure 4-30. Sample of computational contours (West of Cascade Divide)

4.70. Smoothing. The PMP computations thus far made are for finite boxes without a smooth gradient from one to the other. Such smoothing was obtained by overlaying the fields of computations on generalized contour maps which offered guidance in the drawing of isolines of PMP. The computed PMP within each box was first distributed according to the slopes within the box. Other adjustments were made, considering features of the topography not entirely reflected in the profiles. For example, if adjacent 12 n. mi. wide terrain profiles split and thus de-emphasized a prominent but short ridge, decreasing its effect, the PMP windward of this ridge was increased. Samples of computations and final orographic index isolines are shown in figures 4-31 and 4-32.

4.71. Allowance for direction of inflow. East of the Cascades all the southwest-facing slopes and the more prominent south-facing slopes were covered by direct computations. (These were made also near the Continental Divide for spillover from northeast flow.) Both direction computations were enveloped. Where there was a slope facing some other direction between south and west, a PMP value was drawn comparable to a slope facing southwest or south. At pertinent locations, such as the Blue Mountains of Oregon, slopes facing up to northeast are almost as critical as southwest-facing slopes. In other regions in the Upper Snake east-southeast-facing slopes similarly were given full consideration.

4.72. On the windward slopes of the Cascades and Coast Ranges, a graphical approach for generalizing PMP for a range of inflow directions was used. This graphical technique evolved from relations of several topographic parameters to computed PMP. The most useful parameters were found to be elevation and degree of slope. Relations were determined between these two variables and PMP, one for each span of one or two degrees of latitude in order to avoid variation due to change of moisture. Using these graphical relations, orographic PMP was determined over prominent slopes facing west-southwest and southwest. Their validity was checked by the sample PMP computations along southwest-northeast profiles (par. 4.67).

Near 120° longitude two sets of computations were available for consideration: spillover computations from west-of-Cascades and local upslope computations from either southwest or south. These were enveloped areally, control being chiefly from southwest computations.

Near the Continental Divide, upslope computations from southwest and spillover from northeast flow were drawn for and then enveloped. The former prevailed except near the Divide, the distance depending on nearness of the Divide to high terrain to west or east (par. 4.21).

4.73. Checks and controls. The process of converting "box" computations to a chart, illustrated in figures 4-31 and 4-32, was checked and controlled in several ways. First, averages were scaled from a preliminary analysis over each box. The ratios of these to the original computations

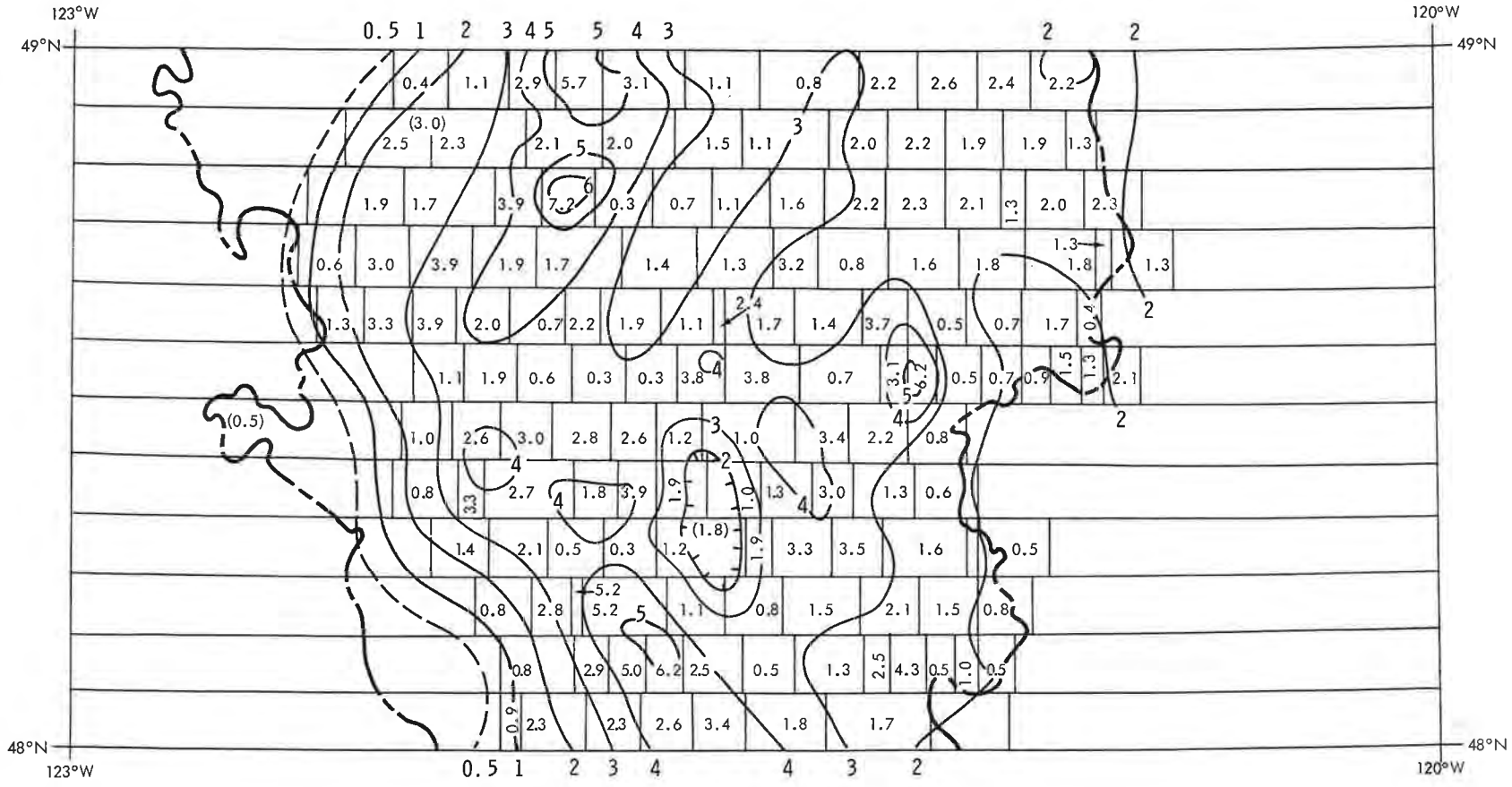

Figure 4-31. Sample of computed 6-hr. January PMP (in.) for westerly inflow and orographic PMP index (West of Cascade Divide)

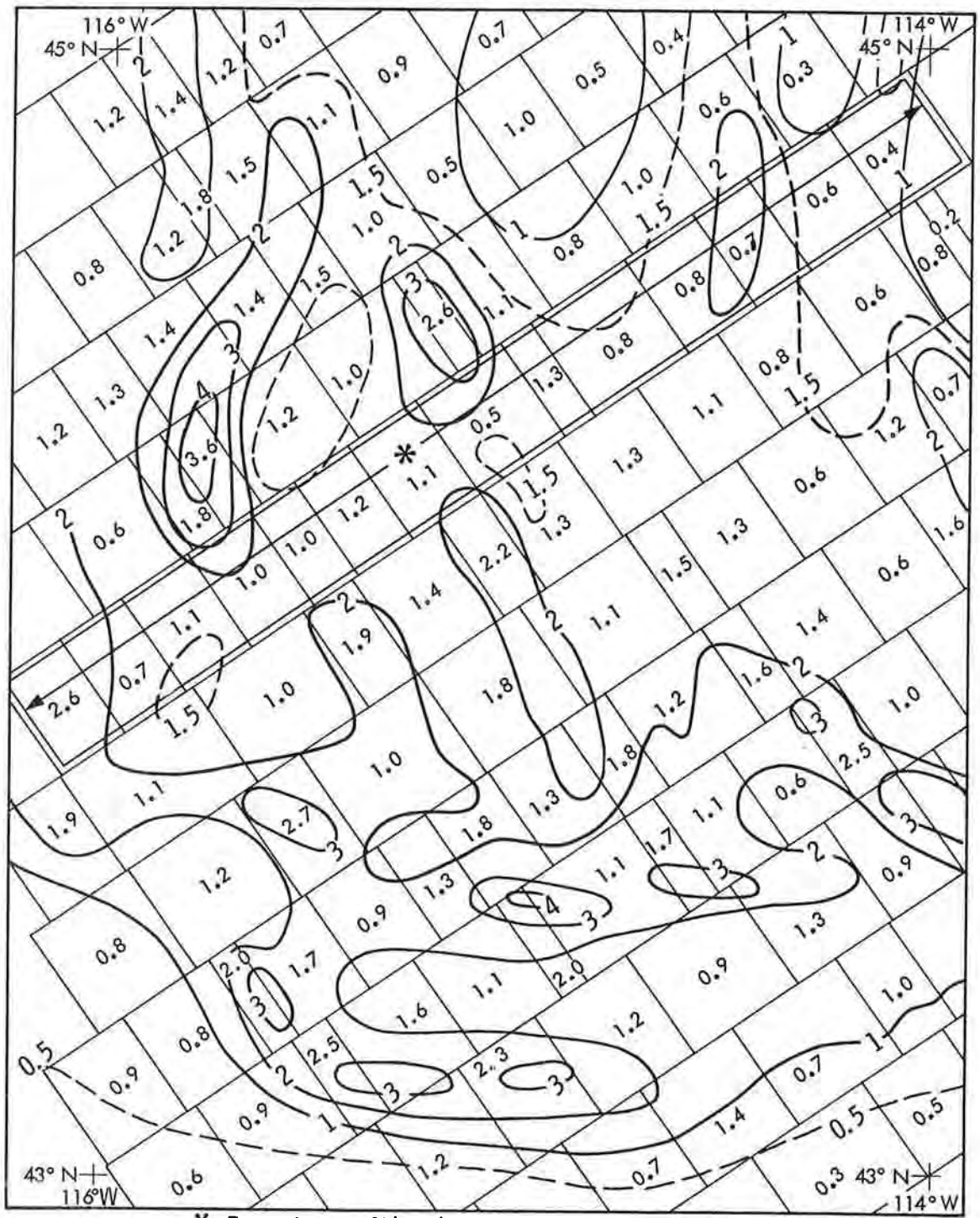

Figure 4-32. Sample of computed 6-hr. May PMP (in.) for SW inflow and orographic PMP index (East of Cascade Divide)

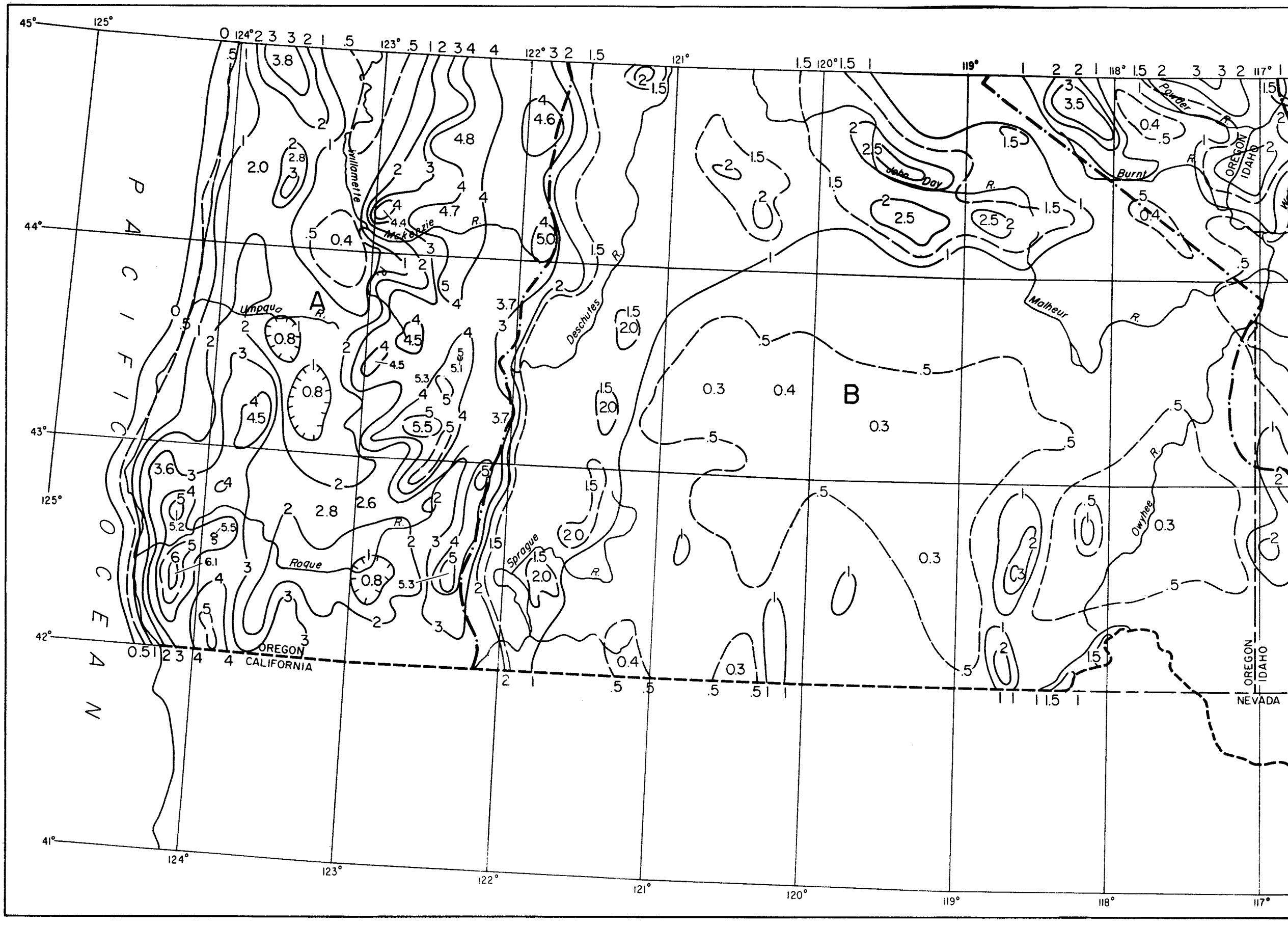
PACIFIC OCEAN
OREGON
CALIFORNIA
OREGON
IDAHO
OREGON
IDAHO
NEVADA
Willamette R.
McKenzie R.
Umpqua R.
Deschutes R.
Rogue R.
Sprague R.
Powder R.
John Day R.
Burnt R.
Malheur R.
Owyhee R.
A
B
C
45°
44°
43°
42°
41°
125°
124°
123°
122°
121°
120°
119°
118°
117°

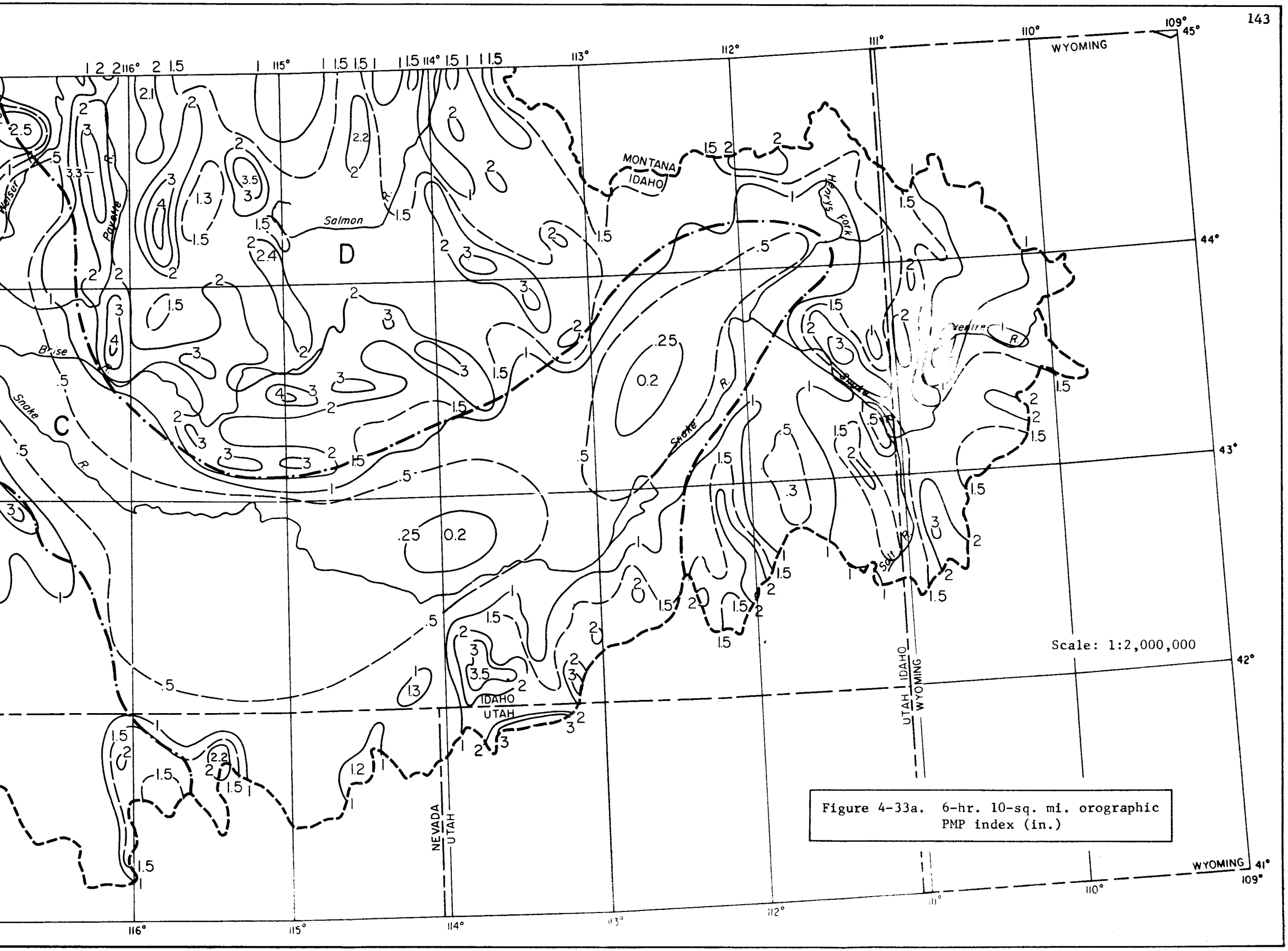

Figure 4-33a. 6-hr. 10-sq. mi. orographic PMP index (in.)

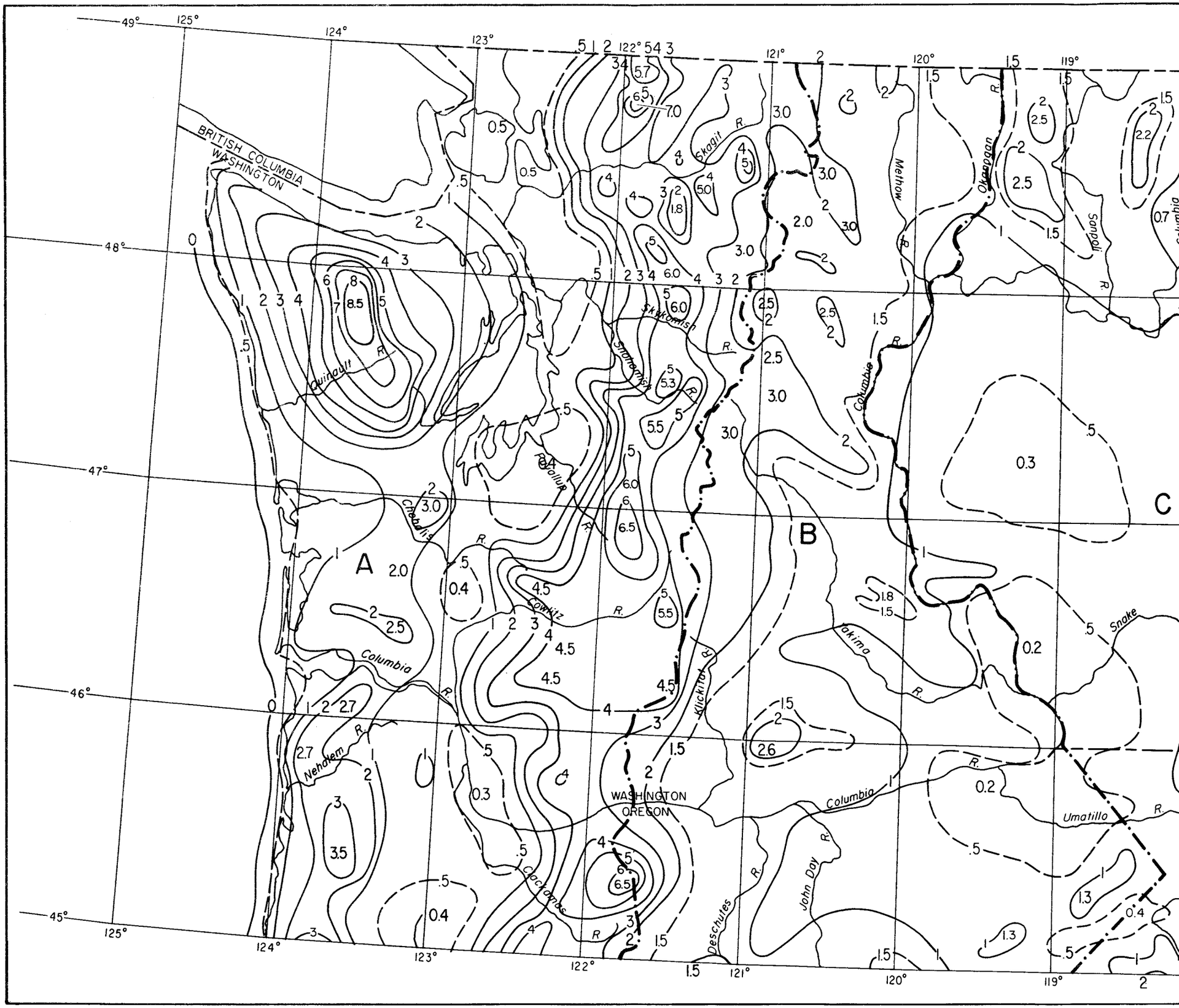
BRITISH COLUMBIA
WASHINGTON
WASHINGTON
OREGON
A
B
C
Quinault R.
Chehalis R.
Cowlitz R.
Columbia R.
Nehalem R.
Clackamas R.
Skagit R.
Skykomish R.
Snoqualmie R.
Methow R.
Okanogan R.
Columbia R.
Yakima R.
Klickitat R.
Deschutes R.
John Day R.
Umatilla R.
Snake R.
Columbia R.
49°
48°
47°
46°
45°
125°
124°
123°
122°
121°
120°
119°

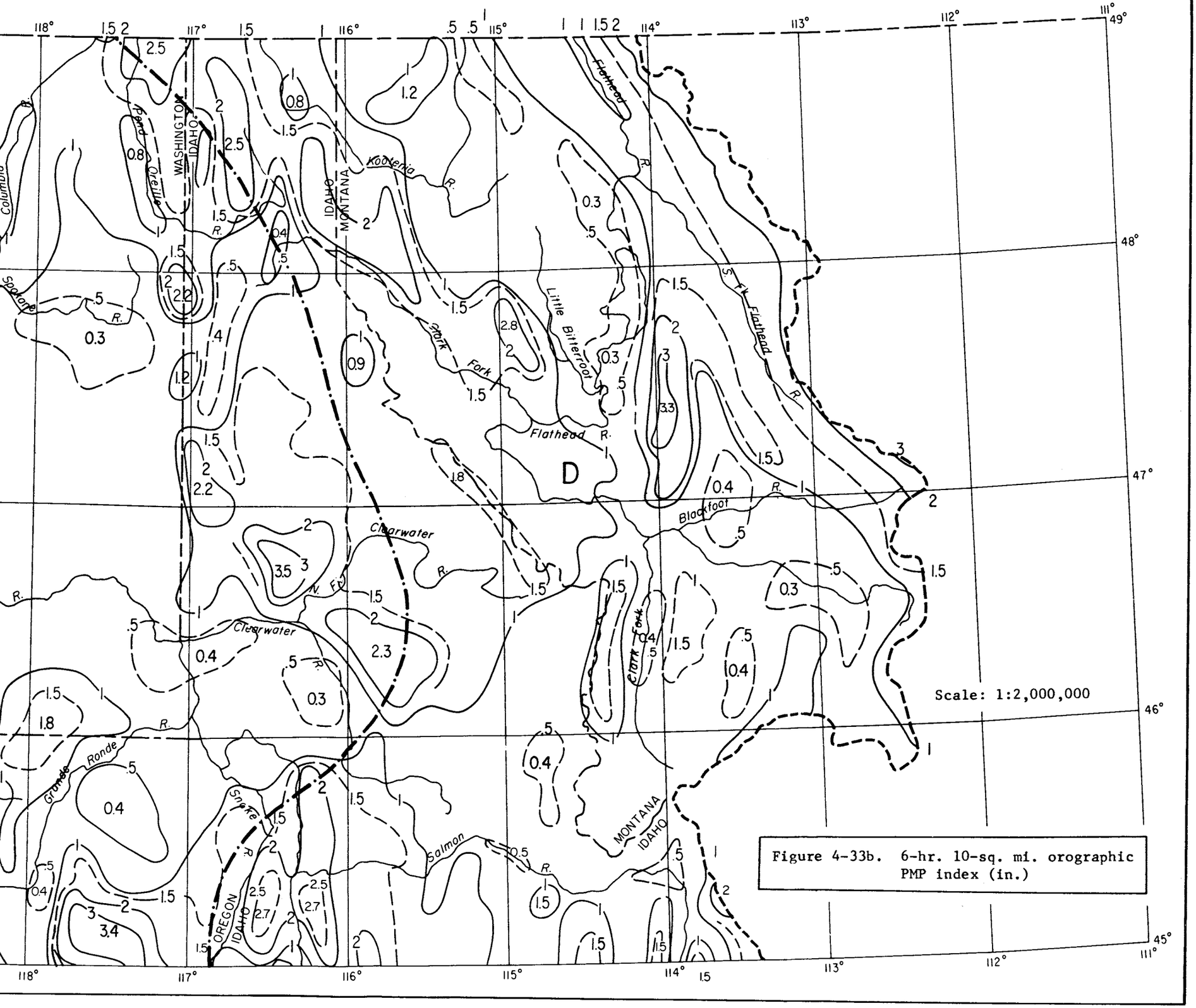

Figure 4-33b. 6-hr. 10-sq. mi. orographic PMP index (in.)

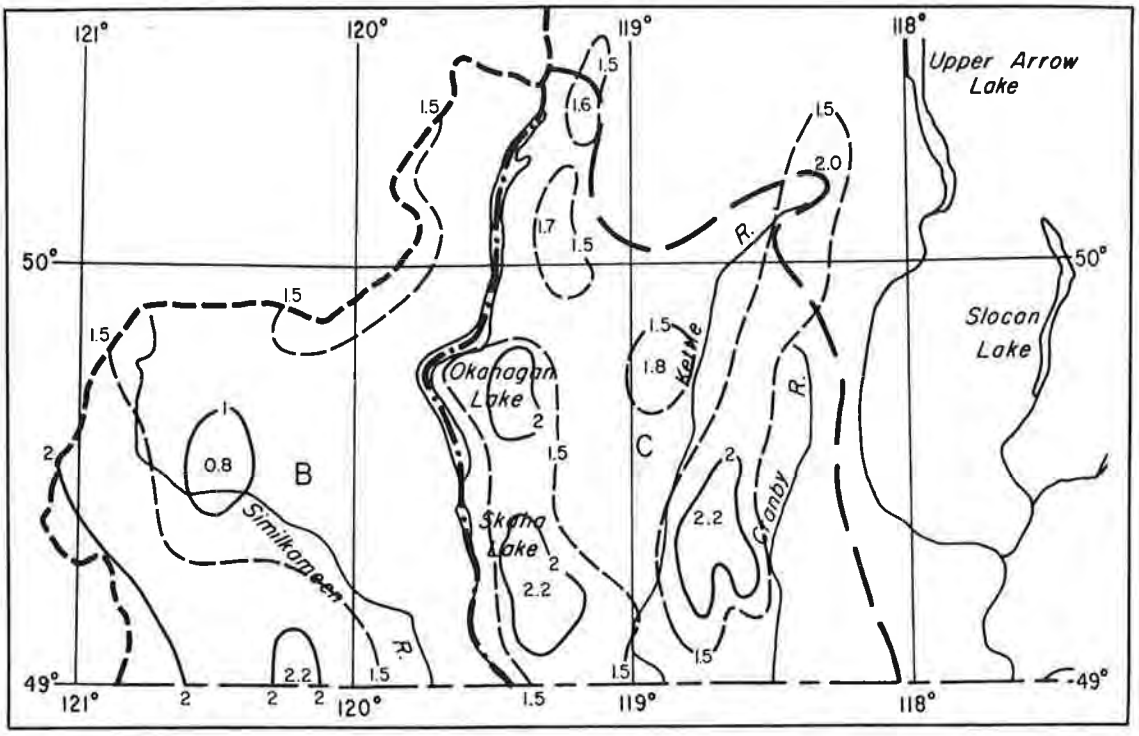

Scale: 1:2,000,000

Figure 4-33c. 6-hr. 10-sq. mi. orographic PMP index (in.)

were studied by the analyst--box by box--to insure that substantial departures from the computed values were deliberate and were justified by details of the topography. After these adjustments, the overall ratios of analysis to computations over large blocks of relatively homogeneous topography were calculated and compared. In the west-of-Cascades test area with S, SW, and W wind computations it was found that enveloping the three directions point by point yielded an index averaging about 1.5 times the west-only computations. The value 1.5 was then used as a calibration factor. Values on the preliminary index map of paragraph 4.70 were cut back to 1.5 times those on the west wind computation map where they were higher.

Over homogeneous blocks east of Cascades smoothing tended to increase the values in lee areas such as in portions of the Salmon River drainage. These areas all had low computed values since windward mountains left only spillover rain for some quite prominent slopes. In some of these blocks slopes facing other than south or southwest accounted for increased values.

4.74. Comparisons were also made between 3-day 10-year values (10) and index map values over the homogeneous blocks. Plots showed a fairly high correlation between latitude and ratio of index map to 3-day 10-year values, the ratio decreasing in northern blocks. While a northward decrease in this ratio was found for California (HMR 36) the decrease here is greater.

4.75. Where the various comparisons of analyses to computed or to the 3-day 10-year precipitation map showed differences that could not be explained by slope or other terrain features, adjustments were made in the analysis.

Use of index map

4.76. The 6-hr. 10-sq. mi. orographic PMP index is given in figures 4-33a to c. Seasonal variation of orographic PMP differs from one portion of the basin to another, as discussed in the previous section and as shown in figure 4-27. Seasonal factors from this figure are to be multiplied by basin average orographic index value to obtain basin average 6-hr. orographic PMP for months October through June. Durational variation of orographic PMP up to 3 days is given in tables 4-8 and 4-9 for west and east of the Cascade Divide, respectively. Because the index envelops orographic rain determined from several directions and maximum moisture inflow in a storm has limited lateral extent, an additional adjustment is required for basin size, figure 4-39.

4-G. DURATIONAL VARIATION OF OROGRAPHIC PMP

4.77. Variations of wind, moisture and relative humidity in storms determine durational variation of orographic precipitation. The durational variations of these variables are first presented individually, and then applied to the orographic precipitation model to obtain computed depth-duration variation of orographic PMP.

Variation of wind

4.78. The data used for determining seasonal variation of wind (par. 4.55) at Boise and Seattle were used also for deriving the durational variation. Direction was restricted to south through west for Seattle, while less restriction on direction was necessary to obtain a satisfactory sample for Boise. Highest wind situations were selected and plots made showing the durational variation. Figure 4-34 illustrates a typical plot of these windspeeds for Seattle (or Tatoosh Island) for directions from southwest to west. With once-a-day observations, one observation was equated to 1 hour, 2 observations to 1 day duration, 3 observations to 2 days, etc. Boise and Seattle data have similar durational trends when adjusted for height above surface. By expressing these durational variations in terms of 6-hr. incremental winds, and smoothing for continuity from level to level, the variation given in figure 4-35 results. At 950 mb. the durational variation is quite similar to that found for stations in California (HMR 36), so the durational variation of 1000-mb. wind from that report is used.

4.79. A check was made to determine if the durational variation of high winds varies with season. Data used were highest winds at the 850-, 700-, and 500-mb. levels at Seattle (1954 to 1961 or 1962) and Boise (1952-1962) for the 1200Z observations. Restrictions on direction were:

500 mb.: S-W
700 mb.: SSE-WNW
850 mb.: SE-NW through W

At the lowest level, less restriction on direction was necessary to obtain cases with appreciable wind persisting for 3 days.

For each month of record, the highest 1-day wind at each station was tabulated for each level. Then the average highest 3-day wind including each highest 1-day wind, was determined. This gave, for each month and level, 11 cases at Boise and 9 or 10 at Seattle which met the above direction restrictions. In order to show that the selection method did not bias 1- to 3-day average wind comparisons, the highest 3-day average wind was similarly found. Almost all highest 3-day cases included a highest 1-day wind, indicating no bias.

The ratios of the 1- to 3-day windspeeds were averaged for each month. These average ratios indicated little trend from month to month. One durational variation of wind was therefore adopted for all months.

Variation of moisture

4.80. As explained in paragraph 3.04, highest 12-hr. persisting surface dew points are used as an index to moisture in depth assuming a pseudo-adiabatic lapse rate. In paragraph 3.10 an average durational variation of moisture is given for all months and regions. This variation was used in determining the variation of orographic PMP due to moisture.

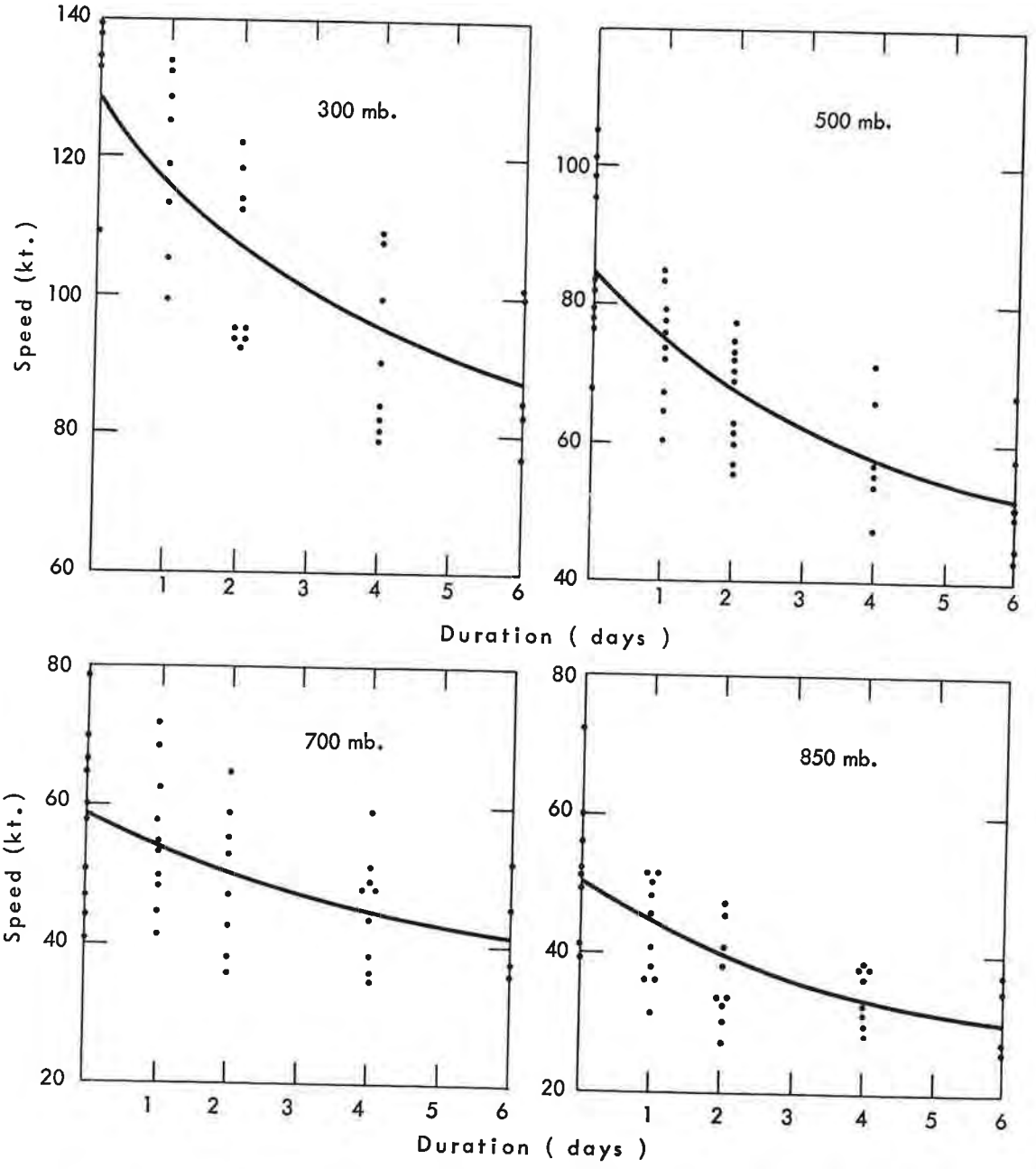

Figure 4-34. Durational variation of highest winds at Seattle or Tatoosh, 1951-1959

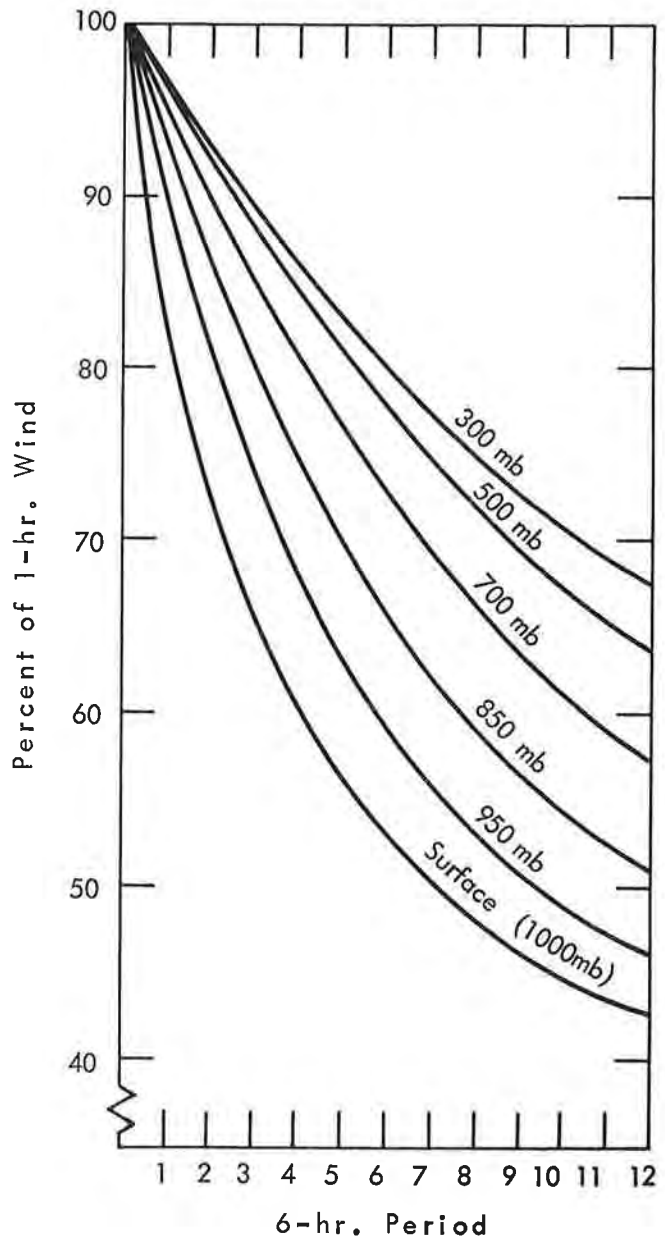

Figure 4-35. Durational variation of PMP winds by 6-hr. increments

Variation of relative humidity

4.81. The constantly varying relative humidity of the air is an important factor in limiting the amount of sustained precipitation over long durations. High moisture in mid-latitude storms is limited by intermittent intrusions of drier air at some levels. To measure this effect, radiosonde measurements of relative humidity were examined in several storm periods. The relative humidity was averaged from surface to 600 mb. Above 600 mb. the contribution of moisture to total precipitation is small. These averages were then placed in descending order, converted to percent of first period and plotted. Curves from 4 storms west of the Cascade Divide and from 1 east of the Divide are shown in figure 4-36. The dashed line enveloping the 4 western storms was adopted as the durational variation of relative humidity west of the Cascades. The durational variation adopted for east of Cascades is that of the record December 1955 storm.

Computed durational variation of orographic PMP due to wind, moisture and relative humidity

4.82. West of Cascade Divide. A generalized slope extending from 0 to 5000 feet in elevation, representative of the west slopes of the Cascades, was used for computing the durational variation of orographic PMP. Precipitation computations were made for each 1000-ft. interval as well as for the entire slope, using each variable separately to assess the effects of each. Figure 4-37 gives the durational decay in orographic PMP due to decay of moisture, expressed in percent of 1st 6-hr. precipitation, for each 1000-ft. layer and for the average over the entire slope. For the sets of computations shown, relative humidity was 100 percent and wind input was that for the 12th (lowest) 6 hours and for 1st (highest) 6 hours. Computations (not shown) were made also for the 12th 6-hr. and 1st 6-hr. winds with 70 percent relative humidity. An average of these four durational decays due to moisture was adopted. The variation due solely to variation in relative humidity was next determined at several levels, holding wind and moisture constant. Finally the variation due solely to wind was found.

4.83. Durational variation of orographic PMP due to each of the three components is given in figure 4-38. The curve showing the combination of the three components is the adopted orographic PMP durational variation. Table 4-8 expresses this durational variation in percent of the 1st 6-hr. orographic PMP increment.

Table 4-8

INCREMENTAL DURATIONAL VARIATION OF OROGRAPHIC PMP
(West of Cascade Divide)

6-Hr. Period											
1	2	3	4	5	6	7	8	9	10	11	12
Percent of 1st. 6-Hr. Increment											
100	89	80	71	63	56	50	44	39	34	30	26

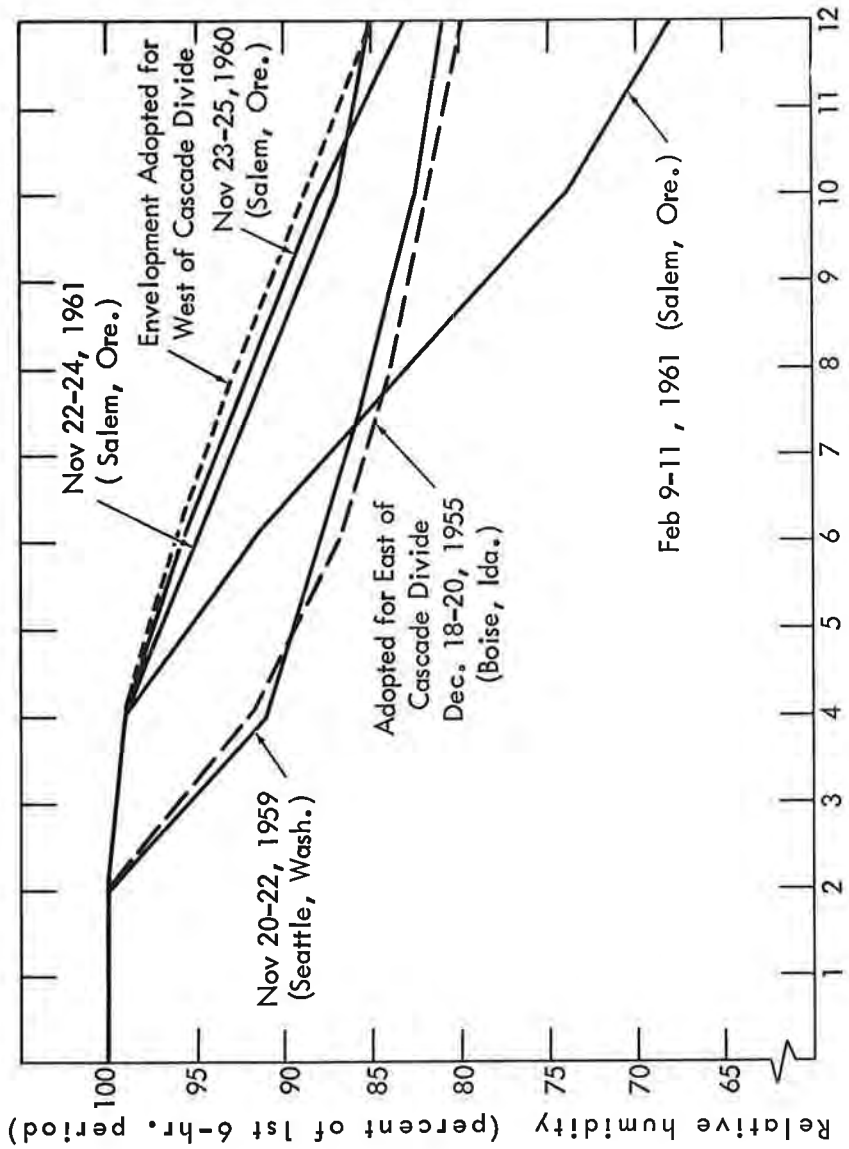

Figure 4-36. Adopted durational variation of relative humidity

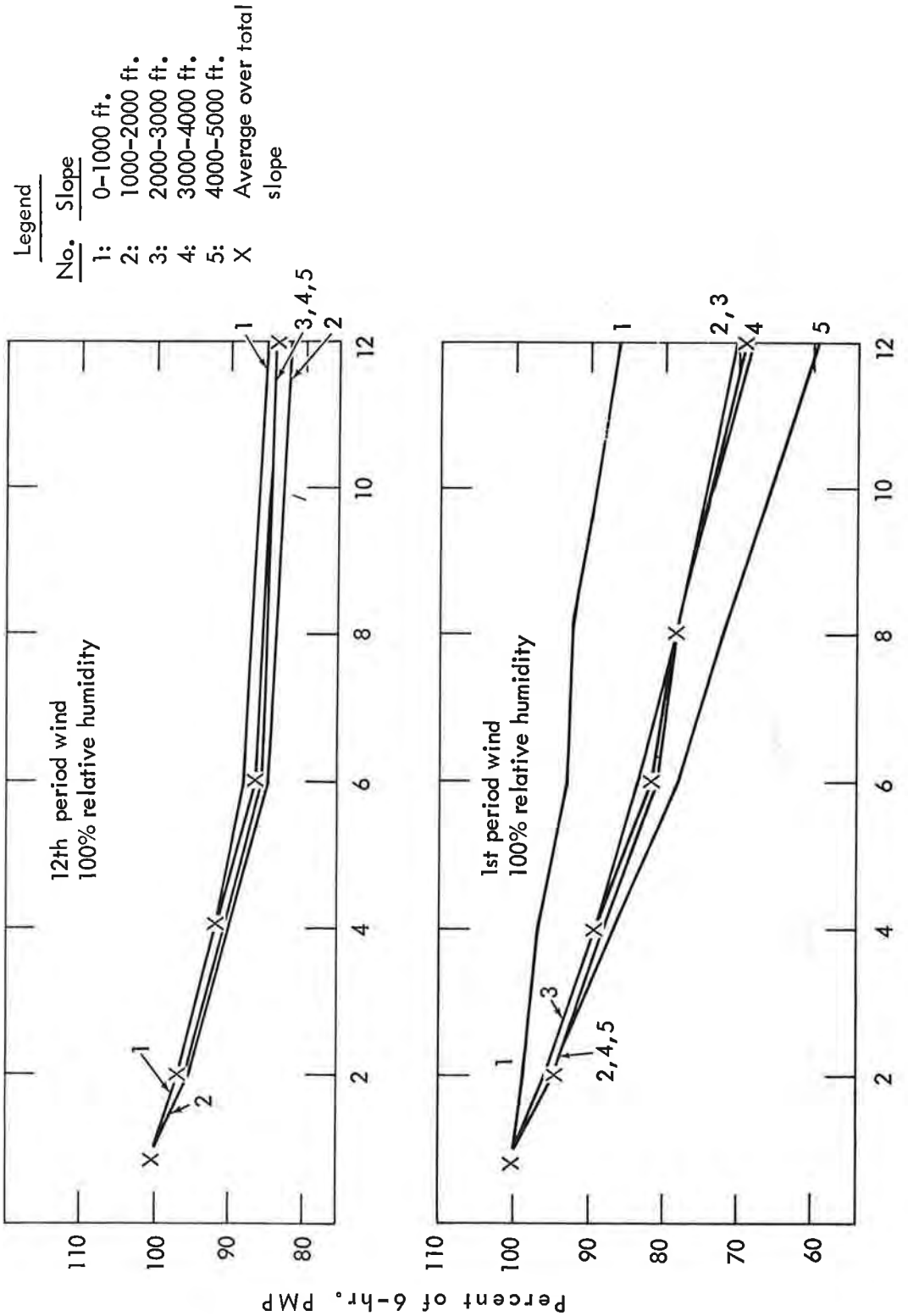

Figure 4-37. Durational variation of orographic PMP due to moisture (West of Cascade Divide)

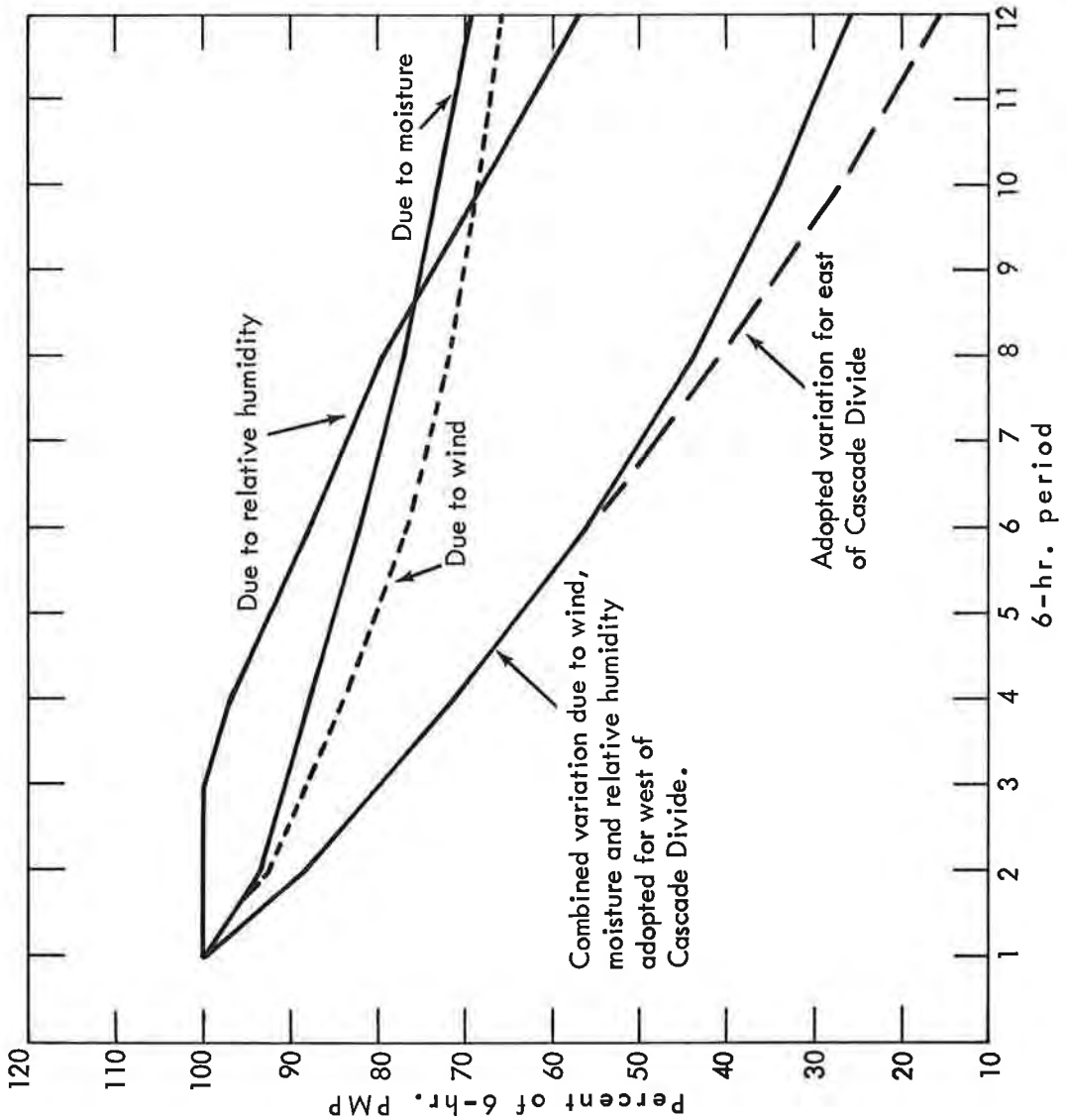

Figure 4-38. Durational variation of orographic PMP

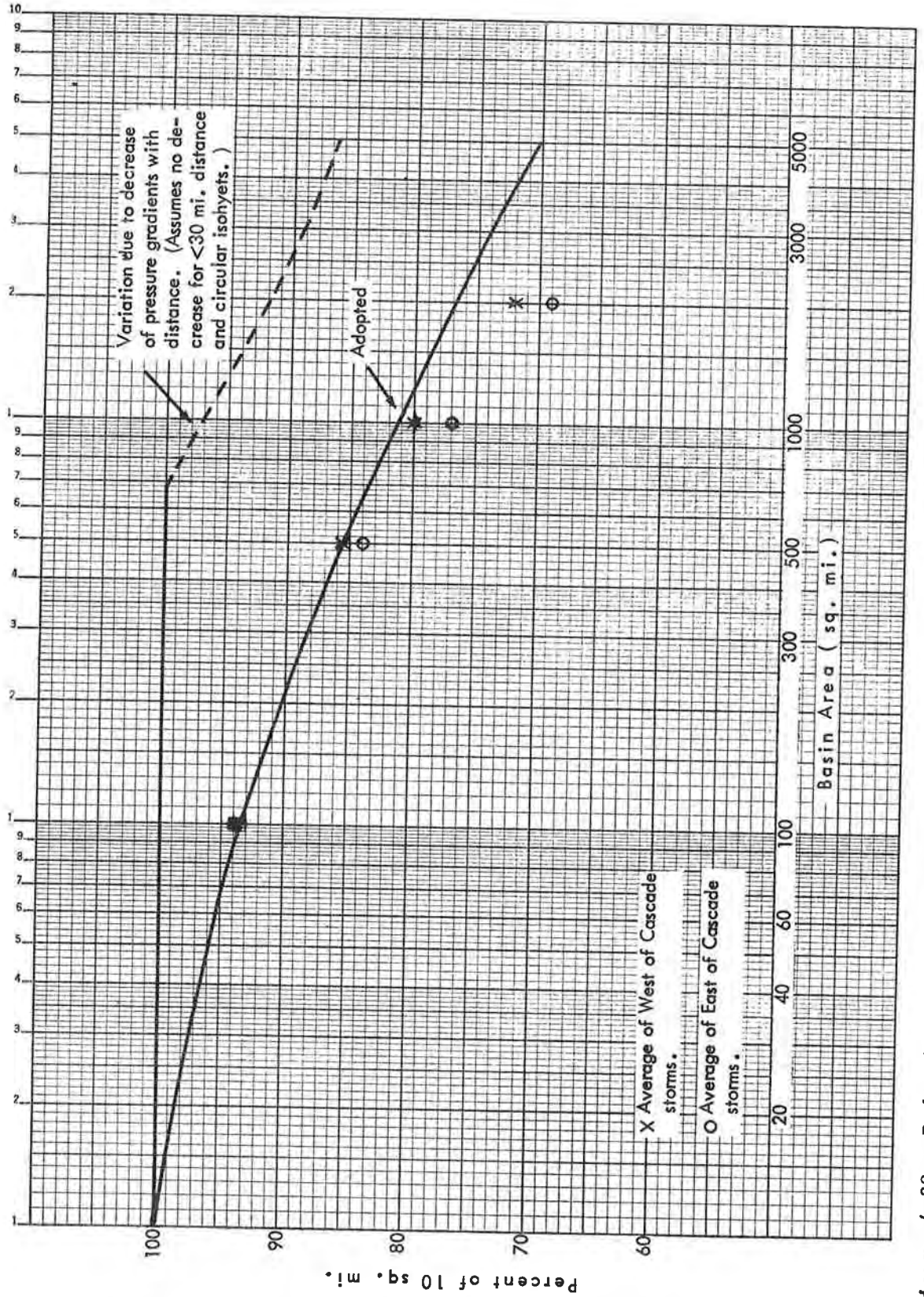

Figure 4-39. Reduction of orographic PMP for basin size

4.84. East of Cascade Divide. Computations analogous to those for west of Cascades were made for a synthetic slope, from 4000 ft. to 9000 ft. in 50 miles. The results (not shown) reflect the effects of the higher elevation of this slope than west of Cascades and of assuming non-saturation below the height of an upwind barrier (below 800 mb.). For highest elevation bands (6000 to 9000 ft.) decrease of orographic precipitation with duration is considerably less than that west of Cascades. At lowest elevations, 4000 to 6000 ft., decrease is considerably more than that west of Cascades. The total slope durational variation of orographic PMP has slightly less decrease for short durations and more decrease at long durations than that west of the Cascades.

The durational decrease adopted for east of the Cascade Divide is given in figure 4-38 and in table 4-9. It is the same as that for the western region to 36 hours; then the decrease is more rapid.

Table 4-9

INCREMENTAL DURATIONAL VARIATION OF OROGRAPHIC PMP
(East of Cascade Divide)

6-Hour Period											
1	2	3	4	5	6	7	8	9	10	11	12
Percent of 1st. 6-Hr. Increment											
100	89	80	71	63	56	48	41	34	27	21	16

4.85. The durational decrease of easterly winds (direction 10° to 130°) east of the Continental Divide is greater than for westerly winds. The easterly wind durational decrease is based on that at Great Falls in six large spring storms at levels from the surface to 9000 meters above sea level. Using persisting dew points for durations to 72 hours listed in Weather Bureau Technical Paper No. 5 (4), the decrease of moisture with duration for four Montana stations east of the Divide averaged over the months of May through July is a little less than that adopted for west of the Divide (upper curve of fig. 4-38). Sample orographic PMP computations at various durations, with these wind and moisture decreases and with a qualitative allowance for relative humidity decay (not specifically evaluated) indicate a depth-duration curve slightly below that in figure 4-38. This permits us to extend use of table 4-9 to the Continental Divide.

Durational variation for short durations

4.86 For small basins it is necessary to compute general storm PMP for durations shorter than 6 hours. Projecting the durational variation of orographic PMP for longer durations back through the origin gives the adopted 20 and 54 percent of the first 6-hr. orographic PMP for 1 and 3 hours, respectively. Orographic PMP for 1 and 3 hours in California (HMR 36), computed over various slopes, averaged these same percents of 6-hr. values.

4-H. VARIATION OF OROGRAPHIC PMP WITH BASIN SIZE

4.87. Areal variation of orographic precipitation is controlled largely by the configuration, location and extent of terrain slopes. The orographic PMP index map reflects these controls. But two additional factors become important in considering the variation of orographic PMP with basin size because of the way the orographic PMP index was developed. One is the lateral extent over which maximum winds and moisture can occur compared to the lateral extent of a basin. The other arises because the orographic PMP index envelops PMP at a location for several inflow directions, a procedure which becomes less realistic as basin size increases.

Lateral extent

4.88. On a steep slope of wide lateral extent, both mean seasonal precipitation and the orographic PMP index map have a similar broad lateral extent of high values. The lateral extent of heavy rain in a particular 3-day storm is limited by the wind and moisture field of that storm. This is demonstrated in storms of record. Such limitations must be included in the final orographic PMP values.

Maximum winds, determined in part from highest pressure gradients between points, decrease with distance between the points. Rainfall, which is proportional to wind inflow, likewise should decrease with basin width. Rain decrease, based on the decrease in maximum windspeed with increasing basin width was adopted from paragraph 5.53 (HMR 36), which assumes no reduction up to 30 miles. This reduction with basin size increase for circular isohyets is shown by the dashed curve in figure 4-39.

Slope orientation

4.89. The other reason for a reduction of orographic PMP with basin size is obvious. The orographic PMP index value on a particular slope is an enveloping value; it considers inflow from several directions and is drawn for the effect of slope on the most favorable direction. But for a sub-basin with slopes facing several directions, maximum lifting cannot occur on all slopes at a given time.

Adopted reduction

4.90. A single basin-size reduction factor was adopted which incorporates both effects. This relation is given in figure 4-39 by the solid line. To about 1000 square miles it is based on the mean of depth-area relations for highest 24 hours in storms over mountain regions both east and west of the Cascade Divide. These storms are listed in table 4-10.

For some of the western storms, two centers were averaged, one on the Olympic Mountains and one over the Cascade slopes. Twenty-four hour durations were used in each case. The adopted curve is to be used for all durations.

Table 4-10

STORMS AVERAGED FOR DEPTH-AREA VARIATION

West of Cascade Divide	East of Cascade Divide
October 26-28, 1937	May 26-30, 1906
December 16-19, 1931	December 18-23, 1933
November 16-20, 1911	January 21-24, 1935
November 2-7, 1934	
January 20-25, 1935	
October 21-26, 1934	
February 23-27, 1932	
November 18-22, 1921	
December 16-19, 1917	

The adopted areal decrease of orographic PMP is made less steep than the average of storm data indicates. The latter is affected by the component of convergence rain. Orographic rain, controlled by terrain, does not have as steep an areal decrease as does convergence rain.

Chapter V

THUNDERSTORM PMP EAST OF CASCADE DIVIDE

5-A. INTRODUCTION

5.01. Intense local summer thunderstorms can produce short duration rains for small basins east of the Cascade Divide which exceed the potential from general storms. Examples of these summer intense rains are the 4 inches in 1/2 hour reported at Girds Creek, Oreg., July 13, 1956 and 7 inches in 1 hour near Morgan, Utah, August 16, 1958. The general storm PMP given in earlier chapters purposely did not include such storms in the development.

5.02. Because summer thunderstorms are very local and in sparsely populated areas are rarely measured, relatively less is known of them than of general storms. Therefore variation with basin size, elevation and duration are facets which are difficult to define.

5.03. Summer thunderstorm PMP is not given west of the Cascade Divide. No summer thunderstorms have been reported there of the intensity of those to the east, for which the moisture source is often the Gulf of Mexico or Gulf of California. The Cascade Divide offers an additional barrier to such moisture inflow to coastal areas where, in addition, the Pacific Ocean to the west has a stabilizing influence on the air to hinder the occurrence of intense summer local storms.

5.04. The first portion of this chapter notes some observations made by various writers on thunderstorms. This is followed by discussion of seasonal trends and thunderstorm weather patterns, and then by the development of thunderstorm PMP.

5-B. BACKGROUND INFORMATION

Characteristics of severe thunderstorms

5.05. Studies on intense thunderstorms have been surveyed for guidance in the development of PMP. Pertinent observations or conclusions from this survey follow.

5.06. Formation. Newton (12) implies that the isolated giant cell has a highly organized complicated structure. Many observations[1] suggest formation is by the amalgamation of two or more separate cells. Battan (13) has

---

[1]Campo, Calif., August 12, 1891
Springfield, Oreg., May 25, 1901
Jacksonville, Oreg., May 27, 1905
Palmetto, Nev., August 11, 1890
Doraville, Oreg., June 15, 1903
Morgan (nr.), Utah, August 16, 1958

noted that the largest, long-lived thunderstorm does not develop as a single convective unit but grows in a series of steps with successive cloud towers which combine to form an intense thunderstorm. This statement is corroborated by Byers and Braham (14). While the presence of large area convergence appears to be a necessary factor for extreme convection and thunderstorm formation, several recent studies hint that the rare giant cell forms in a convergence field not identified with widespread rain and numerous thunderstorms. Thus a logical concept of the PMP thunderstorm is a cell or combination of cells in an area of little rainfall otherwise.

5.07. Location. A supposition that rough topography is conducive to the formation of a PMP thunderstorm is debatable. Convective radar echoes are observed to form with a higher frequency over the higher terrain. But Clark and Fonken (15) suggest that the more intense thunderstorms observed in central Utah are usually at lower elevations.

5.08. Movement. Stagnation or slow motion of a thunderstorm contributes to extreme point rainfall. But migration enhances persistence by replenishing moisture supply (16). Bjerknes (17) notes that "movement over the level plains ordinarily exceeds that over more rugged country" but that occasionally "no storm movement is evident."

Seasonal trends

5.09. While highest monthly rain occurs during winter in all of the Northwest, summer months dominate highest daily rain values east of the Cascade Divide, as shown in chapter III. Even more striking is their domination of short duration local intense rainfall. The farther east, the greater is the summer control.

These climatic trends in thunderstorm rainfall are explained in part by the influence in summer of Gulf of Mexico moisture, especially in the southeast and east portions of the area. But areas nearer the Cascade Divide, and thus less accessible to this moisture source, also experience local intense thunderstorm rain, usually a little earlier in the season. Here the important mechanism involves contrast between moist residual air and cool maritime air during passage of a Pacific storm.

5-C. THUNDERSTORM SYNOPTIC PATTERNS

Storm data

5.10. Intense summer thunderstorms are uncommon enough west of the Continental Divide that they have rarely been observed at the few long-record first-order Weather Bureau Stations, most of which are located in flat terrain or river valleys. Thus record values come from the more plentiful records of cooperative observers or "bucket surveys," usually in somewhat rugged terrain.

The most intense short-period summer rains of record in and near the area of this report are listed in table 5-1, along with pertinent information. Locations of these storms are shown in figure 5-1. These values average nearly five times the average of the maximum observed values at the nearest long-record first-order station.

Table 5-1

DATA IN INTENSE SUMMER THUNDERSTORMS

	Date	Location (see fig. 5-1)	Duration (min.)	Amount (in.)	Moisture from Gulf of Mexico
		Columbia Basin			
1.	June 15, 1954	Richland, Oreg.	10	0.56	No
2.	June 14, 1903	Heppner, Oreg.	20	1.5+	No upper data
3.	July 13, 1956	Girds Cr., Oreg.	30	4.0	Indirectly
4.	July 21, 1956	Simon Ranch, Idaho	20	2.5	Yes
5.	June 22, 1938	Birch Cr., Oreg.	20	2.5	Probably (No upper data)
		Bordering Area			
6.	August 16, 1958	Morgan (nr.), Utah	60	7.0	Yes

Storm characteristics

5.11. A schematic of flow in storms numbered 1, 4, 5 and 6 in table 5-1 is shown in figure 5-2. Meteorological highlights of the storms of table 5-1 are summarized:

1. Storms listed first involved unstable polar maritime air in an eastward-moving Pacific Low; those listed last are more closely associated with a moist south to southeast flow (fig. 5-2). Except for storm No. 5, the order also relates to season and location, the latter storms occurring later in the season and farther southeast.

2. Sea-level isobars had cyclonic curvature except for the Morgan storm. Low-level windspeeds were light and pressure gradients were weak, as is typical of summer.

3. Storms listed occurred in fairly rugged terrain, near but not over steep mountain slopes.

Resume of two storms

5.12. Girds Creek, Oreg. July 13, 1956. About 4 inches of rain was measured in 30 minutes in this thunderstorm. The general area is at an average elevation of about 4000 feet. The slope rises to southeast, to 6000 feet within 10 miles.

Figure 5-1. Intense thunderstorm locations

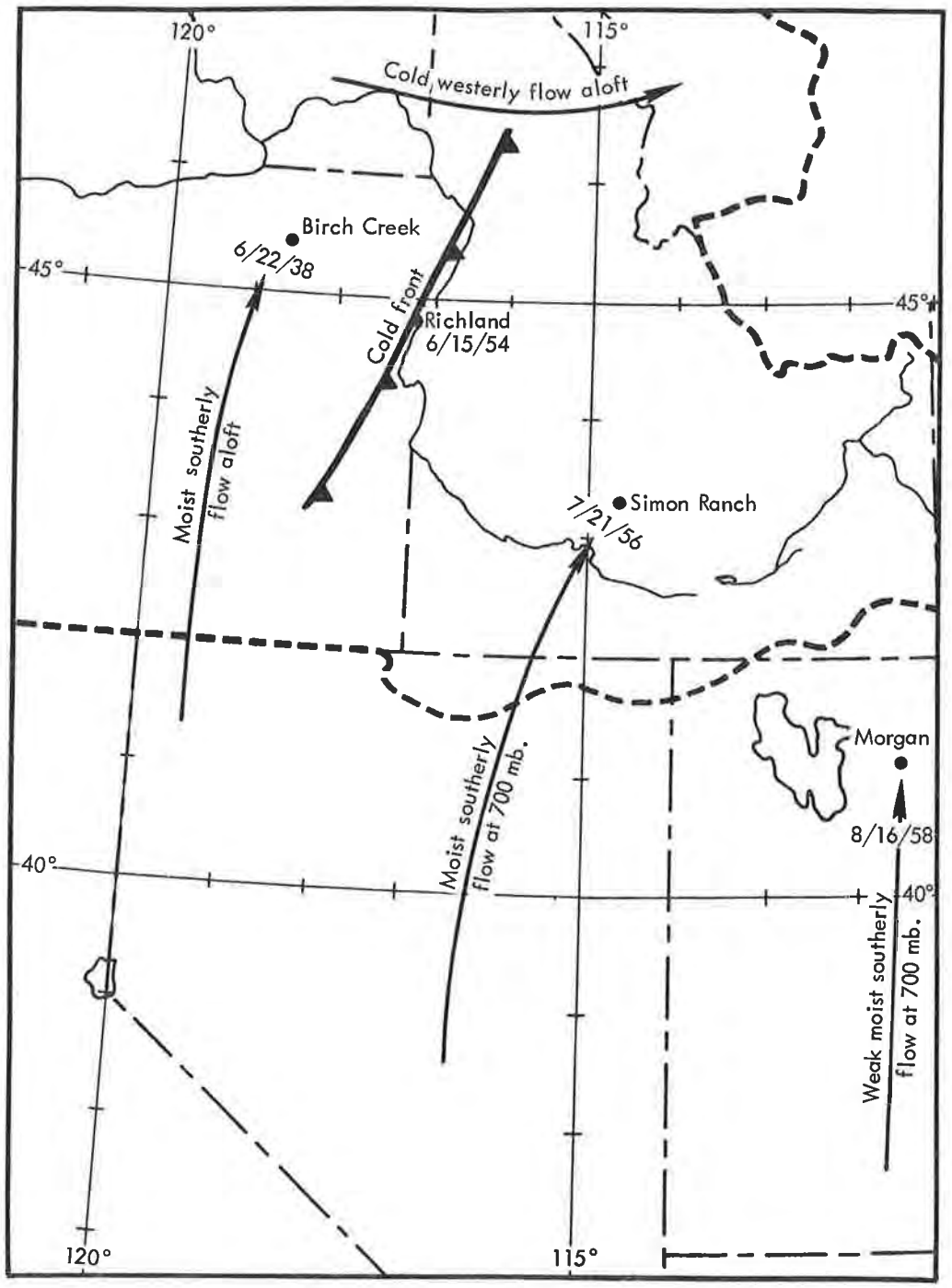

Figure 5-2. Schematic of meteorological factors in 4 intense local thunderstorms

A deep upper Low just off the northern California coast drifted slowly southeastward and onshore on the morning of the 13th; then as it filled it moved rapidly northward and was absorbed in a short-wave upper trough moving southeastward from western British Columbia. The reflection at the surface was a flat 1010-mb. Low over the Pacific Northwest which deepened to 1005 mb. over eastern Washington as the trough passed.

Figure 5-3 shows the path of moisture inflow aloft from the Southwest States northward around the upper Low, then southward into Oregon. This indirect entry of moisture is considered unusual. The axis of the moist tongue was over the upper trough in the area of the storm on the afternoon of the 13th with dry Pacific air on three sides. Thunderstorms had occurred over southern Oregon and southward into the Northern Sierras on the 12th. On the 13th they centered over north-central Oregon northeastward near the location of the moisture axis and upper Low track.

5.13. Morgan (nr.), Utah, August 16, 1958. This storm occurred close to the southeast border of the Columbia Basin. The isohyetal map (fig. 5-4) drawn to U. S. Geological Survey rainfall data and streamflow estimates, suggests two storm centers. Close to 7 inches were measured at each in approximately one hour. The storm centers are east of Morgan in Weber Canyon where it cuts through a north-south ridge about 10 miles east of the front of the Wasatch Range. Within 5 to 10 miles in most directions, peaks are 3000 feet above the valley. The general area experiences occasional severe thunderstorms which usually form over mountains and drift into valleys. Similar topographic features exist elsewhere in the Northwest States.

Precipitation amounts in northern Utah were mostly very light on this date. Measured amounts were about .25 inch in the area just beyond the influence of the main cells, and lighter at greater distances.

The following is a summary description of the storm by local witnesses near its perimeter: Heavy black clouds formed about 7 miles to southeast and about 5 miles to northwest. These cells appeared to move toward the two indicated rain centers, the latter cell prolonging the intense rain observed from the former. Runoff estimates corroborate the storm's intensity and areal extent and show that rain measurements were made close to the rain centers.

The circulation was ideal for bringing Gulf of Mexico air northward into the northern Plateau region. A weak 700-mb. southerly moist flow into northern Utah was present on the 16th, under the combined influence of a High over the Southern Rockies and a north-south trough along the California coast north-northeastward through eastern Washington. Evidence of high moisture content in this flow (fig. 5-2) is the extremely high 700-mb. dew points on the 16th (6°C at Salt Lake City and Grand Junction). Prior to the 16th, moisture had been carried westward along the Southwest Border States on the 14th as the upper High was elongated from the central Plains to central California. Then on the 15th the splitting of this High permitted the northward flow into Nevada and Utah; on that date thunderstorms occurred over the Southwest and in the central Plateau. By the 16th the surface

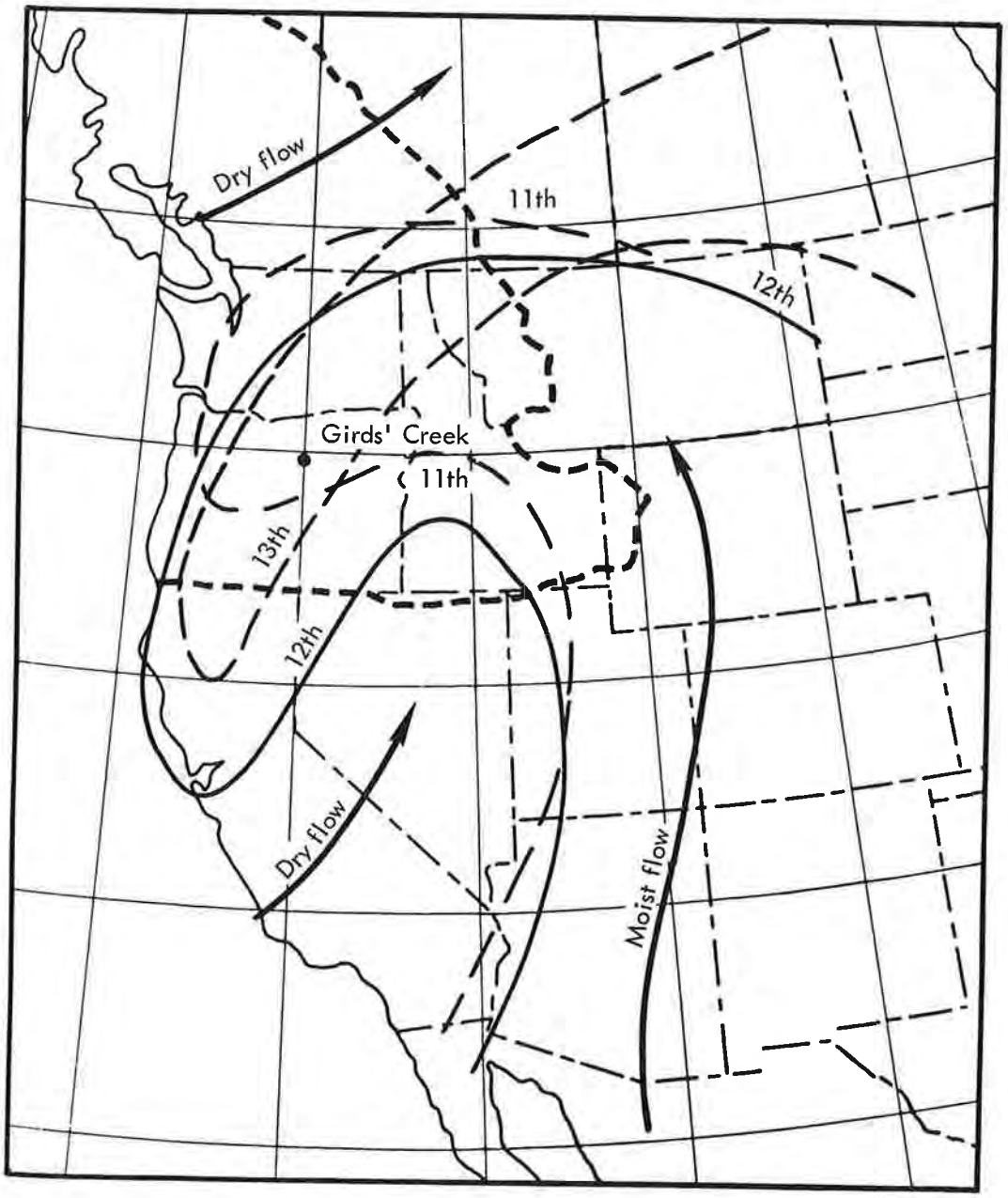

Figure 5-3. Positions of 700-mb. 0°C dew point lines at 1900 PST July 11-13, 1956

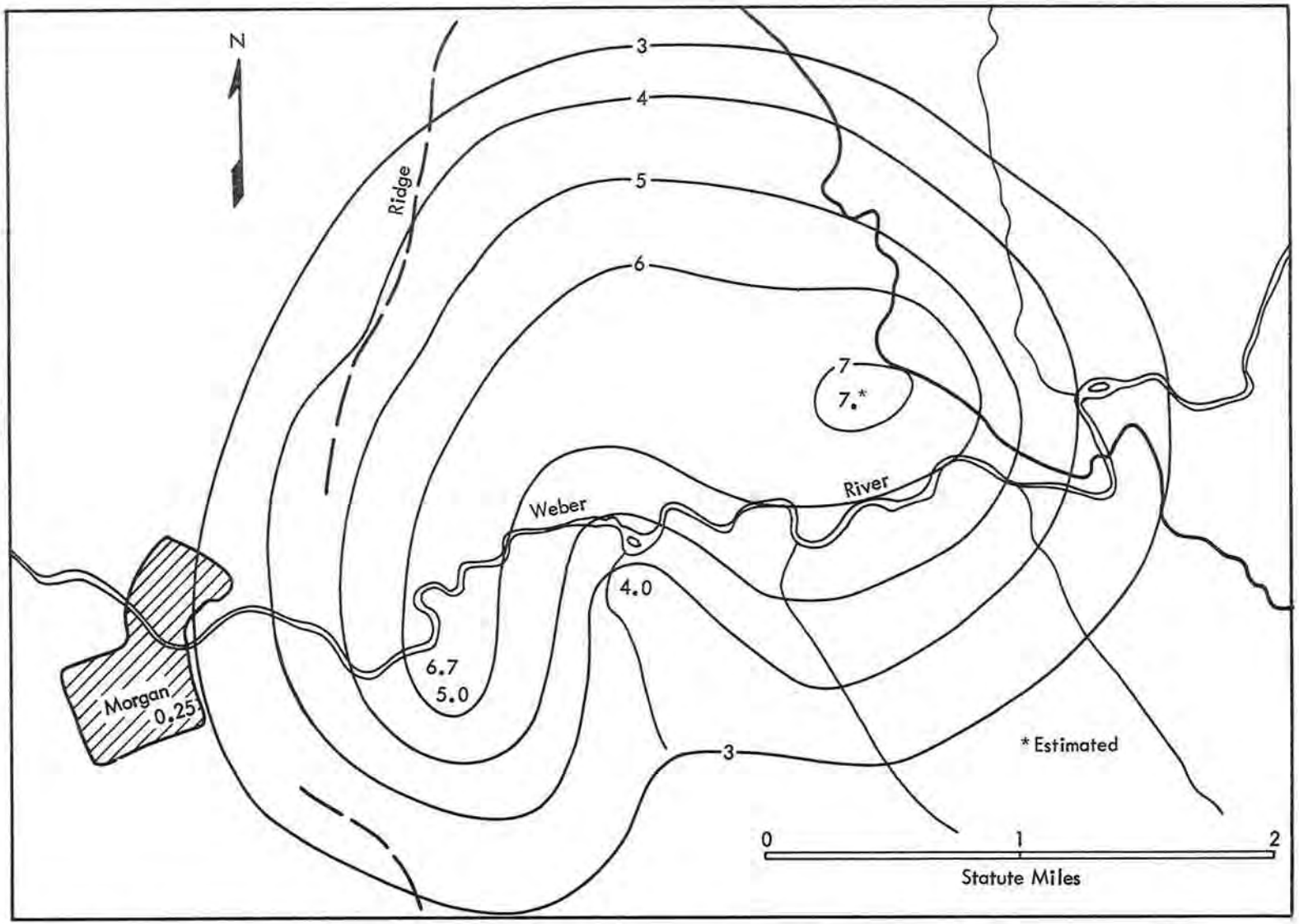

Figure 5-4. Isohyetal map (in.) of Morgan, Utah storm, August 16, 1958

trough had moved eastward ahead of its upper trough to eastern Nevada. Cyclonic circulation was not evident in the southerly flow in the vicinity of and near the time of the thunderstorm.

5-D. POINT PMP AND ITS VARIATIONS

5.14. Point PMP for summer thunderstorms is developed in the following paragraphs for durations to 6 hours. Seasonal, geographic, areal and elevation variations are given.

Envelopment of point thunderstorm rain adjusted for moisture

5.15. Point PMP for the region east of the Cascades is determined from an envelope of moisture-adjusted observed thunderstorm rains in the region, plus that at Morgan, Utah, which is considered transposable to the southeast border of the basin. Pertinent data on these rains (points 1 through 6) and the adopted point PMP envelope are given in figure 5-5. Observed rain values are normalized by maximizing from storm 1000-mb. dew point to a 73°F dew point, the enveloping 12-hr. persisting August 1000-mb. dew point at the southeast border of the Columbia Basin. (Storm rain x [precipitable water for 73°F ÷ precipitable water for storm 1000-mb. dew point] = maximized rain.) This procedure is an alternate to defining P/M ratios for each rain amount, as was done in chapter III for general convergence rain. This alternate is more convenient when only a few rain observations are available. Adjustment to highest dew point in the basin provides a base depth-duration relation to which pertinent seasonal and geographical variations may be applied.

5.16. Points 7 through 10 shown in figure 5-5 are actual rain values (not maximized), measured outside the study region; two exceeded the adopted envelope. All were closely associated with Gulf of Mexico moisture that would be reduced by barriers if transposed to the Northwest. Transposition of storms over extensive and high barriers from other regions no doubt is considerably more complex than techniques to date can cope with. The Buffalo Gap storm in place of occurrence, and other larger storms east of the Continental Divide, such as the Cherry Creek, Colo. storm of May 30, 1935 (24 in. in 6 hr.), were related to a direct flow of moisture from the Gulf of Mexico with no upwind barrier. This in itself will not allow transposition to the Northwest.

5.17. The depth-duration curve of figure 5-5 was extended to 6 hours. Its shape is such that the 1- to 6-hr. ratio is greater than that of an average depth-duration curve of modest thunderstorms selected from Weather Bureau Technical Paper No. 15 (18). This difference is a result of the short durations of the intense thunderstorms observed in the Northwest, as shown in table 5-1.

5.18. Point thunderstorm PMP has been adopted as equal to the PMP for one square mile. This relatively small maximization partially counteracts

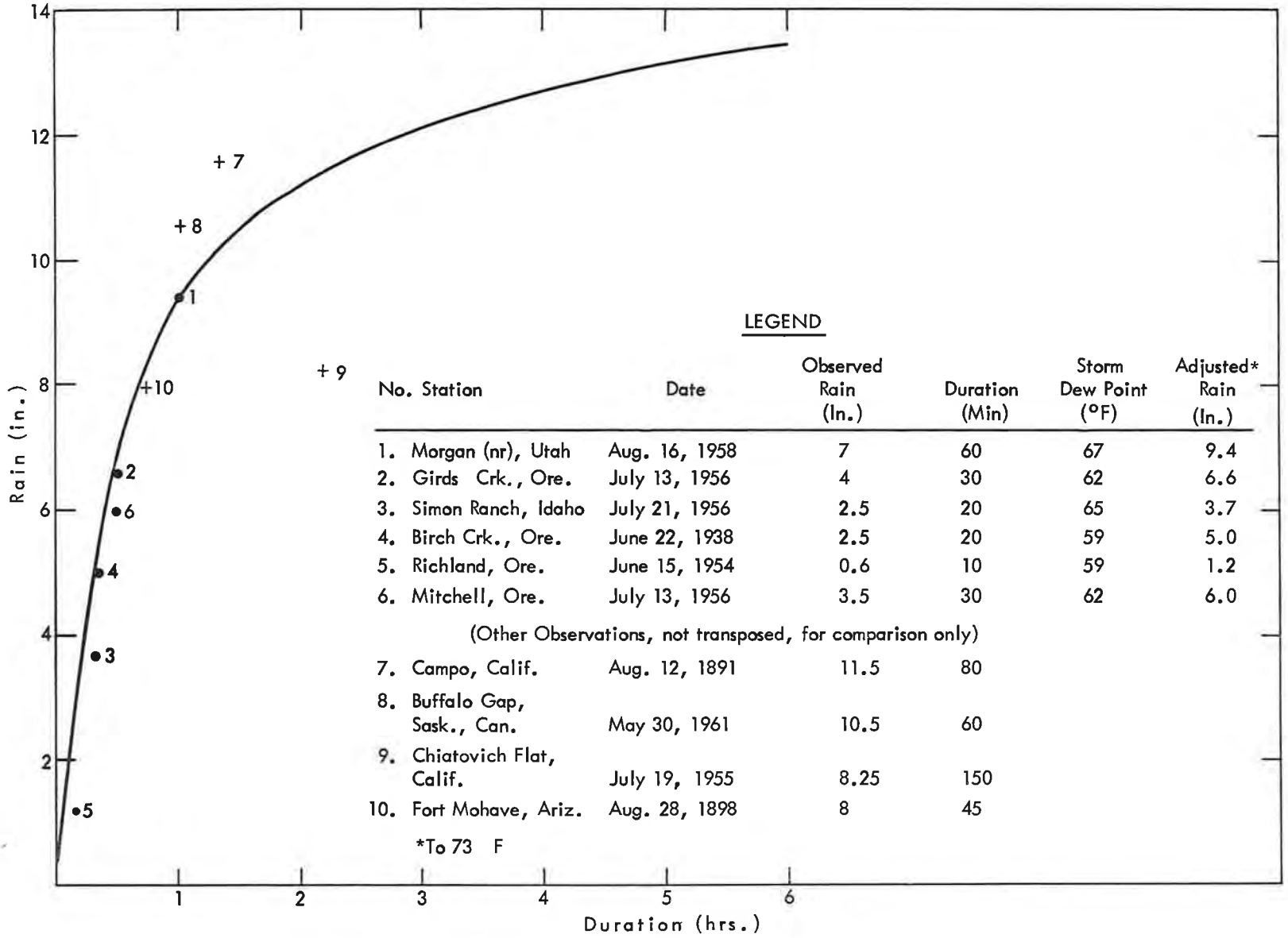

LEGEND

No.	Station	Date	Observed Rain (In.)	Duration (Min)	Storm Dew Point (°F)	Adjusted* Rain (In.)
1.	Morgan (nr), Utah	Aug. 16, 1958	7	60	67	9.4
2.	Girds Crk., Ore.	July 13, 1956	4	30	62	6.6
3.	Simon Ranch, Idaho	July 21, 1956	2.5	20	65	3.7
4.	Birch Crk., Ore.	June 22, 1938	2.5	20	59	5.0
5.	Richland, Ore.	June 15, 1954	0.6	10	59	1.2
6.	Mitchell, Ore.	July 13, 1956	3.5	30	62	6.0
	(Other Observations, not transposed, for comparison only)					
7.	Campo, Calif.	Aug. 12, 1891	11.5	80		
8.	Buffalo Gap, Sask., Can.	May 30, 1961	10.5	60		
9.	Chiatovich Flat, Calif.	July 19, 1955	8.25	150		
10.	Fort Mohave, Ariz.	Aug. 28, 1898	8	45		

*To 73 F

Figure 5-5. Point thunderstorm PMP for 73°F dew point

the fact that undoubtedly there were higher rain rates in the prototype storms than were measured.

Seasonal and geographic variation

5.19. Variation of measured short-duration rains with season and geography is the best available guide to similar variations in the PMP thunderstorm. But guidance may be derived also from the fact that seasonal and geographic variations in short-period rain intensity are related to those of moisture. Evidence of a seasonal relation is the high frequency of excessive 1-hr. amounts shown in figure 5-6 during months of high maximum dew points. Thus dew points and short-period rains together are employed in the following procedure.

5.20. Method of development. Hourly data provide most of the available information on extreme short-period rainfall intensity. Highest monthly clock-hour amounts in summer months listed in Technical Paper 15 were tabulated from 160 hourly reporting stations with records averaging 15 years. These data were grouped in four zones shown in figure 5-7 whose boundaries are August maximum dew point lines (fig. 3-12).

5.21. For each zone, the average of the upper 20 percent of highest clock-hour amounts was obtained for each month. These averages were plotted by months in figure 5-8a for each zone at the mean location of the data. The abscissa corresponds to the line drawn in figure 5-7 from Washington to southeast Utah. Monthly mean lines on figure 5-8a were drawn to these data as shown.

5.22. The seasonal variation of 1-hr. rain (fig. 5-8a) is drawn in figure 5-8b after considering the seasonal variation of moisture (shown by months in parenthesis) at each zone boundary. The latter figures are maximum moisture in percent of August maximum moisture at the southeast boundary of the Columbia Basin. Moisture is relatively low in eastern Washington with relatively little seasonal variation. The set of adjusted lines on figure 5-8b involves the pattern of figure 5-8a but reflects variation of moisture in figure 5-8b, recognizes effect of low frequency of heavy 1-hr. rains to northwest during midsummer and to southeast in spring, and provides seasonal smoothing. These lines on figure 5-8b provide seasonal and geographical variation of thunderstorm PMP.

5.23. Application. Figure 5-9a gives distance of a basin from the southeast border of the region across parallel lines oriented approximately along maximum dew point lines. Figure 5-9b is a replot of figure 5-8b with abscissa as distance from southeast border.

Basin thunderstorm PMP, in percent of August thunderstorm PMP at the southeast border (fig. 5-5), is read from figure 5-9b (May to September) at the distance from the southeast border obtained in figure 5-9a.

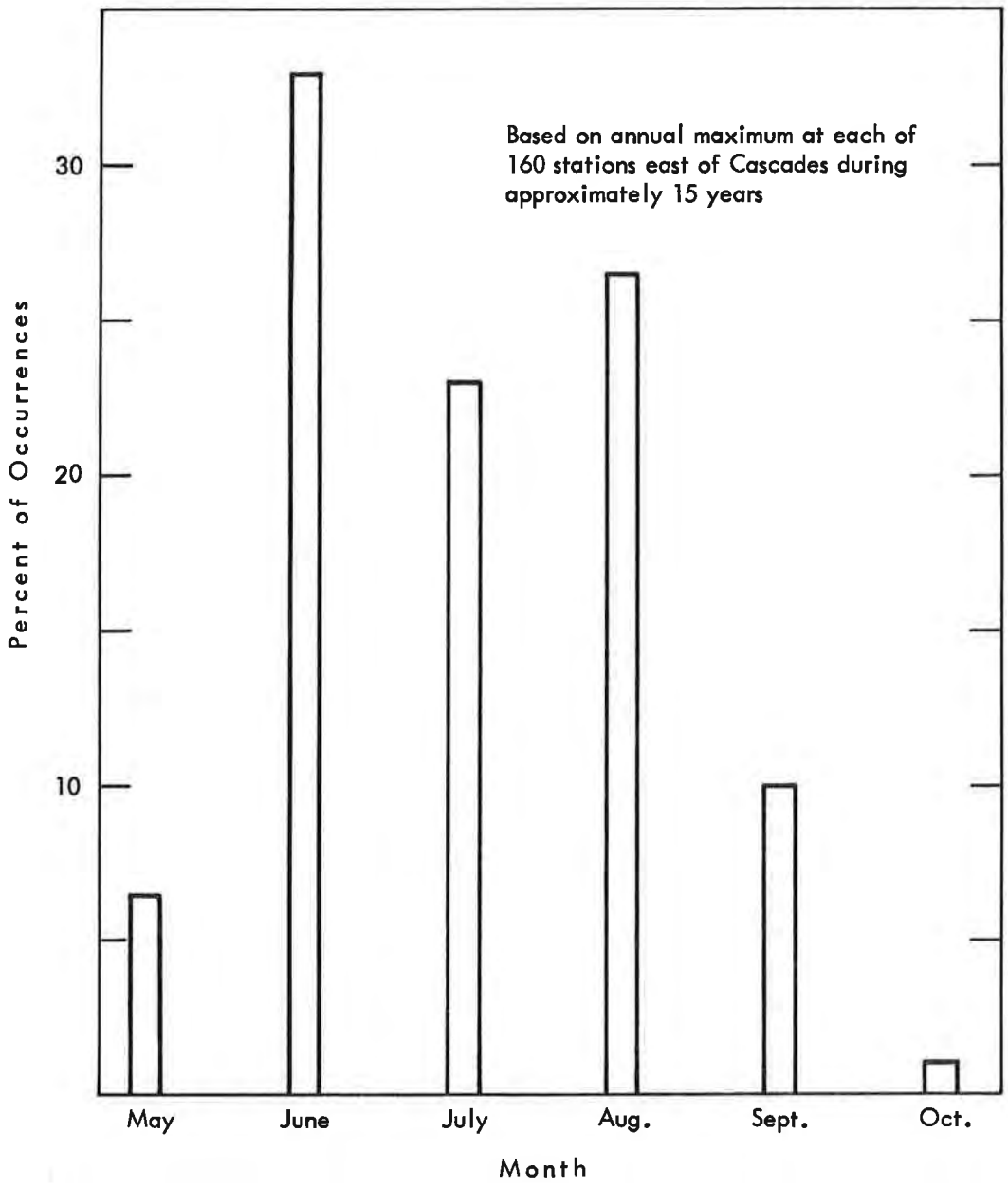

Figure 5-6. Seasonal frequency of hourly amounts over 1 inch

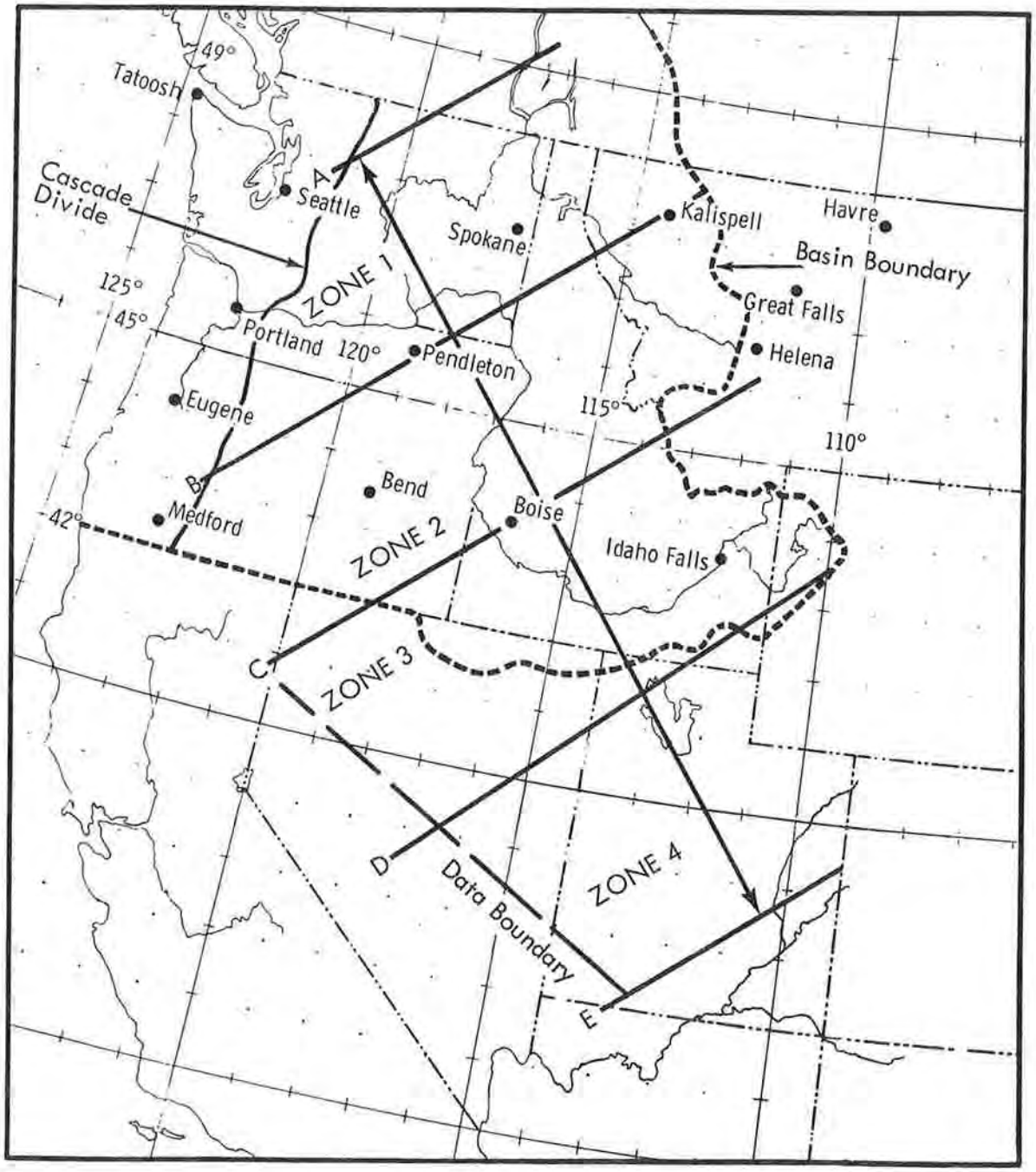

Figure 5-7. Area and zones of clock-hour rain study

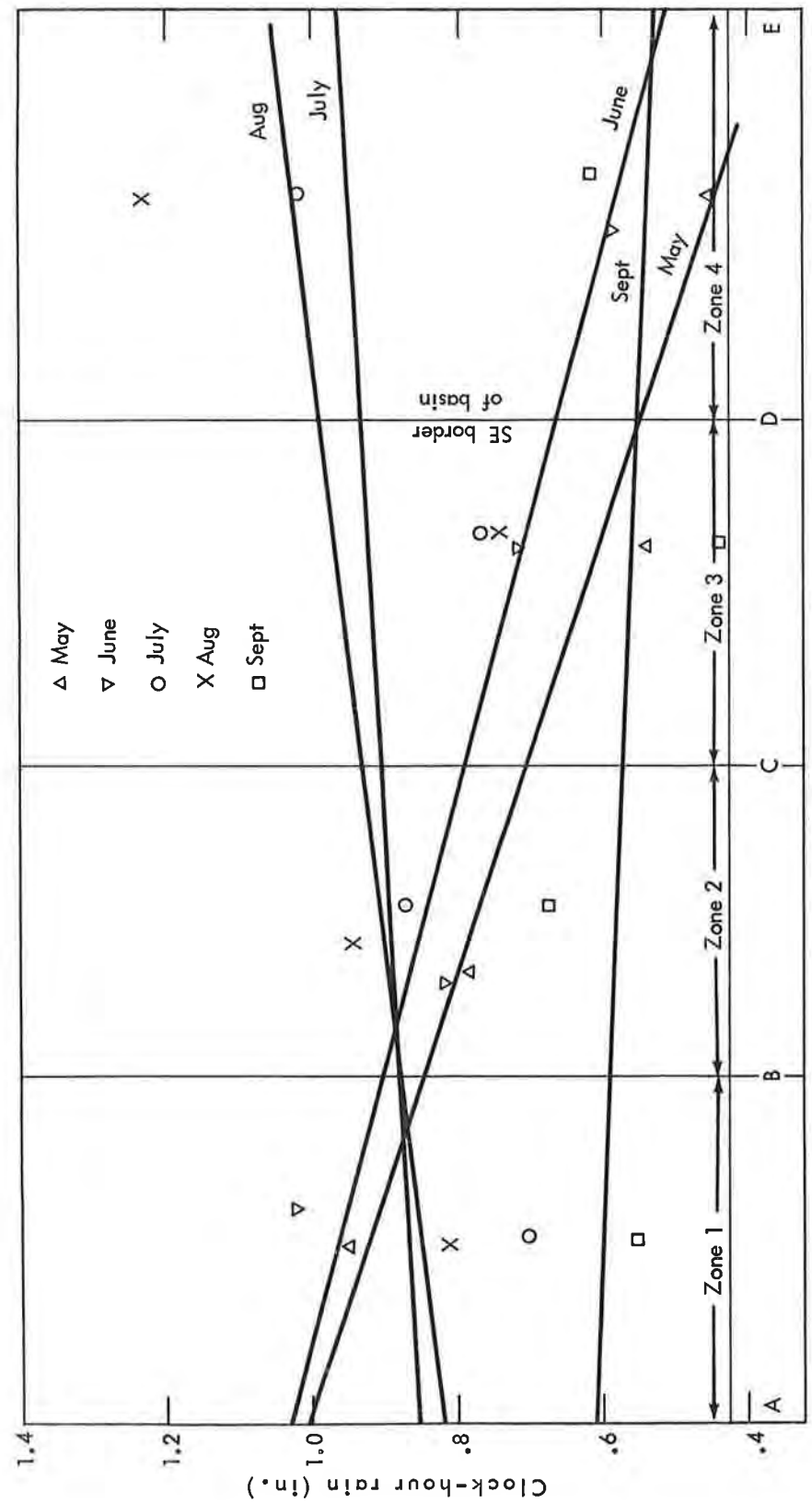

Figure 5-8a. Variation by months and zones of clock-hour rain. (Data are averages of upper 20% of highest monthly amounts. Zone boundaries are shown on fig. 5-7 as A, B, C, D, E.)

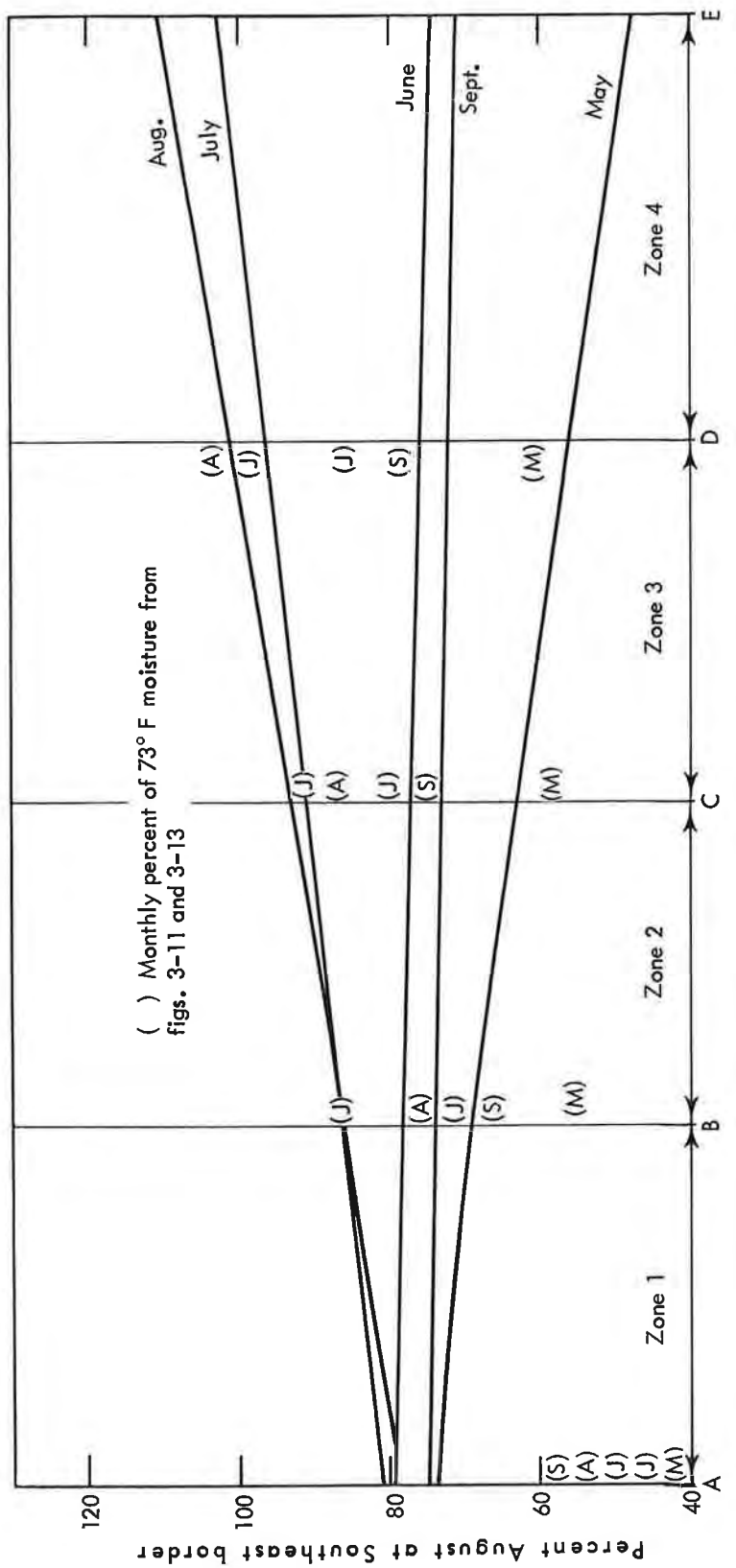

Figure 5-8b. Adjustment of figure 5-8a lines. (Seasonal smoothing, trends of monthly maximum dew point and effect of frequency are involved.)

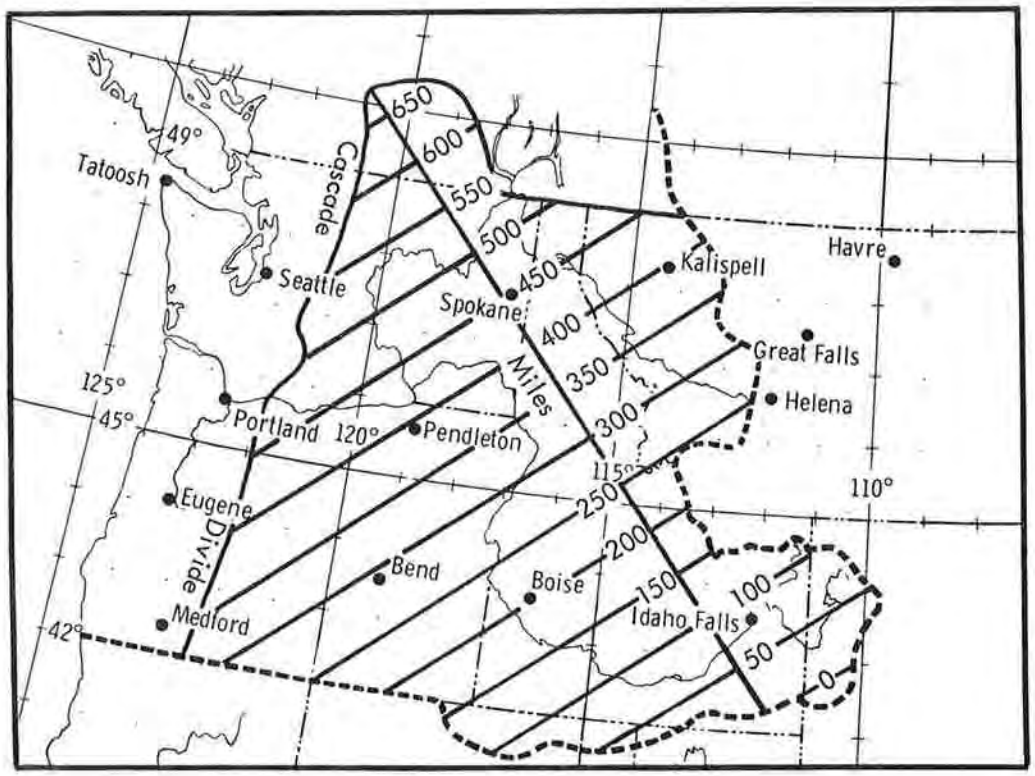

Figure 5-9a. Basin distance from southeast border

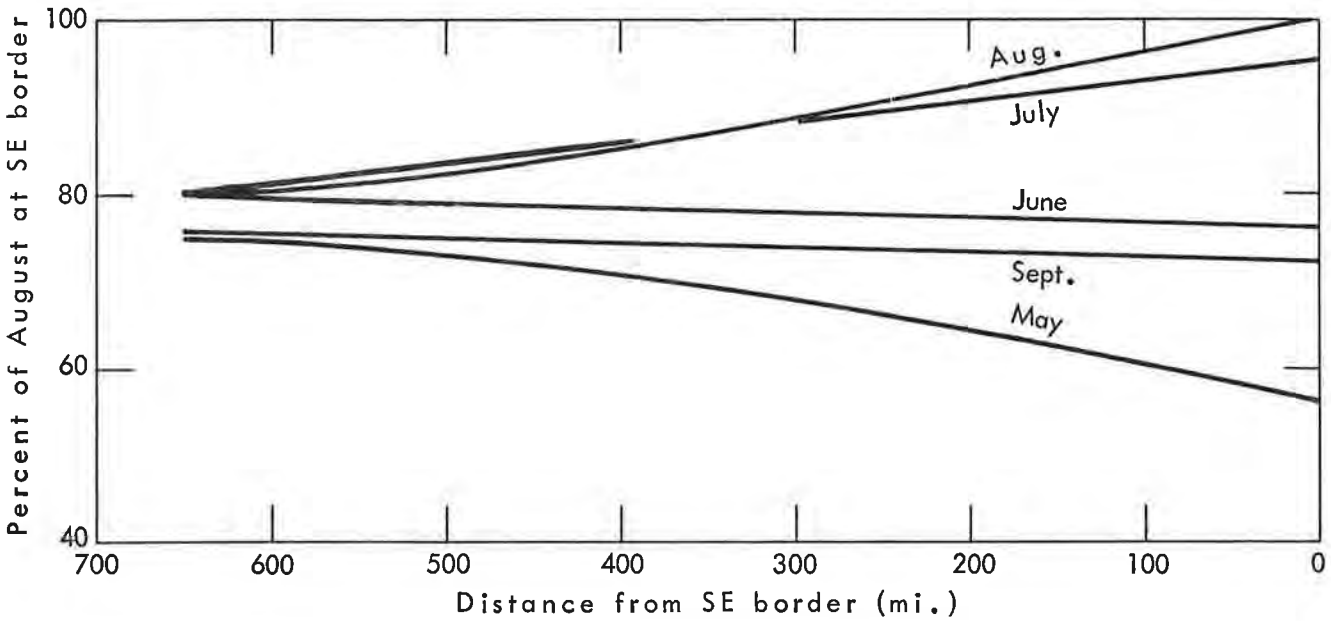

Figure 5-9b. Basin percent of August thunderstorm PMP at southeast border

Elevation variation

5.24. A baffling question concerns the variation of thunderstorm PMP with elevation. The problem has been faced by many investigators. Observational evidence and studies make it clear that the relationship between rainfall and topography differs with storm type. For warm-season short-duration rains, elevation is poorly related to rain magnitude.

5.25. For this purpose the best available data for Idaho and eastern Oregon were studied. These are maximum observed clock-hour rains at recorder stations from Technical Paper No. 15 (18) with extension to an average of 15 years of record from later tabulations. These maxima for the months May through September for stations in Idaho and eastern Oregon were plotted against station elevation (not shown). The trend of precipitation amounts with altitude was not conclusive. An enveloping curve indicates a peak in precipitation at about 2000-3000 feet above the surface.

In the search for a more stable relation between elevation and precipitation, the average of the monthly maximum clock-hour precipitation amounts for the three summer months, June, July and August, were plotted against elevation. Stations in Utah, although outside the basin, were included in order to have values for elevations above 6000 feet. The plots, shown in figure 5-10, do not appear to have a trend with elevation. An envelopment of the data indicates a maximum at about 5000 feet. Unequal number of stations in various elevation bands must account for some of the variation shown, but much is indeterminate.

5.26. Ultimately, as elevation increases, thunderstorm rain must begin to decrease at some level. Using figure 5-10 as a guide, we adopted no change in PMP with elevation up to 5000 feet m.s.l. and a decrease of 5 percent per 1000 feet above. This decrease corresponds closely with the decrease in precipitable water with elevation above 8000 feet, (fig. 3-34).

For the 6-hr. duration, data similar to that analyzed above may show an increase with elevation up to some level since slopes become more effective as duration increases. But the intense thunderstorms of the region are mostly 1-hr. duration or less; the PMP for 1 hour is 70 percent of the 6 hour. Therefore the effect of longer durations on the above adopted elevation variation would be relatively small and has not been included.

Depth-area variation of summer thunderstorm PMP

5.27. In applying summer thunderstorm PMP to a specific basin, an important consideration is how 1-sq. mi. PMP values should decrease with increasing area. This decrease varies widely with individual storms studied, depending largely on storm type but in part on how the isohyets were drawn which is often arbitrary because of sparsity of rain gages.

5.28. Adopted depth-area relations were based on (1) those for eastern type thunderstorms, (2) the few relations available for intense thunderstorms west of the Continental Divide, and (3) those from a model thunderstorm. These steps are elaborated below.

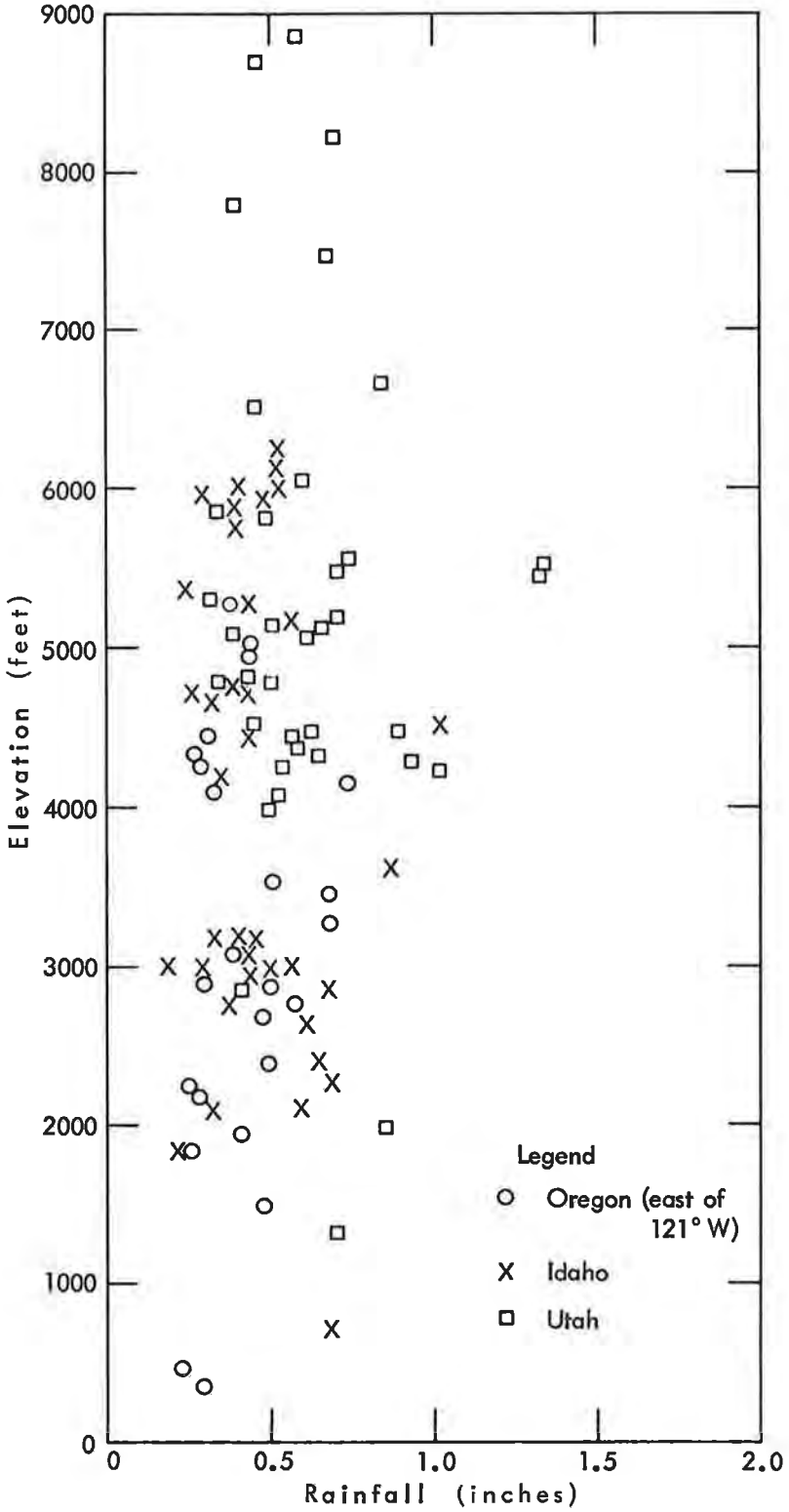

Figure 5-10. Variation of clock-hour rain with elevation

5.29. Depth-area relations from eastern data. Depth-area relations for all storms contained in U. S. Storm Rainfall (19) and in Canadian Storm Data Sheets (20) with time breakdowns to less than 6 hours were compared and summarized. Those with closely spaced isohyets typical of isolated thunderstorms were selected as most nearly representative of thunderstorms in the Columbia River drainage east of the Cascade Divide. On figure 5-11 is a list of eastern storms that were considered. Based on depth-area curves for these storms for 1, 3, and 6 hours, average depth-area curves were drawn for these durations (fig. 5-11, dot-dash curves) consistent from duration to duration. The 6-hr. curve up to 200 square miles quite closely follows that of the Cherry Creek, Colo. storm (May 30-31, 1935) and of the Smethport, Pa. storm (July 17-18, 1942). The 1-hr. curve falls between the depth-area curves of the Gering, Nebr. storm (June 17-18, 1947) and the Buffalo Gap, Saskatchewan storm (May 30, 1961).

5.30. Depth-area relations from western data. Some of the more intense point thunderstorm rains west of the Continental Divide have sufficient surrounding reports from "bucket surveys" to allow determining depth-area relations. These are listed in table 5-2 with other pertinent data and located on figure 5-1.

Table 5-2

INTENSE THUNDERSTORMS WEST OF THE CONTINENTAL DIVIDE

Location	Storm Date	Maximum Point Rain (in.)	Duration of Maximum Rain (min.)	Total Area Covered by Storm (sq. mi.)
Morgan (nr.), Utah	August 16, 1958	7	60	200
Vallecito, Calif.	July 18, 1955	7	70	600
Santa Rita Expt. Sta., Ariz.	June 29, 1959	4.5	55	480
Globe, Ariz.	July 29, 1954	3.5	40	600

5.31. Total area covered by each storm (last column of table 5-2) was determined by extrapolation of isohyets drawn to "bucket survey" data near the storm center and to additional rain amounts from published Weather Bureau records.

5.32. Depth-area relations for these four storms, each expressed in percent of the highest observed point value, are shown in figure 5-12. One way of comparing isohyetal patterns is to assume circular isohyets and to construct isohyetal profiles, plotting depth against distance from center of storm. Such profiles for the same storms, in percent of rain at storm center, are given in figure 5-13. The two figures, based on the same data, are different ways of appraising the variation of rain with area. While

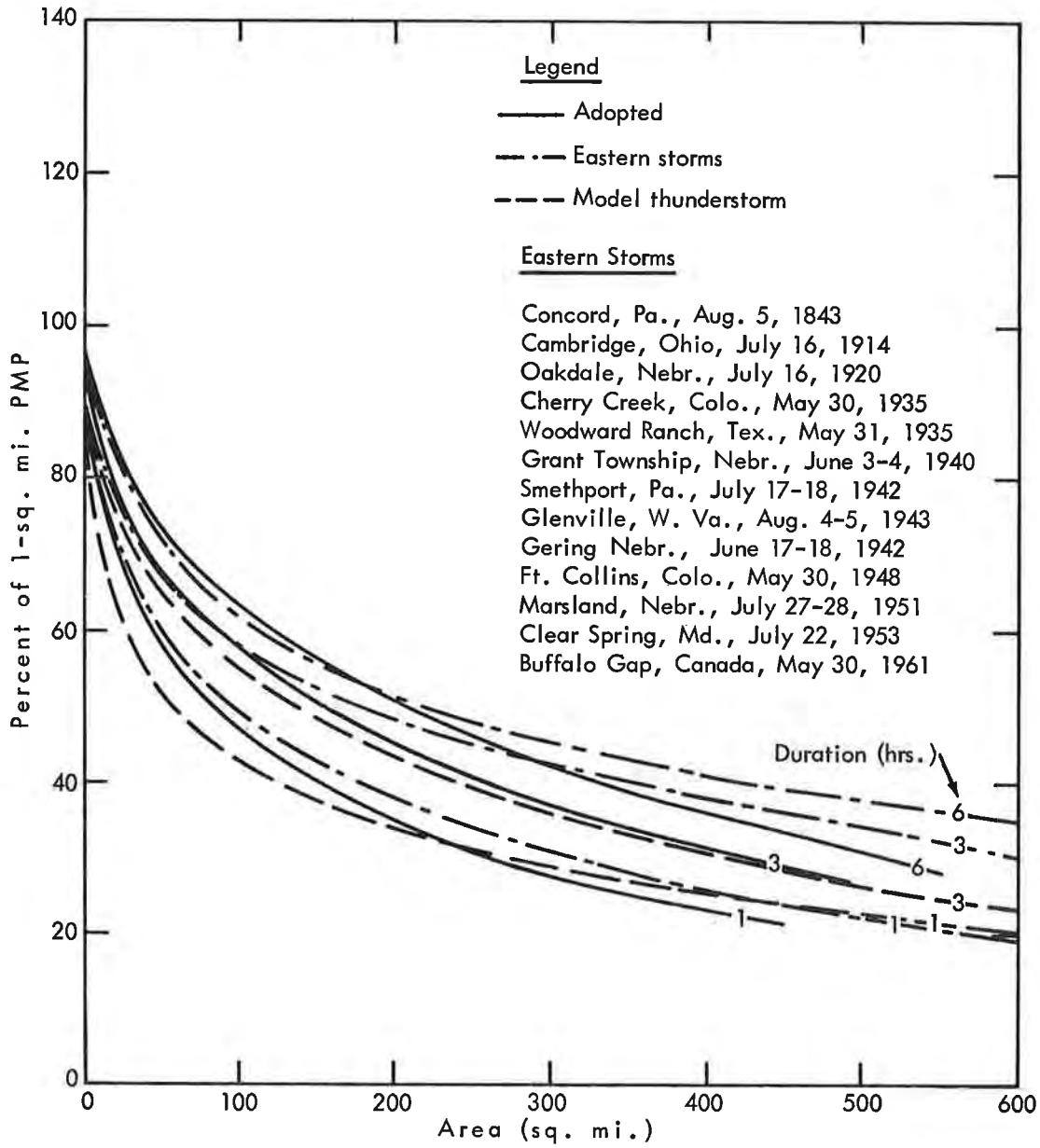

Figure 5-11. Comparison of adopted depth-area relation with eastern data and model thunderstorm

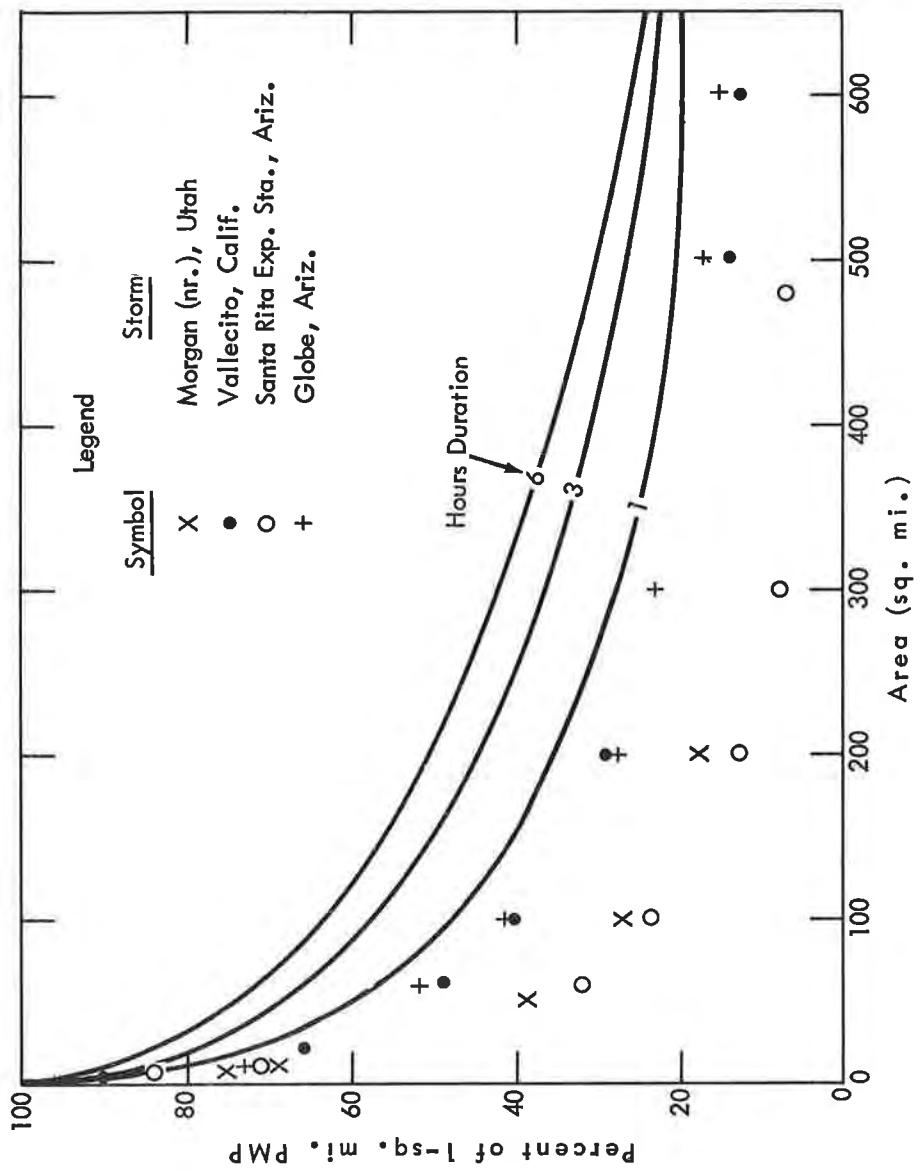

Figure 5-12. Adopted depth-areal relation for thunderstorm PMP

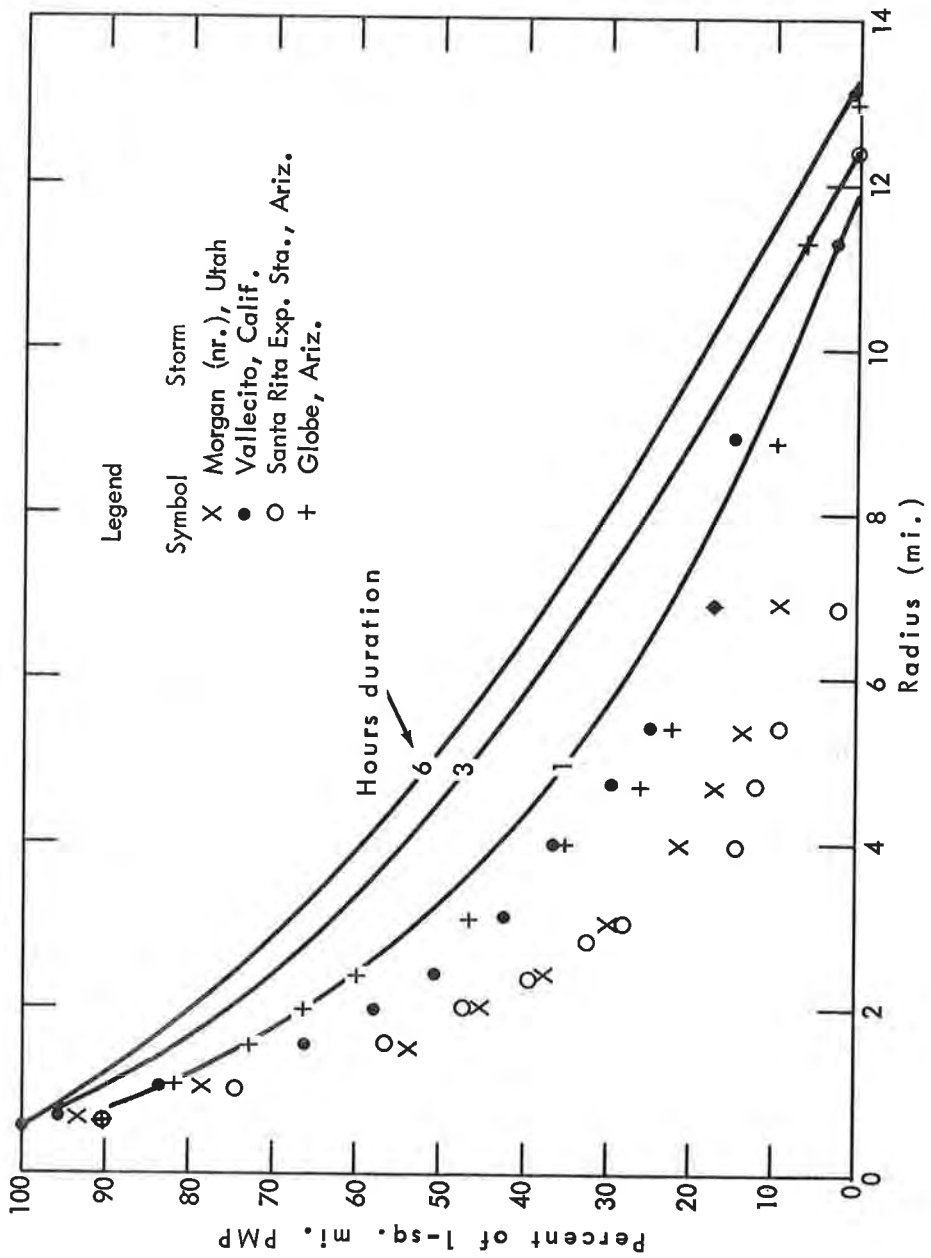

Figure 5-13. Adopted isohyetal profile for thunderstorm PMP

isohyetal profiles show best the areal extent of the storm, depth-area curves are the more familiar method of showing areal relations in rain and provide more directly average rain depth over a basin.

5.33. Depth-area relations for a model thunderstorm. A storm model was developed and analyzed to provide information as to compatibility of an isolated thunderstorm cell with the depth-duration relation given in figure 5-5, and to study effect of storm motion on depth-area relations.

The thunderstorm model involved the following assumptions:

1. Depth-duration relation for 1 square mile from figure 5-5.
2. Circular isohyets.
3. A 4-m.p.h. rate of travel.
4. A rate of storm intensity decay equal to that at a point due to storm motion.

With these assumptions, hourly isohyets were computed for 1, 2, and 3 hours as percent of 1-sq. mi. 1st-hr. values. Then, depth-area relations and isohyetal profiles were drawn, as in paragraph 5.32.

5.34. Comparison with adopted relations. Adopted relations for summer thunderstorm PMP are given in terms of depth-area on figure 5-12 and as isohyetal profiles on figure 5-13. In both relations, the observed western storms are enveloped by PMP except at the outer edge of the storms. This undercutting is consistent with observational data on the smaller area of intense thunderstorms in the Columbia Basin. Similarly the main difference between the adopted depth-area relations and those from eastern storm data (both shown on fig. 5-11) is a reduction of the total area covered by isohyets, especially so for the 6-hr. duration. The profile and areal variations of the adopted PMP and the PMP from the model thunderstorm are quite comparable. Major differences are that the model gives lower percents in small areas and greater percents near the edge of the storm, as is shown for depth-area in figure 5-11. Differing assumptions, such as a slightly slower rate of travel would result in closer agreement.

5.35. Thunderstorm PMP vs. general storm PMP. Although the areal extent of thunderstorm PMP is limited (450 sq. mi. for 1 hr. up to 550 sq. mi. for 6 hr.), this thunderstorm PMP may yet be the most critical for basins larger than these limits. For these larger basins the average depths over 450 square miles for 1 hour and 550 square miles for 6 hours should be computed, placed critically over the basin, and the resulting flood hydrograph compared with that from the general storm PMP (chap. VI).

Steps for obtaining basin average thunderstorm PMP

5.36. Should the areal distribution of thunderstorm PMP not be required, basin average depths are readily obtained by the following steps. (If the areal distribution is required, go to paragraph 5.37 after first 4 steps).

Step

1. Find distance of center of basin from southeast border (fig. 5-9a).

2. Enter figure 5-9b with this distance and read the percent for the required months.

3.* Determine the lowest elevation within the basin boundary.

4. Enter the nomogram of figure 5-14 with the percent found in (2). Proceed vertically to the elevation found in (3), then horizontally to each duration to determine 1-sq. mi. PMP on horizontal scale for indicated durations.

5. Enter figure 5-12 with area of basin to obtain areal reduction for 1, 3, and 6 hours.

6. Multiply the 1-sq. mi. 1-, 3-, and 6-hr. PMP of (4) by the percents of (5).

7. Plot the 1-, 3-, and 6-hr. values of (6) against duration and interpolate for other required durations. Determine hourly increments of PMP.

8. Arrange hourly basin PMP increments in a time sequence for the PMP storm. Highest increment 2d, 3d, or 4th with next highest adjacent on either side, 3d highest adjacent, etc., and lowest 2 increments at beginning and end is recommended. Such arrangement is in agreement with that in Thunderstorm Rainfall (21) and that prescribed in Civil Engineer Bulletin #52-8 (22).

9. Compare resulting thunderstorm PMP with general storm PMP for which a procedure is given in chapter VI.

Procedure for obtaining areal distribution of thunderstorm PMP over basin

5.37. Isohyetal pattern. If the areal distribution of thunderstorm PMP is required within a basin or portion thereof, the isohyetal pattern of figure 5-15 is recommended. It is derived from the model thunderstorm for 2 hours duration, as a compromise for each 1-hr. increment of PMP to avoid complicated procedures.

5.38. Table 5-3 contains information that, together with the isohyetal pattern, permits determining the average depth of PMP over any portion of the basin. This is set up to give PMP for 1/2 hour and for each hour from the 1st (highest) to 6th (lowest) in the 6-hr. PMP storm. Explanation of the table is as follows:

Column (1). Isohyetal letters corresponding to those on the pattern storm.

*Step 3 should read: Determine the mean elevation within the basin boundary and limiting thunderstorm area.

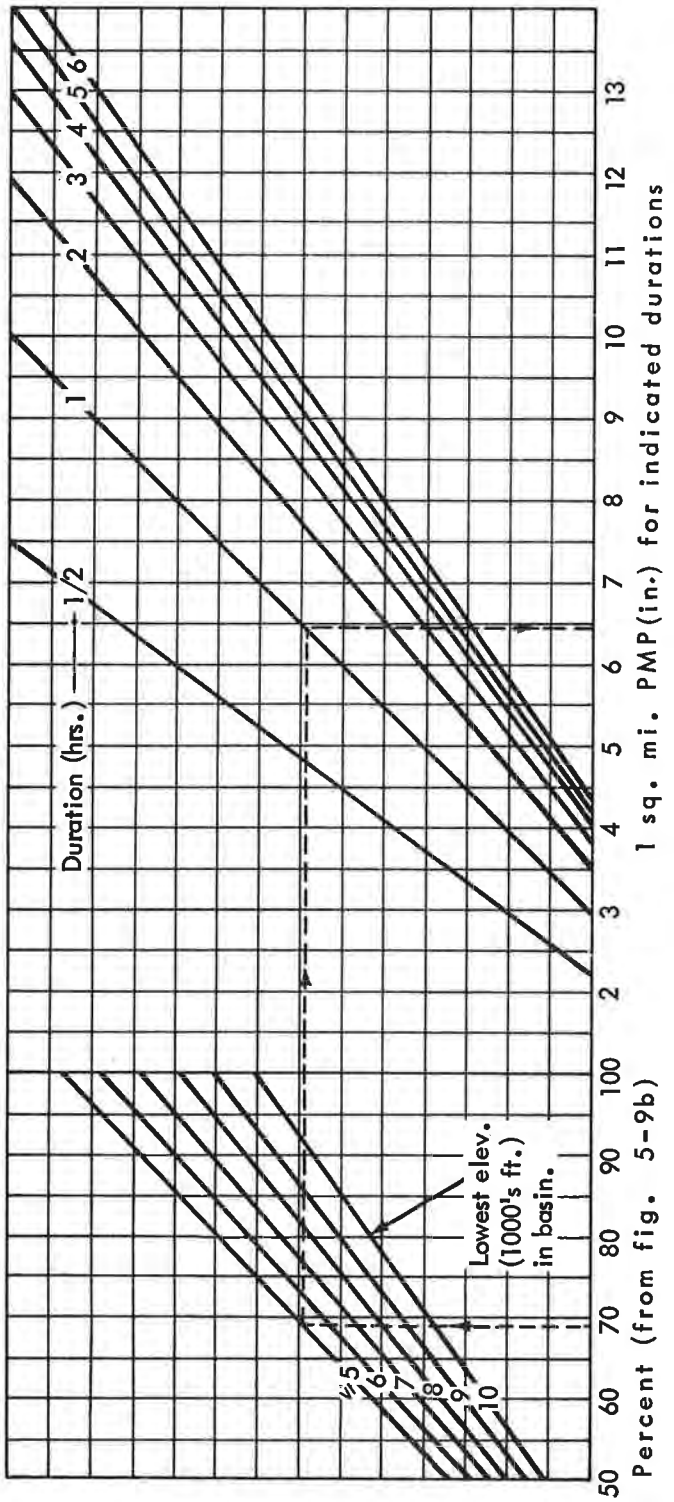

Figure 5-14. Nomogram for obtaining 1-sq. mi. PMP for a basin

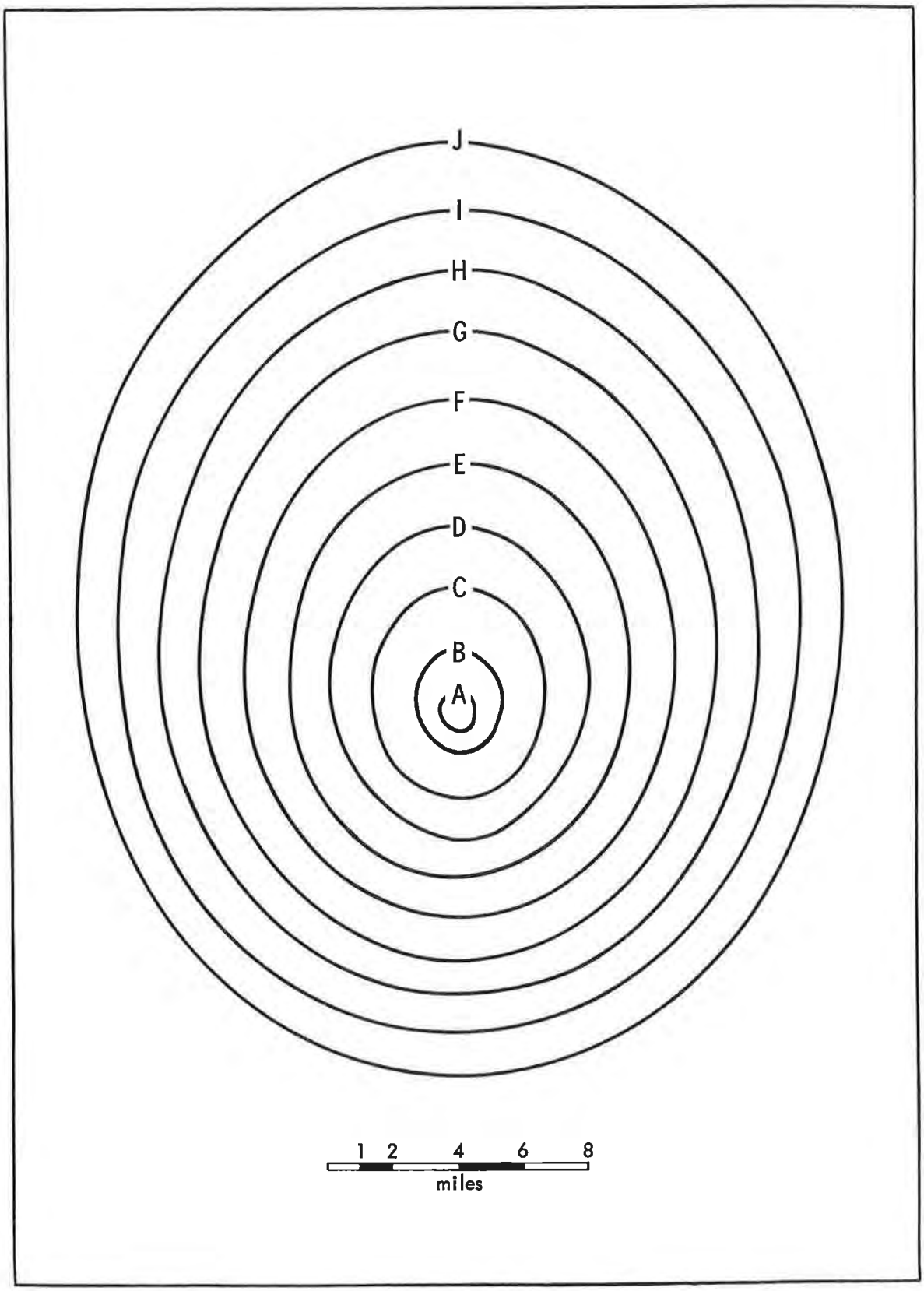

Figure 5-15. Isohyetal pattern for thunderstorm PMP

Column (2). Total area enclosed by each isohyet.

Column (3). Percents of 1-sq. mi. 1-hr. PMP isohyets for 1/2-hr. PMP isohyets. These are used to obtain 1/2-hr. PMP over any portion of a basin.

Columns (4-9). Percents of 1-sq. mi. 1-hr. PMP isohyets for the 1st through 6th-hr. PMP isohyets. These are used to obtain 1st through 6th-hr. PMP over any portion of a basin.

The percent labels were derived from figure 5-13 (PMP isohyetal profiles) and figure 5-5 (PMP depth-duration curve).

Table 5-3

PATTERN STORM ISOHYETAL LABELS

(In percent of 1-sq. mi. 1-hr. PMP isohyets)

(1)	(2)	(3)	(4)	(5)	(6)	(7)	(8)	(9)
Isohyet	Area Enclosed (sq. mi.)	1/2-hr. PMP	(highest) 1st	2nd	Hourly increment of PMP 3rd	4th	5th	(lowest) 6th
A	1	75	100	19	10	6	5	4
B	6	52	76	19	10	6	5	4
C	25	34	54	19	10	6	5	4
D	59	24	40	17	9	6	5	4
E	95	19	32	14	8	5	4	4
F	167	12	21	10	7	4	3	3
G	245	8	14	7	5	4	3	3
H	327	4	8	4	4	3	3	3
I	430	1	1	2	2	2	2	3
J	539	0	0	0	0	0	1	3

5.39. Summary of steps. The following procedure provides areal distribution of PMP within a basin.

Step

1-4. Same as steps 1-4 in paragraph 5.36.

5. Lay the isohyetal pattern, figure 5-15, over the basin outline (both to the same scale). The pattern may be rotated without limit and centered most critically.

6. Note isohyets over (or adjoining) portion of basin (hereinafter referred to as X) for which PMP is required. Obtain labels for these isohyets from table 5-3. (Labels vary with hourly increment of PMP.)

7. Multiply isohyet labels of step 6 by values from step 4. This gives isohyet labels, in inches, for 1/2-hr. PMP and each hourly increment of PMP.

8. Determine average depth over X by standard procedure or alternate.

9. Follow steps 7-9 of paragraph 5.36 if required.

Example of basin average thunderstorm PMP computation

5.40. Steps that follow correspond to those in paragraph 5.36.

Basin: Willow Creek, Oreg.

Area: 96 square miles

Step

1. Distance from southeast border: 390 miles (from fig. 5-9a)

2. Percent of August PMP at southeast border: (fig. 5-9b)

May	June	July	Aug.	Sept.
70	78	86	85	74

3. Lowest elevation within basin: Less than 5000 feet.

   Note: In this example PMP is determined for July.

4. 1-Sq. Mi. PMP (July)

1/2	1	2	3	4	5	6
6.0	8.0	9.6	10.4	10.9	11.3	11.7 (in.)

   (from fig. 5-14)

5. Areal reduction factors for 1, 3, and 6 hours (fig. 5-12)

1	3	6 hr.
.48	.59	.64

6. 1-Sq. mi. PMP of step 4 X areal factors of step 5

3.8 inches	1-hr.
6.1 inches	3-hr.
7.5 inches	6-hr.

7. Interpolated PMP for each duration

1/2	1	2	3	4	5	6	(hr.)
2.4	3.8	5.3	6.1	6.7	7.1	7.5	(in.)

Incremental PMP

1st	2nd	3rd	4th	5th	6th	(hr.)
3.8	1.5	0.8	0.6	0.4	0.4	(in.)

8. Sequence of hourly increments in PMP storm

0.4	1.5	3.8	0.9	0.6	0.4	(in.)

Chapter VI

PMP PROCEDURE AND TIME DISTRIBUTION

Introduction

6.01. For basins east of the Cascade Divide estimates of PMP are made for a general storm type and local summer thunderstorm type. The latter are limited in areal extent to 550 square miles, but even for larger basins may still be more critical than general storm PMP. Both storm types should be evaluated.

West of the Cascade Divide, the orographic storm controls PMP except for small low-lying basins in valleys where PMP for the convergence-only storm (1.23 times convergence PMP for the orographic storm) may be larger.

6.02. PMP can be determined for any basin west of the Cascade Divide up to 5000 square miles in area. East of the Divide PMP is for basin sizes up to 1000 square miles.

6.03. In this chapter stepwise procedures are given for obtaining general storm PMP, followed by several examples. Procedure for obtaining thunderstorm PMP is given in chapter V. A second part of this chapter discusses time distribution of 6-hr. rain in the PMP storm. Procedures are given for sequences that are meteorologically sound and examples are shown.

6.04. Computational forms. Table 6-1 is a form for computing general storm PMP by 6-hr. increments, October through June. The column headings indicate both step and time period. Incremental and accumulated values are entered, obtained by 6-hr. steps from the first (highest) 6 hours through 24 hours, then by 12-hr. steps to 72 hours. The legend at the top of table 6-1, Part I lists the steps, factors involved and data source for convergence PMP. The steps in obtaining orographic PMP are similarly listed in Part II of this table. Part III provides space for sums of orographic and convergence components to obtain total PMP.

6-A. PMP PROCEDURE

Computation of convergence PMP to add to orographic PMP

6.05. Computation of convergence PMP is complicated because four factors are involved, namely index 1000-mb. value, durational variation, depth-area variation and terrain effects. The first two vary both seasonally and geographically, the third varies seasonally and the fourth geographically.

6.06. The procedure for obtaining convergence PMP for a basin either east or west of the Cascade Divide is described by the following steps, in conjunction with table 6-1.

Step A. Use a blank Table 6-1, pp. 199 to 202. Record on line A the basin average stimulation-elevation barrier adjustment from figure 3-37a to c.

Step B. In column B list the basin-average 24-hr. 10-sq. mi. 1000-mb. PMP for the required months from figures 3-23a through 3-31a.

Step C. In column C list the products of A and the monthly values of B.

Step D. In column D list monthly 6/24-hr. ratios at the basin site from figures 3-23b through 3-31b.

Step E. Multiply C by D, each month, and enter in column E. This is basin-average 1st 6-hr. 10-sq. mi. convergence PMP.

Step F. Enter table 3-3 with monthly 6/24-hr. ratios from column D. Read out incremental durational percents for the 2d, 3d, and 4th periods and enter in columns F_2, F_3 and F_4, respectively. Similarly, read out the sums of incremental percents for 5th plus 6th, 7th plus 8th, 9th plus 10th, and 11th plus 12th periods, and record in columns F_6, F_8, F_{10} and F_{12}, respectively. (Use accumulated percents for a 10-sq. mi. basin only.)

Step G. List the basin size adjustments (percents) for the 1st, 2d, 3d, and 4th 6-hr. periods from figures 3-40a to b in columns G_1, G_2, G_3, and G_4, respectively, for each month. This step reduces the 10-sq. mi. values for basin size, required only through the 4th period.

Step H. Record the products of F_1 and G_1, F_2 and G_2, F_3 and G_3, and F_4 and G_4 in columns H_1, H_2, H_3 and H_4, respectively.

Step I. Record H_1 plus H_2 each month in column I_2, I_2 plus H_3 in column I_3, I_3 plus H_4 in column I_4. I_6, I_8, I_{10}, and I_{12} are respectively, the sums $I_4 + F_6$, $I_6 + F_8$, $I_8 + F_{10}$ and $I_{10} + F_{12}$.

Step J. Multiply H_1, I_2, I_3, I_4, I_6, I_8, I_{10} and I_{12} each month by the value E for the same month, and list in columns J_1, J_2, J_3, J_4, J_6, J_8, J_{10} and J_{12}, respectively. These values are 6-, 12-, 18-, 24-, 36-, 48-, 60-, and 72-hr. convergence PMP. (For 1- and 3-hr. convergence PMP, multiply 1st 6-hr. 10-sq. mi. value (E) by percents in figure 3-41* for basins to 500 sq. mi.)

Computation of west-of-Cascades convergence PMP not combined with orographic PMP

6.07. Referring to the reasoning in paragraphs 3.13 and 3.28, a factor 1.23 multiplied by values in paragraph 6.06, step J, gives convergence PMP

*Please see revision of figure 3-41, dated April 1981, which is included at the end of this publication.

not to be combined with orographic PMP, for basins west of the Cascades. This may exceed the combined orographic and convergence PMP for small low-lying basins.

Computation of orographic PMP west of Cascades

6.08. Computation of basin orographic PMP is relatively simple west of the Cascades where 6-hr. January orographic PMP varies with location but seasonal, durational and basin-size factors do not. The products of the seasonal factors (table 4-7) and the durational factors (table 4-8) are shown in tabular form for convenience at the top left of table 6-1, Part II, "Accumulated factors."

The step-by-step procedure for orographic PMP follows:

Step K. Record the basin-size factor from figure 4-39.

Step L. Record a grid-average basin orographic PMP index from figures 4-33a to c.

Step M. Enter the product of K and L on line M. This is 1st 6-hr. basin orographic PMP.

Step Q. Multiply each of the "accumulated factors" (for each month) by M to obtain the orographic PMP. Enter these values in table Q. (For 1- and 3-hr. PMP, multiply 1st 6-hr. PMP by 20% and 54%, respectively.)

Computation of orographic PMP east of Cascades

6.09. East of the Cascade Divide the seasonal variation is differentiated zonally; it depends on elevation in one zone. This adds two steps to the computation. Steps K, L and M are identical to those west of the Cascades:

Step K. Record the basin-size factor from figure 4-39.

Step L. Record a grid-average basin orographic PMP index from figures 4-33a to c.

Step M. Enter the product of K and L on line M. This is 1st 6-hr. basin orographic PMP.

Step N. Determine the zone in which the basin lies from figures 4-33a to c. From table 4-7, copy on line N the seasonal factors for the basin zone. (In zone C, use average basin elevation.)

Step P. On line P list the products of M and accumulated durational factors.

Step Q. Enter in table Q orographic PMP for all durations each month, the products of each value on line N times all values on line P. (For 1- and 3-hr. PMP, multiply 1st 6-hr. values by 20% and 54%, respectively.)

Total PMP comparison

6.10. Total PMP is the sum of orographic and convergence PMP. For instance, 24-hr. total PMP is the value J_4 of table 6-1, Part I plus the 24-hr. value in table Q, Part II. Part III is provided for these sums.

For west-of-Cascades basins, values obtained in this manner are to be compared with values from paragraph 6.07 (1.23 times the J values of convergence PMP from table 6-1, Part I) for areas, months and durations at which the latter may be the larger.

For basins east of Cascades, compare May to September local thunderstorm PMP (from chapter V) with highest October-June values of total PMP from paragraph 6.09.

Examples of PMP computations

6.11. Wynoochee Basin. A stepwise numerical example follows below, using the notation of paragraph 6.06. This is a computation of December PMP for 3, 6, 12, 18, 24, 36, and 72 hours for the 197-sq. mi. area of the Wynoochee Basin on the southern slopes of the Olympic Mountains of Washington. The complete October-June computations are on pages 195 and 196.

I-a. Convergence PMP to combine with orographic PMP

A.	1.12	Fig. 3-37b
B.	8.6 in.	Fig. 3-25a
C.	1.12 x 8.6 in. = 9.6 in.	A x B
D.	.43	Fig. 3-25b
E.	9.6 in. x .43 = 4.1	C x D
F_1	100%	Table 3-3
G_1	81%	Fig. 3-40a
H_1	100% x 81% = 0.81	$F_1 \times G_1$
J_1 (6-hr.)	4.1 in. x .81 = 3.3 in.	$E \times H_1$
F_2	60%	Table 3-3
G_2	92%	Fig. 3-40a
H_2	60% x 92% = .55	$F_2 \times G_2$
I_2	0.81 + 0.55 = 1.36	$H_1 + H_2$
J_2 (12-hr.)	4.1 in. x 1.36 = 5.6 in.	$E \times I_2$
F_3	41%	Table 3-3

G_3	96%	Fig. 3-40a
H_3	41% x 96% = 0.39	$F_3 \times G_3$
I_3	1.36 + 0.39 = 1.75	$I_2 + H_3$
J_3 (18-hr.)	4.1 in. x 1.75 = 7.2 in.	$E \times I_3$
F_4	31%	Table 3-3
G_4	100%	Fig. 3-40a
H_4	31% x 1.00% = 0.31	$F_4 \times G_4$
I_4	1.75 + 0.31 = 2.06	$I_3 + H_4$
J_4 (24-hr.)	4.1 in. x 2.06 = 8.4 in.	$E \times I_4$
F_6	44%	Table 3-3
I_6	2.06 + .44 = 2.50	$I_4 + F_6$
J_6 (36-hr.)	4.1 in. x 2.50 = 10.3 in.	$E \times I_6$
$F_7 - F_{12}$ (Sum of increments 7th thru 12th periods)	79%	Table 3-3
I_{12}	2.50 + .79 = 3.3	$I_6 + F_8 + F_{10} + F_{12}$
J_{12} (72-hr.)	4.1 in. x 3.3 = 13.5 in.	$E \times I_{12}$
J (3-hr.)	4.1 in. x 51% = 2.1 in.	E x % in fig. 3-41

I-b. Convergence PMP not combined with orographic PMP. Multiply above J values by 1.23 for comparison with III.

II. Orographic PMP

K	.90	Fig. 4-39
L	3.4 in.	Fig. 4-33b
M	.90 x 3.4 in. = 3.06 in.	K x L
Q_1 (6-hr.)	3.06 in. x 1.04 = 3.2 in.	M x Dec. Accumulated orographic factors for 6, 12, 18, 24, 36 and 72 hr. Table 6-1 Part II
Q_2 (12-hr.)	3.06 in. x 1.97 = 6.0 in.	
Q_3 (18-hr.)	3.06 in. x 2.80 = 8.6 in.	
Q_4 (24-hr.)	3.06 in. x 3.54 = 10.8 in.	
Q_6 (36-hr.)	3.06 in. x 4.77 = 14.6 in.	
Q_{12} (72-hr.)	3.06 in. x 7.09 = 21.7 in.	
Q (3-hr.)	3.2 in. x 54% = 1.7 in.	Par. 4.86

III. Combined convergence and orographic PMP (in.)

	Conv.		Orog.		Total	
3-hr.	2.1	+	1.7	=	3.8	J + Q
6-hr.	3.3	+	3.2	=	6.5	$J_1 + Q_1$
12-hr.	5.6	+	6.0	=	11.6	$J_2 + Q_2$
18-hr.	7.2	+	8.6	=	15.8	$J_3 + Q_3$
24-hr.	8.4	+	10.8	=	19.2	$J_4 + Q_4$
36-hr.	10.3	+	14.6	=	24.9	$J_6 + Q_6$
72-hr.	13.5	+	21.7	=	35.2	$J_{12} + Q_{12}$

6.12. Willow Creek above Heppner. A similar stepwise December computation is given for the east of Cascades Willow Creek, Oreg. Basin above Heppner. Basin size is 96 square miles. The October-June computations are listed on pages 197 and 198.

I. Convergence PMP to combine with orographic PMP

A.	.77	Fig. 3-37b
B.	8.7 in.	Fig. 3-25a
C.	.77 x 8.7 in. = 6.7 in.	A x B
D.	.57	Fig. 3-25b
E.	6.7 in. x .57 = 3.8 in.	C x D = 6-hr. 10-sq. mi. PMP
F_1	100%	Table 3-3
G_1	87%	Fig. 3-40a
H_1	100% x 87% = 0.87	F_1 x G_1
J_1 (6-hr.)	3.8 in. x 87% = 3.3 in.	E x H_1
F_2	38%	Table 3-3
G_2	94%	Fig. 3-40a
H_2	38% x 94% = 0.36	F_2 x G_2
I_2	0.87 + 0.36 = 1.23	$H_1 + H_2$
J_2	3.8 in. x 1.23 = 4.7 in.	E x I_2
F_3	22%	Table 3-3
G_3	98%	Fig. 3-40a
H_3	22% x 98% = 0.22	F_3 x G_3
I_3	1.23 + 0.22 = 1.45	$I_2 + H_3$
J_3 (18-hr.)	3.8 in. x 1.45 = 5.5 in.	E x I_3

F_4	16%	Table 3-3
G_4	100%	Fig. 3-40a
H_4	16% x 100% = .16	$F_4 \times G_4$
I_4	1.45 + .16 = 1.61	$I_3 + H_4$
J_4 (24-hr.)	3.8 in. x 1.61 = 6.1 in.	E x I_4
F_6	22%	Table 3-3
I_6	1.61 + .22 = 1.83	$I_4 + F_6$
J_6 (36-hr.)	3.8 in. x 1.83 = 7.0 in.	E x I_6
$F_7 - F_{12}$	38% (Sum of increments 7th thru 12th periods)	Table 3-3
I_{12}	1.83 + .38 = 2.21	$I_6 + F_8 + F_{10} + F_{12}$
J_{12} (72-hr.)	3.8 in. x 2.21 = 8.4 in.	E x I_{12}
J (3-hr.)	3.8 x 60% = 2.3 in.	E x % in fig. 3-41
J (1-hr.)	3.8 in. x 30% = 1.1 in.	

II. Orographic PMP

K	.94	Fig. 4-39
L	.90 in.	Fig. 4-33b
M	.94 x .90 = .85 in.	K x L
N	1.04	Fig. 4-33b Table 4-7 (Dec.)
P_1 (6-hr.)	.85 in. x 1.00 = 0.85 in.	
Q_1 (6-hr.)	1.04 x .85 in. = 0.9 in.	
P_2 (12-hr.)	.85 in. x 1.89 = 1.6 in.	
Q_2 (12-hr.)	1.04 x 1.6 in. = 1.7 in.	
P_3 (18-hr.)	.85 in. x 2.69 = 2.3 in.	P M x Dec. accumulated factors for 6, 12, 18, 24, 36 and 72 hr.
Q_3 (18-hr.)	1.04 x 2.3 in. = 2.4 in.	
P_4 (24-hr.)	.85 in. x 3.40 = 2.9 in.	
Q_4 (24-hr.)	1.04 x 2.9 in. = 3.0 in.	Q N (for Dec.) x P for 6, 12, 18, 24, 36 and 72 hr.
P_6 (36-hr.)	.85 in. x 4.59 = 3.9 in.	
Q_6 (36-hr.)	1.04 x 3.9 in. = 4.1 in.	
P_{12} (72-hr.)	.85 in. x 6.46 = 5.5 in.	
Q_{12} (72-hr.)	1.04 x 5.5 in. = 5.7 in.	
Q (3-hr.)	.9 in. x 54% = 0.5 in.	(par. 4.86)
Q (1-hr.)	.9 in. x 20% = 0.2 in.	

III. Combined convergence and orographic PMP (in.)

	Conv.		Orog.		Total	
1-hr.	1.1	+	0.2	=	1.3	$J + Q$
3-hr.	2.3	+	0.5	=	2.8	$J + Q$
6-hr.	3.3	+	0.9	=	4.2	$J_1 + Q_1$
12-hr.	4.7	+	1.7	=	6.4	$J_2 + Q_2$
18-hr.	5.5	+	2.4	=	7.9	$J_3 + Q_3$
24-hr.	6.1	+	3.0	=	9.1	$J_4 + Q_4$
36-hr.	7.0	+	4.1	=	11.1	$J_6 + Q_6$
72-hr.	8.4	+	5.7	=	14.1	$J_{12} + Q_{12}$

Table 6-1

Basin Wynoochee River, Washington Basin Size 197 Sq. Mi.

PART I. CONVERGENCE PMP (in.)

LEGEND

A Stimulation-elevation-barrier factor. Fig. 3-37a to c.
B 24-hr. 1000-mb. 10-sq. mi. PMP. Figs. 3-23a through 3-31a.
C Product of A and B.
D 6/24-hr. ratios. Figs. 3-23b through 3-31b.
E 6-hr. 10-sq. mi. PMP. (Product of C and D)
F Incremental percents. Table 3-3. 6-hr. periods through F_4, 12 hr. for F_6, F_8, F_{10} and F_{12}
G Basin size reduction. Figs. 3-40a and 3-40b. First four periods only.
H Product of F and G (each of first four periods). No entry later periods.
I Accumulated increments. $I_2 = H_1 + H_2$, $I_3 = I_2 + H_3$, $I_4 = I_3 + H_4$, $I_6 = I_4 + F_6$, $I_8 = I_6 + F_8$, etc.
J Accumulated basin average convergence PMP, E x H_1, I_2, I_3, etc.

A = 112

	Through 1st period								Through 2d period				
	B	C	D	E	F_1	G_1	H_1	J_1	F_2	G_2	H_2	I_2	J_2
OCT	8.3	9.3	.50	4.7	1.00	.79	.79	3.7	.48	.91	.44	1.23	5.8
NOV	8.6	9.6	.45	4.3	1.00	.81	.81	3.5	.56	.92	.52	1.33	5.7
DEC	8.6	9.6	.43	4.1	1.00	.81	.81	3.3	.60	.92	.55	1.36	5.6
JAN	8.5	9.5	.43	4.1	1.00	.80	.80	3.3	.60	.92	.55	1.35	5.5
FEB	8.4	9.4	.43	4.0	1.00	.80	.80	3.2	.60	.92	.55	1.35	5.4
MAR	8.2	9.2	.45	4.1	1.00	.80	.80	3.3	.56	.92	.52	1.32	5.4
APR	7.9	8.8	.48	4.2	1.00	.80	.80	3.4	.50	.92	.46	1.26	5.3
MAY	7.4	8.3	.52	4.3	1.00	.79	.79	3.4	.44	.92	.40	1.19	5.1
JUNE	6.5	7.3	.58	4.2	1.00	.76	.76	3.2	.36	.91	.33	1.09	4.6

	Through 3d period					Through 4th period					Through 6th period		
	F_3	G_3	H_3	I_3	J_3	F_4	G_4	H_4	I_4	J_4	F_6	I_6	J_6
OCT	.30	.95	.29	1.52	7.1	.22	.99	.22	1.74	8.2	.30	2.04	9.6
NOV	.38	.96	.36	1.69	7.3	.28	1.00	.28	1.97	8.5	.40	2.37	10.2
DEC	.41	.96	.39	1.75	7.2	.31	1.00	.31	2.06	8.4	.44	2.50	10.3
JAN	.41	.96	.39	1.74	7.1	.31	1.00	.31	2.05	8.4	.44	2.49	10.2
FEB	.41	.96	.39	1.74	7.0	.31	1.00	.31	2.05	8.2	.44	2.49	10.0
MAR	.38	.96	.36	1.68	6.9	.28	1.00	.28	1.96	8.0	.40	2.36	9.7
APR	.32	.96	.31	1.57	6.6	.24	1.00	.24	1.81	7.6	.34	2.15	9.0
MAY	.27	.96	.26	1.45	6.2	.20	.99	.20	1.65	7.1	.28	1.93	8.3
JUNE	.21	.94	.20	1.30	5.5	.15	.99	.15	1.45	6.1	.21	1.66	7.0

	Through 8th period			Through 10th period			Through 12th period		
	F_8	I_8	J_8	F_{10}	I_{10}	J_{10}	F_{12}	I_{12}	J_{12}
OCT	.23	2.27	10.7	.18	2.45	11.5	.16	2.61	12.3
NOV	.30	2.67	11.5	.23	2.90	12.5	.21	3.11	13.4
DEC	.32	2.82	11.6	.25	3.07	12.6	.22	3.29	13.5
JAN	.32	2.81	11.5	.25	3.06	12.5	.22	3.28	13.4
FEB	.32	2.81	11.2	.25	3.06	12.2	.22	3.28	13.1
MAR	.30	2.66	10.9	.23	2.89	11.8	.21	3.10	12.7
APR	.26	2.41	10.1	.20	2.61	11.0	.18	2.79	11.7
MAY	.21	2.14	9.2	.17	2.31	9.9	.14	2.45	10.5
JUNE	.15	1.81	7.6	.12	1.93	8.1	.10	2.03	8.5

PART II. OROGRAPHIC PMP (in.)

LEGEND

K Basin size factor. Fig. 4-39.
L 6-hr. orographic index. Grid average over basin. Figs 4-33a to c.
M Product of K and L

K =	.90
L =	3.4
M =	3.06

Table 6-1 (Cont'd.)

Basin Wynoochee River, Washington

West of Cascade Divide

Table Q obtained by multiplying M times the accumulated orographic seasonal-durational factors below:

Accumulated factors

Per.	1	2	3	4	6	8	10	12
Hr.	6	12	18	24	36	48	60	72
OCT	1.08	2.04	2.91	3.67	4.96	5.97	6.76	7.37
NOV	1.07	2.02	2.88	3.64	4.91	5.92	6.70	7.30
DEC	1.04	1.97	2.80	3.54	4.77	5.75	6.51	7.09
JAN	1.00	1.89	2.69	3.40	4.59	5.53	6.26	6.82
FEB	1.00	1.89	2.69	3.40	4.59	5.53	6.26	6.82
MAR	.95	1.80	2.56	3.23	4.36	5.25	5.95	6.48
APR	.87	1.64	2.34	2.96	3.99	4.81	5.45	5.93
MAY	.76	1.44	2.04	2.58	3.49	4.20	4.76	5.18
JUNE	.68	1.29	1.83	2.31	3.12	3.76	4.26	4.64

East of Cascade Divide

	O	N	D	J	F	M	A	M	J
N									

Accumulated durational factors

Per.	1	2	3	4	6	8	10	12
Hr.	6	12	18	24	36	48	60	72
	1.00	1.89	2.69	3.40	4.59	5.48	6.09	6.46

P* ____

P*= M x durational factors

Multiply values in line P by percents in line N to get basin orographic PMP. Enter in table Q.

Q. Accumulated Orographic PMP (in.)

	Duration (hr.) 6	12	18	24	36	48	60	72
OCT	3.3	6.2	8.9	11.2	15.2	18.3	20.7	22.6
NOV	3.3	6.2	8.8	11.1	15.0	18.1	20.5	22.3
DEC	3.2	6.0	8.6	10.8	14.6	17.6	19.9	21.7
JAN	3.1	5.8	8.2	10.4	14.0	16.9	19.2	20.9
FEB	3.1	5.8	8.2	10.4	14.0	16.9	19.2	20.9
MAR	2.9	5.5	7.8	9.9	13.3	16.1	18.2	19.8
APR	2.7	5.0	7.2	9.1	12.2	14.7	16.7	18.1
MAY	2.3	4.4	6.2	7.9	10.7	12.9	14.6	15.9
JUNE	2.1	3.9	5.6	7.1	9.5	11.5	13.0	14.2

PART III. TOTAL PMP (in.)

	Duration (hr.) 6	12	18	24	36	48	60	72
OCT	7.0	12.0	16.0	19.4	24.8	29.0	32.2	34.9
NOV	6.8	11.9	16.1	19.6	25.2	29.6	33.0	35.7
DEC	6.5	11.6	15.8	19.2	24.9	29.2	32.5	35.2
JAN	6.4	11.3	15.3	18.8	24.2	28.4	31.7	34.3
FEB	6.3	11.2	15.2	18.6	24.0	28.1	31.4	34.0
MAR	6.2	10.9	14.7	17.9	23.0	27.0	30.0	32.5
APR	6.1	10.3	13.8	16.7	21.2	24.8	27.7	29.8
MAY	5.7	9.5	12.4	15.0	19.0	22.1	24.5	26.4
JUNE	5.3	8.5	11.1	13.2	16.5	19.1	21.1	22.7

Table 6-1

Basin Willow Creek above Heppner, Oreg. Basin Size 96 Sq. Mi.

PART I. CONVERGENCE PMP (in.)

LEGEND

A Stimulation-elevation-barrier factor. Figs. 3-37a to c.
B 24-hr. 1000-mb. 10-sq. mi. PMP. Figs. 3-23a through 3-31a.
C Product of A and B.
D 6/24-hr. ratios. Figs. 3-23b through 3-31b.
E 6-hr. 10-sq. mi. PMP. (Product of C and D)
F Incremental percents. Table 3-3. 6-hr. periods through F_4, 12 hrs. for F_6, F_8, F_{10} and F_{12}.
G Basin size reduction. Figs. 3-40a or 3-40b. First four periods only.
H Product of F and G (each of first four periods). No entry later periods.
I Accumulated increments. $I_2 = H_1 + H_2$, $I_3 = I_2 + H_3$, $I_4 = I_3 + H_4$, $I_6 = I_4 + F_6$, $I_8 = I_6 + F_8$, etc.
J Accumulated basin average convergence PMP, E x H_1, I_2, I_3, etc.

A = .77

	Through 1st period								Through 2d period				
	B	C	D	E	F_1	G_1	H_1	J_1	F_2	G_2	H_2	I_2	J_2
OCT	9.0	6.9	.59	4.1	1.00	.86	.86	3.5	.34	.94	.32	1.18	4.8
NOV	8.9	6.9	.58	4.0	1.00	.87	.87	3.5	.36	.94	.34	1.21	4.8
DEC	8.7	6.7	.57	3.8	1.00	.87	.87	3.3	.38	.94	.36	1.23	4.7
JAN	8.5	6.5	.57	3.7	1.00	.86	.86	3.2	.38	.95	.36	1.22	4.5
FEB	8.2	6.3	.57	3.6	1.00	.86	.86	3.1	.38	.95	.36	1.22	4.4
MAR	8.1	6.2	.58	3.6	1.00	.86	.86	3.1	.36	.95	.34	1.20	4.3
APR	8.3	6.4	.59	3.8	1.00	.86	.86	3.3	.35	.95	.33	1.19	4.5
MAY	8.6	6.6	.61	4.0	1.00	.85	.85	3.4	.33	.94	.31	1.16	4.6
JUNE	8.8	6.8	.65	4.4	1.00	.83	.83	3.7	.29	.94	.27	1.10	4.8

	Through 3d period					Through 4th period					Through 6th period		
	F_3	G_3	H_3	I_3	J_3	F_4	G_4	H_4	I_4	J_4	F_6	I_6	J_6
OCT	.20	.96	.19	1.37	5.6	.14	.99	.14	1.51	6.2	.19	1.70	7.0
NOV	.21	.98	.20	1.41	5.6	.15	1.00	.15	1.56	6.2	.21	1.77	7.1
DEC	.22	.98	.22	1.45	5.5	.16	1.00	.16	1.61	6.1	.22	1.83	7.0
JAN	.22	.97	.21	1.43	5.3	.16	1.00	.16	1.59	5.9	.22	1.81	6.7
FEB	.22	.97	.21	1.43	5.1	.16	1.00	.16	1.59	5.7	.22	1.81	6.5
MAR	.21	.97	.20	1.40	5.0	.15	1.00	.15	1.55	5.9	.21	1.76	6.3
APR	.20	.97	.19	1.38	5.2	.15	1.00	.15	1.53	5.8	.20	1.73	6.6
MAY	.19	.97	.18	1.34	5.4	.13	1.00	.13	1.47	5.9	.18	1.65	6.6
JUNE	.15	.96	.14	1.24	5.5	.10	.99	.10	1.34	5.9	.14	1.48	6.5

	Through 8th period			Through 10th period			Through 12th period		
	F_8	I_8	J_8	F_{10}	I_{10}	J_{10}	F_{12}	I_{12}	J_{12}
OCT	.13	1.83	7.5	.10	1.93	7.9	.09	2.02	8.3
NOV	.15	1.92	7.7	.12	2.04	8.2	.10	2.14	8.6
DEC	.16	1.99	7.6	.12	2.11	8.0	.10	2.21	8.4
JAN	.16	1.97	7.3	.12	2.09	7.7	.10	2.19	8.1
FEB	.16	1.97	7.1	.12	2.09	7.5	.10	2.19	7.9
MAR	.15	1.91	6.9	.12	2.03	7.3	.10	2.13	7.7
APR	.14	1.87	7.1	.11	1.98	7.5	.09	2.07	7.9
MAY	.12	1.77	7.1	.10	1.87	7.5	.08	1.95	7.8
JUNE	.09	1.57	6.9	.08	1.65	7.3	.07	1.72	7.6

PART II. OROGRAPHIC PMP (in.)

LEGEND

K Basin size factor. Figs. 4-39.
L 6-hr. orographic index. Grid average over basin. Figs. 4-33a to c.
M Product of K and L.

K =	.94
L =	.90
M =	.85

Table 6-1 (Cont'd.)

Basin Willow Creek, Oreg.

West of Cascade Divide

Table Q obtained by multiplying M times the accumulated orographic seasonal-durational factors below:

Accumulated factors

Per.	1	2	3	4	6	8	10	12
Hr.	6	12	18	24	36	48	60	72
OCT	1.08	2.04	2.91	3.67	4.96	5.97	6.76	7.37
NOV	1.07	2.02	2.88	3.64	4.91	5.92	6.70	7.30
DEC	1.04	1.97	2.80	3.54	4.77	5.75	6.51	7.09
JAN	1.00	1.89	2.69	3.40	4.59	5.53	6.26	6.82
FEB	1.00	1.89	2.69	3.40	4.59	5.53	6.26	6.82
MAR	.95	1.80	2.56	3.23	4.36	5.25	5.95	6.48
APR	.87	1.64	2.34	2.96	3.99	4.81	5.45	5.93
MAY	.76	1.44	2.04	2.58	3.49	4.20	4.76	5.18
JUNE	.68	1.29	1.83	2.31	3.12	3.76	4.26	4.64

East of Cascade Divide

	O	N	D	J	F	M	A	M	J
N	1.08	1.07	1.04	1.00	1.00	.95	.90	.90	.85

Accumulated durational factors

Per.	1	2	3	4	6	8	10	12
Hr.	6	12	18	24	36	48	60	72
	1.00	1.89	2.69	3.40	4.59	5.48	6.09	6.46
P*	.85	1.61	2.29	2.89	3.90	4.66	5.18	5.49

P* M x durational factors

Multiply values in line P by percents in line N to get basin orographic PMP. Enter in table Q.

Q. Accumulated Orographic PMP (in.)

	Duration (hr.) 6	12	18	24	36	48	60	72
OCT	.9	1.7	2.5	3.1	4.2	5.0	5.6	5.9
NOV	.9	1.7	2.5	3.1	4.2	5.0	5.5	5.9
DEC	.9	1.7	2.4	3.0	4.1	4.8	5.4	5.7
JAN	.9	1.6	2.3	2.9	3.9	4.7	5.2	5.5
FEB	.9	1.6	2.3	2.9	3.9	4.7	5.2	5.5
MAR	.8	1.5	2.2	2.7	3.7	4.4	4.9	5.2
APR	.8	1.5	2.1	2.6	3.5	4.2	4.7	4.9
MAY	.8	1.5	2.1	2.6	3.5	4.2	4.7	4.9
JUNE	.7	1.4	2.0	2.5	3.3	4.0	4.4	4.7

PART III. TOTAL PMP (in.)

	Duration (hr.) 6	12	18	24	36	48	60	72
OCT	4.4	6.5	8.1	9.3	11.2	12.5	13.5	14.2
NOV	4.4	6.5	8.1	9.3	11.3	12.7	13.7	14.5
DEC	4.2	6.4	7.9	9.1	11.1	12.4	13.4	14.1
JAN	4.1	6.1	7.6	8.8	10.6	12.0	12.9	13.6
FEB	4.0	6.0	7.4	8.6	10.4	11.8	12.7	13.4
MAR	3.9	5.8	7.2	8.6	10.0	11.3	12.2	12.9
APR	4.1	6.0	7.3	8.4	10.1	11.3	12.2	12.8
MAY	4.2	6.1	7.5	8.5	10.1	11.3	12.2	12.7
JUNE	4.4	6.2	7.5	8.4	9.8	10.9	11.7	12.3

Table 6-1

Basin _____ Basin Size _____ Sq. Mi.

PART I. CONVERGENCE PMP (in.)

LEGEND

A Stimulation-elevation-barrier factor. Figs. 3-37a to c.
B 24-hr. 1000-mb. 10-sq. mi. PMP. Figs. 3-23a through 3-31a.
C Product of A and B.
D 6/24-hr. ratios. Figs. 3-23b through 3-31b.
E 6-hr. 10-sq. mi. PMP. (Product of C and D)
F Incremental percents. Table 3-3. 6-hr. periods through F_4, 12 hrs. for F_6, F_8, F_{10} and F_{12}
G Basin size reduction. Figs. 3-40a or 3-40b. First four periods only.
H Product of F and G (each of first four periods). No entry later periods.
I Accumulated increments. $I_2 = H_1 + H_2$, $I_3 = I_2 + H_3$, $I_4 = I_3 + H_4$, $I_6 = I_4 + F_6$, $I_8 = I_6 + F_8$, etc.
J Accumulated basin average convergence PMP, E x H_1, I_2, I_3, etc.

A =

	Through 1st period								Through 2d period				
	B	C	D	E	F_1	G_1	H_1	J_1	F_2	G_2	H_2	I_2	J_2
OCT					1.00								
NOV					1.00								
DEC					1.00								
JAN					1.00								
FEB					1.00								
MAR					1.00								
APR					1.00								
MAY					1.00								
JUNE					1.00								

	Through 3d period					Through 4th period					Through 6th period		
	F_3	G_3	H_3	I_3	J_3	F_4	G_4	H_4	I_4	J_4	F_6	I_6	J_6
OCT													
NOV													
DEC													
JAN													
FEB													
MAR													
APR													
MAY													
JUNE													

	Through 8th period			Through 10th period			Through 12th period		
	F_8	I_8	J_8	F_{10}	I_{10}	J_{10}	F_{12}	I_{12}	J_{12}
OCT									
NOV									
DEC									
JAN									
FEB									
MAR									
APR									
MAY									
JUNE									

PART II. OROGRAPHIC PMP (in.)

LEGEND

K Basin size factor. Figs. 4-39
L 6-hr. orographic index. Grid average over basin. Figs. 4-33a to c.
M Product of K and L.

K =
L =
M =

Table 6-1 (Cont'd.)

Basin _____

West of Cascade Divide

Table Q obtained by multiplying M times the accumulated orographic seasonal-durational factors below:

	Accumulated factors							
Per.	1	2	3	4	6	8	10	12
Hr.	6	12	18	24	36	48	60	72
OCT	1.08	2.04	2.91	3.67	4.96	5.97	6.76	7.37
NOV	1.07	2.02	2.88	3.64	4.91	5.92	6.70	7.30
DEC	1.04	1.97	2.80	3.54	4.77	5.75	6.51	7.09
JAN	1.00	1.89	2.69	3.40	4.59	5.53	6.26	6.82
FEB	1.00	1.89	2.69	3.40	4.59	5.53	6.26	6.82
MAR	.95	1.80	2.56	3.23	4.36	5.25	5.95	6.48
APR	.87	1.64	2.34	2.96	3.99	4.81	5.45	5.93
MAY	.76	1.44	2.04	2.58	3.49	4.20	4.76	5.18
JUNE	.68	1.29	1.83	2.31	3.12	3.76	4.26	4.64

East of Cascade Divide

	O	N	D	J	F	M	A	M	J
N	___	___	___	___	___	___	___	___	___

	Accumulated durational factors							
Per.	1	2	3	4	6	8	10	12
Hr.	6	12	18	24	36	48	60	72
	1.00	1.89	2.69	3.40	4.59	5.48	6.09	6.46

P* ___ ___ ___ ___ ___ ___ ___ ___

P*= M x durational factors

Multiply values in line P by percents in line N to get basin orographic PMP. Enter in table Q.

O. Accumulated Orographic PMP (in.)

	Duration (hr.)							
	6	12	18	24	36	48	60	72
OCT								
NOV								
DEC								
JAN								
FEB								
MAR								
APR								
MAY								
JUNE								

PART III. TOTAL PMP (in.)

	Duration (hr.)							
	6	12	18	24	36	48	60	72
OCT								
NOV								
DEC								
JAN								
FEB								
MAR								
APR								
MAY								
JUNE								

Table 6-1

Basin _____ Basin Size _____ Sq. Mi.

PART I. CONVERGENCE PMP (in.)

LEGEND

A Stimulation-elevation-barrier factor. Figs. 3-37a to c.
B 24-hr. 1000-mb. 10-sq. mi. PMP. Figs. 3-23a through 3-31a.
C Product of A and B.
D 6/24-hr. ratios. Figs. 3-23b through 3-31b.
E 6-hr. 10-sq. mi. PMP. (Product of C and D).
F Incremental percents. Table 3-3. 6-hr. periods through F_4, 12 hr. for F_6, F_8, F_{10} and F_{12}.
G Basin size reduction. Figs. 3-40a or 3-40b. First four periods only.
H Product of F and G (each of first four periods). No entry later periods.
I Accumulated increments. $I_2 = H_1 + H_2$, $I_3 = I_2 + H_3$, $I_4 = I_3 + H_4$, $I_6 = I_4 + F_6$, $I_8 = I_6 + F_8$, etc.
J Accumulated basin average convergence PMP, E x H_1, I_2, I_3, etc.

A =

	Through 1st period								Through 2d period				
	B	C	D	E	F_1	G_1	H_1	J_1	F_2	G_2	H_2	I_2	J_2
OCT					1.00								
NOV					1.00								
DEC					1.00								
JAN					1.00								
FEB					1.00								
MAR					1.00								
APR					1.00								
MAY					1.00								
JUNE					1.00								

	Through 3d period					Through 4th period					Through 6th period		
	F_3	G_3	H_3	I_3	J_3	F_4	G_4	H_4	I_4	J_4	F_6	I_6	J_6
OCT													
NOV													
DEC													
JAN													
FEB													
MAR													
APR													
MAY													
JUNE													

	Through 8th period			Through 10th period			Through 12th period			
	F_8	I_8	J_8	F_{10}	I_{10}	J_{10}	F_{12}	I_{12}	J_{12}	
OCT										
NOV										
DEC										
JAN										
FEB										
MAR										
APR										
MAY										
JUNE										

PART II. OROGRAPHIC PMP (in.)

LEGEND

K Basin size factor. Fig. 4-39.
L 6-hr. orographic index. Grid average over basin. Figs. 4-33a to c.
M Product of K and L

K =
L =
M =

Table 6-1 (Cont'd.)

Basin _____

West of Cascade Divide

Table Q obtained by multiplying M times the accumulated orographic seasonal-durational factors below:

Accumulated factors

Per.	1	2	3	4	6	8	10	12
Hr.	6	12	18	24	36	48	60	72
OCT	1.08	2.04	2.91	3.67	4.96	5.97	6.76	7.37
NOV	1.07	2.02	2.88	3.64	4.91	5.92	6.70	7.30
DEC	1.04	1.97	2.80	3.54	4.77	5.75	6.51	7.09
JAN	1.00	1.89	2.69	3.40	4.59	5.53	6.26	6.82
FEB	1.00	1.89	2.69	3.40	4.59	5.53	6.26	6.82
MAR	.95	1.80	2.56	3.23	4.36	5.25	5.95	6.48
APR	.87	1.64	2.34	2.96	3.99	4.81	5.45	5.93
MAY	.76	1.44	2.04	2.58	3.49	4.20	4.76	5.18
JUNE	.68	1.29	1.83	2.31	3.12	3.76	4.26	4.64

East of Cascade Divide

	O	N	D	J	F	M	A	M	J
N	___	___	___	___	___	___	___	___	___

Accumulated durational factors

Per.	1	2	3	4	6	8	10	12
Hr.	6	12	18	24	36	48	60	72
	1.00	1.89	2.69	3.40	4.59	5.48	6.09	6.46

P* ___ ___ ___ ___ ___ ___ ___ ___

P*= M x durational factors

Multiply values in line P by percents in line N to get basin orographic PMP. Enter in table Q.

Q. Accumulated Orographic PMP (in.)

	Duration (hr.) 6	12	18	24	36	48	60	72
OCT								
NOV								
DEC								
JAN								
FEB								
MAR								
APR								
MAY								
JUNE								

PART III. TOTAL PMP (in.)

	Duration (hr.) 6	12	18	24	36	48	60	72
OCT								
NOV								
DEC								
JAN								
FEB								
MAR								
APR								
MAY								
JUNE								

6-B. TIME DISTRIBUTION

6.13. Development of PMP in this report is by 6-hr. increments where the "1st" 6-hr. increment or period refers to the highest amount and the "12th" the lowest. A necessary step for determining a probable maximum flood hydrograph is to arrange these 6-hr. increments in a time sequence during the PMP storm. If the "2nd" increment is placed next to the "1st", PMP for 12 hours duration is obtained. Similarly each smaller increment, strictly speaking, needs to be placed adjacent to the next higher to obtain PMP for each duration through 3 days.

6.14. Guidance in setting up time sequences is obtained from sequences as observed in storms. These show much variation. For example, one of the first four highest rain increments in nine western Washington storms occurred in each of the 12 6-hr. periods. Yet there was a decided tendency for two to four of the higher rain increments to occur adjacent to each other.

6.15. Since storms show characteristic grouping of highest increments in several bursts it is reasonable to allow some deviation from the strict sequential requirement resulting from the method of developing PMP. The following guidelines allow such a compromise.

(a) Group the four heaviest 6-hr. increments of the 72-hr. PMP in a 24-hr. sequence, the middle four increments in a 24-hr sequence, and the smallest four increments in a 24-hr. sequence.

(b) Within each of these 24-hr. sequences arrange the four increments such that the second highest is next to the highest, the third highest adjacent to these, and the fourth highest at either end.

(c) Arrange the three 24-hr. sequences so that the second highest 24-hr. period is next to the highest with the third at either end.

6.16. Examples of rain sequences arranged according to these guidelines are shown in figure 6-1. Other distributions patterned after major storms in the basins may be used provided they do not give appreciably less critical flood hydrographs.

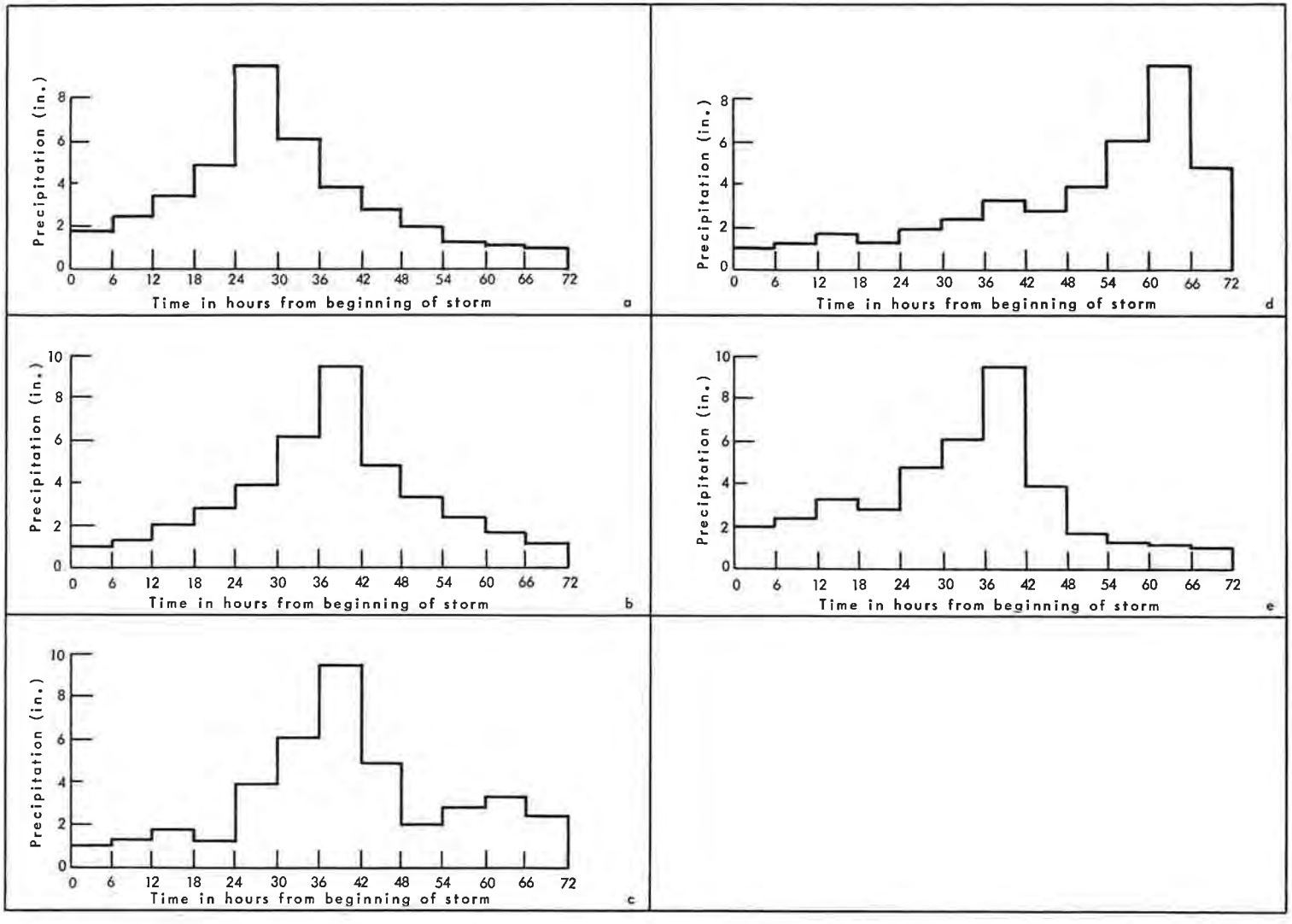

Figure 6-1. Sample PMP time sequences

Chapter VII

COMPARISON OF PMP WITH MAXIMUM OBSERVED PRECIPITATION

PMP compared with observed point precipitation

7.01. Comparisons between observed extreme point precipitation and 10-sq. mi. PMP values from this report are shown for west and east of the Cascade Divide in tables 7-1 and 7-2, respectively. PMP for the month in which the rain occurred is given, along with the highest PMP for the October through June season. The ratio of observed to highest PMP is in the last column. In table 7-2 (east of Cascade Divide comparisons) 10-sq. mi. 6-hr. thunderstorm PMP is in parenthesis if it exceeds general storm PMP. Figure 7-1 is a location map.

7.02. Most of the observed values are once-daily measurements taken from Technical Paper No. 16 (7), listing maximum daily values through 1949. These values were supplemented by an inspection of published once-daily values (23) for the period 1950 to the present. A few are maximum 24-hr. values from first-order Weather Bureau station autographic records or from clock-hour tabulations from autographic records (18) for a relatively short period. Mass curves were used to a limited extent to estimate some additional maximum 24-hr. amounts. The 48- and 72-hr. maximum observed values were obtained by adding amounts adjacent to the 24-hr. maximum amounts or were found in the Corps of Engineers storm studies (19). Some of the observed amounts are quite low, for example, 2.5 inches in 24 hours at Wilson Creek, Wash. (table 7-2). Such values are listed to provide comparisons for many parts of the study region.

7.03. Some of the closest approaches to PMP were found along the coast or on slopes near the coast. Elk Park and Quinault, Wash., and Gold Beach, Cave Junction, and Brookings, Oreg. have had 60 percent or more of PMP for some duration. Nearby mountains with slopes extending to the coast in a favorable orientation (as near Brookings) enhance opportunities for high rainfalls at these stations, all of which are in areas where stimulation is an important component of PMP. Ratios of rain to PMP were high also in the June 1964 Continental Divide storm, for example at Lake McDonald Lodge (table 7-2 and fig. 7-2).

7.04. Portland's record values of 7.7 inches in 24 hours and 10.7 inches in 48 hours observed in December 1882 are 76 and 85 percent of PMP, respectively. Portland has a 95-yr. record. In non-orographic areas, amounts approaching PMP have rarely been experienced because of the limited area of such regions. It should be expected that in large non-orographic regions, such as the Central or Southern States, opportunity for observed rains to approach PMP proportions is greater.

PMP compared with observed areal precipitation

7.05. Some of the highest areal depths of precipitation are compared with PMP both for the month in which the storm occurred and for the October

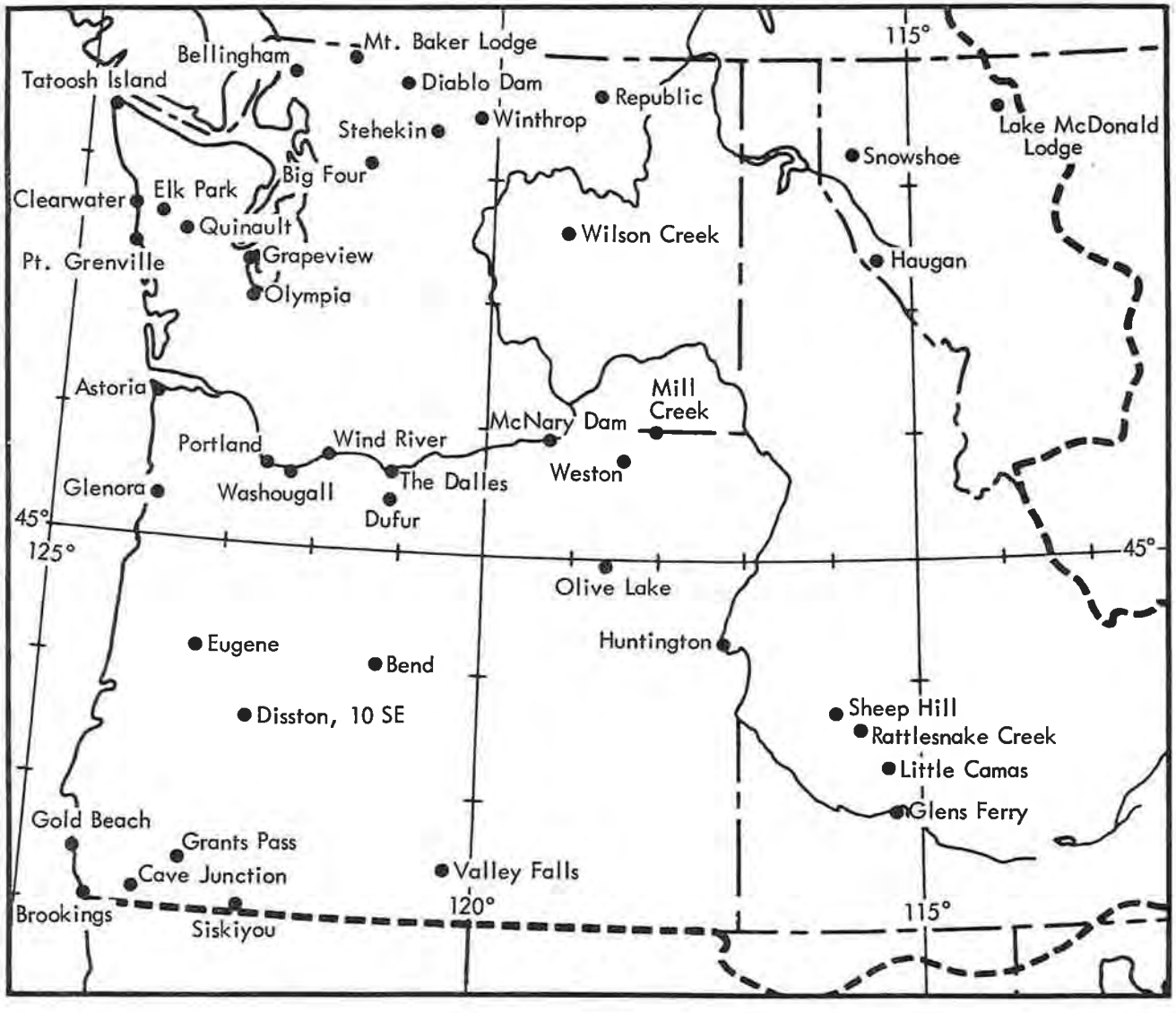

Figure 7-1. Locations of places listed in tables 7-1 and 7-2

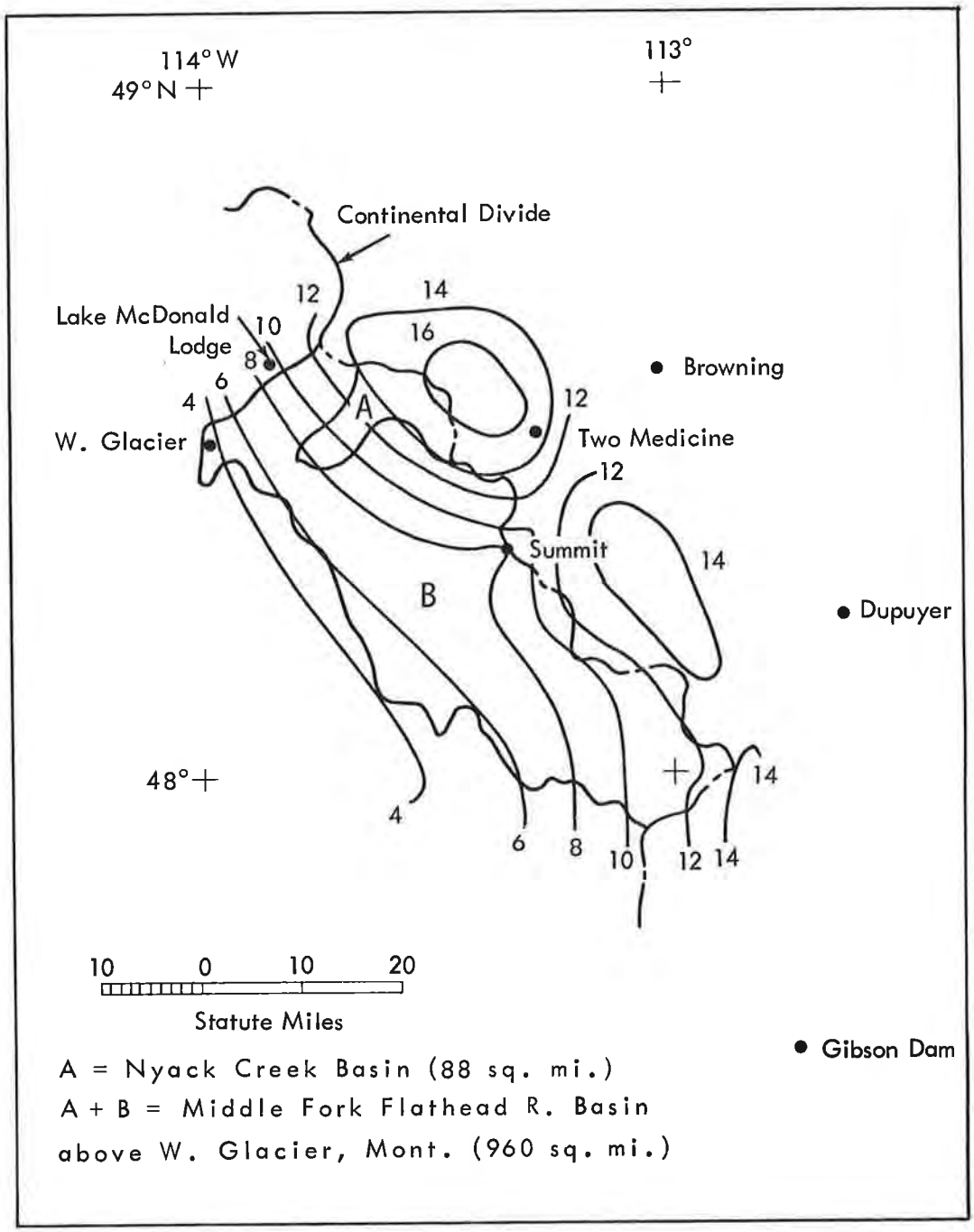

Figure 7-2. June 7-8, 1964 storm isohyets (in.) and locations of test areas in table 7-3

to June season in table 7-3. Ratios of observed to highest PMP are given. Storms and observed depths were taken from Preliminary Storm Part II's analyzed by the Corps of Engineers except for the June 1964 storm. Outstanding in the ratios of observed to PMP is the January 1935 storm on the Olympic Mountains with the 6-hr. average depth over 1000 square miles (6.0 in.) 80 percent of the PMP. This observed value, however, is based on liberally drawn isohyets through very little data. Comparable ratios occurred west of the Continental Divide in the Nyack Creek Basin and Middle Fork of the Flathead River Basin above West Glacier for 12-24 hours in the June 1964 storm (table 7-3). Storm isohyets are shown in figure 7-2. The third highest storm ratio of observed to PMP is 0.66 for a duration in the March-April, 1931 storm over the Clearwater drainage of Idaho.

7.06. Tables 7-1 to 7-3 indicate that storms west of the Cascade Divide have approached PMP magnitude more frequently than storms east of the Divide. One reason for this is that storms are more frequent nearer the coast, allowing more opportunity for extreme rains. Another is that observation stations are less plentiful east of the Cascades and therefore the chances of measuring highest amounts are less.

Comparison with Weather Bureau Technical Paper No. 38 (3)

7.07. There is a general similarity in estimates from this report and those from Technical Paper No. 38 in that high and low centers approximately coincide. The most obvious difference is the degree of detail. Technical Paper No. 38 considers all the United States west of the 105th meridian while the present report covers only about one-third of this area. The scope of Technical Paper No. 38 does not allow the degree of detail shown in the present report. Small centers and minor variations in the isolines were necessarily smoothed out in Technical Paper No. 38.

7.08. 10-sq. mi. PMP west of the Cascades. Over low-lying regions such as the Willamette Valley floor, 24-hr. 10-sq. mi. PMP values from this report are lower than those of Technical Paper No. 38. These differences are the result of different limits of transposition imposed on small-area convective storms in the two reports, the limitations of the present report being the more restrictive west of Cascades. In regions of strong orographic control the 24-hr. 10-sq. mi. PMP values of the present report are higher, primarily because of more reliance on terrain influence on precipitation.

7.09. 10-sq. mi. PMP east of the Cascades. The 24-hr. 10-sq. mi. PMP values from Technical Paper No. 38 are generally higher than those of this report. More liberal transposition of general storms in Technical Paper No. 38 is the most likely reason. However, where 6-hr. thunderstorm PMP values control 24-hr. PMP, the 24-hr. estimates presented in the two reports are close. Six-hour 10-sq. mi. PMP of this report tends to be higher than that of Technical Paper No. 38. Data for several intense local thunderstorms were not available for analysis at the time Technical Paper No. 38 was written (1959).

7.10. PMP for larger areas. As area increases, PMP from Technical Paper No. 38 decreases more slowly than PMP from the present report. This again results partially from the more generalized nature of that report in which one depth-area relation is applied to all storms.

Comparison with PMP estimates for selected watersheds

7.11. Figures 7-3 to 7-7 give PMP estimates for three watersheds west of the Cascade Divide and for two watersheds east of the Divide. Preliminary estimates of PMP previously made for these basins are shown, as well as estimates from Technical Paper No. 38 for the basins less than 400 square miles in area. The estimates labeled "October-June PMP" are a composite; for example, the 6-hr. PMP may not be from the same month as the 72-hr. PMP.

7.12. Differences between the various estimates for a basin are quite small for some basins and large for others. Differences sometimes depend on duration being compared. One of the largest is between 72-hr. PMP in this report, and a preliminary estimate dated July 1947. Revised techniques in estimating PMP account for some differences.

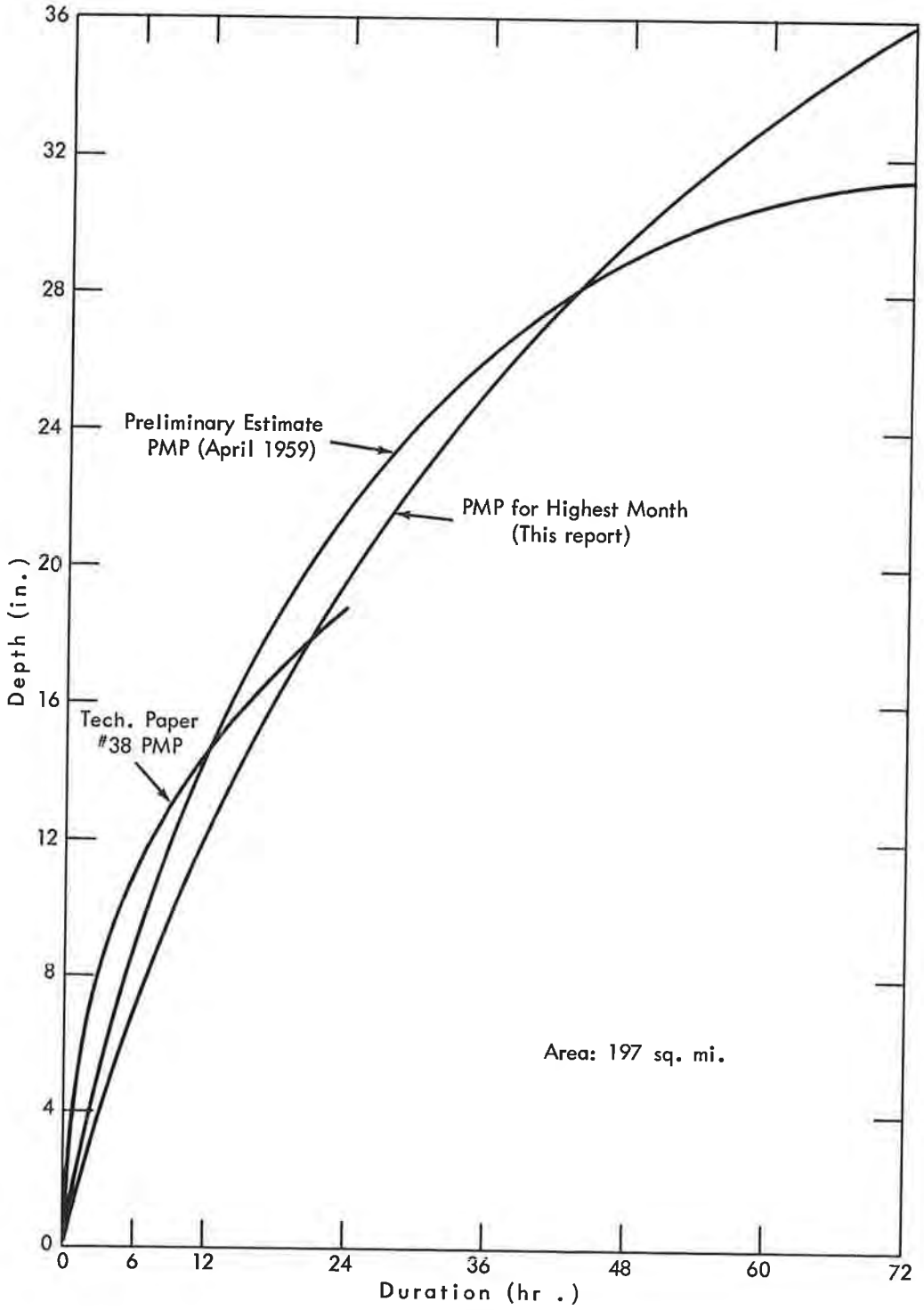

Figure 7-3. Comparison of PMP estimates for Wynoochee River Basin, Wash.

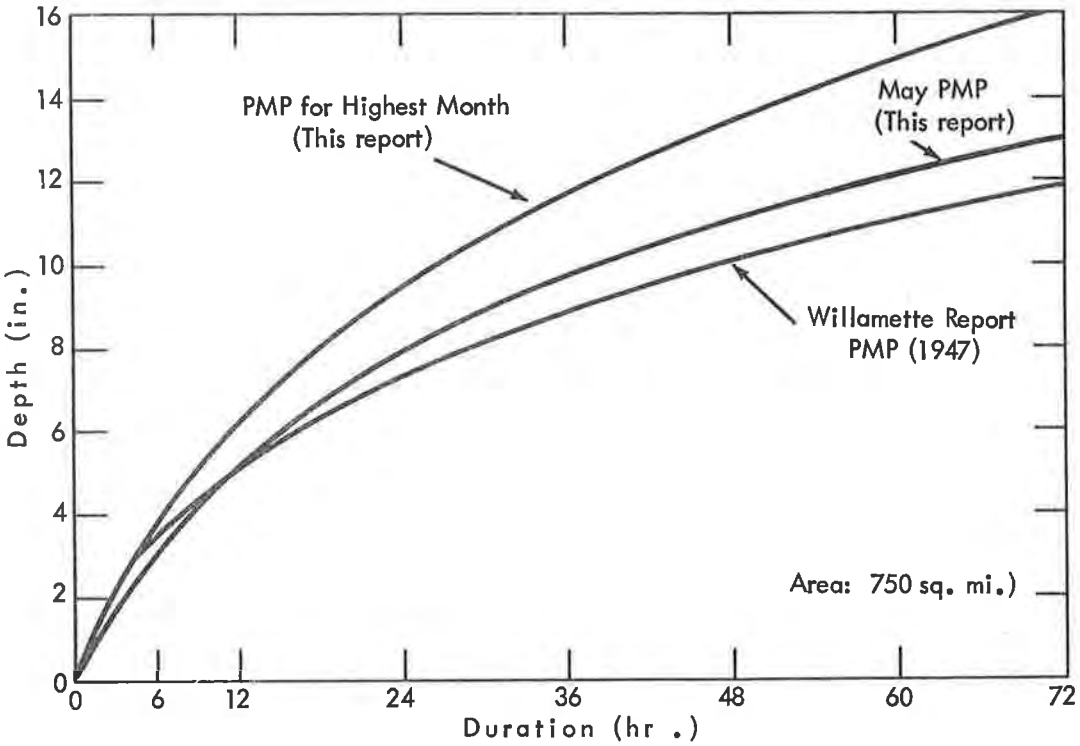

Figure 7-4. Comparison of PMP estimates for Yamhill River Basin, Oreg.

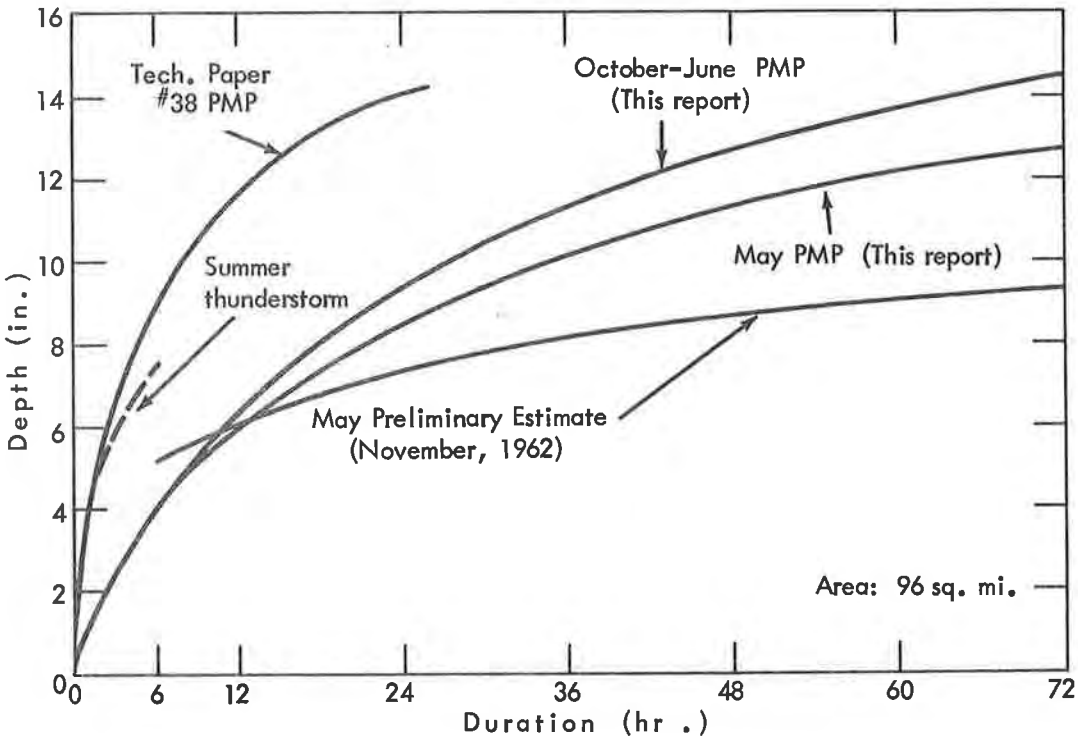

Figure 7-5. Comparison of PMP estimates for Willow Creek Basin, Oreg.

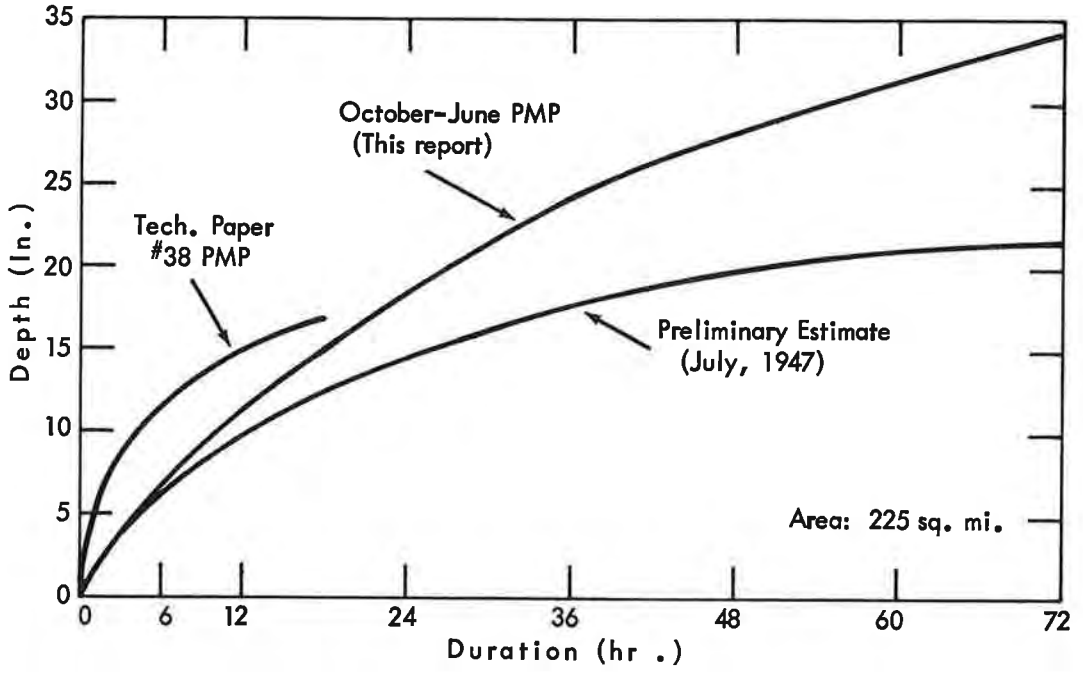

Figure 7-6. Comparison of PMP estimates for Green River Basin, Wash.

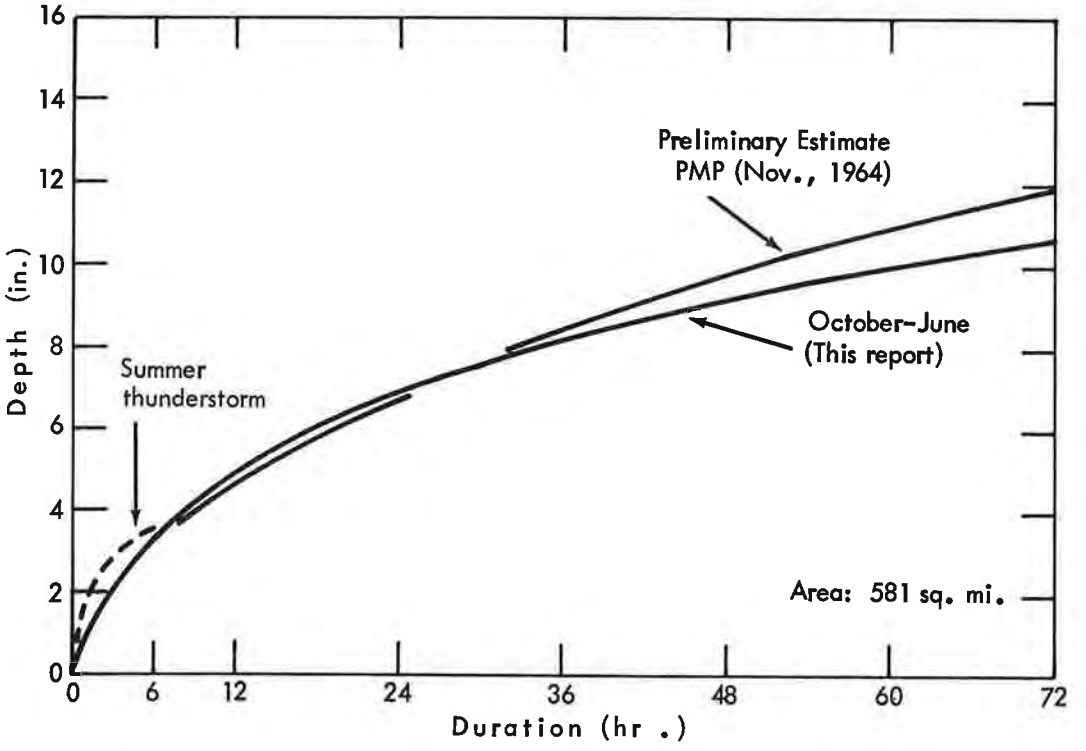

Figure 7-7. Comparison of PMP estimates for Blackfoot River Basin, Idaho

Table 7-1

COMPARISON OF MAXIMUM OBSERVED PRECIPITATION WEST OF CASCADE DIVIDE WITH PMP
(Point rainfall compared with 10-sq. mi. PMP)

Location	Date	Duration (hr.)	Observed Pcpn (in.)	PMP for Month of Storm (in.)	PMP for Highest Month (in.)	Ratio: Obs. Value / Highest PMP
Astoria, Oreg.	1/22/19	24	7.0	11.8	11.9	.59
	2/1-2/16	48	9.0	15.9	16.2	.56
Bellingham, Wash.	1/21/35	24	5.4	9.9	10.3	.52
Big Four, Wash.	2/26/32	24	10.7	19.6	21.1	.51
Brookings, Oreg.	6/9/33	24	9.1	10.1	14.0	.65
	3/16-18/32	72	15.2	20.9	22.8	.67
Cave Junction, Oreg.	12/22/64	24	8.1	13.2	13.6	.60
	12/21-22/64	48	12.0	18.9	19.2	.62
	12/21-23/64	72	15.0	22.5	22.9	.67
Clearwater, Wash.	2/9-10/51	48	11.2	19.3	19.8	.57
Diablo Dam PH, Wash.	10/24/45	24	6.5	17.3	17.3	.38
Disston 10SE, Oreg.	1/5-6/48	24	8.7	21.7	22.8	.38
	1/5-6/48	48	12.0	32.8	34.4	.35
Elk Park, Wash.	1/21/35	24	11.8	21.2	22.1	.53
	1/21-22/35	48	23.6	31.7	32.9	.72
	1/21-23/35	72	27.7	38.1	39.5	.70
Eugene, Oreg.	12/21-23/64	72	8.6	16.4	16.8	.51
Gold Beach, Oreg.	1/16-18/53	72	15.3	24.2	24.5	.62
Glenora, Oreg.	11/8/93	24	10.4	19.8	19.8	.53
	12/20-21/15	48	13.2	27.8	28.2	.47
Grants Pass, Oreg.	2/20-22/56	72	10.3	21.6	22.3	.46
Grapeview, Wash.	1/22/35	24	5.9	10.0	10.3	.57
Mt. Baker Lodge, Wash.	10/27/37	24	8.8	19.1	19.1	.46
Olympia, Wash.	2/9/51	24	4.9	10.9	11.4	.43
Pt. Grenville, Wash.	11/20/59	24	7.1 (a)	12.0	12.0	.59
	11/20-22/59	72	11.5 (a)	19.1	19.4	.59
Portland, Oreg.	12/12/82	24	7.7	10.0	10.1	.76
	12/11-12/82	48	10.7	12.5	12.5	.85
Quinault, Wash.	1/21/35	24	12.0	25.2	26.4	.45
	1/21-22/35	48	23.5	36.8	38.6	.61
	1/21-23/35	72	28.8	46.0	48.2	.60
Siskiyou, Oreg.	1/2/01	24	6.0	14.7	15.3	.39
Tatoosh, Wash.	10/17/30	24	5.9	12.2	12.6	.47
Washougall, Wash.	1/19/11	24	7.7	16.6	17.4	.44
Wind River, Wash.	11/20/21	24	8.0	18.9	18.9	.42

(a) Observed data questionable

Table 7-2

COMPARISON OF MAXIMUM OBSERVED PRECIPITATION EAST OF CASCADE DIVIDE WITH PMP
(Point rainfall compared with 10-sq. mi. PMP)

Location	Date	Duration (hr.)	Observed Pcpn (in.)	PMP for Month of Storm (in.)	*PMP for Highest Month (in.)	Ratio: Obs. Value / Highest PMP
Bend, Oreg.	10/27/50	24	3.3	11.0	11.0	.30
Dufur, Oreg.	11/21/21	24	4.0	11.8	11.8	.34
Glens Ferry, Idaho	5/16/25	24	3.5	7.1	(11.2)	.31
Haugan, Mont.	3/25/35	24	4.5	9.0	12.6	.36
Huntington, Oreg.	10/24/13	24	4.1	8.4	(11.0)	.37
Little Camas, Idaho	1/26/20	24	4.0	10.7	12.6	.32
McNary Dam, Wash.	10/1-2/57	24	3.2	9.2	(10.4)	.31
Mill Creek, Wash.	3/16/21	24	4.2	10.9	12.5	.34
Olive Lake, Oreg.	11/20/21	24	3.3	9.8	(10.2)	.32
Rattlesnake Cr., Idaho	11/23/09	6	3.7	6.3	(11.3)	.33
	11/23/09	12	6.4	10.0	(11.3)	.57
	11/23/09	18	7.2	13.0	14.1	.51
	11/22-23/09	36	8.6	19.7	20.6	.42
	11/21-23/09	48	10.7	22.7	23.6	.45
Republic, Wash.	4/7/37	24	3.5	10.5	11.8	.30
Sheep Hill, Idaho	11/21-22/09	24	4.5	15.5	16.4	.28
		48	6.1	22.5	23.3	.26
Snowshoe, Mont.	11/21-22/09	48	7.0	19.3	22.5	.31
Stehekin, Wash.	2/16/49	24	6.6	12.6	13.5	.49
The Dalles, Wash.	11/19-21/21	24	4.9	10.0	(10.2)	.48
		48	7.0	13.5	13.5	.52
		72	8.9	15.5	15.5	.57
Weston, Oreg.	5/30/06	24	4.6	9.5	(10.6)	.43
Wilson Cr., Wash.	6/22/37	24	2.5	8.2	(10.1)	.25
Winthrop, Wash.	1/21/35	24	4.2	14.0	15.3	.27
Valley Falls, Oreg.	11/24/10	24	3.5	7.3	(11.0)	.32
Lake McDonald Lodge, Mont.	6/7-8/64	30	9.6	14.3	14.3	.68

*Values for 6-hr. 10-sq. mi. thunderstorm PMP in parentheses if higher than general storm PMP.

Table 7-3

COMPARISON OF MAXIMUM OBSERVED AREAL PRECIPITATION WITH PMP
(1000-sq. mi. areas except as noted)

Location	Date	Duration (hr.)	Observed Pcpn (in.)	PMP for Month of Storm (in.)	PMP for Highest Month (in.)	Ratio: Obs. Value / Highest PMP
			West of Cascade Divide			
Cascades (Wind River), Wash.	10/21-26/34	6	1.7	5.4	5.4	.31
		12	2.4	9.5	9.5	.40
		24	4.2	15.7	15.8	.38
		72	8.6	28.9	29.4	.29
Cascades, Northern Wash.	1/20-25/35	6	2.8	4.7	5.3	.53
		12	4.8	8.5	9.2	.52
		24	7.2	14.2	15.4	.47
		72	16.0	27.0	28.7	.56
Cascades (Columbia Gorge), Wash.-Oreg.	11/18-22/21	6	2.2	5.7	5.7	.39
		12	3.9	10.0	10.0	.39
		24	7.0	17.0	17.0	.41
		72	11.7	30.6	31.1	.38
Olympic Mountains, Wash.	1/20-25/35	6	6.0	7.2	7.4	.81
		12	10.4	13.3	13.7	.76
		24	14.0	23.0	23.6	.59
		72	30.1	43.2	44.5	.68
Olympic Mountains, Wash. (5000 sq. mi.)	1/20-25/35	6	3.5	4.1	4.4	.80
		12	6.4	7.8	8.3	.77
		24	8.8	14.2	14.8	.59
		72	19.9	27.1	28.1	.71

Table 7-3, Cont'd.

COMPARISON OF MAXIMUM OBSERVED AREAL PRECIPITATION WITH PMP
(1000-sq. mi. areas except as noted)

Location	Date	Duration (hr.)	Observed Pcpn (in.)	PMP for Month of Storm (in.)	PMP for Highest Month (in.)	Ratio: Obs. Value / Highest PMP
			East of Cascade Divide			
Clearwater, Idaho	3/31-4/2/31	6	1.8	2.9	4.1	.44
		12	2.9	4.6	6.1	.48
		24	5.5	7.2	8.6	.64
		36	6.8	8.8	10.3	.66
		48	7.0	10.0	11.5	.61
		72	7.4	11.5	13.1	.56
Rattlesnake Cr., Idaho	11/22-23/09	6	1.6	3.7	4.1	.39
		12	2.9	6.1	6.4	.45
		24	3.4	9.7	9.9	.34
		36	4.5	12.0	12.2	.37
		48	6.2	14.2	14.3	.43
Snowshoe, Mont.	11/17-20/09	6	1.6	3.5	4.7	.34
		12	2.3	5.6	7.1	.32
		24	3.1	9.0	10.6	.29
		36	4.8	11.2	12.9	.37
		48	5.6	12.8	14.7	.38
Nyack Cr. Basin, Mont. (88 sq. mi.)	6/7-8/64	6	4.7	7.2	7.2	.66
		12	8.4	10.7	10.7	.78
		24	11.9	15.7	15.7	.76
		30	12.6	17.7	17.7	.71
Middle Fork Flathead River above West Glacier, Mont. (960 sq. mi.)	6/7-8/64	6	3.2	5.0	5.0	.64
		12	6.0	7.8	7.8	.76
		24	8.1	11.7	11.7	.69
		30	8.6	13.2	13.2	.65

Chapter VIII

TEMPERATURE AND WIND FOR SNOWMELT COMPUTATIONS

Introduction

8.01. Evaluation of runoff involves the contribution of snowmelt. Snowmelt computations require generalized temperature and wind sequences during the 3-day PMP storm and for 3 days prior. Their derivation is given in this chapter. A procedure for obtaining these values is outlined, and an example is presented for a specific basin.

Temperatures and dew points during PMP storm

8.02. Temperatures during the PMP storm are equal to maximum dew points, using the simplifying assumption of a saturated adiabatic atmosphere. Maximum storm dew points were determined for the development of convergence and orographic PMP (pars. 3.03-3.10).

Temperatures and dew points prior to PMP storm

8.03. For combined rain and snowmelt flood determinations a sequence of high temperatures for several days prior to rain is generally the most critical situation. With this in mind, highest temperatures observed prior to major storms in the Northwest were determined. An envelope of the difference between these prior temperatures and the temperatures during the storms was then assumed applicable to PMP temperatures at the beginning of the PMP storm.

Sources of storms surveyed included preliminary Corps of Engineers storm data, the controlling storms listed in Cooperative Studies Snake River Report No. 11 (11) and Weather Bureau Technical Paper No. 38 (3), as well as storms giving record 24-hr. rainfall amounts. Daily mean temperatures and precipitation amounts were obtained for a mountain station near the 24-hr. heavy rain center and for a nearby upwind first-order valley station. For a particular season and region the critical temperature differences were approximately the same at the two stations.

Temperature differences for establishing the critical upper envelope plotted by dates of occurrence showed significant seasonal trends. These trends and the range of temperature differences depended on whether the storm was east or west of the Cascade Divide. Durational curves of the temperature differences through 3 days were therefore drawn for each region. These appear in figure 8-1. Cool-season antecedent temperatures are at least as low as during the storm. In late spring and early autumn, antecedent temperatures are higher than during the storm.

8.04. Dew points prior to the PMP storm are determined from the dew point difference curves of figure 8-1, which are applicable for all months.

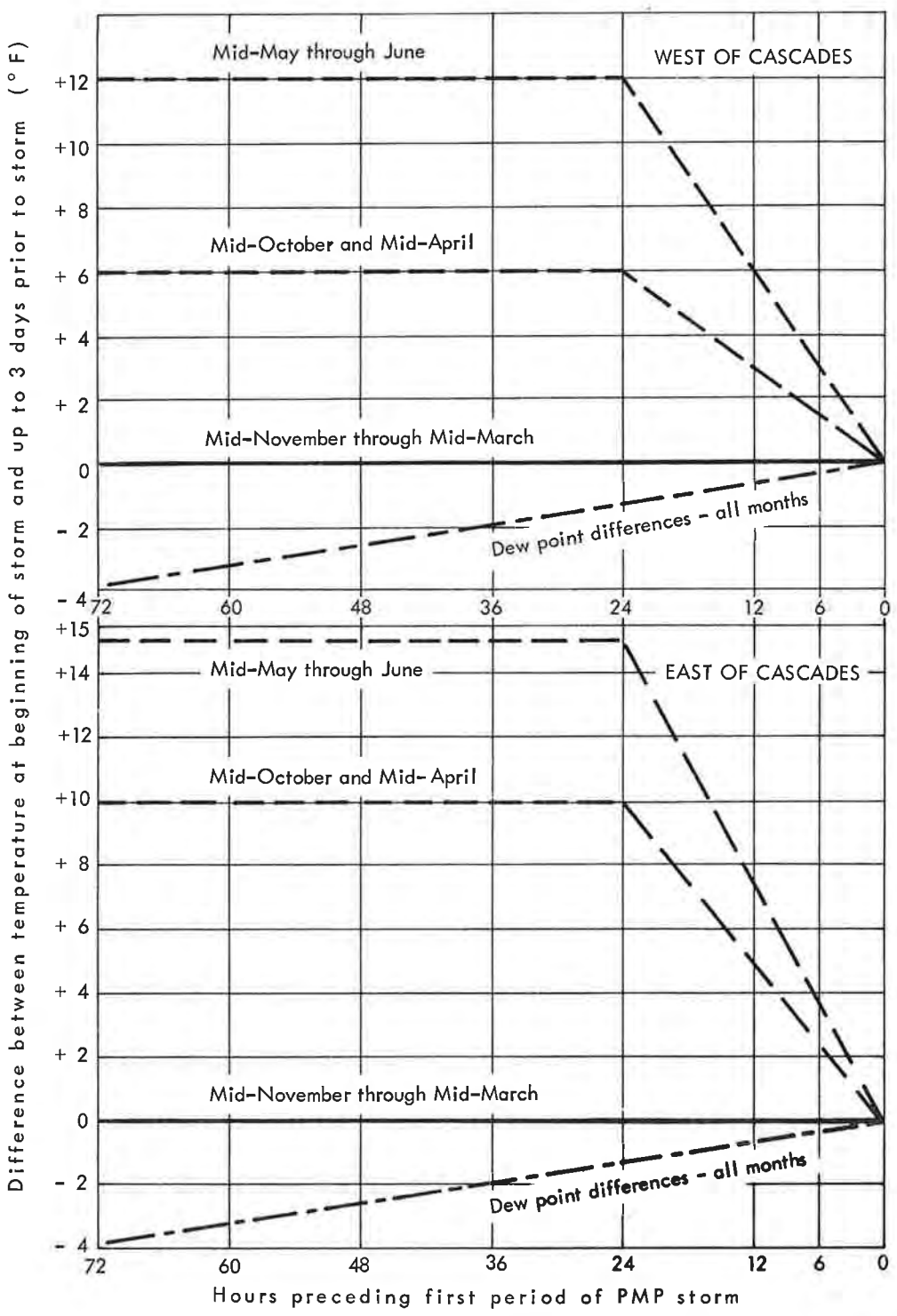

Figure 8-1. Highest temperatures prior to PMP storm

These were derived from Weather Bureau Technical Paper No. 5 (4) which gives highest persisting dew points for up to 5 days duration.

Snowmelt winds during PMP storm

8.05. Maximum winds through height in the atmosphere and their seasonal and durational variations used to derive orographic PMP are the basis for snowmelt winds during the PMP storm.

8.06. West of Cascade Divide. Figure 4-18 shows the maximum (i.e., January) free-air 6-hr. winds west of the Cascade Divide. The seasonal variation of these maximum winds is given in figure 4-24. For obtaining anemometer-level winds from these free-air winds, the result of a comparison study at Blue Canyon, Calif. is recommended (HMR 36, par. 10.09). At that location the average ratio of anemometer-level to free-air winds was .75. A smaller ratio for sheltered areas and a higher ratio for very exposed locations at high elevations would be appropriate. Durational variation of these winds is given in figure 4-35.

8.07. East of Cascade Divide. Maximum (January) 6-hr. winds for east of the Cascade Divide are given in figure 4-19. The dashed curve at the lower left of this figure shows the variation of anemometer-level winds with station elevation. Windspeeds read from this curve for basin elevations may be used with no adjustment. Somewhat higher or lower winds would be reasonable for a basin more or less exposed than the stations supplying the data for the curve of figure 4-19. Durational variation of wind is given in figure 4-35 and seasonal variation in figure 4-24.

Snowmelt winds prior to PMP storm

8.08. Prior to the PMP storm it is suggested that the PMP winds for the 12th 6-hr. period prevail for three days.

Procedure for determining temperatures, dew points and winds prior to and during the PMP storm

8.09. The steps in working out temperature, dew point and wind sequences prior to and during a PMP storm follow.

A. Temperatures and dew points during PMP storm

(1) Read the 12-hr. 1000-mb. dew point (temperature) from figures 3-11 to 3-13 for desired month at the basin location.

(2) Obtain the precipitable water (W_p) corresponding to this temperature from figure 8-2. Enter this figure with 12-hr. temperature on the abscissa and read the corresponding W_p on the ordinate.

(3) Read the percentage ratios of W_p for each of the twelve 6-hr. periods to W_p for the maximum 12-hr. dew point from figure 3-14.

(4) Multiply the 12-hr. W_p by the percentages from step A (3). This gives W_p for each 6-hr. increment during the PMP storm.

(5) Using the W_p values from step A (4) enter figure 8-2 to obtain the corresponding 1000-mb. temperatures for each duration for the required month.

(6) Adjust these temperatures to the elevation of the area of interest. This is accomplished by use of figure 8-3. Starting with the 1000-mb. temperature on the abscissa, proceed parallel to the sloping lines to the basin elevation and read the adjusted temperature on the abscissa.

(7) Rearrange temperatures in A (6) to conform to the adopted PMP storm sequence (par. 6.15).

B. Temperatures prior to PMP storm

1. From A (7) find the temperature for the first 6-hr. period of the storm in sequence.

2. Read difference between the temperature at the storm beginning and the temperature at each 6-hr. duration prior to storm from figure 8-1.

3. Add the differences determined in B (2) to the first 6-hr. temperature to determine the temperatures for each antecedent 6-hr. period.

C. Dew points prior to PMP storm

1. From the dew point curve of figure 8-1 determine the differences between the first period dew point and the dew point for each duration prior to storm.

2. Subtract differences from the temperature (dew point) determined in B (1).

D. Winds during PMP storm

1. To use the figures pertaining to wind relationships, transform the basin average elevation to pressure by the pressure-height relation shown in figure 8-4.

2. a. West of Cascade Divide Basin. Determine January maximum free-air wind at basin pressure from figure 4-18.

b. East of Cascade Divide Basin. Determine January maximum surface wind at basin pressure from dashed curve on figure 4-19.

3. Figure 4-24 shows the adopted seasonal variation of maximum wind expressed in percent of the mid-January value. These percent ratios apply either east or west of the Cascades.

4. Multiply windspeed of D (2) by ratio for desired month from D (3).

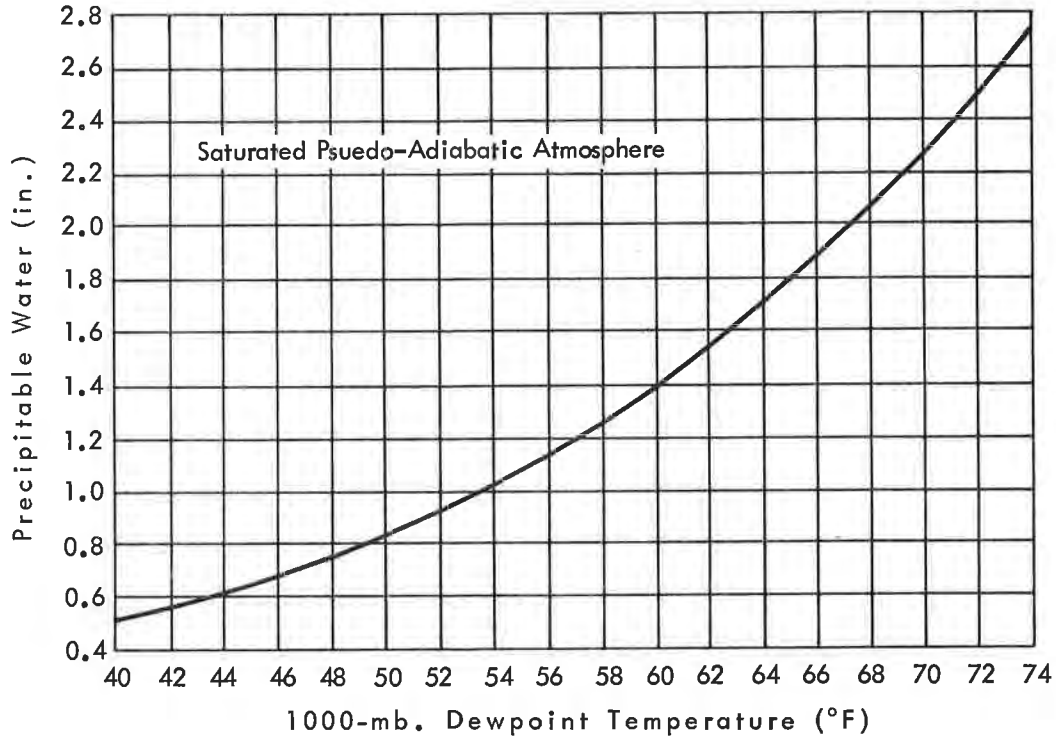

Figure 8-2. Variation of precipitable water with 1000-mb. dew point temperature

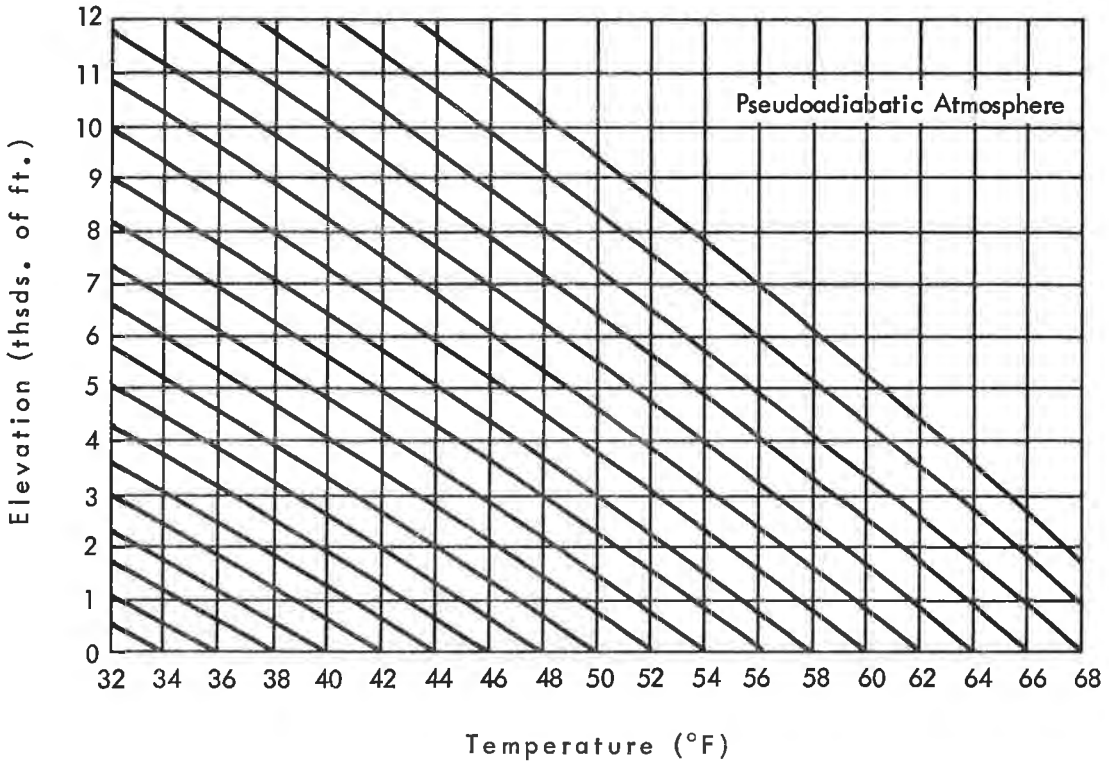

Figure 8-3. Decrease of temperature with elevation

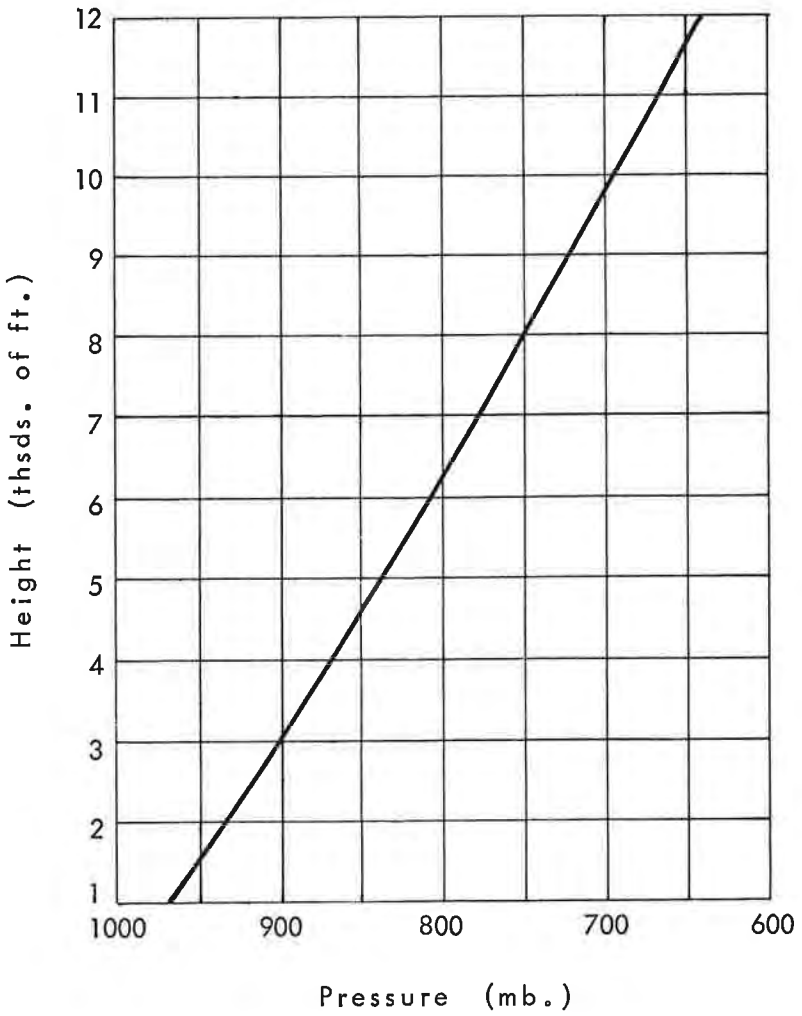

Figure 8-4. Pressure-height relation

5. Obtain durational wind factors given in figure 4-35.*

6. Multiply maximum 6-hr. windspeed of D (4) by the D (5) ratios to obtain all 6-hr. speeds for the 3-day storm. For west of Cascade Divide Basins multiply these by 0.75 for anemometer-level winds.

7. Arrange 6-hr. winds to conform to the selected PMP storm sequence.

E. Winds prior to PMP storm

The least of the twelve windspeeds calculated in D (6) may be maintained for the 72-hr. period prior to the PMP storm.

Example of snowmelt winds and temperatures for a basin

8.10. As an example snowmelt data for mid-May for the Blackfoot River drainage above Blackfoot Reservoir, Idaho, will be determined.

Basin average elevation: 7000 feet.

Lettered and numbered steps in this example are identical to those in the outlined procedure.

A. Temperatures and dew points during PMP storm

(1) Average 12-hr. mid-May maximum dew point over basin (fig. 3-12): 63.0°F.

(2) Precipitable water (W_p) for 63.0°F (fig. 8-2): 1.59 inches.

	6-hr. period											
	1st	2d	3d	4th	5th	6th	7th	8th	9th	10th	11th	12th
(3) Ratios of W_p each 6-hr. period to maximum 12-hr. W_p (fig. 3-14)	1.04	1.00	0.97	0.95	0.92	0.90	0.89	0.87	0.85	0.84	0.82	0.81
(4) = (2) x (3) W_p (ins.)	1.65	1.59	1.54	1.51	1.46	1.43	1.42	1.38	1.35	1.34	1.30	1.29
(5) Mid-May 1000-mb. temperatures (°F) each period (fig. 8-2):	63.6	63.0	62.4	61.9	61.4	61.0	60.6	60.2	59.8	59.4	59.0	58.7

*Durational variation of figure 4-35 is in percent of 1-hr. winds. To obtain durational factors in terms of 1st 6-hr. winds, multiply the percents for each period from figure 4-35 by the ratio of 1.00 to the percent of figure 4-35 for the 1st 6-hr. period.

	6-hr. period											
	1st	2d	3d	4th	5th	6th	7th	8th	9th	10th	11th	12th
(6) Mid-May temperatures (°F) reduced to 7000 ft. (fig. 8-3):	45.4	44.7	44.0	43.2	42.5	41.9	41.3	40.8	40.3	39.8	39.4	39.0
(7) Rearrangement of temperatures to conform to sequence of PMP increments (sequence (a) of fig. 6-1 used in this example): °F	40.3	41.3	42.5	44.0	45.4	44.7	43.2	41.9	40.8	39.8	39.4	39.0

B. Temperatures prior to PMP storm

(1) Temperature for first 6-hr. period of PMP storm: 40°F

	Hrs. prior to storm											
	6	12	18	24	30	36	42	48	54	60	66	72
(2) Mid-May differences between temperatures at indicated times prior to first 6-hr. period of storm (fig. 8-1):	4	7	11	15	15	15	15	15	15	15	15	15
(3) Sum of (1) and (2) °F	44	47	51	55	55	55	55	55	55	55	55	55

C. Dew points prior to PMP storm

	Hrs. prior to storm											
	6	12	18	24	30	36	42	48	54	60	66	72
(1) Difference between dew point at beginning of storm and at indicated times prior to storm (fig. 8-1) °F	0	1	1	1	2	2	2	3	3	3	4	4
(2) = B(1) - C(1) °F	40	39	39	39	38	38	38	37	37	37	36	36

D. Winds during PMP storm

(1) Basin average elevation: 7000 feet. Basin average pressure (fig. 8-4): 775 mb.

(2-b) 6-hr. January anemometer-level winds at 775 mb. (fig. 4-19): 45 kts.

(3) May 6-hr. percentage of January wind (fig. 4-24): 69%

(4) Wind of D(2-b) x percent of D(3) = 31 kts.

	6-hr. period											
	1st	2d	3d	4th	5th	6th	7th	8th	9th	10th	11th	12th
(5) Duration factor for each 6-hr. period (fig. 4-35 and p. 102)	1.00	.93	.87	.83	.77	.73	.69	.66	.64	.61	.59	.57
(6) Anemometer winds in descending order D(4) x D(5) kts.	31	29	27	26	24	23	21	20	20	19	18	18
(7) Windspeeds re-arranged after PMP sequence (a) of fig. 6-1. Kts.	20	21	24	27	31	29	26	23	20	19	18	18

E. Winds prior to PMP storm

Lowest windspeed during mid-May PMP storm period over Blackfoot Basin is 18 kts. from D (6). This value continues for 72 hours prior to beginning of storm.

ACKNOWLEDGMENTS

This report was prepared by the staff of the Hydrometeorological Branch, Office of Hydrology, ESSA, under the direct supervision of V. A. Myers, Chief of the Branch. Principal project leaders were J. T. Riedel, F. K. Schwarz and R. L. Weaver. Meteorologists C. W. Cochrane, G. A. Lott, W. W. Swayne and R. R. Watkins assisted in varying degrees. S. Molansky was responsible for editing and coordination of drafting. The staff of the Meteorological Technician Pool provided detailed research support.

Corps of Engineers personnel from the States of Washington and Oregon and in the Washington, D. C. Office of the Chief offered many suggestions, particularly Mr. D. E. Nunn. Review by various responsible individuals in the Water Management Information Division of the Office of Hydrology is also gratefully acknowledged.

REFERENCES

1. U. S. Weather Bureau, "Interim Report - Probable Maximum Precipitation in California," Hydrometeorological Report No. 36, Washington, 1961.

2. U. S. Weather Bureau, "Seasonal Variation of Probable Maximum Precipitation East of the 105th Meridian," Hydrometeorological Report No. 33, Washington, 1956.

3. U. S. Weather Bureau, "Generalized Estimates of Probable Maximum Precipitation West of the 105th Meridian," Technical Paper No. 38, Washington, 1960.

4. U. S. Weather Bureau, "Highest Persisting Dewpoints in Western United States," Weather Bureau Technical Paper No. 5, Washington, 1948.

5. Canada Department of Agriculture, "Persisting Dewpoints in the Prairie Provinces," Meteorological Report No. 11, 1963.

6. U. S. Weather Bureau, "Meteorology of Hydrologically Critical Storms in California," Hydrometeorological Report No. 37, Washington, 1962.

7. U. S. Weather Bureau, "Maximum 24-Hour Precipitation in the United States," Technical Paper No. 16, Washington, 1952.

8. Showalter, A. K., "An Approach to Quantitative Forecasting of Precipitation Part II, Formulas for Quantitative Rainfall Forecasting," Washington, 1944, p. 14.

9. Myers, V. A., "Airflow on the Windward Side of a Large Ridge," Journal of Geophysical Research, Vol. 67, No. 11, October 1962.

10. Corps of Engineers, U. S. Army, "Ten-Year Storm Precipitation in the Pacific Northwest," Technical Bulletin No. 10, Sacramento, 1964.

11. U. S. Weather Bureau, "Critical Meteorological Conditions for Design Floods in the Snake River Basin," Cooperative Studies Report No. 11, Washington, 1953.

12. U. S. Weather Bureau, "Dynamics of Severe Convective Storms," National Severe Storm Project No. 9, Washington, 1962.

13. Battan, L. J., "Some Properties of Convective Clouds," Nubila., Anno. 4-n, 1, 1961, pp. 1-12.

14. U. S. Weather Bureau, "The Thunderstorm," Report of the Thunderstorm Project, Washington, 1949.

15. Bureau of Reclamation, "Design Storms for Central Utah Project Area," Denver, 1958.

16. Weickman, H., Thunderstorm Electricity, University of Chicago Press, 1953, pp. 108-109.

17. Bjerknes, J., "Memorandum on Local Summer Storms," U. S. Engineer Office, South Pacific Division, San Francisco, Calif., 1940, 12 pp.

18. U. S. Weather Bureau, "Maximum Station Precipitation for 1, 2, 3, 6, 12 and 24 Hours," Technical Paper No. 15, Parts I, II, XII.

19. Corps of Engineers, U. S. Army, "Storm Rainfall in the United States," Washington, 1945.

20. Meteorological Branch, Department of Transport, Canada, "Storm Data Sheets," Toronto, Ontario.

21. U. S. Weather Bureau, Hydrometeorological Section Report No. 5, Part II, Thunderstorm Rainfall, August 1945.

22. Department of the Army, Office of the Chief of Engineers, Civil Engineer Bulletin No. 52-8, "Standard Project Flood Determinations," Washington, D. C., March 26, 1952.

23. U. S. Weather Bureau, "Climatological Data for the United States by Sections," Washington, D. C.

U.S. DEPARTMENT OF COMMERCE
National Oceanic and Atmospheric Administration
National Weather Service

Revisions of April 1981 to

Hydrometeorological Report No. 43

PROBABLE MAXIMUM PRECIPITATION, NORTHWEST STATES

For distribution to all users of
Hydrometeorological Report No. 43

Prepared by

Hydrometeorological Branch
Office of Hydrology

April 1981

Probable Maximum Precipitation, Northwest States
Revision of April 1981

Introduction

Probable maximum precipitation (PMP) for the northwestern United States was prepared by the Hydrometeorological Branch, National Weather Service in 1965-66. The results of this study were published in November 1966 as Hydrometeorological Report No. 43, "Probable Maximum Precipitation, Northwest States," (USWB 1966), (HMR 43). That report provides generalized procedures for preparing estimates of a general storm PMP for the entire region and a local or thunderstorm PMP for that portion of the region east of the crest of the Cascade Range. Primary emphasis for the general storm PMP was on durations from 6 to 72 hours, though procedures were provided for determining 1- and 3-hour values within the general storm for small basins.

Subsequent experience with the procedure proposed in HMR 43, indicates that the PMP estimates for the 1- and 3-hour duration during the general storm situation may be too small. This is particularly true in the region west of the Cascades. There is no absolute standard by which such estimates may be measured qualitatively but, they can be compared with like values from similar regions and with ratios to other measures of extreme rain. One such extreme rain index is the value for the 100-year recurrence interval. A specific recurrence interval for PMP can not be determined nor can a relationship be developed that permits obtaining one directly from the other. Examination of such ratios between these two factors in many regions have suggested some qualitative relations as general guides to an approximate level for PMP. An examination of these ratios indicate regions in both Oregon and Washington where PMP values for those short durations may be too low. Other comparisons such as ratios between maximum observed point values and PMP estimates and with statistical estimates of PMP (Hershfield 1965) also indicate PMP values for the 1- and 3-hour duration in the general storm determined by HMR 43 procedures are not comparable to similar values in other regions. Similar comparisons for 1- and 3-hour values east of the Cascade Range for the local or thunderstorm PMP did not indicate these values were too low.

Computation of 1- and 3-hour PMP Values

The procedure used for estimating PMP values in general storms involved computing convergence and orographic components separately and then combining them for the total precipitation value.

Convergence PMP

The convergence component of PMP for the 6-hour duration was first determined and index relations used to obtain values for both longer and shorter durations.

The ratios applied to the 6-hour index values to obtain shorter duration values were developed from smooth extrapolation of depth-duration

curves drawn primarily for 24/6 and 72/6-hour storm data. Review of these curves suggested considerable flexibility in the curves that could be developed.

To determine more accurately appropriate 1/6 and 3/6-hour ratios, we examined the ratios used for PMP studies in California (USWB 1961). These ratios were considerably higher than those used in the northwestern states. Another comparison was 1/6 and 3/6-hour values for the 2- and 100-year recurrence interval. Again, ratios used for estimating PMP values for the northwest states appeared too low. Ratios were also computed between large 1- and 3-hour amounts and corresponding 6-hour amounts in major recent storms.

These studies were used to develop revised ratios for application to the 6-hour convergence index map. It was impossible to detect significant seasonal or geographic differences in the 1/6 and 3/6-hour ratios within the northwest states when consideration was limited to general storms in the northwest. Thus, one set of curves were developed applicable to the entire region. The greatest differences between the new and old curves are in 1-hour values for the region west of the Cascade Crest. The least differences are for the 3-hour duration east of the Cascade Crest. The revised curves (figure attached) should be used in place of figure 3-41 of HMR 43.

Orographic PMP

The orographic index was based on computation involving a laminar flow orographic precipitation model. Durational variations were developed based upon observed durational variations in moisture and inflow winds. Re-examination of these durational variations did not suggest any reason to prepare revised durational curves.

Summary

Preparation of PMP estimates for short durations for small basins in Washington and Oregon indicate the values for the 1- and 3-hour durations for area sizes of less than 300 square miles were probably too low. Review of values for these durations and area sizes indicate the greatest differences were in regions of little or no orographic precipitation. A review of the procedures for computing these values suggest the error is in the 1/6-and 3/6 hour convergence PMP. Revision of these ratios were required to provide values consistent with PMP estimates for the same durations in surrounding regions and with values for other durations in the northwest.

References

1. U.S. Weather Bureau, 1966: Probable Maximum Precipitation, Northwest States, Hydrometeorological Report No. 43, Department of Commerce, Washington, D.C., 228 pp.
2. U. S. Weather Bureau, 1961: Interim Report, Probable Maximum Precipitation in California, Hydrometeorological Report No. 36, Department of Commerce, Washington, D.C., 202 pp.
3. Hershfield, David M., 1965: Methods for estimating Probable Maximum Precipitation, Journal of American Waterworks Association, 57, 965-972.

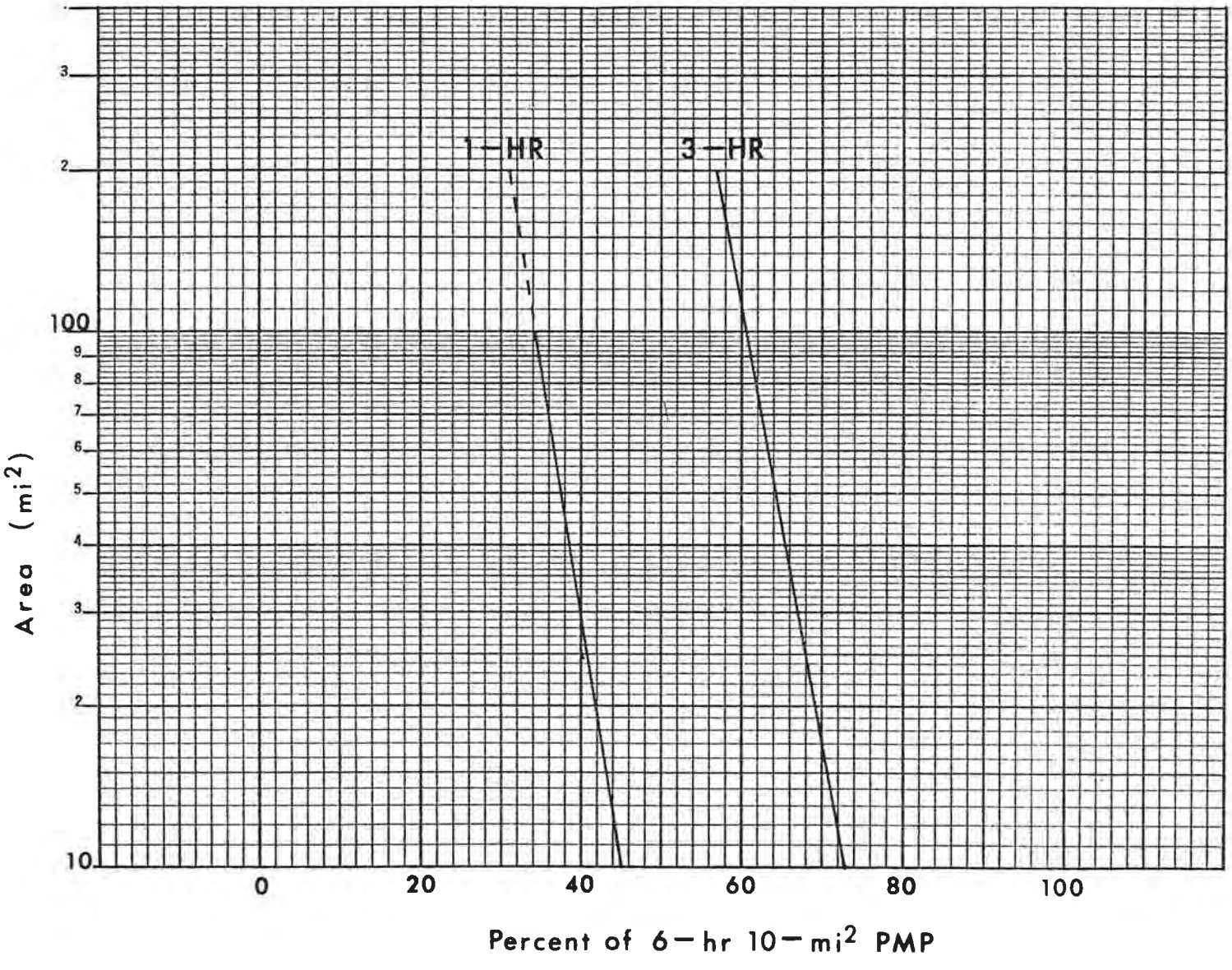

Figure 3-41 (Rev.) - Variation of short duration PMP in percent of 1st 6-hr amount. Applicable to entire region for October to June.